

**PETROLEUM SOURCE ROCK POTENTIAL OF SUBMARINE FAN
AND DELTAIC CENOZOIC SEQUENCES OF WESTERN SABAH AND
SARAWAK, MALAYSIA**

TOGUNWA SERIFAT OLAYINKA

**DEPARTMENT OF GEOLOGY
FACULTY OF SCIENCE
UNIVERSITY OF MALAYA
KUALA LUMPUR**

2015

**PETROLEUM SOURCE ROCK POTENTIAL OF SUBMARINE FAN
AND DELTAIC CENOZOIC SEQUENCES OF WESTERN SABAH AND
SARAWAK, MALAYSIA**

TOGUNWA SERIFAT OLAYINKA

**DISSERTATION SUBMITTED IN FULFILMENT OF THE
REQUIREMENTS FOR THE DEGREE OF
MASTER OF SCIENCE**

**DEPARTMENT OF GEOLOGY
FACULTY OF SCIENCE
UNIVERSITY OF MALAYA
KUALA LUMPUR**

2015

UNIVERSITY OF MALAYA
ORIGINAL LITERARY WORK DECLARATION

Name of Candidate: Togunwa Serifat Olayinka (I.C/Passport No: A05191256)

Registration/Matric No: SGR120088

Name of Degree: Master of Science

Title of Project Paper/Research Report/Dissertation/Thesis:

**PETROLEUM SOURCE ROCK POTENTIAL OF SUBMARINE FAN AND
DELTAIC CENOZOIC SEQUENCES OF WESTERN SABAH AND SARAWAK,
MALAYSIA**

Field of Study: **Petroleum Geology/ Geochemistry**

I do solemnly and sincerely declare that:

- (1) I am the sole author/writer of this Work;
- (2) This Work is original;
- (3) Any use of any work in which copyright exists was done by way of fair dealing and for permitted purposes and any excerpt or extract from, or reference to or reproduction of any copyright work has been disclosed expressly and sufficiently and the title of the Work and its authorship have been acknowledged in this Work;
- (4) I do not have any actual knowledge nor do I ought reasonably to know that the making of this work constitutes an infringement of any copyright work;
- (5) I hereby assign all and every rights in the copyright to this Work to the University of Malaya ("UM"), who henceforth shall be owner of the copyright in this Work and that any reproduction or use in any form or by any means whatsoever is prohibited without the written consent of UM having been first had and obtained;
- (6) I am fully aware that if in the course of making this Work I have infringed any copyright whether intentionally or otherwise, I may be subject to legal action or any other action as may be determined by UM.

Candidate's Signature

Date:

Subscribed and solemnly declared before,

Witness's Signature

Date:

Name: Dr.Wan Hasiah Abdullah

Designation: Professor and Supervisor

ABSTRACT

The study area is in the northwest Borneo which extends between Sarawak and Sabah, Malaysia. This research presents geochemical and petrographical data from outcrop samples distributed in the northern part of Sarawak and western part of Sabah, which are considered amongst areas with many uncertainties in terms of hydrocarbon prospectivity. A total number of sixty samples were analyzed to evaluate the organic matter content, hydrocarbon generating potential, kerogen type, thermal maturity, source input and depositional conditions. The samples were collected from fluvio-deltaic deposits (Meligan, Belait, Miri, Lambir, Tunku formations) and deep water turbidite sediments (West Crocker and Temburong formations) of Eocene to Miocene age. Most of the deltaic sequences samples contain above average levels of organic matter content (TOC >1 wt. %) and possess fair to good hydrocarbon generating potential. The samples from the deepwater turbiditic sequences show poor to fair organic matter content and hydrocarbon generating potential except for few samples from West Crocker formation with significantly higher values of TOC. Based on the dominance of Type III and Type III/IV kerogen within these formations that are supported by low Hydrogen Index (HI) values in the range of 20-150 mg/g HC, as well as low atomic hydrogen to carbon ratios (H/C <1), and pyrolysis-gas chromatography (Py-GC) fingerprints displaying dominance of aromatic compounds over n-alkane/alkene doublets, all of which suggest ability to generate gas rather than oil. However, presence of oil prone Type II/III kerogen is observed in the slump deposits within the West Crocker Formation. The thermal maturity assessment based on pyrolysis T_{max} and vitrinite reflectance (VR) indicate an immature to very early mature stage for hydrocarbon generation amongst the Belait, Lambir, Miri and Tunku formations. On the other hand, the West Crocker, Temburong, and Meligan formations are generally mature to late mature corresponding to peak oil and gas generation stages. Distribution of n-alkanes and isoprenoids indicate land derived organic matter source input

that were preserved under alternating oxidizing and reducing conditions for all of the studied sequences. This is further supported by palynofacies assemblages (abundance of woody fragments), low total sulphur (TS) content, and based on the source and redox sensitive trace elements such as V, Ni, Cr, Co, Sc concentrations and their ratios.

ABSTRAK

Kawasan kajian adalah terletak di Barat Laut pulau Borneo yang bersempadanan antara Sarawak dan Sabah, Malaysia. Kajian geokimia dan data daripada sample batuan singkapan, taburan petrografi di kawasan bahagian Utara Sarawak dan Barat Sabah mempunyai banyak ketidakpastian dari segi prospektiviti hidrokarbon. Sebanyak 60 sample dianalisa untuk menilai kandungan bahan organik, potensi penjanaan hidrokarbon, jenis kerogen, kematangan terma, sumber bahan organik, dan keadaan semasa pengapungan. Pengutipan sampel dilakukan daripada enapan fluvial-delta (Meligan, Belait, Miri, Lambir, Tunku formation) dan sedimen turbidit laut dalam (West Crocker and Temburong Formation) yang dalam lingkungan umur Eocene ke Miosene. Kebanyakan sampel dari jujukan delta adalah diatas purata kandungan bahan organik ($\text{TOC} > 1 \text{ wt.}\%$) dan mempunyai potensi penjanaan hidrokarbon dari sederhana ke bagus. Sampel dari jujukan turbidit laut dalam menunjukkan potensi kurang ke sederhana kandungan bahan organik serta penjanaan hidrokarbon kecuali beberapa sampel dari Formasi Crocker Barat. Jenis kerogen adalah ditakrifkan dalam jenis III dan III/IV, yang mana menyokong nilai HI yang rendah (dalam lingkungan 20-150 mg / g HC), nisbah H/C yang rendah ($\text{H} < 1$), kandungan aromatic yang dominan berbanding kembar n-alkenes/alkanes pada data PyGC semuanya menunjukkan keupayaan menjana gas berbanding minyak. Walaubagaimanapun, kewujudan jenis II/III di dalam Formasi Crocker Barat menunjukkan potensi penjanaan minyak dari sedimen tersebut. Penilaian kematangan terma daripada pirolisis Tmax dan pantulan vitrinit (VR) menunjukkan sampel berada pada tahap tidak matang ke awal matang untuk penjanaan hidrokarbon pada Formasi Belait, Lambir, Miri and Tunku. Selain itu, Formasi Crocker Barat, Temburong, dan Meligan secara keseluruhannya adalah matang ke lewat matang yang sejajar dengan kemuncak penjanaan minyak dan gas. Taburan n-alkanes dan isoprenoid menunjukkan keadaan sedimen semasa

kemasukkan bahan organic adalah pertengahan antara oksid-tidak oksid bagi kesemua jujukan yang dikaji. Penemuan ini juga turut disokong oleh data palynologi yang mempunyai kandudugan bahan kayuan yang tinggi, kandungan sulphur yang rendah, serta kandungan punca dan unsur surih redox yang rendah.

ACKNOWLEDGEMENTS

The thesis compiled here is the result of immense support provided by individuals whose inspiration, ideas, time, funding, and love were instrumental in its completion.

I want to thank my supervisor Prof. Wan Hasiah for tremendous guidance throughout my research process and writing. I am also grateful to Prof. Felix Tongkul and Dr. Meor Hakif for helping out during fieldwork. Thank you for sharing your knowledge with me. A deep sense of gratitude to my committee members, Dr. Ralph Kugler, Dr. Joe Lambiasi and Dr. Aqeel Ashraf for their constructive comments and guidance. My sincere thanks also go to Dr. Mohammed Hakimi for his help and guidance during my research.

I am grateful to University of Malaya for providing facilities to complete this research and IPPP for providing research grant No. PG043-2013A. Many thanks to Mr. Khairul Azlan for his technical support of SRA operation and maintenance, and to Mr. Yousif Makeen and Mr. Baleid Hatem for their help in sample preparation and analysis. I want to acknowledge the entire faculty and staffs of the Department of Geology, for technical and administrative support.

I am especially thankful for my best friend Dr. Olumide Ayodele, for intellectual and moral support, encouragement and inspiration. Thank you for keeping life normal and reminding me of the important things in life. A special thank you to Susan, Salvation, Shirin, Samah and Taofeekat for all their contributions to the success of this research. I express my deepest gratitude to all my family members. Thank you for your love, patience, support and for always believing in me. My most special thanks to Engr. Kayode Adebisi for supporting me this far. With a family like you, every goal is within reach, and no dream is too big. I thank God for His blessings to make all these happen.

TABLE OF CONTENTS

| | Page no. |
|---|-----------|
| Abstract..... | iii |
| Abstrak | v |
| Acknowledgements..... | vi |
| List of Figures..... | xi |
| List of Tables..... | xiii |
| List of Plates..... | xiv |
| List of Appendices..... | xv |
| CHAPTER 1: INTRODUCTION | 1 |
| 1.1 Background | 1 |
| 1.2 Problem Statement | 2 |
| 1.3 Objectives..... | 3 |
| 1.4 Study Area..... | 3 |
| CHAPTER 2 : GEOLOGICAL FRAMEWORK..... | 7 |
| 2.1 Regional Geological Setting | 7 |
| 2.2.1 Tectonic Evolution | 9 |
| 2.2.1.1 Paleocene to Eocene | 9 |
| 2.2.1.2 Oligocene to Early Miocene | 11 |
| 2.2.1.3 Early Miocene to Middle Miocene | 12 |
| 2.2.1.4 Late Miocene to Pliocene..... | 13 |
| 2.2.2 Lithostratigraphy | 13 |
| 2.2.2.1 West Crocker Formation..... | 14 |
| 2.2.2.2 Temburong Formation | 15 |
| 2.2.2.3 Meligan Formation | 15 |
| 2.2.2.4 Belait Formation | 16 |
| 2.2.3 Petroleum System Overview of Western Sabah..... | 17 |
| 2.2.3.1 Source Rocks | 17 |
| 2.2.3.2 Reservoirs, Traps and Seals | 18 |
| 2.3 GENERAL GEOLOGY OF NORTHWEST SARAWAK..... | 20 |
| 2.3.1 Tectonic Evolution | 20 |
| 2.3.2 Lithostratigraphy | 21 |
| 2.3.2.1 Lambir Formation | 21 |
| 2.3.2.2 Miri Formation..... | 21 |

| | | |
|--|---|-----------|
| 2.3.2.3 | Tukau Formation | 22 |
| 2.3.3 | Petroleum System Overview | 22 |
| 2.3.3.1 | Source Rocks | 22 |
| 2.3.3.2 | Reservoirs Traps and Seals | 23 |
| CHAPTER 3: REVIEW OF SOURCE ROCK EVALUATION PRINCIPLE | | 24 |
| 3.1 | Petroleum Source Rock Evaluation | 24 |
| 3.1.1 | Quantity of Organic Matter | 26 |
| 3.1.2 | Genetic Potential | 27 |
| 3.1.3 | Quality of Organic Matter | 27 |
| 3.1.4 | Thermal Maturation..... | 29 |
| 3.2 | Molecular Geochemistry | 31 |
| 3.2.1 | Source Input and Depositional Conditions Indicators..... | 31 |
| 3.2.2 | Thermal Maturity Indicators..... | 34 |
| 3.3 | Trace Elements application in paleoredox conditions | 35 |
| CHAPTER 4: METHODOLOGY | | 38 |
| 4.1 | Introduction | 38 |
| 4.2 | Fieldwork and Sampling | 38 |
| 4.3 | Petrological Analyses..... | 42 |
| 4.3.1 | Polished Block Preparation | 42 |
| 4.3.2 | Vitrinite Reflectance Measurement..... | 42 |
| 4.3.3 | Maceral Analysis | 42 |
| 4.3.4 | Palynofacies Analysis..... | 43 |
| 4.4 | Geochemical Analyses | 43 |
| 4.4.1 | Source Rock Analysis | 43 |
| 4.4.2 | Bitumen Extraction..... | 43 |
| 4.4.3 | Liquid Column Chromatography | 44 |
| 4.4.4 | Gas Column Chromatography-Mass Spectrometry | 44 |
| 4.4.5 | Kerogen Isolation | 45 |
| 4.4.6 | Open Pyrolysis-Gas Chromatography (Py-GC) | 45 |
| 4.4.7 | Elemental Analysis (TS, and CHN) | 46 |
| 4.4.8 | Inductively Plasma Mass Spectrometry (ICP-MS) | 46 |
| CHAPTER 5: RESULTS | | 47 |
| 5.1 | Introduction | 47 |
| 5.2 | Lithofacies Description | 47 |
| 5.2.1 | Tukau Formation | 47 |
| 5.2.2 | Miri Formation | 51 |
| 5.2.3 | Lambir Formation..... | 55 |
| 5.2.4 | Belait Formation..... | 60 |

| | | |
|-------------------------------------|--|------------|
| 5.2.5 | Meligan Formation | 63 |
| 5.2.6 | Temburong Formation..... | 63 |
| 5.2.7 | West Crocker Formation | 68 |
| 5.2.8 | Undifferentiated Formation | 71 |
| 5.3 | Organic Petrographic Data..... | 72 |
| 5.3.1 | Maceral Analysis | 72 |
| 5.3.2 | Palynofacies analysis..... | 76 |
| 5.3.3 | Vitrinite Reflectance..... | 79 |
| 5.4 | Organic Geochemistry | 79 |
| 5.4.1 | Extractable Organic Matter and Hydrocarbons Yield..... | 81 |
| 5.4.2 | Total Organic Carbon | 81 |
| 5.4.3 | Pyrolysis | 85 |
| 5.4.3.1 | Source Rock Analysis | 85 |
| 5.4.3.2 | Py-GC | 86 |
| 5.4.4 | Elemental Analytical Data..... | 93 |
| 5.4.5 | Molecular Composition | 93 |
| 5.4.5.1 | n-alkanes and isoprenoids..... | 93 |
| 5.4.5.2 | Phenanthrene and alkyl derivatives | 96 |
| 5.5 | Trace elements distributions | 96 |
| CHAPTER 6: DISCUSSION | | 108 |
| 6.1 | Introduction | 108 |
| 6.2 | Source Rock Evaluation | 108 |
| 6.2.1 | Organic matter richness and hydrocarbon generative potential | 108 |
| 6.2.2 | Bulk kerogen Characteristics..... | 112 |
| 6.2.3 | Thermal Maturity of Organic Matter..... | 119 |
| 6.2.4 | Prospect for Liquid Hydrocarbon Generation..... | 123 |
| 6.3 | Source of Organic Matter and Depositional Conditions | 126 |
| 6.3.1. | Palynofacies Indicators..... | 126 |
| 6.3.2 | Molecular Indicators for Source Input and Depositional Conditions..... | 127 |
| 6.3.3. | Elemental Indicators | 130 |
| 6.3.4 | Trace Elements | 133 |
| CHAPTER 7: CONCLUSIONS | | 138 |
| REFERENCES..... | | 140 |
| LIST OF PUBLICATIONS..... | | 160 |
| APPENDICES..... | | 161 |

LIST OF FIGURES

| | Page No |
|---|---------|
| Figure 1.1. Satellite image shows the Borneo Island, and highlighted are the location of the study area (in red rectangles). | 5 |
| Figure 1.2. Geological map of Borneo showing the distributions of the studied formations (Hall, 2002). | 6 |
| Figure 2.1. (a) Schematic cross sections across the NW Borneo collisional margin during the Late Cretaceous and Oligocene to Miocene. | 10 |
| Figure 2.2. The amalgamated tectono-stratigraphic terranes of northwest Borneo (Tjia, 2012). | 19 |
| Figure 2.3. Simplified stratigraphy of the offshore and onshore sediments of western Sabah and northern Sarawak (West Baram Delta) with principal unconformities. | 19 |
| Figure 4.1. Simplified geological map showing sampling location in areas within western Sabah and northern Sarawak | 39 |
| Figure 4.2. Flowchart of the methods adopted in this study | 46 |
| Figure 5.1. Sedimentary Log of Tukai Formation. | 49 |
| Figure 5.2. Sedimentary Log of Miri Formation. | 53 |
| Figure 5.3. Sedimentary Log of Lambir Formation. | 58 |
| Figure 5.4. Summary Log of Belait Formation in Batu Luang showing wide range of depositional environments | 63 |
| Figure 5.5 Sedimentary Log of Meligan Formation. | 64 |
| Figure 5.6. Sedimentary log of Temburong Formation. | 66 |
| Figure 5.7. Sedimentary log of West Crocker Formation in Locality (145) KK, popularly known as the kingfisher outcrop. | 69 |
| Figure 5.8. Map showing distribution of vitrinite reflectance in the western Sabah and northern Sarawak studied formations. | 80 |
| Figure 5.9. Concentrations of EOM fractions in the studied samples. | 82 |
| Figure 5.10. Pyrograms of the studied formations showing quality of kerogen. | 89 |
| Figure 5.11. Representative m/z 85 fragmentogram showing the distribution of n-alkanes and isoprenoids. | 99 |
| Figure 5.12. m/z 178 +192 fragmentograms showing the distribution of phenanthrenes (P) and methyl-phenanthrenes (MP) in the studied formations. | 103 |
| Figure 6.1. Plot of total organic carbon (TOC) versus hydrocarbon yield (S ₂) showing the hydrocarbon generative potential of the studied deltaic and submarine fan samples. | 110 |
| Figure 6.2. TOC versus hydrocarbon yield plot showing source rock richness and hydrocarbon potential. | 111 |

| | |
|---|-----|
| Figure 6.4. Crossplot of total organic carbon (TOC in wt. %) and remaining hydrocarbon potential (S ₂ in mg HC/g rock) showing the quality of kerogen in the studied..... | 133 |
| Figure 6.3 Modified van Krevelen diagram of Hydrogen index (HI) versus Oxygen index (OI) showing kerogen quality of the studied formations..... | 115 |
| Figure 6.4. Crossplot of total organic carbon (TOC in wt. %) and remaining hydrocarbon potential (S ₂ in mg HC/g rock) showing the quality of kerogen in the studied formations..... | 116 |
| Figure 6.5. The ternary diagram to assess the kerogen characteristics by using the relative percentages m-p-xylene, phenol, and n-octene (Larter, 1984)..... | 117 |
| Figure 6.6. Ternary plot of classification of kerogen type based on major organic constituents observed under reflected light microscopy (modified after Cornford et al., 1998)..... | 118 |
| Figure 6.7 Plot of Hydrogen Index versus T _{max} showing the type of kerogen and thermal maturity of the studied samples..... | 122 |
| Figure 6.8. Predicted hydrocarbon in the studied sequences | 125 |
| Figure 6.9. Ternary amorphous organic matter–phytoclast–palynomorph (APP) kerogen plot based to characterize the kerogen assemblage and environments under transmitted light microscopy (modified after Tyson, 1995)..... | 128 |
| Figure 6.10. Plot of Pr/n-C ₁₇ vs Ph/n-C ₁₈ showing the deposition conditions of the preserved organic matter in the studied formations..... | 131 |
| Figure 6.11 . Plot of 9MP/9MP+1MP ratio against aquatic macrophyte n-alkane proxy (Paq) of the analysed samples (Ficken et al., 2000)..... | 132 |
| Figure 6.12. Relationship between total organic carbon (TOC) and total sulphur (TS) showing the depositional conditions of the analysed samples (Trendline from Hedges and Keil, 1996)..... | 135 |
| Figure 6.13 a) Plot of Ni/Co against V/Sc ratios (modified after Powell et al. 2003), b) Plot of Ni/Co and V/Cr (modified after Jones and Manning, 1994)..... | 137 |

LIST OF TABLES

| | Page No |
|---|---------|
| Table 3.1. Generative potential, kerogen type, expelled products and thermal maturity of source rock (Peters and Cassa, 1994)..... | 32 |
| Table 4.1 Lithological description and location of the studied formations samples. | 40 |
| Table 5.1. Organic petrology results including palynofacies (under transmitted light (%), kerogen composition (under reflected light (%)) and thermal maturity indicators (vitrinite reflectance measurements (%Ro))..... | 73 |
| Table 5.2. Extractable organic matter and hydrocarbon yield from the studied samples... | 83 |
| Table 5.3 Bulk geochemical characteristics (TOC content , pyrolysis) of the studied formations..... | 87 |
| Table 5.4. TOC and elemental analysis data of the studied formations..... | 94 |
| Table 5.5. Source and maturity parameters derived from n-alkanes, isoprenoids and phenanthrenes..... | 97 |
| Table 5.6. Trace elements concentrations and ratios in the studied samples..... | 106 |

LIST OF PLATES

Page No

| | |
|--|----|
| Plate 5.1. Field observation in studied Tukai Formation outcrop..... | 50 |
| Plate 5.2 : Field observation in studied Miri Formation outcrop..... | 54 |
| Plate 5.3: Field observation in Lambir Formations..... | 59 |
| Plate 5.4. Field Observation of Belait Formation in Batu Luang part of Klias Peninsula... | 62 |
| Plate 5.5. Field Observation of Meligan Formation in Sipitang area | 65 |
| Plates 5.6. Field observation in Temburong Formation..... | 67 |
| Plate 5.7. Field observation in West Crocker Formation..... | 70 |
| Plate 5.8. Field Observations of the undifferentiated Formations..... | 71 |
| Plate 5.9. Photomicrograph of common maceral constituents of the studied northwest Sarawak formations..... | 74 |
| Plate 5.10. Photomicrograph of common maceral constituents of the studied in western Sabah..... | 75 |
| Plate 5.11. Common palynofacies types in the studied formations..... | 78 |

LIST OF APPENDICES

| | Page No |
|--|---------|
| Appendix A: Vitrinite Reflectance Data and Histograms..... | 161 |
| Appendix B: Py-GC Pyrogram Quantitative Data..... | 173 |

CHAPTER 1

INTRODUCTION

1.1 Background

The Cenozoic sedimentary basins of the NW Borneo margin covers an area of over 260,000 km² encompassing both onshore and offshore Sarawak, Brunei and Sabah (Morrison and Lee, 2003). Hydrocarbon exploration started onshore in the late 1800's with the first discovery (the Miri Field) being made in 1910 (Rijks 1981, Tan et al.1999; Morrison and Lee, 2003). Subsequent discoveries transformed the margin into a prolific hydrocarbon region with the most significant provinces being the Central Luconia and Baram Delta. The recent discovery of Adong Kecil West in Sarawak reported to produce over 440 barrels of crude oil per day and 11.5 million standard cubic feet of gas per day (PETRONAS, 2013). Combined discovered reserves for the margin now exceed 20 billion barrels of oil equivalent (Sandal, 1996; PETRONAS, 1999, Morrison and Lee, 2003).

To date, the NW Borneo petroleum system has never been truly defined despite prolific hydrocarbon occurrence, often fraught by the inability to identify discrete source intervals. The economic importance of the NW Borneo margin combined with academic interest in the complex geology has resulted in a considerable body of research on the region, much of which is excellently summarized by previous workers (e.g. Abdul Jalil and Mohd Jamaal, 1992; Azlina Anuar and Abdul Jalil, 1997, 1999; Wan Hasiah, 1999; Abdullah, 2003; Morrison and Lee, 2003; PETRONAS, 1999; Anuar and Hoesni, 2008; Hakimi et.al, 2013) yet the source of the oils is still under debate. The scant geological and geochemical evidence for the origin of oils suggests that terrigenous organic matter is the most likely source (e.g. Azlina Anuar and Kinghorn, 1994; Madon and Abolins, 1999; Algar, 2012). Although such disseminated land plant debris is conventionally considered to

be gas-prone, the search for the oil prone source rock is still inconclusive. Preliminary study on the deep water (submarine fan) sequence in western Sabah revealed the occurrence of a substantial hydrogen-rich (oil prone) stringers of allochthonous terrestrial-derived organic matter as reported by Algar (2012). However there has been no direct study on the petroleum source rock potential of the onshore deepwater and deltaic sequences in western Sabah and northern Sarawak to possibly indicate their contribution to the hydrocarbon accumulations in NW Borneo. Therefore this study is aimed at evaluating the petroleum source rock potential of West Crocker and Temburong (Submarine Fan), Meligan, Belait, Lambir, Miri and Tukai (Deltaic) formations in Sabah and Sarawak which may likely provide relevant information for better understanding of the petroleum system, especially the roles these sedimentary units played in the generation and expulsion of hydrocarbon in the NW Borneo basins.

Estimation of hydrocarbon source potential by characterization of the dispersed organic matter or kerogen using geochemical and petrological techniques has become an integral part of hydrocarbon exploration in frontier basins (Tissot and Welte, 1984; Hunt, 1996; Peters et al., 2005). This involves identifying the potential source rocks, measuring the total amount of organic matter present, the type and quality of the organic matter and the level of thermal maturity attained (Hunt, 1996; Peters et al., 2005). In addition, the understanding of organic matter source input, preservation and depositional conditions help to determine the evolution of organic matter and tectonic setting (Peters et al., 2005).

1.2 Problem Statement

Based on summary of the previous work, various geological and geochemical studies have been done in the NW Borneo especially in the offshore area with little to no investigation of potential source rocks in the onshore area. Few geochemical studies carried out in the onshore area are limited to basic geochemical methods with little to no

information on hidden potentials of the studied sequences. Therefore, this research will provide better understanding on the variation and quality of organic matter, source input and depositional conditions as well as the thermal maturation for hydrocarbon generation and expulsion by integrating geochemistry and petrology.

1.3 Objectives

The main objective of this study is to show the hydrocarbon potentiality of the selected Cenozoic formations in parts of western Sabah and northern Sarawak that will be performed by;

- i. Evaluating the type and quantity of organic matter contents within the studied formations.
- ii. Assessing the source input and depositional conditions of the organic matter.
- iii. Determine the level of maturity of the existing organic matters in the studied formations and their potential for hydrocarbon generation.

1.4 Study Area

The study area is located in western Sabah and northernwest Sarawak (Figure 1.1) and is bounded by latitude from N2.00 and longitude E116.30. The major outcrop locations are in Klias Peninsula, Sipitang, Kota Kinabalu and South Miri areas. The distribution of the studied formations is shown in Figure 1.2.

The Klias Peninsula is a prominent rectangular geomorphic feature (~1500 km²) that juts abruptly from the NE-trending shoreline of Sabah between Brunei Bay and the small Papar River delta (Cullen, 2010). This region developed as a Neogene foreland basin and its modern coastline study can serve as an analogue for clastic depositional systems ancient foreland basins. Belait Formation and Setap Shale are widely distributed in this area.

The Sipitang area of western Sabah consists mainly of hilly to steep terrain trending north-south with narrow valleys. A number of rivers such as Sungai Long Pa Sia, Sungai Mai drain the area and flow into the Sungai Padas. The geology of Sipitang area as studied by Wilson (1964) consist of the Crocker, Temburong and Melingan formations with Quaternary alluvial deposits of riverine terraces and recent riverine alluvia occur in the valleys. The geomorphology of the area consists of almost vertically dipping sandstones and shales forming a dip slope and face slope in a step-like morphology (Paramanthan, 1998).

The landscape of Kota Kinabalu (KK) forms the foothill part of the Crocker Range. A remarkable geologic feature of this area in western Sabah is the wide distribution of turbidites of the Crocker Formation. These are interbedded sandstone and shale sedimentary rocks deposited in a deepwater basin (submarine fan) during the latest Eocene (37 Ma) through to the earliest Miocene (21 Ma) with thickness up to 1,000m (Crevello, 2006). The Crocker turbidites are also exposed on islands offshore KK, and extend offshore western Sabah below the Miocene-Quaternary deltaic sediments (Tongkul, 1989).

The Lambir, Miri and Tukai Formation are well exposed in the South of Miri along Miri-Bintulu and Miri-Bekenu roads. The three formations are interfingering stratigraphically and belong to the Miocene West Baram delta system (Hutchison, 2005). The West Baram Delta is characterized by the deposition of a northwestward prograding delta since Middle Miocene times.

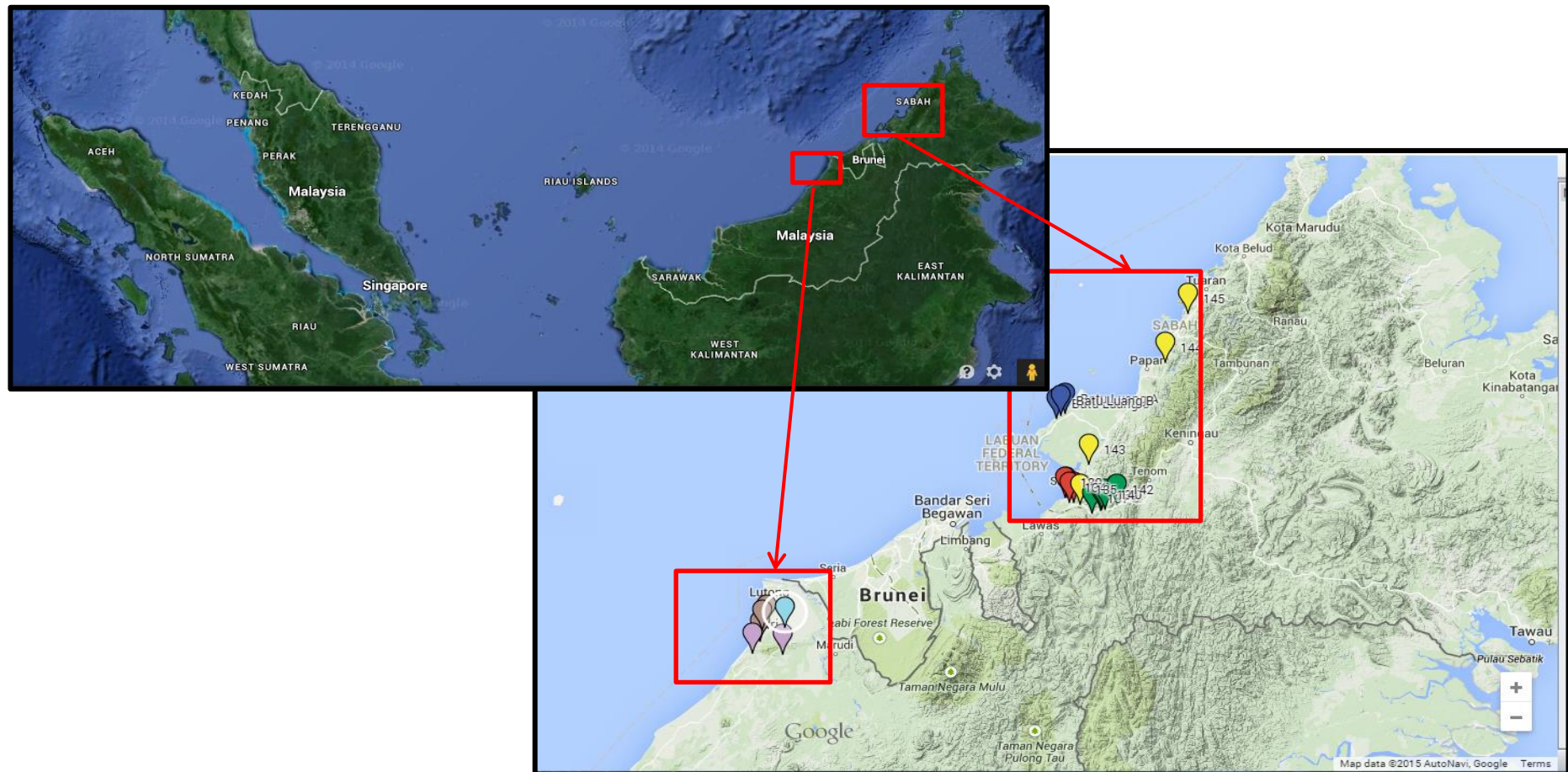


Figure 1.1. Satellite image shows the Borneo Island, and highlighted are the location of the study areas (in red rectangles).

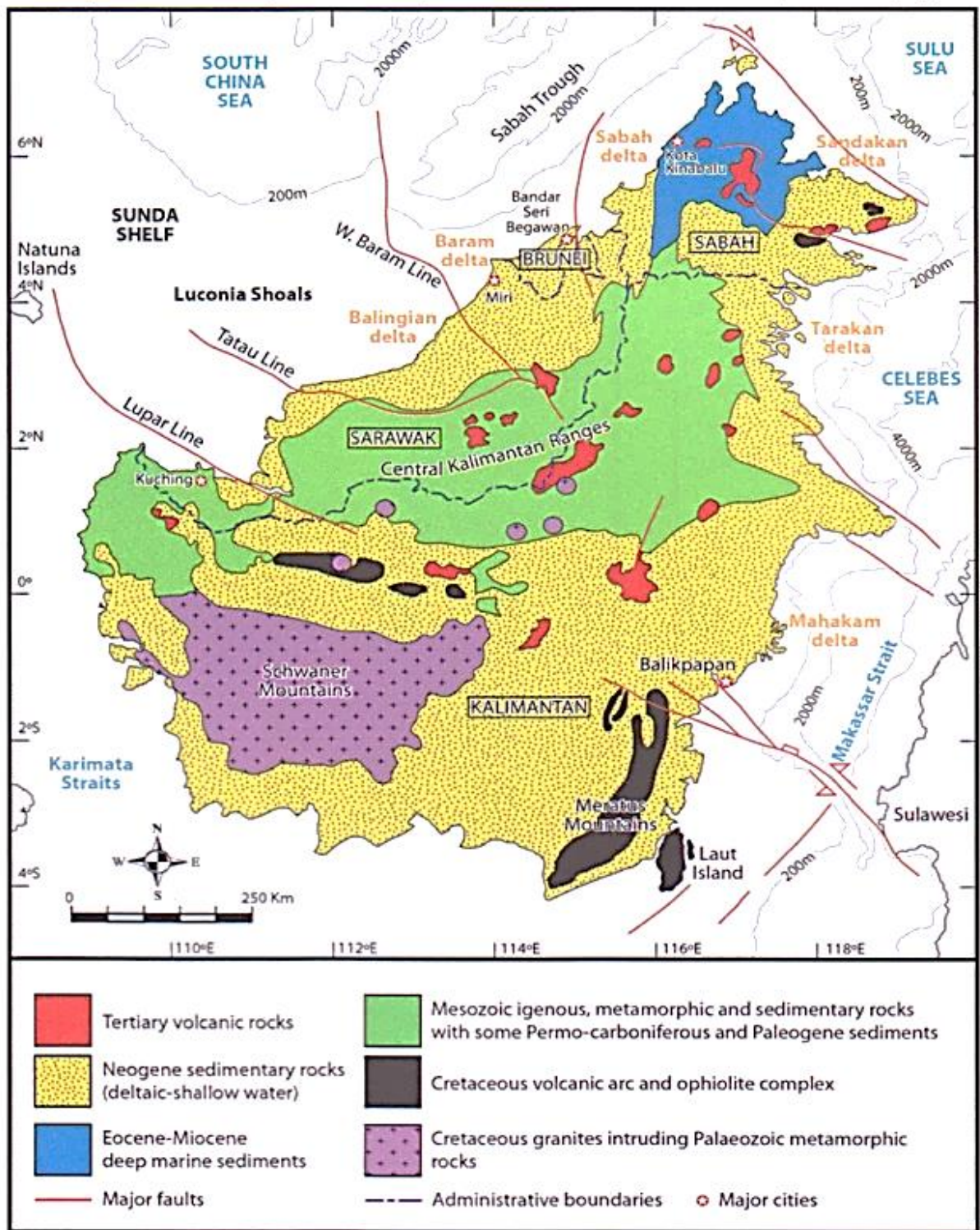


Figure 1.2. Geological map of Borneo showing the distributions of the deltaic and deep water sequences in the study areas (after Hall, 2002).

CHAPTER 2

GEOLOGICAL FRAMEWORK

2.1 Regional Geological Setting

The principal features of the geological evolution of NW Borneo are summarized in Hinz et al. (1989), Hutchison (1996a, 1996b), Milsom et al. (1997), PETRONAS (1999), Hutchison et al. (2000), Hall and Nichols(2002), Morley et al. (2003), Morley and Back (2008), Hall et al. (2008), Hesse et al., 2009 . NW Borneo was built from the Mesozoic to Holocene, and records a complex plate tectonic history involving oceanic and continental crust (Figure 2.1). Convergence between a proto-South China Sea plate and the Luconia “block”, and NW Borneo led to the Cenozoic development of a heterogeneous collisional margin: the NW Borneo collisional margin. During Oligocene–early Miocene times, the South China Sea was opened by seafloor spreading. With the opening of the South China Sea, the thinned continental crust of the Dangerous Grounds region was rifted away from the southern margin of China (e.g.Hinz and Schlüter, 1985; Taylor and Hayes, 1983; Briais et al., 1993). On the southeastern side of the Dangerous Grounds, Hinz and Schlüter (1985) interpreted an older region of oceanic crust, the proto–South China Sea. During the Paleogene, this proto–South China Sea closed, most likely due to a SE-directed subduction beneath NW Borneo. Following complete subduction of the proto–South China Sea oceanic crust, continental crust of the Dangerous Grounds region was partially subducted beneath the Crocker Formation basin of NW Borneo in the latest early Miocene before its buoyancy locked the system (James, 1984; Levell, 1987; Hazebroek and Tan, 1993; Hutchison, 1996a, 1996b; Sandal, 1996; Hall, 1996; Milsom et al., 1997). Subsequently, northern Borneo experienced significant compressional deformation, as documented onshore in folded sedimentary units of late early Miocene to middle Miocene ages (e.g., Sandal, 1996; Morley et al., 2003; Back et al., 2001, 2005, 2008), as well as offshore in

folded and thrust middle Miocene to present-day shelf and slope sequences (e.g., Levell, 1987; Hinz et al., 1989; Hazebroek and Tan, 1993; Morley et al., 2003; Ingram et al., 2004). On the shallow NW Borneo shelf, late Neogene compression coincided with the development of major synsedimentary normal faults and the up to 10-km-thick late Neogene deltaic overburden (Hesse et al., 2009). This “thin-skinned” extensional deformation was superimposed on deep-seated compressional structures and generated, particularly in the southern part of the NW Borneo shelf, a multitude of complex tectonic features that resulted in the reactivation of major thrusts as normal faults and the inversion of synsedimentary normal faults (Morley et al., 2003). The complex interference of extensional and compressional features ceased in the vicinity of the shelf break, beyond which a purely compressional fold-and-thrust belt developed (Hesse et al., 2009).

The coastal and offshore regions of the NW Borneo collisional margin are divided into two basins: the Sarawak and Sabah basins (Hall and Morley, 2004; Tjia, 2012) (Figure 2.2). The NW - SE trending West Baram Line, thought to be a transform fault related to the ancient subduction zone, divides the two basins (Agostinelli et al., 1990; King et al., 2010). The West Baram Line is considered to have separated the deposition of predominantly carbonate sediments in the Sarawak Basin and siliciclastic sediments in the Sabah Basin (Madon et al., 1999). Uplift and deformation of the inboard areas of the NW Borneo collisional margin continued to the latest Cenozoic and has significantly influenced the depositional systems and structure of the two basins (Madon, 1999a; Morley et al., 2000). The West Baram Line presently divides active W - WNW directed convergence in the Sabah Basin from smaller amounts of S-SW directed convergence in the Sarawak Basin (Figure 2.2), as demonstrated by recent Global Positioning System measurements (Simons et al., 2007).

The Sarawak Basin is situated onshore and near coast regions from the West Baram Line east of Miri, to the western extent of the Malaysian province Sarawak and offshore for approximately 400 km (King et al., 2010). The Sabah Basin is located NE of the West Baram Line to the most northern tip of Borneo, extending from onshore to approximately 200 km offshore, where it is bounded by the NW Borneo Trough (King et al., 2010).

2.2 General Geology of Western Sabah

2.2.1 Tectonic Evolution

In this study, the review on the general geology of western Sabah has been grouped into Paleocene to Eocene, Oligocene to Early Miocene, Early Miocene to Middle Miocene, and Late Miocene to Pliocene.

2.2.1.1 Paleocene to Eocene

The Paleogene regional tectonic setting of Sabah is very complex with southeasterly subduction of the proto-South China Sea in NW Borneo (Hall 1996), followed by a period of continued deposition of deep marine Rajang Group turbidites. The Rajang Group is a widespread association of Late Cretaceous to Eocene deep water mudstones and turbiditic sandstones which include the Sapulut, Trusmadi and East Crocker formations. All are thought to have been deposited in the large NE-SW trending Crocker Basin and all are highly deformed with tight isoclinal folds and thrusts (Hutchison, 1996a).

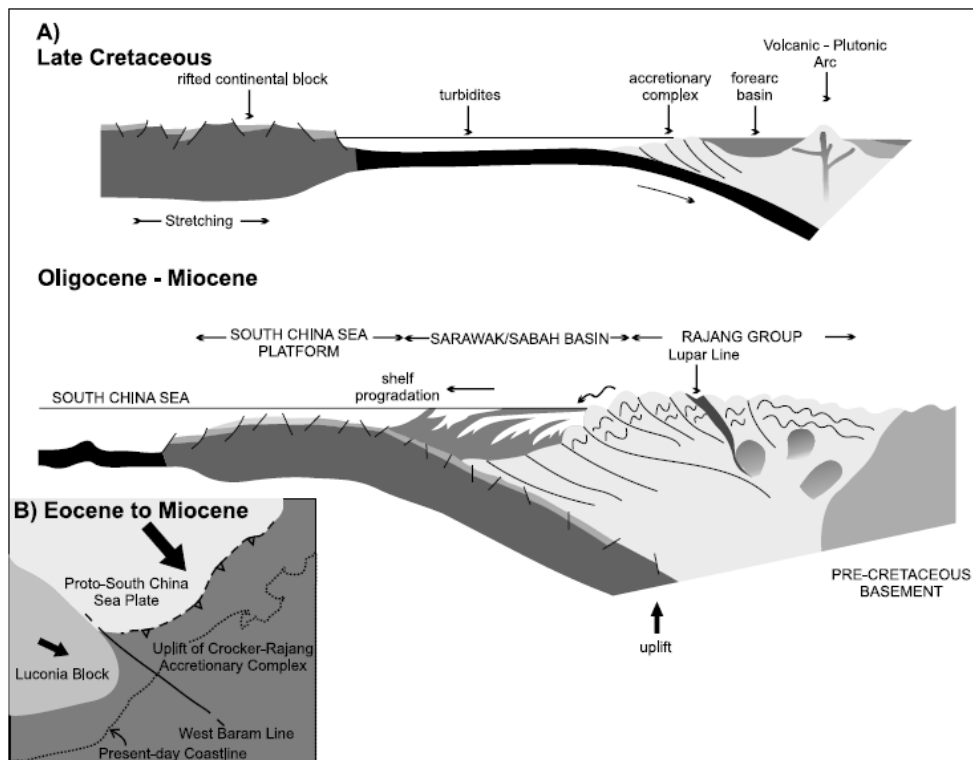


Figure 2.1. (a) Schematic cross sections across the NW Borneo collisional margin during the Late Cretaceous and Oligocene to Miocene, illustrating the subduction of the proto-South China Sea plate beneath the Crocker-Rajang Accretionary Complex (King et al., 2010). (b) A schematic map illustrating the plate configuration at the NW Borneo collisional margin during the Eocene to Miocene (after King et al., 2010)

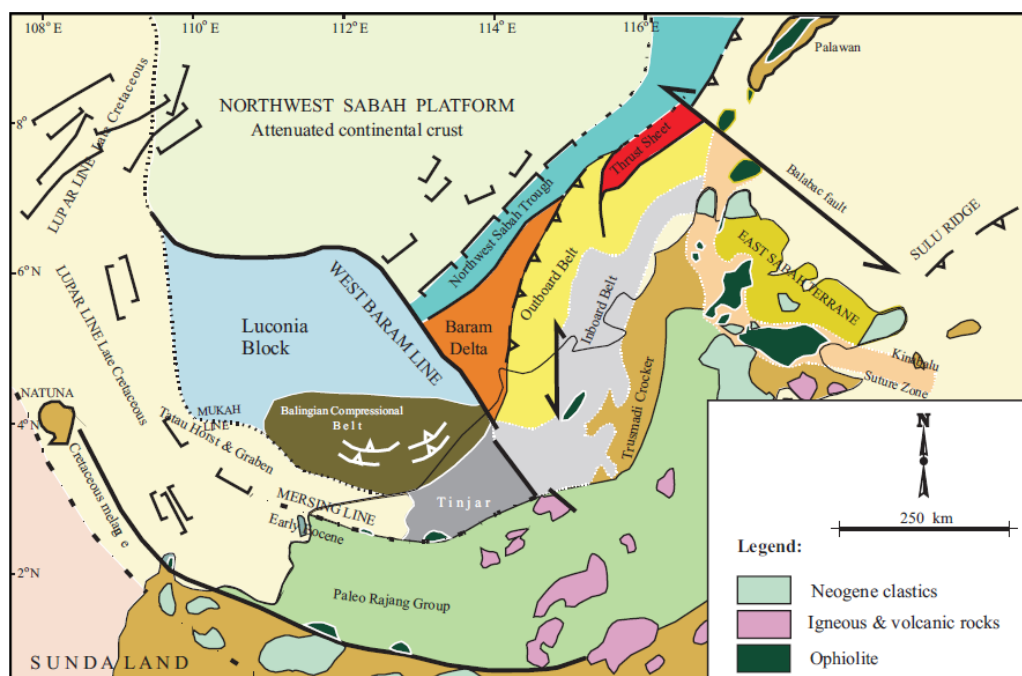


Figure 2.2. The amalgamated tectono-stratigraphic terranes of northwest Borneo (afterTjia, 2012).

The Palaeogene was therefore a period of continued deposition of deep marine turbidites. The strongly deformed turbiditic Rajang Group is interpreted as a part of an accretionary prism related to southeasterly subduction of the proto-South China Sea in the NW Borneo. The Late Eocene tectonic deformation is characterized by folding, thrusting and regional uplift related to the collision of the Luconia Continental Block against NW Borneo (Sarawak Orogeny; Hutchison, 1996a). An unconformity within the succession of Palaeogene turbidites between the Middle and Upper Eocene is inferred by Rangin et al. (1990) on the evidence of reworking of nannofossils and Hutchison (1996a) also argues that the West Crocker Formation includes detritus from uplifted and eroded Rajang Group and East Crocker Formation rocks. Hutchison (1996a) refer to this uplift as the 'Sarawak orogeny' and suggest it was probably driven by collision along the northern Borneo margin at this time. The unconformity is generally difficult to recognize in outcrop in Sabah because of similarities in lithologies either side of it and the strong Neogene deformation.

2.2.1.2 Oligocene to Early Miocene

Following the Late Eocene deformation, uplift and erosion of the Rajang Fold-Thrust Belt provided a source of sediment for the Borneo trough to the NW and also the SE where material was deposited in deep water setting as the West Crocker and Temburong Formations in western Sabah. The fold-thrust belt of the West Crocker Formation, which is well exposed in western Sabah, represents the accretionary complex related to continued southeasterly subduction of the proto-South China Sea in the NW Borneo (Balaguru and Nichols, 2004). Southward directed movement of the NW Sabah continental plate linked to the opening of the South China Sea resulted in the initial uplift of the Temburong and West Crocker formations. Barckhausen & Roeser, (2004) reinterpreted paleomagnetic data and concluded that the sea floor spreading in the South China Sea, which began at 32 Ma, had already ceased by 20 Ma. This indicates that

subduction ceased in the Early Miocene as opposed to the previously interpreted Middle Miocene (Brias et al. 1993) when the Dangerous Grounds micro-continental fragments collided with NW Borneo (Hutchison et al., 2000). This predates the timing of the Sabah Orogeny including the earlier 20 Ma timing proposed by Balaguru & Hall (2003), and it coincides with the Base Miocene Unconformity (BMU) in Sabah. The Early Miocene (22-20 Ma) deformation is a major tectonic event involving the formation of the Sabah mélanges significant uplift and erosion; patches of Burdigalian limestone formed during this uplift. This period was followed by a change in depositional environment from deep-water clastics to a shallow-water deltaic setting called the Meligan Delta (Stage III). To the south, shallow marine sediments of the Meligan Formation and shale- dominant Setap Formation were deposited. However to the north, deep marine clastic deposition continued (Kudat Formation). Prior to impending intensified deformation, widespread carbonates were deposited manifesting initial uplift of Crocker Fold-Thrust Belt (Leong,1999). All of offshore Sabah was under slope- to deep-marine conditions during Early Miocene to early Middle Miocene time.

2.2.1.3 Early Miocene to Middle Miocene

Arc-continent collision in the northern Borneo between the Cagayan Arc and Palawan Continental Block (Rangin, 1991) created another Middle Miocene Unconformity (MMU, 15.5 Ma) which marks the Deep Regional Unconformity (DRU) in onshore and offshore Sabah. This significant Middle Miocene unconformity separates the Meligan Delta from the overlying middle to late Miocene Champion Delta (Stage IV-ABC). This stage generally is characterized by coastal aggradation and progradation sequences comprising the onshore outcrop equivalents of the Belait Formation of NW Sabah. The Stage IVA is a widespread regressive lower coastal plain to marginal marine (deltaic to shoreface) succession, whereas the Stage IVB is a major transgressive sequence of

offshore marine deposits. The Stage IVC is a major regressive sequence with widespread coastal to shallow marine and deep-water deposits followed by a period of prolonged sea-level lowstand. The Belait Formation is dominated by fluvio-deltaic sandstones with laterally equivalent coastal plain to marine sandstone successions that comprise the topsets of the Champion Delta depositional system. Outcrop studies indicate that the Champion Delta is a complex NW prograding delta system with stacked sequences (from bottom to top) of fluvial sands, marginal marine (estuarine & deltaic) and shoreface deposits (van Hattum et al., 2006; Lambiase and Ovinda, 2006; Hall et al., 2008; Lambiase and Cullen, 2013).

2.2.1.4 Late Miocene to Pliocene

The late Miocene Shallow Regional Unconformity (SRU) separates the Champion Delta sequence from the younger Baram Delta (Stage IV-DEFG) succession (Balaguru and Hall, 2003) this most prominent unconformity in Sabah coincides with significant regional uplift and erosion. Stage IV (DEFG) of the Late Miocene to Pliocene is composed of stacked fluvio-deltaic sequence of the Baram Delta System with equivalent offshore shales and deep-water turbidite deposits. The late Miocene to Pliocene was a period of active regression with moderate aggradation punctuated by short periods of minor transgression. The deposits include the onshore equivalent of the Liang Formation of NW Sabah and Brunei that unconformably overlie the Belait and Seria formations. The Liang formation also consists of fluvial sandstones and conglomerates, marginal marine sediments and shoreface sandstones and shales (Hutchison, 1996a; 2005).

2.2.2 Lithostratigraphy

The stratigraphic subdivision of western Sabah is based on correlation of unconformities recognized in the Tertiary of the west Sabah mainland and the adjacent offshore (Figure 2.3). The sedimentary sequences in between these unconformities are

informally called ‘Stages’ (Bol and van Hoorn, 1980; Gartrell et.al., 2011) in the offshore and formations in the onshore (Hall, 2013).

2.2.2.1 West Crocker Formation

The West Crocker formation is an informal name for distinguishing the western and northwestern outcrops of a Paleogene succession in northwest Borneo that constitutes the sand rich Crocker Formation (Hutchison et al., 2000; Lambiase et.al. 2008). The studied West Crocker Formation outcrops in Kota Kinabalu and Sipitang areas of Sabah. The formation comprises predominantly turbidites and other deepmarine sediments of Oligocene-Early Miocene age (Wilson, 1964). They are generally well-deformed, imbricated and thrust (Tongkul, 1989; Leong, 1999). This essentially siliciclastic succession has been interpreted as flysh, turbidites submarine fans, and/or “mass-flow” deposits (e.g. Hutchison, 2005; Crevello, 2006; Jackson et al., 2009; Algar et al., 2011) of a foreland basin that developed along the Oligocene-Miocene subduction zone along the NW Sabah margin. The West Crocker formation lies directly below the Top Crocker Unconformity of van Hattum et al. (2013). The TCU has previously been correlated in different ways with unconformities offshore, typically in sequences deposited above the Crocker Fan (van Hattum et al., 2013). This profound angular unconformity that was generated during an orogenic event that uplifted Paleogene and older rocks and marks the transition from that uplift to the rapid subsidence that accompanied deposition of the thick overlying Neogene shallow marine clastic succession. In the offshore, this unconformity was identified by earlier workers (e.g. Bol and van Hoorn, 1980, Levell, 1987 and Hazebroek and Tan, 1993) as an unconformity below the Miocene hydrocarbon-producing strata of NW Borneo, but was left unnamed (van Hattum, 2013).

2.2.2.2 Temburong Formation

The Temburong Formation firstly introduced by Brondijk (1962) and then revised by Wilson (1964). This formation is dominantly argillaceous, characterized by rhythmic repetition of siltstone and shale, and some rare lenticles of limestone. The formation is remarkably uniform in lithology, being mainly a flysch deposit, with common intercalations of slightly calcareous pelagic shale (Wilson, 1964; Hutchison, 2005). Wilson (1964) has described some turbidite sedimentary structures in the siltstones, such as graded bedding and flute and groove casts which can be seen in the eastern Brunei and south of Beaufort, Sabah. Over two decade several studies have been conducted on the Temburong Formation and can be concluded that this formation has been deposited in deep marine environment by weak turbidity currents as a flysch deposits (Wilson, 1964; Madon, 1997). The age of the formation ranges from Oligocene to Lower Miocene based on planktic foraminiferal assemblage (Wilson, 1964).

The Temburong formation has been interpreted to be the coeval shaly equivalent of the Crocker Formation and has been long recognized as a thick succession of turbidites with northward-directed paleocurrents that was deposited in response to collisional tectonics associated with Late Cretaceous to early Miocene rifting in the South China Sea (Stauffer, 1967; Wilson, 1964; Tan and Lamy, 1990; Hutchison, 1996). The rock units are made of irregular rhythmic repetition of steeply dipping interbedded turbidite sandstone and partially metamorphosed black shales (Hutchison, 1996; 2005).

2.2.2.3 Meligan Formation

The Meligan Formation (Middle Oligocene - Early Miocene) is a lithostratigraphic unit which belongs to a proto-Champion delta (Meligan Delta). The formation is deeply truncated at the present day surface, and only preserved from erosion in the centres of a number of synclines, in the Temburong area of Brunei Darussalam and in adjacent

Sarawak and Sabah (Sandal, 1996; Hutchison, 2005). The Meligan Formation consists dominantly of white-grey, thick bedded, well cemented, frequently cross-bedded medium to coarse grained sandstones. Sandstones belonging to the Meligan Formation were possibly deposited in delta plain and braided river environments (Hutchison, 2005).

In Sabah the Meligan Formation unconformably overlies the West Crocker Formation (Liechti et al., 1960). The base of the Meligan Formation is generally conformable with the partly older Setap Shale Formation, and locally the two formations interfinger (Liechti et al., 1960; van Hattum et al., 2013). The Meligan and Temburong Formations are both truncated at a semi-regional unconformity of Early Miocene age (Top Crocker Unconformity; TCU). This unconformity grades into a conformable contact over a relatively short distance in basinward direction, as is also demonstrated on seismic from offshore northwest Sabah (Sandal, 1996; van Hattum et al., 2013).

2.2.2.4 Belait Formation

The Belait Formation is dominantly sandstone succession with interbedded shales and coals of middle Miocene age. This formation is part of the petroleum bearing succession of the Champion delta in NW Borneo. It has been interpreted as coastal and coastal plain deposits from a range of sedimentary environments associated with a relatively large delta (Wilford, 1961, Curiale et al., 2000, Lambiase 2000). Facies associations suggest that much of the Belait Formation was deposited in structurally-controlled, tide dominated coastal embayments and an open marine coastline well exposed in Klias Peninsula. Fluvial, tidal and shore face sandstones dominate the Belait Formation and the exposed coals are closely associated with tidal and fluvial deposits suggesting deposition in coastal swamps (Madon, 1997; Hutchison, 2005; Tan, 2010; Lambiase and Tulot, 2013).

2.2.3 Petroleum System Overview of Western Sabah

Hydrocarbons in the offshore equivalent of the study area are found in mainly in the Stages IVA, IVC, and IVD (Leong, 1999; Figure 2.3). There are minor occurrences in other stratigraphic units, including Stage III (e.g. at SE Collins). The occurrence of onshore oil seepages in the NW Sabah Province is evidence for a viable petroleum system in the vicinity of the study area although, is still relatively poorly explored (Leong and Azlina, 1999).

2.2.3.1 Source Rocks

Hydrocarbons in the Sabah Basin are very similar in composition and could have originated from source rocks rich in mainly terrigenous organic matter (Scherer, 1980; Abdul Jalil and Mohd Jamaal, 1992; Azlina Anuar and Abdul Jalil, 1997). The source rocks are most likely within the Post-DRU (Stage IV) sequences as the pre-DRU deep marine shales are generally lean and thermally over-mature (Leong and Azlina, 1999). Widespread erosion of the NW Sabah margin during the early Middle Miocene and the extensive outbuilding of the stage IV siliciclastic wedge, resulted in deposition of source beds that are rich in terrigenous organic matter, interbedded with sand prone reservoir facies (Mazlan et al., 1999). Source rock preservation in the Sabah basin is the result of the high input of terrigenous organic matter and high sedimentation rates and seemingly not due to anoxicity (Azlina Anuar and Abdul Jali, 1997). Coaly and carbonaceous shales are the most prolific source rocks in the Sabah basin because of the abundance in large volumes (>2000m thick in some areas) and are closely interbedded with sandstones which act as migration conduits for hydrocarbon migration once the saturation threshold is reached. This efficiency in expulsion allows liquid hydrocarbons to leave the source rocks, as opposed to being retained and converted to gas (Mazlan et al., 1999).

2.2.3.2 Reservoirs, Traps and Seals

The hydrocarbon reservoirs in the Sabah Basin are predominantly siliciclastic. Good quality reservoirs are formed by coastal to fluvio-marine and stacked shallow marine sandstones. Also, the marine turbidites in stages IVC/IVD also form thick, high –quality reservoirs (Leong and Azlina, 1999). Carbonate reservoirs, although a minor component, have fair to excellent reservoir quality. These carbonate mounds and reefs occur on the Kudat Platform in the Northern Sabah Province. Most of the hydrocarbons occur in complex wrench-induced faulted anticlines, rollover anticlines associated with deltaic growth faults, and other fault-related closures. The main structural traps in the western Sabah are fault propagation folds and fold anticlines (Scherer, 1980). The hydrocarbons migrations are generally through faults and intrabedding movement (Nor Azidin et al., 2011). The seal in NW Sabah is mainly provided by intraformational shale and mudstone with effective top and flank seals in many proven accumulations (Erb West, Kinabalu, St Joseph). In some places, shale filled slump scars and shale diapirs act as seal (Leong and Azlina, 1999).

| | | WESTERN SABAH | | NORTHERN SARAWAK | |
|----------|----------------------|--------------------|------------------------|--------------------|-----------------------|
| CENOZOIC | AGES Not to Scale | Offshore Stages | Onshore Formations | Offshore Cycles | Onshore Formations |
| | PLIOCENE | IVF | LIANG | VII | LIANG |
| | LATE MIOCENE | IVE | PLU | VI | TUKAU |
| | | IVD | BELAIT | UPPER | |
| | | IVC | | V MIDDLE | |
| | | IVB | | LOWER | |
| | MIDDLE MIOCENE | IVA | | IV | LAMBIR |
| | | III | MELIGAN SETAP SHALE | III | SETAP SHALE |
| | OLIGOCENE | II | TEMBURONG | I | |
| | EOCENE | | WEST CROCKER | | |
| | | I | EAST CROCKER | | |
| | | | TCU | | |
| | | | DRU | | |

Figure 2.3. Simplified stratigraphy of the offshore and onshore sediments of western Sabah and northern Sarawak (West Baram Delta) with principal unconformities (after Leichti, 1960; Rijks, 1981; Hall, 2013; Gartrell et al., 2011;). Pliocene Unconformity (PLU), Shallow Regional Unconformity (SRU), Deep Regional Unconformity (DRU), and the Top Crocker Unconformity (TCU) otherwise called Base Miocene Unconformity (BMU).

2.3 General Geology of Northwest Sarawak

2.3.1 Tectonic Evolution

The Baram Delta Province is roughly in triangular shape, extends offshore and onshore in northeast-southwest direction lying on both sides of northwestern Sarawak and western Sabah including Brunei water. Towards southwest, the province extends into the northeastern coastal area of Sarawak, which is named as West Baram Delta (Tan et al., 1999). West Baram Line is marked as western margin of the Baram Delta. It separates the delta from the old Balingian and Central Luconia Provinces to the west. Morris Fault – Jerudong Line is the eastern margin of the Baram Delta and it separates the delta from the older, intensely tectonised Inboard Belt of offshore NW Sabah (Figure 2.1). The West Baram Delta is characterized by the deposition of a northwestward prograding delta since Middle Miocene times. Growing in sedimentary section thickness was accompanied by growth faulting trending in NE-SW direction towards the west of Baram Delta (Madon, 1999; Tan et al., 1999).

Following an Early Miocene tectonic event, uplift and erosion were accompanied by the deposition of a thick pile of clastic sediments which prograde seaward. Periods of delta outbuilding were separated by rapid transgressions, represented by marine shale intervals that form the base of eight sedimentary cycles in the offshore (Tan et al., 1999). The regressive sequences of each depositional cycle grade northwestwards from coastal-fluviomarine sands to neritic, marine shales (Tan et al., 1999; Hutchison, 2005). Since the Middle Miocene, the Baram Delta has been subsiding relative to the more stable Central Luconia and Balingina provinces to the west (Tan et al., 1999).

2.3.2 Lithostratigraphy

The Neogene formations crop out in onshore northwest Sarawak to form an integral part of the clastic wedge passing laterally basinward into the Setap Shale Formation. Their stratigraphic relationships are depicted in Figure 2.3

2.3.2.1 Lambir Formation

The Lambir Formation of middle Miocene age consists predominantly of sandstones and alternating shales with minor limestone and marl in some places (Liechti et al., 1960; Tan et. al., 1999; Haile and Ho, 2014). They are increasingly less consolidated towards the upper part of the formation, which consists of sandstone alternating with shales and clays, partly coarse grained or gritty, with quartz pebbles (Leichti et al., 1960). The formation is made up of tidal facies rich in carbonaceous materials in the form of coaly debris and laminations as observed in the Lambir Hills area. The Lambir Formation interfingers with Miri and Tukai formations (Rijk, 1981; Hutchison, 2005) as shown the Figure 2.3. and it has a slightly diachronous transitional contact with the underlying Setap Shale (Tan et al., 1999).

2.3.2.2 Miri Formation

The Miri Formation of middle Miocene age is a siliciclastic succession of coarsening upwards clay-sand packages that is restricted to the coastal area between Miri city in Sarawak basin and Jerudong in Brunei. The studied outcrops are located within the coastal part of Miri city. The Miri Formation are the uplifted part of the subsurface, oil-bearing sedimentary strata of the Miri oilfield possibly corresponds to upper Cycle IV to Cycle V of the offshore stratigraphic units (Tan et al. 1999; Warnier et al, 2011). Based on lithological differences and micropaleontology, the Miri Formation was subdivided into Lower Miri which consists of interbedded shale and sandstone overlying the Setap Shale Formation, and Upper Miri which is characterised

by irregular sandstone and shale alternations (Tan et.al.1999; Hutchison, 2005; Warnier et al, 2011).

2.3.2.3 Tukai Formation

The sedimentary rocks of the Tukai Formation belong to the age range between Late Miocene and Early Pliocene and conformably overlie the Lambir Formation near Sungai Liku in the eastern Lambir Hill. The Tukai Formation is preserved in a relatively simple synclinal structure dissected by strike–slip fault systems and consists of both clay and sandstone beds (Nagarajan et al., 2013). They are made up of mainly fluvial deposits with characteristics including lenticular-shaped channels present at the lower and upper parts of the succession and composed of medium to coarse grained sandstone (Kessler, 2010; Nagarajan et al., 2013). The absence of brackish water forms of foraminifers, presence of lignite layers and amber balls in layered strata suggested that the Tukai Formation was possibly deposited in a upper coastal plain (Hutchison, 2005).

2.3.3 Petroleum System Overview

2.3.3.1 Source Rocks

No distinct source rock interval that gives rise to oil accumulated has been identified in the West Baram Delta. In contrast with the majority of the world's deltas which are mostly built upon passive margins, the West Baram Delta is deposited on an actively subducting margin located offshore NW Borneo (Anuar and Hoesni, 2008). Rapid clastic influx, due to the Middle Miocene uplift and subsequent erosion of the Sabah and Sarawak landmass, with simultaneous space creation led to the accumulation of the West Baram Delta's 8-9km thick depositional sequence of predominantly terrigenous origin (Tan et al., 1999). The source of the West Baram Delta hydrocarbons was intuitively subscribed to Type III land-derived kerogen. Information from offshore

exploration concluded that the West Baram delta oils were generated from land – derived organic materials deposited and preserved in a deltaic setting. These source rocks began accumulating during the Late Miocene with the deposition of Middle and Upper Cycle V sediments and continued into the Pliocene with the deposition of Cycle VI sediments. Mainly humic to mixed, landplant-derived organic material, dispersed within the early-mid Miocene mudstones and sandstones is thought to constitute the source rocks for the oil and gas (Anuar and Hoesni,2008).

2.3.3.2 Reservoirs Traps and Seals

During the overall regressive Cycles V to VIII times a thick sequence of regressive coastal plain and fluvio-marine sediments with generally good reservoir characteristics were deposited (Rijks, 1981; Seah et al., 1987). The principal reservoirs are beach sands, coastal barriers sands and shallow neritic sand -sheets deposited in a coastal environment and channel sands belonging to the deltaic coastal plain environment of deposition (Rijks,1981). The economic floor is at a shallower depth in the southern part of the Baram Delta Province, where erosion has removed the thick overburden and tectonism has increased the intensity of diagenesis (Rijks, 1981; Tan et al., 1999).

In the Baram Delta Province hydrocarbon accumulations are predominantly found to be present in fault dipclosed structures (Tan et al., 1999). Although a large portion of the hydrocarbons is trapped by later faults, the major growth faults form the principal trapping mechanism. This is due to their synsedimentary origin and the very large throws which can place a thick paralic (sand/shale) down thrown block sequence against a fully marine shale sequence in the upthrown block. This juxtaposition of sands against shales appears to be the critical factor for the sealing of the faults.

CHAPTER 3

REVIEW OF SOURCE ROCK EVALUATION PRINCIPLE

3.1 Petroleum Source Rock Evaluation

A petroleum source rock may be defined as fine grained sediment that has generated and expelled enough hydrocarbons to form an accumulation of oil and gas while potential source rock is one that is not mature to generate petroleum in its natural setting but will form significant quantities of petroleum when required thermal maturity is attained (Hunt, 1996; Hunt et al., 2002). Accurate evaluation of the hydrocarbon generation potential of source rocks is essential for hydrocarbon accumulation assessment in a petroleum system (Hunt, 1996). The petroleum potential of any source rock is evaluated by determining the organic matter richness (quantity), type (quality) and thermal maturity of organic matter contained in such rock. There is no single petrological or geochemical parameter that is universally accepted as an accurate measure of the petroleum source potential thus the need to integrate petrology and geochemistry.

The quantity and quality of organic matter (OM) preserved during diagenesis and level of thermal maturity eventually establishes the petroleum-generative potential of the source rock (Demaison and Moore, 1980; Emerson, 1985; Meyers, 1997). The profusion and distinctiveness of OM is associated with the environment of deposition. The OM may be autochthonous (originated in the water column above or within the sediments in which it is buried) or allochthonous (foreign to the environment of deposition). The autochthonous OM may include phytoplankton (diatoms and algae), bacteria, zooplankton, corals and sponges while allochthonous OM is sourced from terrestrial plants and animals debris, spores and pollens transported by air or water to deposition place (Hunt, 1996).

The three major domains of life include archaea, eubacteria (prokaryotes) and eukarya (eukaryotes or higher organisms) that contribute OM to the carbon cycle on Earth. The OM in sedimentary rocks is microscopically heterogeneous. Its chemical composition is related to biological activity, sedimentation and diagenetic processes. The preservation of OM is favored by anaerobic conditions and rapid sedimentation rate. Most petroleum is produced from source rocks sediments preserved in anoxic to dysoxic/suboxic environment since they hold more hydrogen rich OM than do oxic sediments. Sediments are classified as oxic, dysoxic, suboxic and anoxic based on the oxygen contents of the overlying water. Anoxic environments are formed from the lack of water circulation below the photic zone in marine or lacustrine sediments (Peters et al., 2005).

Thermal maturity demonstrates the extent of heat-driven reactions that change sedimentary OM into petroleum. For example, kerogen in fine-grained source rocks can be transformed thermally to oil and gas, which migrate to coarser-grained reservoir rocks. Early diagenetic processes, convert bacterial and plant debris in sediments to kerogen (insoluble particulate OM) and bitumen (extractable OM). Thermal processes usually related with burial then convert part of this OM to petroleum and, ultimately, to gas and graphite (Peters et al., 2005).

It is thought that both kerogen and oil are unstable during catagenesis and progressively decompose to pyrobitumen and gases (e.g. Tissot and Welte, 1984; Hunt, 1996). Crude oil and gas originate by direct thermal decomposition of kerogen and also hydrocarbons in oils crack thermally and produce gas and condensate in the earth (Mango, 1991). Potential source rocks consist of ample amounts of the proper type of dispersed kerogen to generate significant amounts of petroleum but are not yet thermally mature. A potential source rock turns into an effective source rock only at the appropriate level of thermal maturity (Peters et al., 2005).

3.1.1 Quantity of Organic Matter

The quantity of organic matter (OM) in source rocks is usually expressed as the total organic carbon (TOC). TOC is a measure of the organic richness of a rock, i.e. it is the quantity of organic carbon (both kerogen and bitumen) in a rock sample (Jarvie, 1991; Peters and Cassa, 1994; Peters et al., 2005). Three factors are mainly responsible for the organic contents of sediments namely the primary biological productivity, OM preservation and deposition rate of OM versus minerals (Tissot and Welte, 1984).

It is not easy to define the minimum level of TOC a formation must contain in order to qualify as a source sequence. Source qualities are dependent not only on the amount of OM, but also on the type of OM, maturity etc. In general, the higher the TOC value, the better is the source potential. According to published data (e.g., Tissot and Welte, 1984; Peters and Moldowan, 1993; Hunt, 1996) minimum values of TOC for potential source rocks are 0.5% for shales and 0.3% for carbonates. Average values for shaly source rocks world-wide are 1.5% to 2%, for carbonates approximately 0.6% (Tissot and Welte, 1984).

Samples with TOC values exceeding these limits should be analyzed further, as TOC values alone do not necessarily characterize the potential to generate oil/gas. TOC only establish the amount of OM, not the category of OM. Very high levels of TOC can be due to dead carbon. TOC values of 10% or more in coaly sediments are common, but data from subsequent pyrolysis (and organic petrology) sometimes indicate that a major proportion of the organic material is “dead” i.e. Reworked and not capable of generating hydrocarbons any more. Differences in maceral distributions play a crucial role; a sample with 2% TOC in which the OM is predominantly vitrinite, is a much poorer source than a sample with the same amount of TOC in which the OM consists of Type-I and Type-II kerogen mixture.

3.1.2 Genetic Potential

The total amount of hydrocarbons present in source rocks is $S_1 + S_2$ which represents the genetic potential (GP) and allows a semi-quantitative evaluation of potential source rocks based on Rock-Eval analysis. It characterizes the total amount of hydrocarbons which can be released during maturation. S_1 corresponds to the fraction of the genetic potential which has been effectively transformed into hydrocarbons. S_2 represents the potential which has not yet generated hydrocarbons. Thus $S_1 + S_2$ articulated in milligram hydrocarbons per gram of rock, is an evaluation of the genetic potential. The high genetic potential (>2 mg HC/g rock) suggest oil prone source rock whereas low values (generally <2 mg HC/g rock) indicates gas prone source rock (Dyman et al., 1996; Ehinola et al., 2008).

The percent of bitumen in sediments, also called extractable organic matter (EOM) can be used to assess the source rock generative potential. A low percentage <0.05 % indicates poor potential; 0.05-0.1 % stands for fair and 0.1-0.2 % for good whereas 0.2-0.4 % for very good and >0.4 represents excellent quality source rock (Peters and Cassa, 1994).

3.1.3 Quality of Organic Matter

The organic matter in a potential source rock must be capable of generating petroleum. Kerogens capable of generating hydrocarbons are derived from both marine and terrestrial sources. Kerogen can be classified based on chemical composition and visual properties. Macerals are the individual organic components making up kerogen and they are classified by optical properties determined by organic petrology. The four maceral groups are liptinite or exinite, vitrinite, and inertinite. The groups are determined by the type of organic material that the macerals are derived from. Organic geochemical techniques are used to classify kerogen into four types, I, II, III, and IV.

These four types are based on chemical composition and the relative amounts of carbon, Hydrogen, and oxygen present in the sample. Relatively high hydrogen contents in kerogen correspond to greater oil-generating potential. During burial and resulting thermal maturation as oil and gas form/crack from the source rock, the kerogen becomes depleted in hydrogen and oxygen relative to carbon. The amount of petroleum generated and expelled from a source rock increases as the atomic hydrogen-to-carbon (H/C) ratio of the organic matter increases (Hunt, 1996). Thus, the most useful classifications of kerogen types are based on hydrogen, carbon, and oxygen compositions of the organic matter.

Type I kerogen has high atomic hydrogen-to-carbon atomic (H/C) ratio (~ 1.5) and low atomic oxygen-to-carbon (O/C) ratio (< 0.1) (Peters and Moldowan, 1993). It is predominately composed of the most hydrogen-rich organic matter known in the geologic record. The organic matter is often structureless (amorphous) alginite of algal or bacterial origin. Petrographically Type I kerogens consist mostly of liptinite macerals, with trace to minor amounts of vitrinite and inertinite sometimes present. Type II kerogen has high atomic H/C ($1.2 - 1.5$) and low O/C ratios compared to Types III and IV (Peters and Moldowan, 1993). It originates from mixtures of zooplankton, phytoplankton, and bacterial debris in marine sediments. Type II kerogens are dominated by liptinite macerals with lesser amounts of vitrinite and inertinite. Type II kerogens account for most petroleum source rocks (Peters and Moldowan, 1993). Type III kerogen has low H/C (< 1.0) and high O/C (up to ~ 0.3) (Peters and Moldowan, 1993). Such low hydrogen content in organic matter is associated with polyaromatic compounds and derived mostly from higher plants. The chemical composition of Type III kerogen is equivalent to vitrinite, telinite, collinite, huminite, and so-called humic or woody kerogen. It produces natural gas and occasionally associated condensate if the thermal maturation is adequate. Type IV kerogen has low H/C (≈ 0.5) and relatively high

O/C (0.2 – 0.3). Type IV kerogen is predominantly oxidized organic matter and is hydrogen-poor.

The Hydrogen Index (HI) is the ratio of the S_2 to TOC of the rock, expressed as mg hydrocarbon per g TOC. The HI is the chief source parameter used in the quantitative modeling of phase and volume of the generated hydrocarbons (Pepper and Corvi, 1995; Arfaoui et al., 2007). The marine organisms and algae are generally comprised of lipid and protein-rich OM, where the ratio of hydrogen to carbon is elevated compared to land plants. The Oxygen Index (OI) is the ratio of the S_3 to TOC of the rock, expressed as mg CO_2 per gram of TOC. The OI is a factor that shows a relationship with the ratio of oxygen to carbon, which is high for remains of land plants and inert organic material than in marine sediments.

The HI versus OI plot is broadly employed to classify the dominant type of OM in potential source rocks (Bordenave et al., 1993; Schwark et al., 2009) and is reliable indicator of kerogen type (Peters and Cassa, 1994). The HI vs. Tmax plot can substitute HI vs. OI plot when the reliability of S_3 results is doubtful (Espitalie et al., 1984). The different kerogen types produced from source rocks can be obtained from HI or S_2/S_3 ratio (Peters, 1986). The samples with the HI values >250, 150-250 and <150 milligram hydrocarbon per gram of rock are classify the OM as Type II (liptinite), Type II-III (mixed) and Type III (humic) respectively (Yensepbayev et al., 2010). Type I (algal) kerogen generally possess HI values >600 mg HC/g TOC (Peters and Cassa, 1994).

3.1.4 Thermal Maturation

When sedimentary organic matter is buried in basins it is exposed to increasingly higher subsurface temperatures. It is generally accepted that, following diagenesis, thermal maturation or catagenesis is the predominant process by which economic quantities of hydrocarbons are produced from the kerogen in source rocks

(Hunt, 1996). At temperatures of approximately 60°C and higher, the thermal degradation of kerogen yields hydrocarbons under reducing conditions (Hunt, 1996). Type I and II kerogens generate most of the world's oil when subjected to burial temperatures between 60°C and 160°C. Type III kerogen generates natural gas, condensate, and waxy oil. Type IV kerogen generates small quantities of methane (CH₄) and carbon dioxide (CO₂). Most oil expulsion occurs within this burial temperature range too, when the organic matter is in the “oil window”. Petroleum expulsion from the source rocks is very inefficient; roughly 85% of the hydrocarbons generated in a mature source rock are retained within the micropores of the fine-grained sediments (Hunt, 1996). These hydrocarbons are eventually cracked to natural gas as temperatures increase beyond the oil window. Three levels of maturity are recognized by petroleum geochemists, early, peak, and late mature. Hunt (1996) “Postmature for oil is mature for the gas window. Between one-half to two-thirds of thermogenic gas forms during the thermal cracking of previously generated oil in both source rocks and in reservoir rocks and in coal.

The Tmax parameter is considered a very reliable indicator of thermal maturity of Type II and Type III kerogens, but not for Type I (Espitalie, 1986). The chemical changes that occur within the kerogen are reflected in the changing optical properties of the microscopically recognizable constituents (Peters and Cassa, 1994). Changes in the reflectance of vitrinite-like components express the increasing aromatization of the kerogen and decreasing H/C as hydrocarbons are released due thermal rupturing of C-C and C-heteroatom bonds, in much the same way as vitrinite reflectance changes with increasing coalification (Teichmüller et al., 1998). Espitalie (1986) demonstrated good correlations between the Tmax parameter derived by Rock-Eval Pyrolysis and vitrinite reflectance (VR) for organic matter of Type II and III, up to a VR of 1.5% (after this the S₂ peak disappears and Tmax cannot be determined). Bostick (1979) showed that the

optical properties of vitrinite from finely dispersed organic matter in sedimentary rocks could be used to assess thermal maturity. Vitrinites are maceral group derived from terrigenous higher plants. Vitrinite reflectance is a widely used indicator of thermal stress since it extends over a longer maturity range than any other indicator (Hunt et al., 2002). Vitrinite reflectance can be used to assess thermal maturity in types II and III but cannot be used for type I kerogen due to absence of vitrinite. Vitrinite reflectance values for main phase of oil generation ranges from 0.6-1.35%Ro and values greater than 1.35% indicate dry gas generation (Peter and Cassa, 1994; Taylor et al., 1998).

3.2 Molecular Geochemistry

The use of biomarkers and non-biomarker compounds as indicators of organic matter source input, paleoenvironment and thermal maturity has been widely accepted (Mackenzie et al., 1984; Simoneit, 2004; Peters et al., 2005; Hakimi et.al. 2012). Biomarker or geochemical fossils are organic compounds found in geosphere whose structure can be unambiguously linked to their biological origin, despite the possibility of some structural alteration due to diagenetic or other processes (Peters et al., 2005; Adedosu et al., 2012). Polycyclic aromatic hydrocarbons (PAH) are a suite of organic compounds that are ubiquitous in sediments. The possible source of PAH may be oil, coal, air-transported particles combustion of fossil fuel, plant material, algae and bacteria or diagenesis (Pereira et. al., 1999).

3.2.1 Source Input and Depositional Conditions Indicators

n-Alkanes are widely distributed in various plants and other organisms and are probably the most exploited class of biomarkers (Philp, 1985). Waxes present in higher plants have significant concentrations of long chain homologues of *n*-alkanes in C₂₂-C₃₆ region with a pronounced odd/even carbon number predominance and their occurrence reveals the land plant input (Eglinton and Hamilton, 1967; Tulloch, 1976;

Table 3.1. Generative potential, kerogen type, expelled products and thermal maturity of source rock (Peters and Cassa, 1994).

| Potential (Quantity) | | | | | | |
|----------------------|---------------------|------------------|----------------|------------|--|--------------------|
| Petroleum Potential | TOC (wt.%) | S ₁ | S ₂ | Bitumen | | Hydrocarbons (ppm) |
| | | | | (wt.%) | (ppm) | |
| Poor | 0-0.5 | 0-0.5 | 0-2.5 | 0-0.05 | 0-500 | 0-300 |
| Fair | 0.5-1 | 0.5-1 | 2.5-5 | 0.05-0.10 | 500-1000 | 300-600 |
| Good | 1-4 | 1-2 | 5-10 | 0.10-0.20 | 1000-2000 | 600-1200 |
| Very Good | 2-4 | 2-4 | 10-20 | 0.20-0.40 | 2000-4000 | 1200-2400 |
| Excellent | >4 | >4 | >20 | >0.40 | >4000 | >2400 |
| Kerogen (Quality) | | | | | | |
| Kerogen Type | Kerogen Composition | HI (mg HC/g TOC) | S2/S3 | Atomic H/C | Main Expelled Product at Peak Maturity | |
| I | amorphous/alginate | >600 | >15 | >1.5 | Oil | |
| II | liptinite | 300-600 | 10-15 | 1.2-1.5 | Oil | |
| II/III | liptinite/vitrinite | 200-300 | 5-10 | 1.0-1.2 | Oil &Gas | |
| III | vitrinite | 50-200 | 1-5 | 0.7-1.0 | Gas | |
| IV | inertinite | <50 | <1 | <0.7 | None | |
| Maturation | | | | | | |
| Maturity | | Tmax | PI | | Ro (%) | |
| Immature | | <435 | <0.10 | | 0.2-0.6 | |
| Early Mature | | 435-445 | 0.10-0.15 | | 0.6-0.65 | |
| Peak Mature | | 445-450 | 0.25-0.40 | | 0.65-0.9 | |
| Late Mature | | 450-470 | >0.40 | | 0.9-1.35 | |
| Post mature | | >470 | - | | >1.35 | |

Gogou et al., 2000). Microbial n-alkanes typically indicate a smooth distribution of carbon numbers whereas those resulting from terrestrial source have a noticeable prevalence of the odd carbon numbered compounds, especially in the range of C₂₅, C₂₇, C₂₉ compounds (Tissot and Welte, 1984). Similarly algal input will be characterized by n-alkanes in the C₁₆-C₁₈ region of the chromatogram. The predominance of n-C₂₂ suggests a hypersaline depositional environment and an even/odd preponderance is indicative of a highly reducing environment. The relative proportion of terrestrial versus aquatic OM in crude oils or sediment extracts can be identified by using terrigenous-aquatic ratio (TAR). The higher values reflect high relative profusion of terrestrial compared to aquatic OM (Bourbonniere and Meyers, 1996).

$$\text{TAR} = (\text{nC}_{27} + \text{nC}_{29} + \text{nC}_{31})/(\text{nC}_{15} + \text{nC}_{17} + \text{nC}_{19})$$

The ratio must be used carefully as it is sensitive to secondary alteration processes like maturation and biodegradation. Moreover, certain non-marine algae (e.g. *Botryococcus braunii*) may contribute to C₂₇-C₃₁ n-alkanes (Moldowan et al., 1985; Derenne et al., 1988). However TAR measurements are significant to estimate changes in contribution of land versus aquatic flora in immature samples (e.g. Meyers, 1997).

The most copious source of pristane (C₁₉) and phytane (C₂₀) is the phytol side chain of chlorophyll in phototrophic organisms and bacteriochlorophyll in purple sulphur bacteria (e.g. Brooks et al., 1969; Powell, 1988). The Pr/Ph ratio can be applied to ascertain redox conditions of sediments throughout the deposition period under the supposition that both pristane and phytane were derive from phytol side chain of chlorophyll. Low values of this ratio (Pr/Ph <1) in crude oils and extracts indicate anoxic environment of deposition (Didyk et al., 1978; Tissot and Welte, 1984; Hunt, 1996; Harris et al., 2004; Peters et al., 2005), particularly when accompanied by high prophyrin and sulfur contents, while Pr/Ph >1 designate oxic deposition (Didyk et al.,

1978). The Pr/Ph ratio may undergo an increase under the influence of thermal maturity due to cracking of phytane compared to pristane or preferential net production of the former over the latter (Peters et al., 2005).

3.2.2 Thermal Maturity Indicators

Pristane/n-C₁₇ and phytane/n-C₁₈ ratios decrease with thermal maturity since cracking produces more n-alkanes from kerogen (Tissot et al., 1971). These isoprenoid/n-alkanes ratios can be used to assess thermal maturity of oils and bitumens. However, OM input (Alexander et al., 1981) and secondary processes can affect these ratios. So, it is recommended to use the ratio (Pr + nC₁₇)/ (Ph + nC₁₈) instead of using Pr/nC₁₇ and Ph/nC₁₈ as it is supposed to be least effected by maturation process (Alexander et al., 1981). Biodegradation increases these ratios because of preferential removal of n-alkanes prior to isoprenoids (Peters et al., 2005).

The comparative profusion of odd versus even carbon numbered n-alkanes; CPI (Bray and Evans, 1961) and OEP (Scalan and Smith, 1970) can be used to estimate thermal maturity levels of petroleum. CPI or OEP values significantly above or below 1.0 indicate thermally immature OM. Values of 1.0 propose, but not prove, that the crude oil or rock extract is thermally mature. CPI or OEP values below 1.0 are unusual and typify low-maturity oils or bitumen from carbonate (Peters et al., 2005).

$$CPI = \left[\frac{C_{21} + C_{23} + C_{25} + C_{27} + C_{29}}{C_{22} + C_{24} + C_{26} + C_{28} + C_{30}} + \frac{C_{23} + C_{25} + C_{27} + C_{29} + C_{31}}{C_{24} + C_{26} + C_{28} + C_{30} + C_{32}} \right]$$

$$OEP (1) = (C_{21} + 6C_{23} + C_{25}) / (4C_{22} + 4C_{24})$$

Bray and Evans (1961) infer that a source rock is thermally mature when it has generated enough hydrocarbons to bring down the odd/even ratio of C₂₅-to-C₃₃ n-paraffin to the ratio in crude oil, which is about 0.9 to 1.3. Values of CPI will initially

be >1 but will be inclined towards a final value of 1 with increasing maturity. Sediments from purely marine source show CPI value of 1 at all depths while land plants input enhanced the range up to about 20. High CPI values above 1.5 always pass on to relatively immature samples. Low CPI values, though, do not essentially mean higher maturity; they can also be indicative of OM deficient in terrestrial input.

Alkylated polycyclic aromatic hydrocarbons (PAHs) have received attention as indicators of thermal maturity (Budzinski et al., 1995). Throughout the oil window, aromatic maturity indicators are thought to be more sensitive to maturity effects than many biomarker maturity parameters (Alexander et al., 1986). A variety of aromatic maturity parameters have been proposed on the basis of ratios of the relative concentration of more thermally stable isomers to less stable ones (Radke and Welte, 1983; Bastow et al., 2000). Several maturity ratios involving phenanthrenes have been developed over the years and used to assess thermal maturity ((Alexander et. al., 1985; Radke et al., 1986, 1998; Bastow et al., 1998). Phenanthrene maturity parameters are based on the greater stability of 3-methyl phenanthrene and 2-methylphenanthrene compared to 9-methylphenanthrene and 1-methylphenanthrene (Radke and Welte, 1983). The methyl phenanthrene index (MPI) proposed by Radke is a widely used molecular maturity parameter and depends on the relative stability of the isomers (Radke and Welte, 1983).

3.3 Trace Elements application in paleoredox conditions

Redox-sensitive trace element (TE) concentrations or ratios are among the most widely used indicators of redox conditions in modern and ancient sedimentary systems (e.g., Jones and Manning, 1994, Wignall, 1994; Alberdi-Genolet and Tocco, 1999; Akinlua et. al., 2010; Adegoke et al., 2014). Elements providing good potential for palaeo-redox determination are those which are predicted or observed as being more insoluble in anoxic

water, which can be expected to be enriched relative to detrital inputs in normal oxic sediments.

The presence of trace elements in the organic matter depends mainly on the following factors (Tribovillard et al. 2006): (1) metals used in metabolic processes of living organisms (biogenic elements), (2) the pH and Eh of the sedimentary environment, especially the existence of sulfate-reducing conditions, (3) metals in the sedimentary environment; this is related to the chemical composition of the fluid phase interacting with the sediments during diagenesis, (4) the mineralogy of the sedimentary rock (carbonate or siliciclastic), especially the type and amount of clay minerals of which the clays from the smectite group (expanding clays) have the largest sorption capacity, (5) the type of organic matter related to the presence of functional groups that can form organometallic complexes. The last three points are very important for the distribution of trace elements in a system comprising a sulphide phase, organic matter, and clay minerals.

Tribovillard et al. (2006) indicated that the trace elements, like V, Ni, Cr, Cu, and Mo, can be used as paleoredox proxies for paleoenvironmental analysis. These redox-sensitive trace elements tend to be more soluble under oxidizing conditions and less soluble under reducing conditions, resulting in authigenic enrichment in oxygen-depleted sedimentary facies (Tribovillard et al., 2006). Under reducing conditions, sedimentary accumulations of these trace elements may be hosted by various phases, e.g., metal sulfides, in solid solution in pyrite, insoluble oxides and oxyhydroxides, phosphate, sulfate, organometallic complexes and adsorbed onto organic or mineral surfaces (Tribovillard et al., 2006). In addition, with no postdepositional replenishment of oxidizing agents, sulfides are stable and the elements engaged in or co-precipitated with (iron-) sulfides typically do not move during diagenesis (Tribovillard et al., 2006). As a result, the more reducing condition in depositional environments, the more

enrichment of these trace elements in sedimentary rocks. The enrichment of these trace elements can be used as paleoredox proxies to indicate the reducing conditions in depositional environments.

Lewan and Maynard (1982), Lewan (1984) reported that source rock type and depositional environment have a profound effect on the predicted levels of nickel in the source rocks. This implies that the source depositional environment determines the proportion of vanadium to nickel in crude oil. It has been proved that high V/Ni ratio is associated with anoxic palaeoenvironment of deposition ((Lewan, 1984) whilst both V/Ni and Co/Ni ratios have been shown to be anoxic/oxic related parameters (Jones and Manning, 1994). The concentrations and ratios of trace metals such as V, Ni and Co are of particular importance in trace metal geochemistry. These ratios are used in the determination of source rocks types, depositional environment and maturation of crude oils. This is because these ratios remain unchanged irrespective of diagenetic and in – reservoir alteration (Lewan, 1984; Barwise, 1990).

CHAPTER 4

METHODOLOGY

4.1 Introduction

This chapter discusses the methods adopted in this research to achieve the proposed objectives. This includes fieldwork and laboratory studies. The laboratory studies are categorized into petrological and geochemical analyses performed on sandy and shaly sediments of the Cenozoic sequences within the study areas.

4.2 Fieldwork and Sampling

Fieldwork exercise was carried out in Klias Peninsula, Kota Kinabalu, Beaufort and Sipitang areas of western Sabah and South Miri area of Sarawak. The locations of representative outcrops were plotted on the map (Figure 4.1) with the aid of a Global Positioning System (GPS) and assignment to typical Formation was based on published information from past workers (e.g Tongkul, 1994; Jackson et al. 2009, Hutchison, 2005; Tan, 2010; Wannier et al., 2011). Sedimentary logging was limited to well preserve exposures and photographs were taken for illustration purposes. Sampling was done very carefully to avoid contamination and weathered samples were avoided in the field. The samples description is shown in Table 4.1.

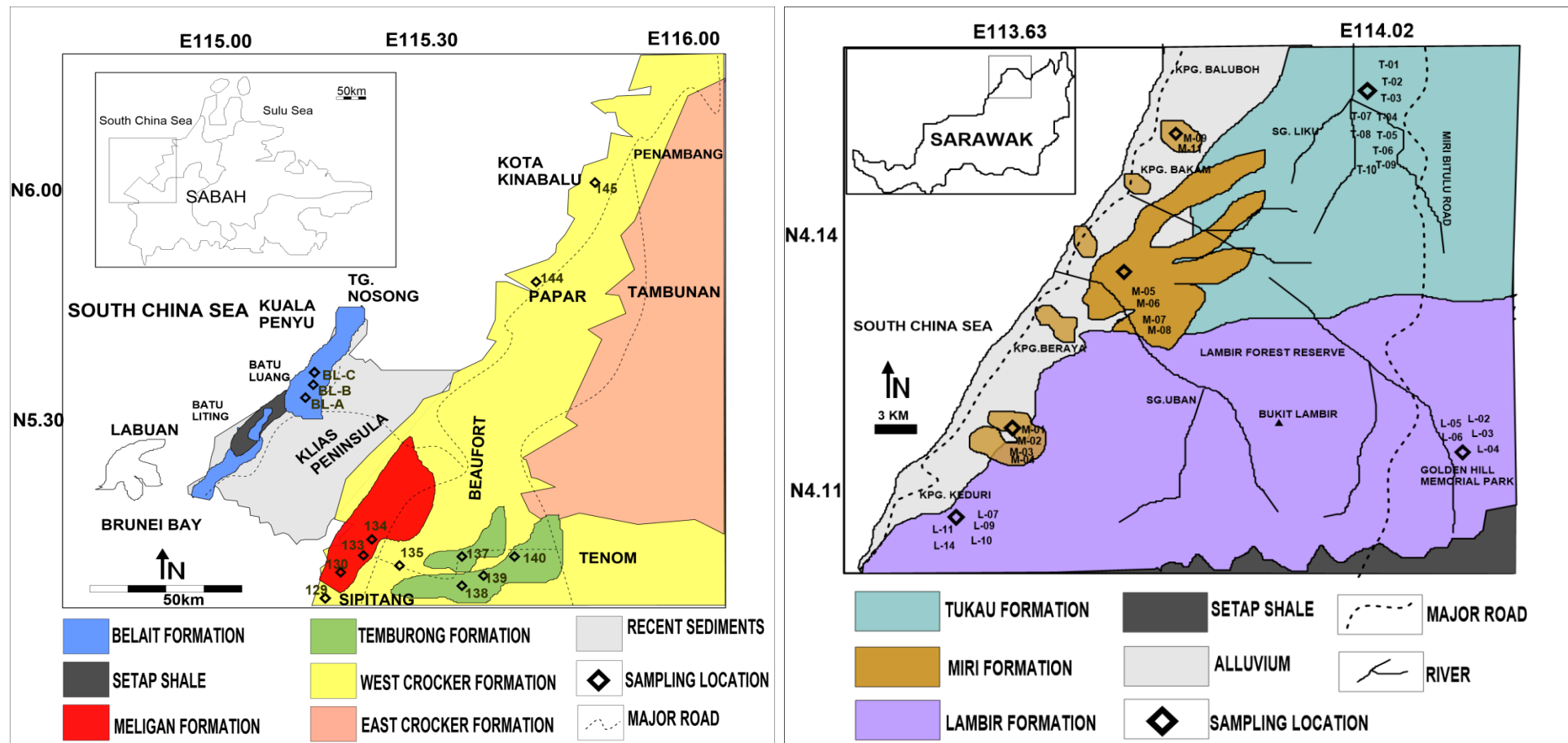


Figure 4.1 Simplified geological map showing sampling location in areas within western Sabah and northern Sarawak

Table 4.1 Lithological description and location of the studied formations samples.

| | Formation | Sample | Coordinates | | Locality | Lithology |
|------------------|-------------------|------------|---------------|----------------|-------------------------------------|-------------------------------|
| | Northwest Sarawak | | | | | |
| WEST BARAM DELTA | Lambir | L-02-SS | 4° 11.271' N | 114° 2.437' E | Miri Bintulu Road | Carbonaceous Sandstone |
| | | L-03-SH | 4° 11.271' N | 114° 2.437' E | | Mudstone |
| | | L-04-SS | 4° 11.271' N | 114° 2.437' E | | Mudstone |
| | | L-05-SS | 4° 11.230' N | 114° 2.399' E | | Carbonaceous Sandstone |
| | | L-06-SH | 4° 11.230' N | 114° 2.399' E | | Carbonaceous Sandstone |
| | | L-07-SH | 4° 11.215' N | 114° 2.410' E | | Mudstone |
| | | L-09-SH | 4° 11.215' N | 114° 2.410' E | | Mudstone |
| | | L-10-SH | 4° 11.190' N | 114° 2.195' E | | Mudstone |
| | | L-11-SH | 4° 11.190' N | 114° 2.195' E | | Mudstone |
| | | L-14-SH | 4° 11.190' N | 114° 2.195' E | | Mudstone |
| | Miri | M-01-SH | 4° 11.618' N | 113°50.778' E | Miri- Bintulu Coastal Road | Mudstone |
| | | M-02-SH | 4° 11.618' N | 113° 50.778' E | | Mudstone |
| | | M-03-SH | 4° 12.718' N | 113°53.661' E | | Mudstone |
| | | M-04-SH | 4° 12.718' N | 113°53.661' E | | Mudstone |
| | | M-05-SH | 4° 12.718' N | 113°53.661' E | | Mudstone |
| | | M-06-SH | 4° 12.718' N | 113°53.661' E | | Mudstone |
| | | M-07-SH | 4° 12.718' N | 113 53.661' E | | Mudstone |
| | | M-08-SS | 4° 15.193' N | 113°54.227' E | | Carbonaceous Sandstone |
| | | M-09-SH | 4° 15.193' N | 113°54.227' E | | Mudstone |
| | | M-10-SS | 4° 15.193' N | 113°54.227' E | | Carbonaceous Sandstone |
| | Tukau | T-01-SS | 4° 15.519' N | 114°2.156' E | Miri- Bintulu Road | Carbonaceous Sandstone |
| | | T-02-SH | 4° 15.519' N | 114°2.156' E | | Mudstone |
| | | T-03-SH | 4° 15.519' N | 114°2.156' E | | Mudstone |
| | | T-04-SH | 4° 15.519' N | 114°2.156' E | | Mudstone |
| | | T-06-SH | 4° 15.519' N | 114°2.156' E | | Mudstone |
| | | T-07-SH | 4° 15.519' N | 114°2.156' E | | Mudstone |
| | | T-08-SH | 4° 15.519' N | 114°2.156' E | | Mudstone |
| | | T-09-SH | 4° 15.519' N | 114°2.156' E | | Mudstone |
| | | T-10-SS | 4° 15.519' N | 114°2.156' E | | Carbonaceous Sandstone |
| | | T-12-SH | 4° 15.519' N | 114°2.156' E | | Mudstone |
| CHAMPION DELTA | Western Sabah | | | | | |
| | Belait | BL-A2-SH | 5° 52.415' N | 115°52.573'E | Batu Luang | Mudstone |
| | | BL-A3-SH | 5° 52.415' N | 115°52.573'E | | Carbonaceous mudstone |
| | | BL-A5-SS | 5° 52.415' N | 115°52.573'E | | Organic laminated sandstone |
| | | BL-A6-SS | 5° 52.415' N | 115°52.573'E | | Sandstone |
| | | BL-A7-SH | 5° 52.415' N | 115°52.573'E | | Mudstone |
| | | BL-A8-SS | 5° 52.415' N | 115°52.573'E | | Carbonaceous sandstone |
| | | BL-B1-SH | 5° 52.365' N | 115°52.520'E | | Mudstone |
| | | BL-C2-SH | 5° 52.350' N | 115°52.475'E | | Mudstone associated with coal |
| MELIGAN DELTA | Meligan | ME-130B-SH | 5° 02 .157' N | 115° 32.355'E | Sipitang | Mudstone |
| | | ME-130C-SS | 5° 02.157' N | 115° 32.355'E | | Carbonaceous sandstone |
| | | ME-130F-SH | 5° 02.157' N | 115° 32.355'E | | mudstone |
| | | ME-133A-SS | 5° 00.651' N | 115° 33.254'E | | Carbonaceous sandstone |
| | | ME-133C-SH | 5° 00.651' N | 115° 33.254'E | | mudstone |
| | | ME-134A-SH | 5° 00.651' N | 115° 33.254'E | | Coaly mudstone |

Table 4.1 Lithological description and location of the studied formations samples
(continuation)

| | Formation | Sample | Coordinates | | Locality | Lithology |
|----------------------|-------------------------------|-------------|--------------|---------------|----------------------------|------------------------|
| SUBMARINE FAN | Temburong | TE-137A-SH | 4° 30.212' N | 115° 40.254'E | Sipitang- Tenom | Dark shale |
| | | TE-137B-SS | 4° 30.212' N | 115° 40.254'E | | Sandstone |
| | | TE-138-SH | 4° 35.156' N | 115° 42.210'E | | Dark shale |
| | | TE-139-SH | 4° 58.147' N | 115° 42.054'E | | Dark shale |
| | | TE-139-SS | 4° 58.147' N | 115° 42.054'E | | Sandstone |
| | | TE-140-SH | 4° 58.124' N | 115° 42.054'E | | Dark shale |
| | West Crocker | WC-129B-SH | 5° 02.376' N | 115° 30.998'E | Sipitang | Dark shale |
| | | WC-129E-MTD | 5° 02.376' N | 115° 30.998'E | | Slump deposit (silty) |
| | | WC-129D-MTD | 5° 02.376' N | 115° 30.998'E | | Slump deposit(shaly) |
| | | WC-129F-MTD | 5° 02.376' N | 115° 30.998'E | | Slump deposit (sandy) |
| | | WC-135B-SST | 4° 59.835' N | 115° 34.441'E | | Carbonaceous sandstone |
| | | WC-144A-MTD | 5° 46.563' N | 116° 01.333'E | Kota Kinabalu | Slump deposit (sandy) |
| | | WC-144B-SH | 5° 46.563' N | 116° 01.333'E | | Dark shale |
| | | WC-145A-SST | 6° 02.527' N | 116° 08.486'E | | Sandstone |
| | | WC-145B-MTD | 6° 02.527' N | 116° 08.486'E | | Slump deposit (sandy) |
| | | WC-145C-SH | 6° 02.527' N | 116° 08.486'E | | Dark shale |
| | Undifferentiated Formation | UD-01-SS | 5°45.951' N | 115°45.961'E | Batu | Carbonaceous sandstone |
| | | UD-02-SS | 5°45.951' N | 115°45.961'E | Liting | Laminated sandstone |

4.3 Petrological Analyses

Organic petrographic analyses used in this study involved the use of a LEICA CTR 6000 photometry microscope. The main objective of this technique is to provide information about the maceral composition, vitrinite reflectance and fluorescence characteristics of the dispersed organic matter in order to assess the type, maturity and source input of organic matter within the studied sequences.

4.3.1 Polished Block Preparation

Rock samples were crushed into small pieces (2-3mm) using pastel and mortar. Samples then were, embedded in 30 mm diameter latex moulds with liquid epoxy resin and hardened for 48 hours at 30°C. Samples were then gradually ground with 350 (coarse), 550 (intermediate), 800 (fine), 1200 (very fine) abrasive powder and finally polished with 1 µm alumina powder-deagglomerate, 0.3 µm alumina powder-deagglomerate, and 0.04 µm OP-S suspension solution for final polishing.

4.3.2 Vitrinite Reflectance Measurement

Measurement of vitrinite reflectance was carried on polished blocks under reflected white light, with x50 oil immersion objectives using immersion oil with a refractive index (ne) of 1.518 at 23°C. A sapphire glass standard with 0.589% reflectance value was used for calibration. Reflectance measurements were determined in the random mode (Rrand) on vitrinite maceral at a wavelength of 546 nm, and the values reported were arithmetic means of at least 25 measurements per sample.

4.3.3 Maceral Analysis

The maceral analysis procedure was carried out in reflected white light and fluorescence mode using 50x oil immersion objectives. Semiquantitative analysis was carried out to estimate maceral abundance in dispersed organic matter in the shaly and sandy samples. Fluorescence microscopy was carried out to identify the liptinite macerals.

4.3.4 Palynofacies Analysis

Palynofacies analysis consisted of observations of isolated kerogen under transmitted light microscopy to identify different organic matter type. A count of 200 organic matter particles was carried out for each slide to document changes in the frequency of organic matter and to calculate their percentage frequency according to Nøhr-Hansen (1989).

4.4 Geochemical Analyses

Geochemical techniques were used to determine the type, abundance and thermal maturity of organic matter as well as source input and depositional conditions.

4.4.1 Source Rock Analysis

The rock samples were crushed to less than 200 mesh and analysed using (SRA-Weatherboard)-TOC/TPH instrument (equivalent to Rock Eval equipment) to identify the organic matter richness, kerogen type and maturation for the preserved organic matter. Pyrolysis analysis was performed on approximately 50-100 mg crushed samples, which were heated to 600°C in a helium atmosphere and measured several parameters such as S1, S2, S3 and temperature of maximum pyrolysis yield (Tmax). TOC was also determined using the SRA instrument. Hydrogen index (HI), oxygen index (OI), production yield (PY), and production index (PI) were calculated as described by Espitalie et al. (1977) and Peters and Cassa (1994).

4.4.2 Bitumen Extraction

Fine powdered rock samples were measured and placed in the pre-extracted thimble capped with pre-extracted cotton wool. Samples were subsequently extracted in a Soxhlet Apparatus for 72 hours using an azeotropic mixture of dichloromethane and methanol in (93:7) ratio. Metallic copper was added into the flask during the extraction process to remove the elemental sulphur and anti-bumping granules was added to avoid

burst out. After that, the solvent was removed through evaporation process by the use of Rotary evaporator under low pressure. The recovered fractions were air dried and the weight was measured and recorded as the extractable organic matter (EOM).

4.4.3 Liquid Column Chromatography

The extractable organic matter (EOM) was separated into saturated and aromatic hydrocarbons and polar compounds (NSO compounds) by column chromatography on neutral alumina over silica gel. Chromatographic column (length/width ratio 50:1) was slurry packed with activated silica gel and aluminum oxide using petroleum ether. Aliphatic, Aromatic and NSO fractions were eluted with petroleum ether (100 ml), dichloromethane (100ml), and methanol (50 ml) respectively. The solvent was distilled off using rotary evaporator to about 3 ml and thereafter transferred into a weighed clean vial. The remaining solvent was removed under nitrogen gas flow at temperature below 50°C.

4.4.4 Gas Column Chromatography-Mass Spectrometry

Gas Chromatography - Mass Spectrometry (GC-MS) was used to analyze the aliphatic and aromatic hydrocarbon fractions of the samples. The saturated fractions were dissolved in hexane while the aromatic fractions were dissolved in dichloromethane (DCM) and analyzed by GC-MS. The analyses were performed on an Agilent Gas Chromatograph 6890N combined with 5975 Inert Mass Selective Detector. The GC temperature was programmed from 40°C to 300°C (30 min hold) at 4 °C min⁻¹ in an oven for 95 minutes. The injected fractions were vaporized and mixed with helium as a carrier gas. The separated compounds were transferred to the source of the mass spectrometer where they were ionized by an electron beam. Data were acquired and processed using Agilent ChemStation software.

4.4.5 Kerogen Isolation

Extracted rock samples were treated with hydrofluoric acid (48-68%) to remove the silicates. The samples were left overnight to ensure the clastic fraction was completely removed and subsequently diluted with distilled water until neutral pH is reached. The sample was treated with a concentrated hot bath of hydrochloric acid, 1:1 (HCl: distilled water) to remove any remnants of carbonates. Samples were allowed to cool and were then diluted with distilled water until a neutral pH is reached and transferred to a centrifuge tube. A mixture of ZnBr (1kg: 370ml distilled water) with specific gravity 2.2 was prepared and then poured into the centrifuge tube and was left overnight. The floated kerogen was pipetted and washed with distilled water.

4.4.6 Open Pyrolysis-Gas Chromatography (Py-GC)

The Pyrolysis analysis was carried out using a Frontier Lab Pyrolyser System which can perform thermal desorption from 40 to 300°C and pyrolysis at 600°C. The system is coupled to an inert (quartz and Ultra ALLOY-5) column fitted to an Agilent GC chromatography equipped with a flame ionization detector. The pyrolysis products were trapped after passing through GC column and released over the range 300-600 °C at (25 °C/min). Identification of peaks based on reference chromatograms was done manually with Agilent ChemStation software and comparison to published data (e.g., Abdullah, 1999; Dembicki, 2009; Hakimi and Abdullah, 2013).

4.4.7 Elemental Analysis (TS, and CHN)

Total Sulphur (TS) was measured on whole rock by combustion in an induction furnace in a flow of oxygen, using a LECO carbon –analyser IR112. Whole rock and selected isolated kerogen samples were subsequently analysed on a Perkin-Elmer 2400 Series CHNS/O Analyzer at the Department of Chemistry to determine carbon (C), hydrogen (H), and nitrogen (N) ratios.

4.4.8 Inductively Plasma Mass Spectrometry (ICP-MS)

Concentrations of trace elements were determined using an Agilent Technologies 7500 Series Inductively-coupled plasma mass spectrometer (ICP-MS). The samples were pulverized into fine powder and prepared for the analysis by Microwave-assisted digestion as outlined by Pi et al. (2013). Anton 3000 microwave oven was used for the Microwave assisted digestion, and the chemicals used comprise a mixture of HNO_3 , HF and HClO_4 . HF was neutralized by fresh addition of HClO_4 to the sample solution and evaporated to near dryness. 10 ml of 5 M HNO_3 was further added and the solution was slowly digested at low temperature. The obtained sample solution was diluted with deionized water to 50 ml in a volumetric flask and were diluted a further 5-fold for ICP-MS analysis. The minimum detection limit of the equipment is less than 1 ppb. Results were corrected to the weight of bulk rock, and analytical precision for trace element concentration was better than 5%.

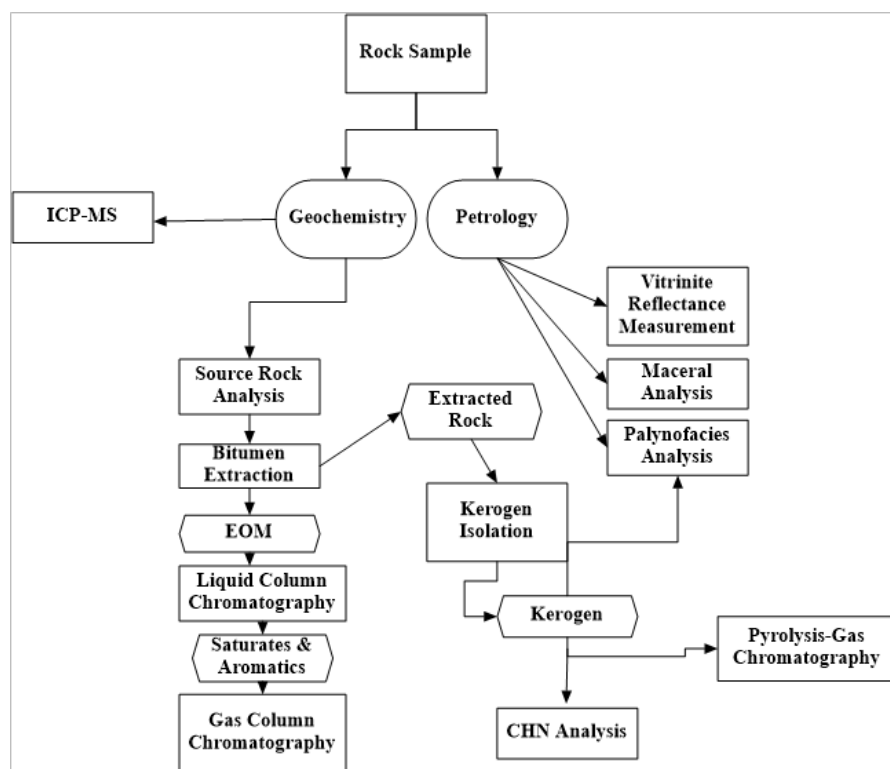


Figure 4.2. Flowchart of the methods adopted in this study.

CHAPTER 5

RESULTS

5.1 Introduction

This chapter presents the results obtained from geochemical and petrological study carried out on the samples collected from western Sabah and northwest Sarawak representing the Tukai, Miri, Lambir, Belait, Meligan, Temburong and West Crocker formations. This chapter also discusses the lithofacies observed in the field.

5.2 Lithofacies Description

The lithologic log used to characterize the lithofacies of the analysed samples at the outcrop locations are shown in Figs. 5.1-5.7. The visited outcrops were assigned to the already established formations by previous workers. Detailed logging was not carried out especially in the western Sabah areas because much detailed sedimentological information has been recorded by previous workers (e.g. Tongkul, 1994; William et al., 2003; Jackson et al. 2009, Hutchison, 2005; Tan, 2010). Selected sedimentological logs are presented in this section to describe the main lithofacies of the studied formations.

5.2.1 Tukai Formation

The Tukai Formation is well exposed in the Sungai Ukong area, in South Miri District. Three lithofacies associations were identified which includes fluvial channel, crevasse splay and flood plain associations.

Fluvial Channel facies association is characterized by structureless massive and trough cross stratified sandstone facies with small scale trough cross stratification that is often associated with parallel lamination at the top of the sequence and erosive base. Flood plain facies association is characterized by carbonaceous mudstone and sandstone facies with dispersed organic matter in the form of amber. Amber is fossilized resin or gum

produced by plants. The association of amber in the Tukai sandstone and mudstone indicate terrestrial origin which suggests that there was a swamp close by to the sedimentary environment. The Crevasse Splay facies association is characterized by parallel laminated sandstones with mudstones interbeds. . This lamination indicates an abrupt change in energy in the channels where the fine grained sediments in suspensions are deposited as lamina.

From field observations (Plate 5.1) and lithofacies analysis, it is apparent that the Tukai sequence in the study area was deposited by means of tractive processes by a river system. This indicates a fluviatile environment of deposition. This fluviatile environment is further supported by the presence of sedimentary structures and total absence of marine fossils as described in the stratigraphic log section (Figure 5.1). The sedimentary structures present are channels, graded beddings, cross beddings and laminations which were formed in a fluvial environment especially a meandering stream.

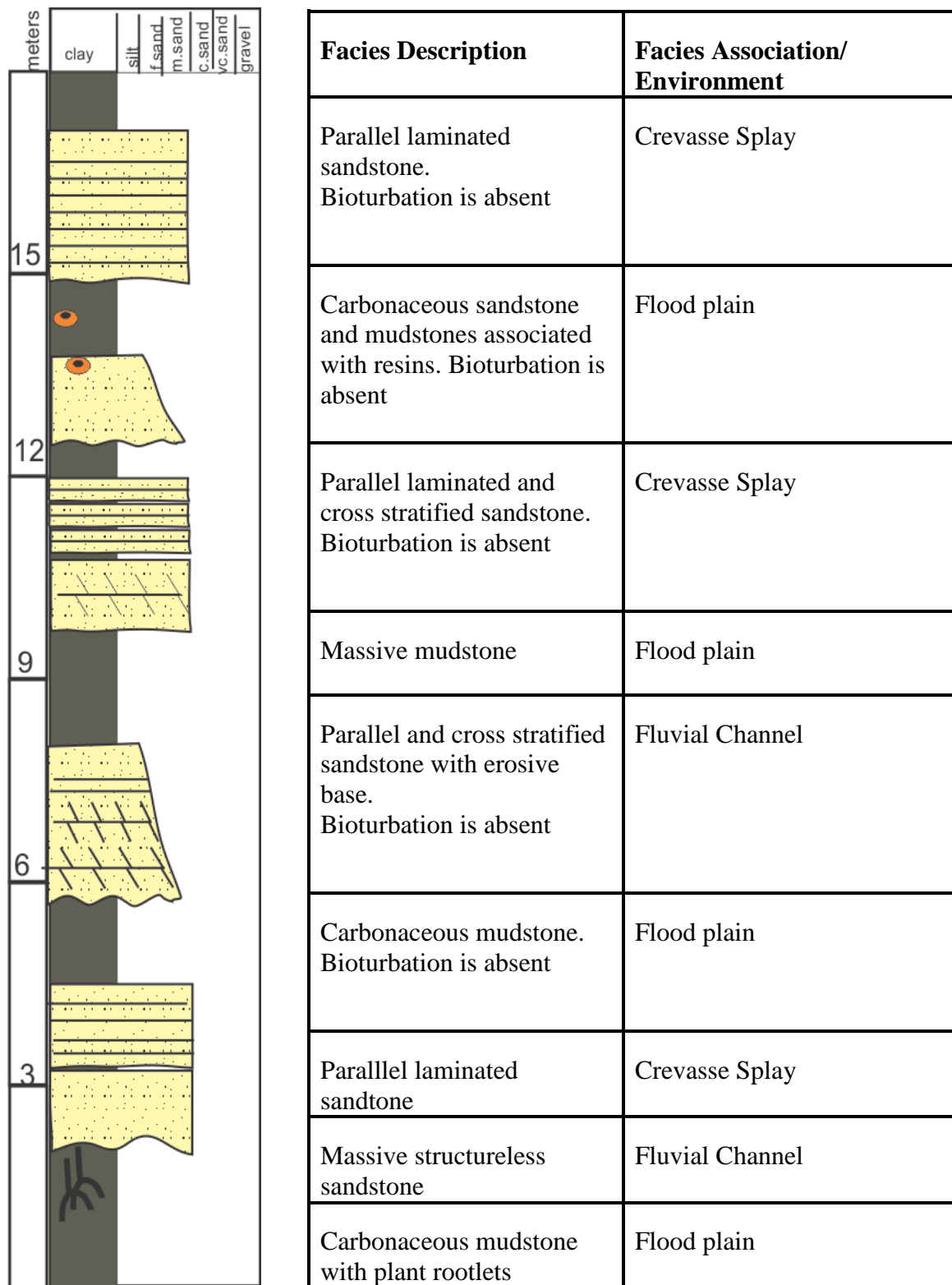


Figure 5.1 Log of Tukau Formation at Sungai Ukong Locality

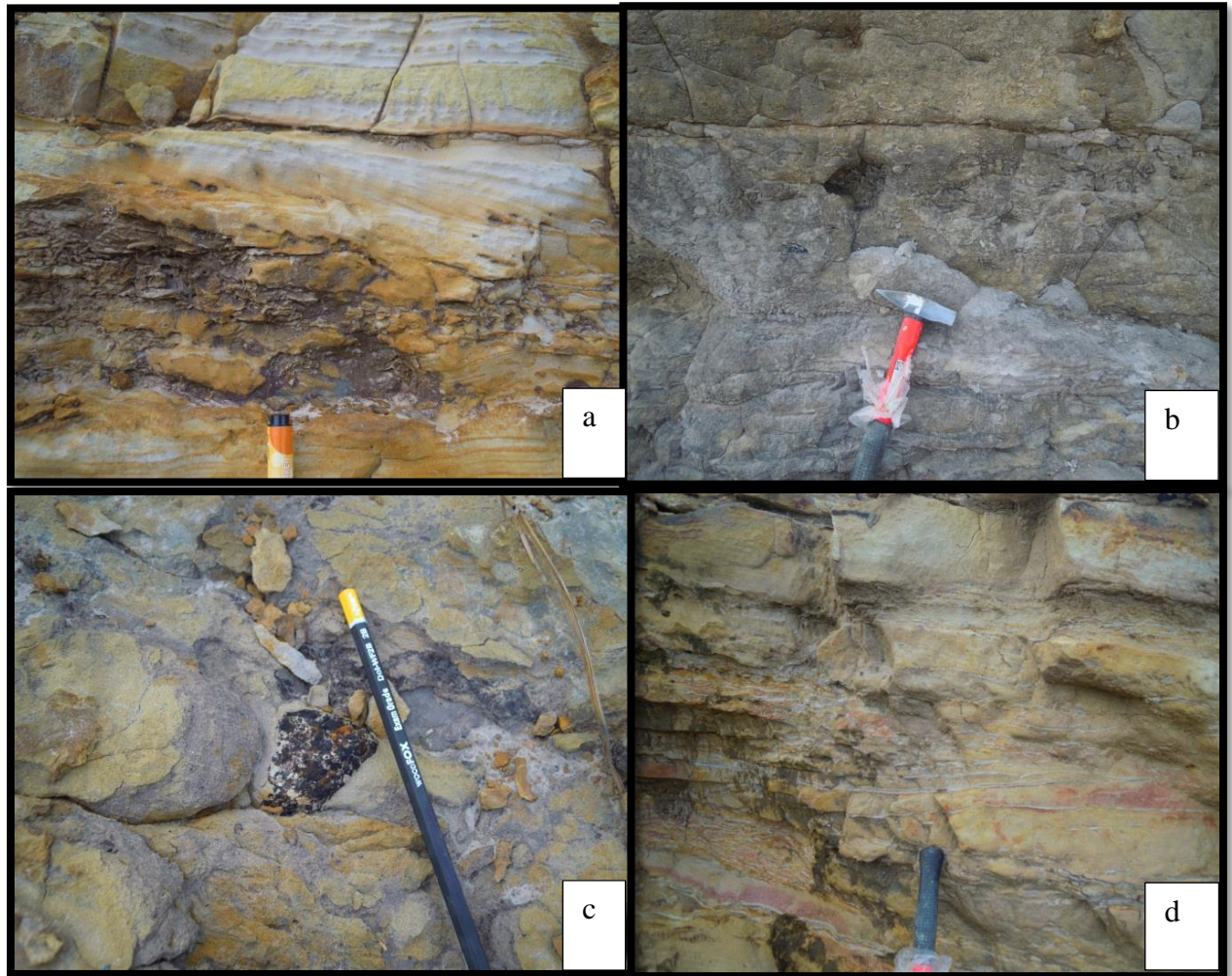


Plate 5.1. Field observation in Tukai Formation at Sungai Ukong : a) Trough cross bed in between parallel laminated sandstone;(b) Carbonaceous mudstone with resin clasts;(c) carbonaceous sandstone with resin clasts; (d) Parallel laminated sandstone interbedded with thick whitish mud.

5.2.2 Miri Formation

The studied Miri Formation is well exposed in the coastal part of Miri-Bitulu coastal road. Nine facies were recognized from the studied Miri Formation and characterized based on the integration of sedimentological and field observations. These facies have been grouped into four facies association which are intertidal, tidal channel, bay head delta, and shore face lithofacies associations.

The identified bay head delta facies association is characterized by massive gravely sandstone facies with abundant lignite clasts. The bay-head delta is the zone where fluvial processes are dominant. As the river flow enters the central lagoon it decelerates and sediment is deposited. The form and processes of a bay-head delta will be those of a river-dominated delta because the tidal effect is minimal and the barrier protects the central lagoon from strong wave energy (Dalrymple et al, 1992). A coarsening-up, progradational succession will be formed, with channel and overbank facies building out over sands deposited at the channel mouth, which in turn overlies fine-grained deposits of the central lagoon. The estuarine association which is made up of tidal channel and intertidal facies associations is characterised by distinct and diagnostic tidal signatures –tidal dune cross bedding with mud draped cosets and foresets including mud couplets, bidirectional (herringbone) cross bedding, rhythmic stratifications, and wave bedding. The tidal estuarine deposits represent the early phase of a significant relative sea level rise, and possibly reflect a southward migration of the paleo Miri shoreline. This phase is also characterized by great wave actions coinciding with abrupt sea level rising, which resulted in the deposition of several tempestites (subtidal sandwaves) at estuary mouth. The shoreface association is represented by hummocky cross stratified sandstones, bioturbated sandstones and associated mudstones. They must have been developed as a result of complete drowning event of the estuarine system which represents the final phase of transgressive system. According to previous works, shallow marine deposits in the south

Miri area represents the upper portion of the exposed Miri Formation, which was possibly deposited during stable high and slowly falling sea level (Tan et al., 1999; Lesslar and Wannier 2001; Abeida et al., 2005).

Based on the facies analysis, trace fossils, and sedimentary structures the environment of deposition of the studied Miri Formation is shallow marine (lower shoreface) to tide dominated estuary. The tide-dominated estuary system of the Miri Formation has been interpreted as open-end tide-dominated estuary includes a variety of sub-environments; tidal channels and bars of estuary mouth, estuarine-upper flow regime sand flat, and restricted tidal flats. The estuarine succession has been interpreted to have been formed during an early transgressive event, representing the lower portion of the investigated Miri section (Tan et al., 1999; Hutchison, 2005). The shallow marine deposits combined to form coarsening-upward, wave-and storm parasequence sets, which were formed during late transgressive event (offshore transition and lower shoreface) which is in agreement with Abeida et al. (2005).

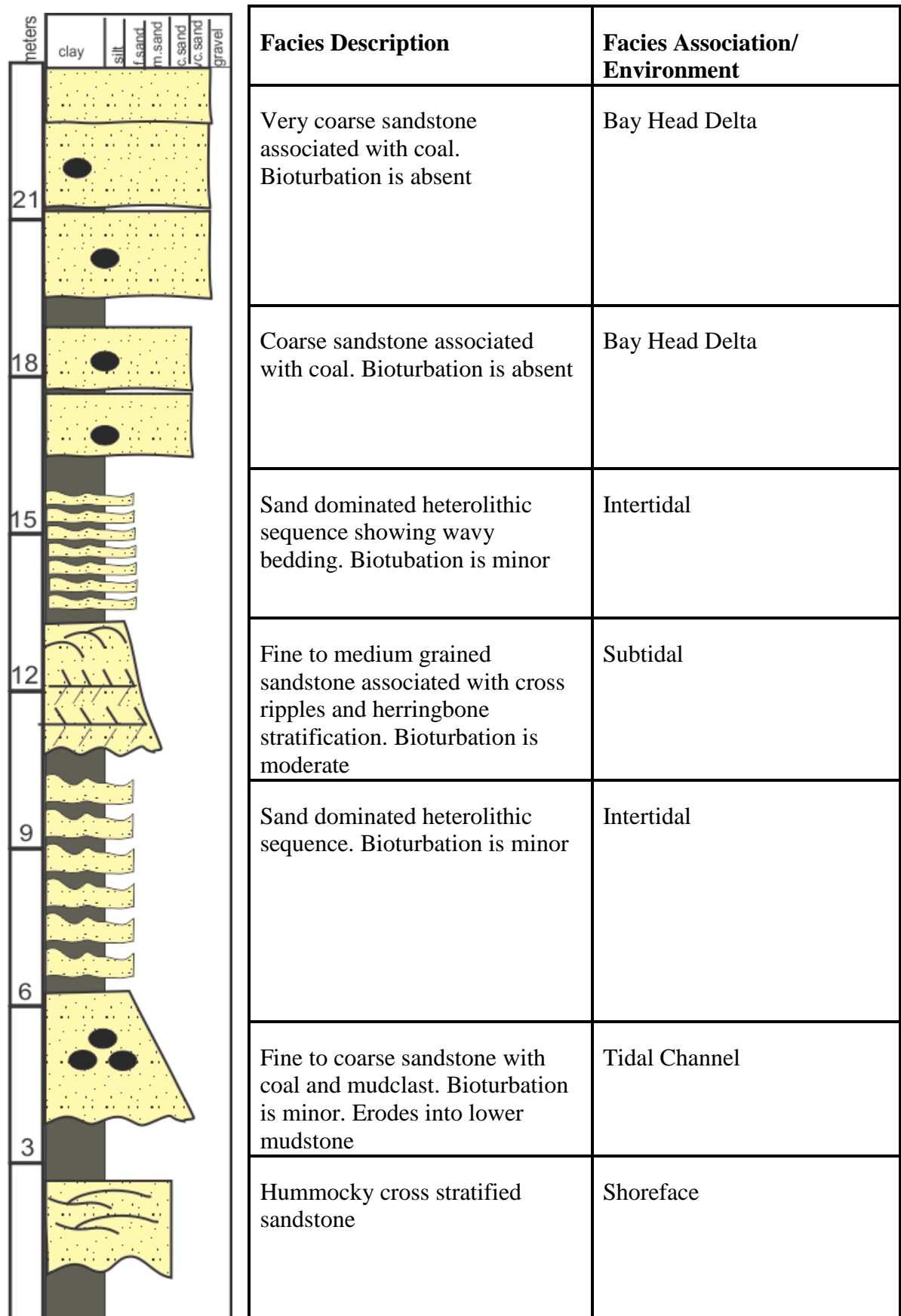


Figure 5.2. Summarised Log of identified facies in the studied Miri Formation at the coastal areas of Miri.

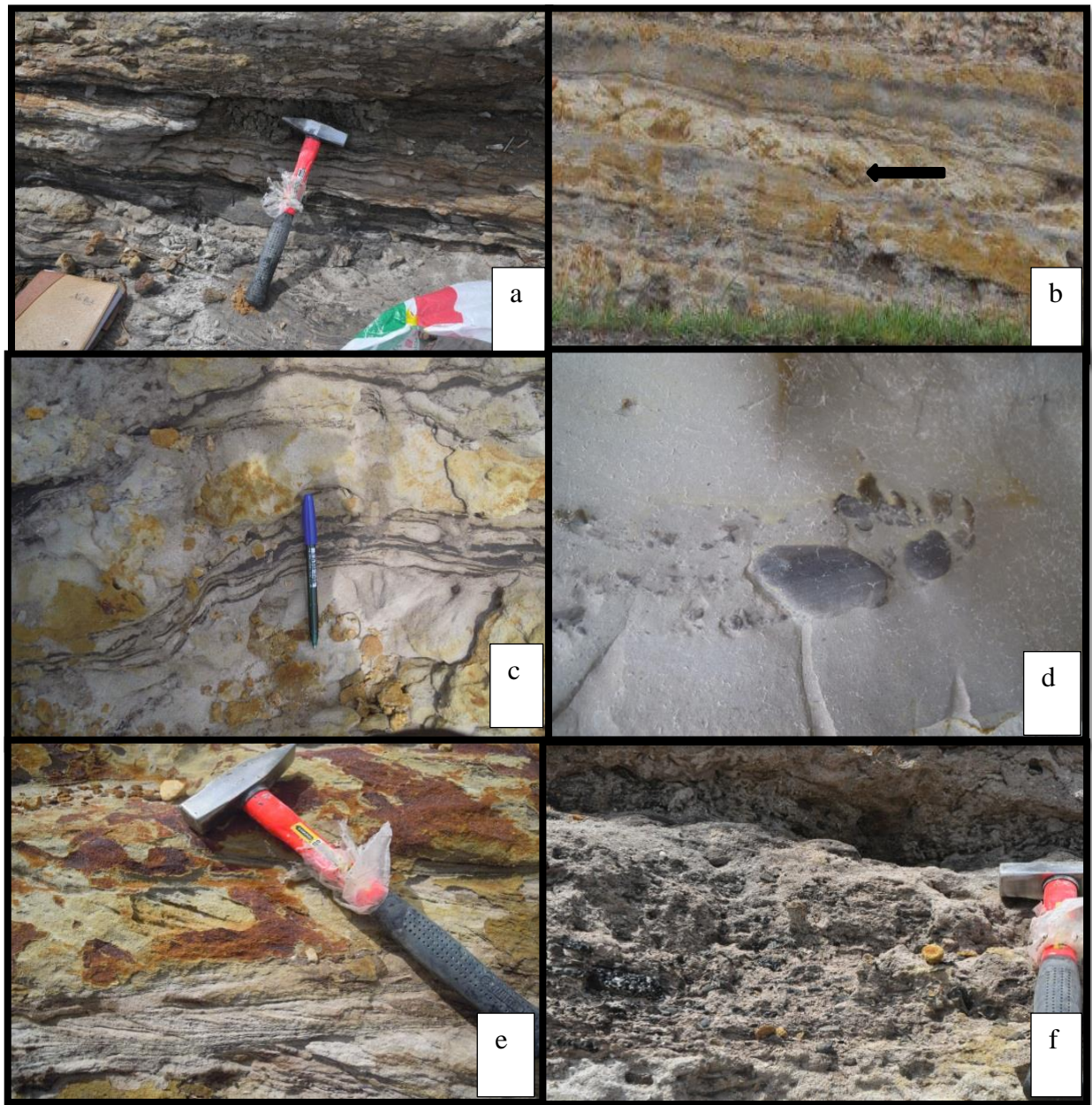


Plate 5.2 Field observation in studied Miri Formation at outcrops along Miri-Bintulu coastal road: a) ripple drift feature in sand dominated heterolithic sequence .b) Hummocky cross stratification in sand bed (highlighted by black arrow).c) mud drapes associated with trough cross bed facies.d) Fine grained sandstone with mud clast in outcrop. e) bi directional current sedimentation displayed by herringbone in studied Miri Formation outcrop.

5.2.3 Lambir Formation

The studied Lambir Formation is located in Lambir Hills National park area and Miri-Bitulu coastal road. Nine lithofacies were identified from the outcrops of the Lambir Formation based on the lithology, sedimentary structures, trace fossils and bed geometry which includes laminated mudstone facies, nodular mudstone facies, carbonaceous facies, heterolithic sequences, and cross laminated facies. These lithofacies has been grouped into intertidal, subtidal, tidal channel and fluvial channel facies associations.

The intertidal mudflat is an environment where there is more deposition of muds through suspension than bedload deposition and is associated with parallel laminated mudstones and nodular mudstones. The parallel laminated mudstone facies is characterized by light grey to light brown mudstone with light grey silty laminations of few centimeters thick. The boundaries of the mudstone and silty laminations are characterized by minor trace fossils. Nodular mudstone facies is grey in color with nodular siderite concretion and lack of bioturbation toward the base. The texture varies from structureless mainly thicker beds, through weakly to strongly laminated very fine sand streaked towards the upper part of the bedding. Siderite concretions within the mudstone layer associates with this facies (Figure 5.3). Siderite concretion formed from the chemical precipitation of iron in a reducing environment. Chemical precipitation of iron and carbonate were preferred in a limited amount of water and oxygen circulation which is isolated for the formation of siderite nodules (Pearson, 2005). It may indicate abundance of iron present in the area. This facies suggest a short-lived phase of low energy condition during which mud and silt were deposited alternately by slack water and current wave action respectively.

The intertidal mix-flat indicates alternation of bedload transport during current flow and the settling of suspended load during periods of slack waters, a short period during high or low tide when the current changes direction makes mud to settle from suspension. This is associated with heterolithic sequences which are characterized by regular

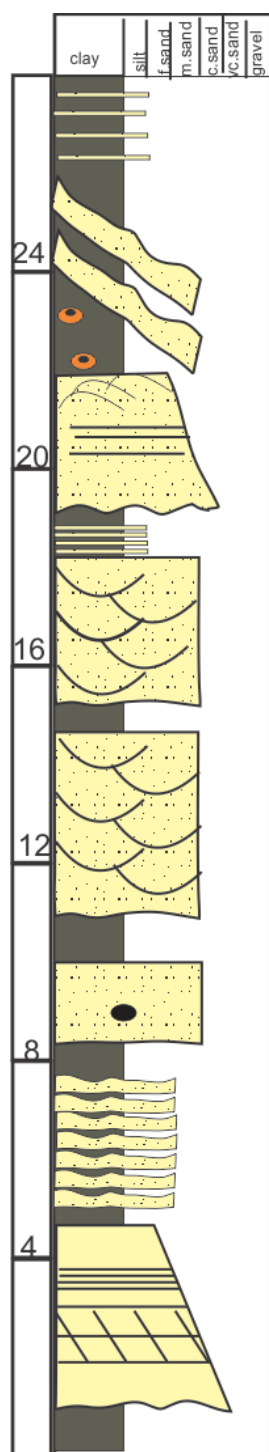
alternation of sandstone and mudstone with wavy bedding. The thickness of the sandstone range from 5cm-30cm, especially in sand dominated heterolithic sequence. The sand dominated heterolithic sequence consists of thin, horizontal fine grained sand and silt layers alternating with clay layers and characterized by dispersed to lamination of organic debris. The sand fraction is more than 50%.

The subtidal environment is associated with parallel laminated sandstones, trough cross stratified sandstones with mud drapes, and ripple cross laminated sandstones. The fining upward parallel laminated sandstone facies sequence is characterized by parallel laminations at the upper part, faint trough cross stratification was observed in the lower part of the sequence. Trace fossils increases from bottom to top. Minor amount of carbonaceous layers are present and occur as thin laminations. Discontinuous mud drapes occur in the sandstone as well. Tiny holes can be found as a result of weathering and the lamination can be wavy due to relief. Trough cross stratified sandstone facies is characterized by light brown, fine –medium grained sandstone with medium scale trough cross bedding, blocky and with a sharp base. The thickness of this facies is up to several meters across. Thin mud and lignite laminations are common throughout with coal clasts. Trace fossils with irregular margins filled with muds or organic matter are abundant. Trough cross bedding are formed by the migration of subaqueous dunes. This bedforms could be deposited by tidal influenced channels at the outer margin. They were deposited during periods when bedload movement ceased. The hardened muds were ripped off from the surface and formed detrital mud clasts when the tidal environment were reactivated. Ripple cross laminated sandstone facies is dominated by climbing asymmetrical ripple lamina and thin muddy lamina. It is often found in the upper section associated with planar and cross laminated beds. The presence of ripple lamination indicated the environment was exposed to seasonal flooding.

Tidal Channel is associated with inclined heterolithic strata characterised by alternating sandstone/mudrock; sandstone beds (25-40cm) thick with ripples, horizontal lamination, wavy bedding, some cross beds; tops of beds can have straight crested symmetrical ripples. Laminated silt beds are (1–10 cm) thick; sandstone makes up 20–90% fine to lower medium sand. Burrows are abundant. Surfaces are inclined up to 12 degrees. Some part of the surfaces is overlain by continuous mud drapes. This suggests deposition in a tidal point bar part of the channel.

Fluvial channel deposit is characterized by massive lunate trough cross bedded sandstone with scouring and erosive base into the underlying mudstones. In some part shows normal grading with no structure observed which might be due to weathering.

The proposed depositional environment for the studied Lambir formation is a tide dominated estuary. An estuary is the marine influenced portion of a drowned valley (Dalrymple et al. 1992). A drowned valley is the seaward portion of a river valley that becomes flooded with seawater when there is a relative rise in sea level. Tide dominated estuaries receive sediment both from river at the head of the estuary, and from the adjacent shelf by tidal currents. The depositional environment interpretation is in good agreement with previous workers (e.g Tan et al., 1999; Kessler, 2000).



| Facies Description | Facies Association/ Environment |
|---|------------------------------------|
| Parallel laminated mudstone. Moderate bioturbation | Intertidal |
| Inclined heterolithic sequence | Tidal Channel |
| Mudstone associated with siderite concretions | Intertidal |
| Cross ripples, parallel laminated sandstone. Bioturbation is intense at the top | Subtidal |
| Cross stratified sandstone with erosive base. Bioturbation is absent | Fluvial channel |
| Carbonaceous sandstone associated with coal | Intertidal |
| Sand dominated heterolithic sequence. Bioturbation is minor | Intertidal |
| Parallel laminated and cross stratified sandstone. Bioturbation is moderate | Subtidal |

Figure 5.3. Log of the studied Lambir Formation outcrop at Lambir Hills National Park area.

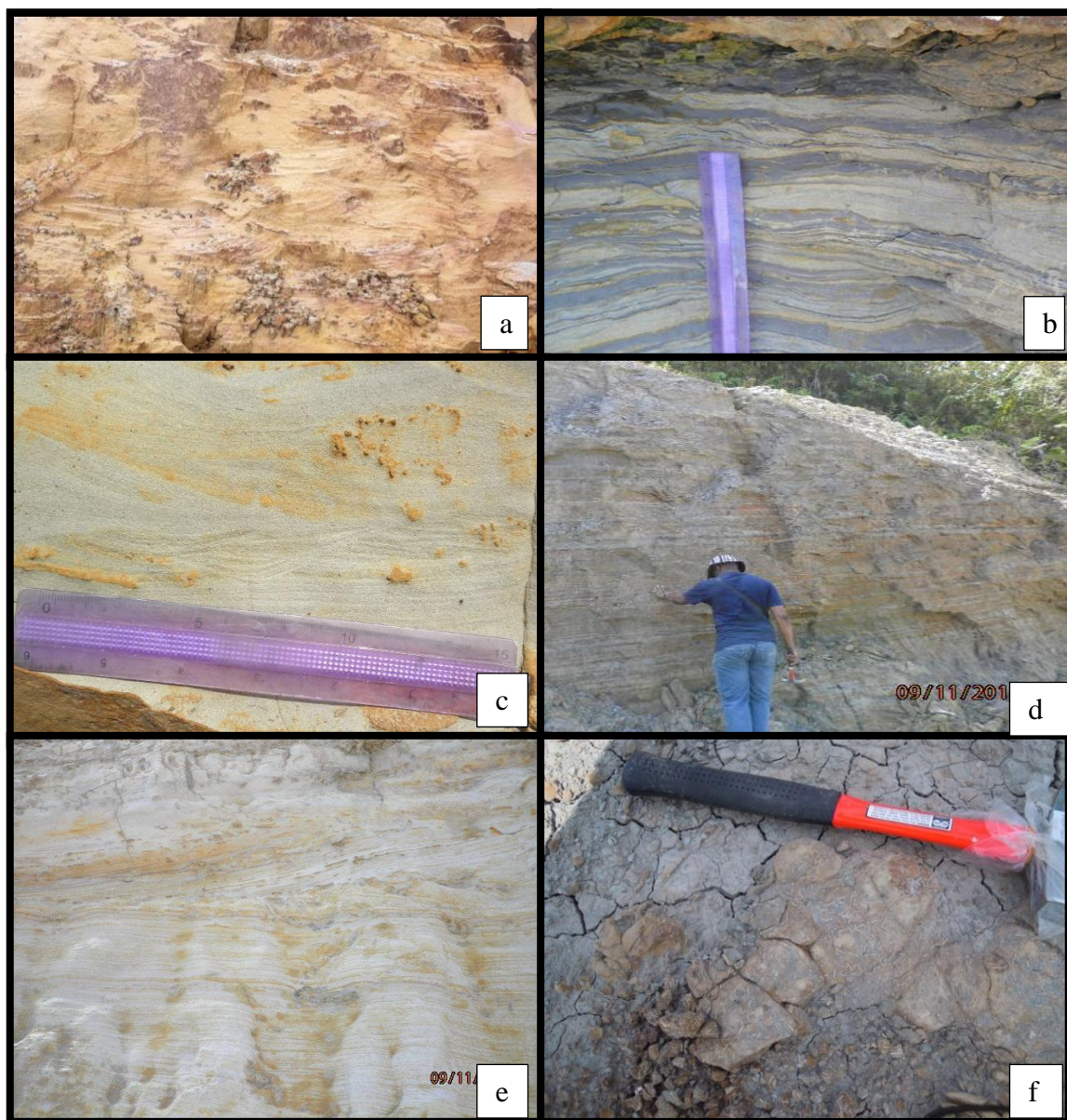


Plate 5.3. Field evidences of the common lithofacies identified at Lambir Hills National Park area (a) lunate trough cross bed in fluvial channel sandstone.(b) Wavy heterolithic sequence (c) ripple cross lamination in sandstone. (d) Parallel laminated mudstone.(e) Trough cross bed with mud drapes. (f) Siderite concretions

5.2.4 Belait Formation

The Belait Formation in western Sabah has been well studied and interpreted as the product of one relatively large deltaic system, the Champion Delta (e.g. Hutchison, 2005; Tan, 2010; Lambiase and Cullen, 2013)

The lithofacies of the Belait Formation consist of sandstones, mudstones and conglomerates associate with coal debris. Batu Luang section includes a wide range of environments in the vertical succession (Fig 5.4) ranging from fluvial channel, distributary channels and tidal flats. The fluvial deposits consist of conglomerate with lenses of sandstone and mudstones. No trace fossils were found in the conglomerates. The poorly sorted clast supported conglomerates with sub-angular to rounded clasts in a matrix of fine sand and mud is also associated with coaly debris (Figure 5.4) . The preserved section above the fluvial deposits as seen in the Batu Luang section is interpreted as deltaic deposits comprising distributary channels, mouth bar sands, interdistributary deposits and prodelta sediments. The prodelta shale associated with coaly debris is capped with tidal flat sediments. Tidal flat deposits is associated with parallel laminated sandstones, sand dominated heterolithics, cross beddings with mud drapes. Distributary channels are associated with cross bedded and parallel laminated sandstones with gravely lag base. Interdistributary bay consists of thick bedded mudstone with thin layer of fine sandstone. Mouth bar is associated with parallel-laminated and massive fine sandstones. Bioturbation is common in the coastal plain deposits.

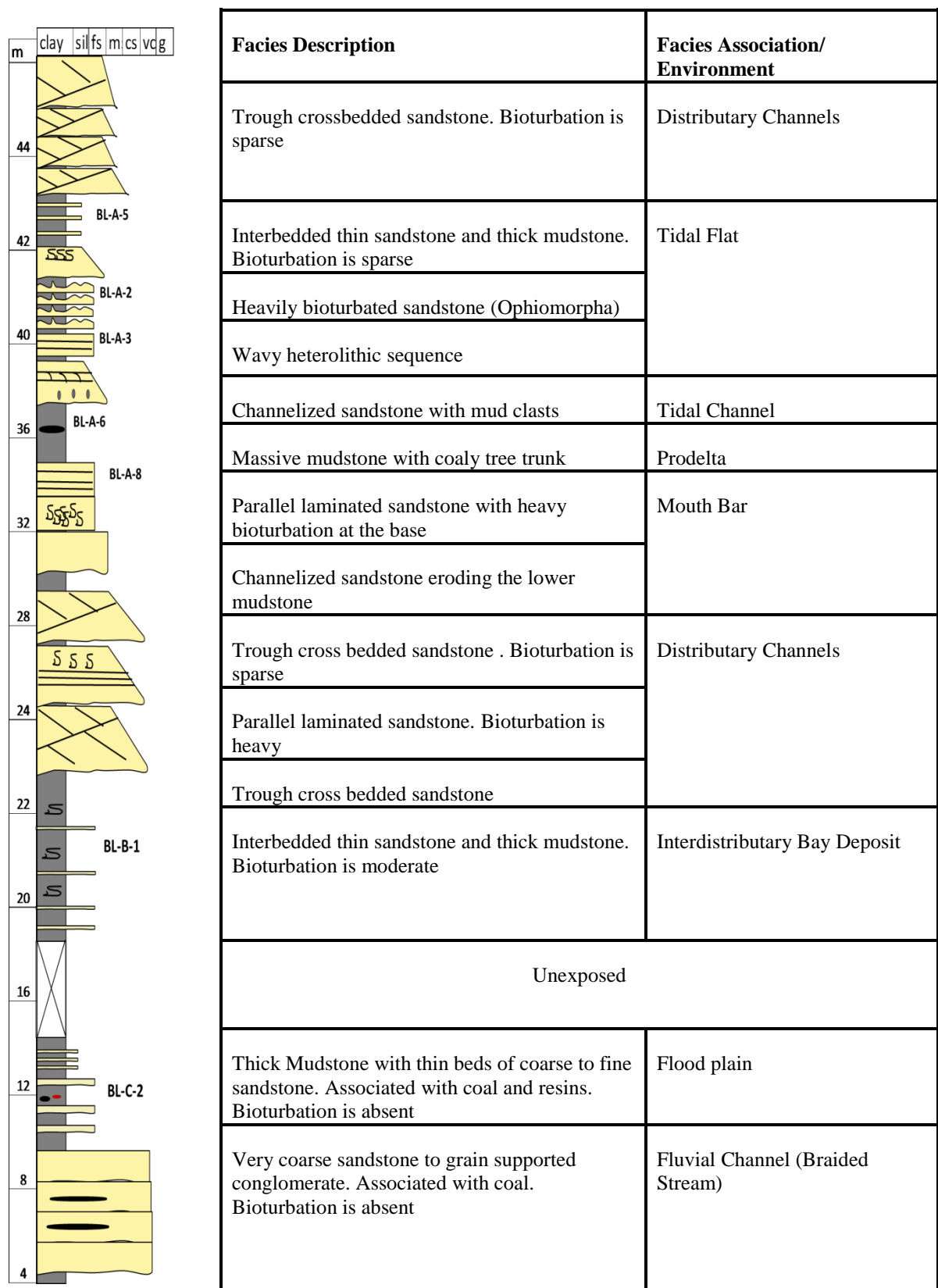


Figure 5.4. Summary Log of Belait Formation in Batu Luang showing wide range of depositional environments

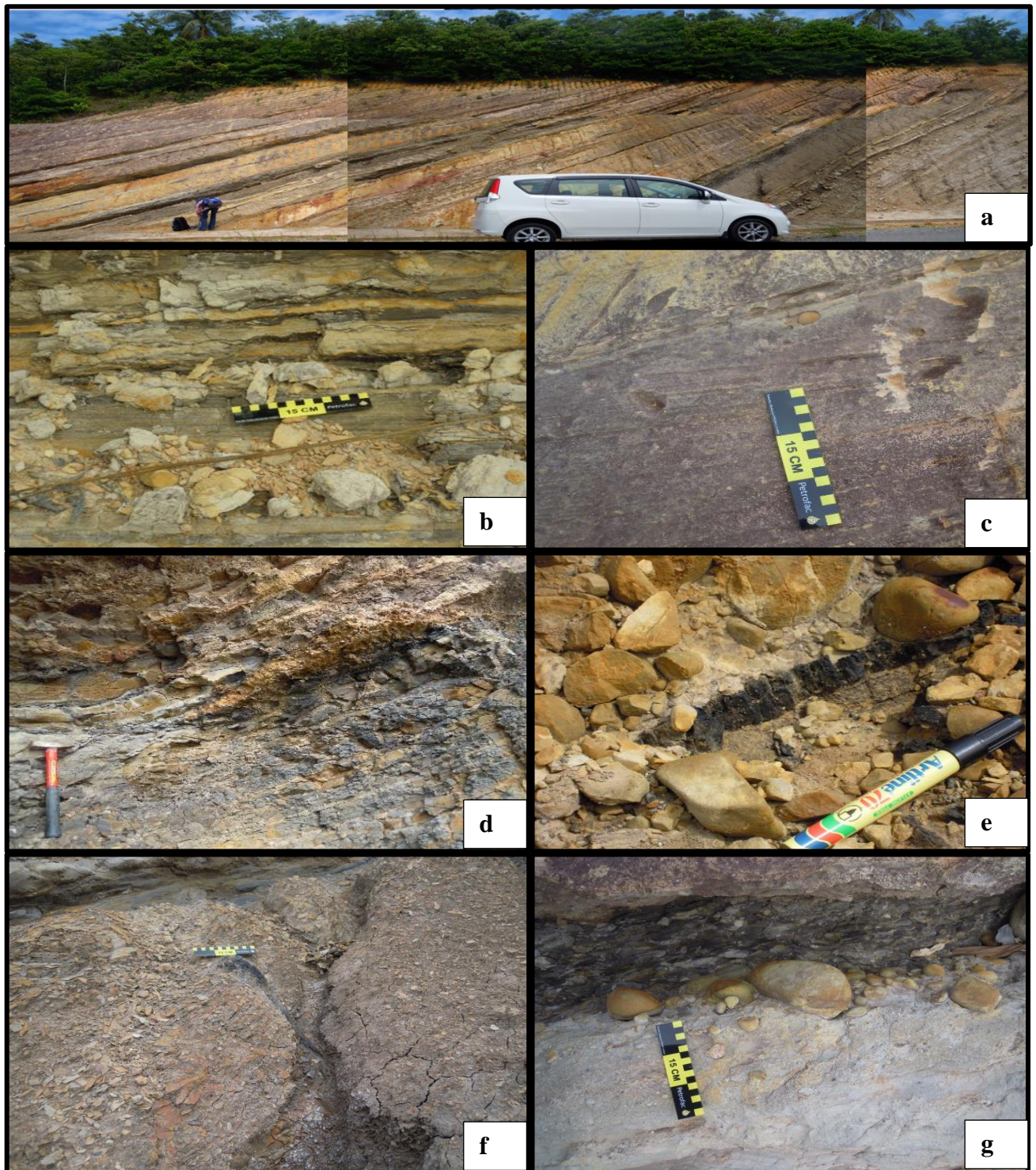


Plate 5.4. Field Observation of Belait Formation in Batu Luang part of Klias Peninsula; a) outcrop view ; b) tidal flat deposits; c) cross bedded distributary channel; d) interdistributary bay deposit; e) braided stream deposit with coal lenses; f) prodelta deposit (associated with allochthonous tree trunks) ; g) gravelly base of distributary channels.

5.2.5 Meligan Formation

There are many descriptions for the typical Meligan Formation (e.g Hutchison, 2005; Tan, 2010). For this study, Meligan Formation was identified based on description with reference to Hutchison (2005). The characteristics of Meligan Formation was discussed in Section 2.2.2.3.

The studied Meligan Formation outcrop that is exposed in major quarries in Sipitang area consists of massive sandstones and shales, laminated mudstones, organic rich-laminated sandstones and mudstones associated with siderite concretions. These facies are interpreted to be associated with lower delta plain. There is a suspected facies transition from the shallow marine Setap Shale to Meligan Formation which is characterized by onlapping and change in dip direction as observed in Sabah Forestry Quarry (Fig.5.5). This facies transition in the Early Miocene has been well described by previous workers (e.g Hall, 2013; Lambiase and Cullen, 2013).

5.2.6 Temburong Formation

The Temburong Formation commonly referred to as the muddy facies transition of the West Crocker Formation is exposed in the Sipitang –Tenom areas of Sabah (Hutchison, 2005). The outcrops are not well preserved due to the low resistance shales. The beds are steeply dipping and calcite veins are common, thus suggests brittle deformation in the Temburong Formation.

The lithofacies consists of dominantly thick shale and interbedded with thin sandstones. This section shows less turbiditic structure. The prevalent Bourma Sequences are Td and Te (massive mudstone and parallel laminated fine sandstones). This rock sequence is interpreted as a distal (outer lobe) of a submarine fan. The deep water environment interpretation is also supported by the presence of *Paleodictyon* ichnofossils and other neritics burrow tracks (Plate 5.6).

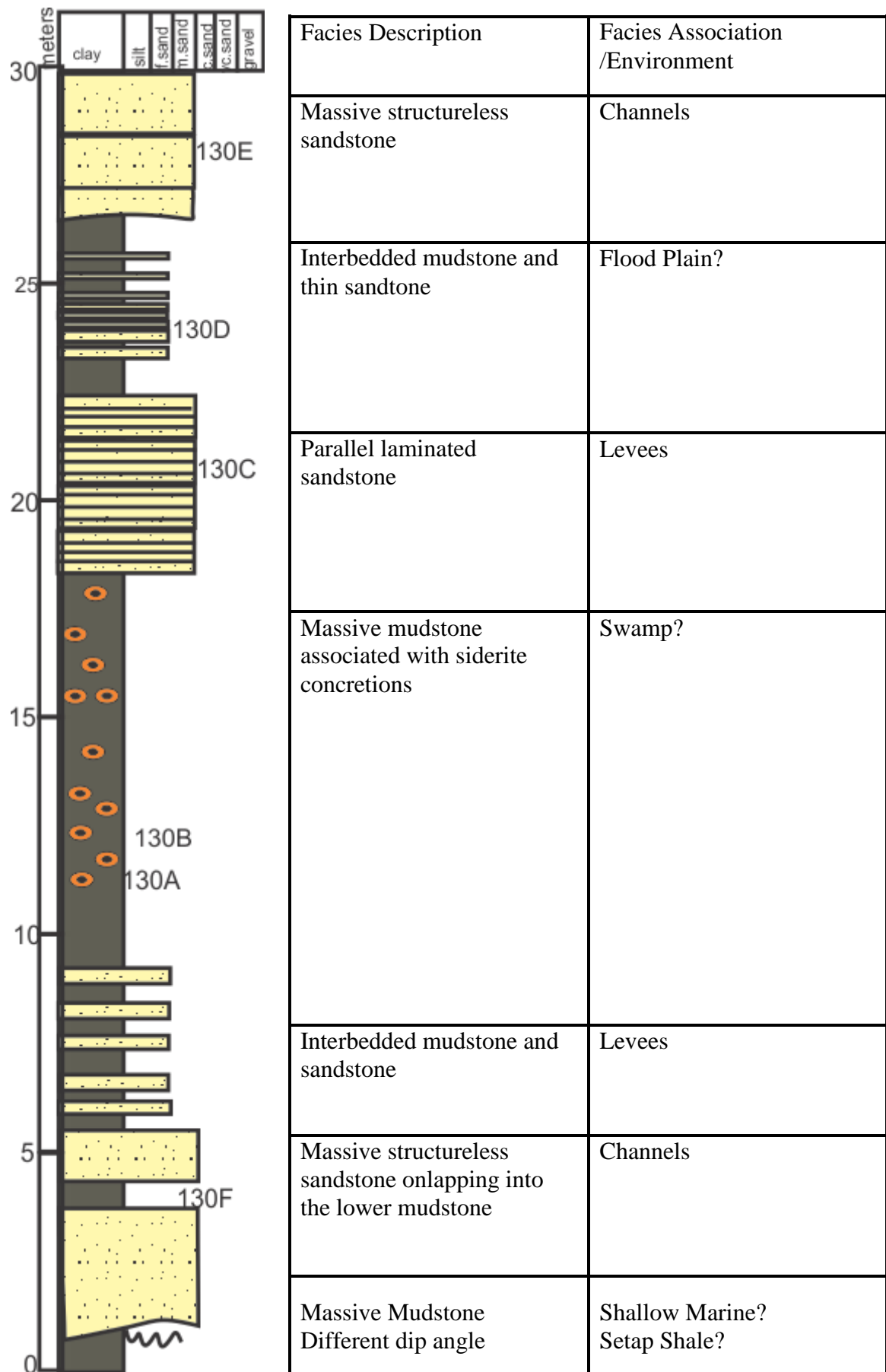


Figure 5.5 Log of Meligan Formation/Setap Shale? at SFI quarry in Sipitang.

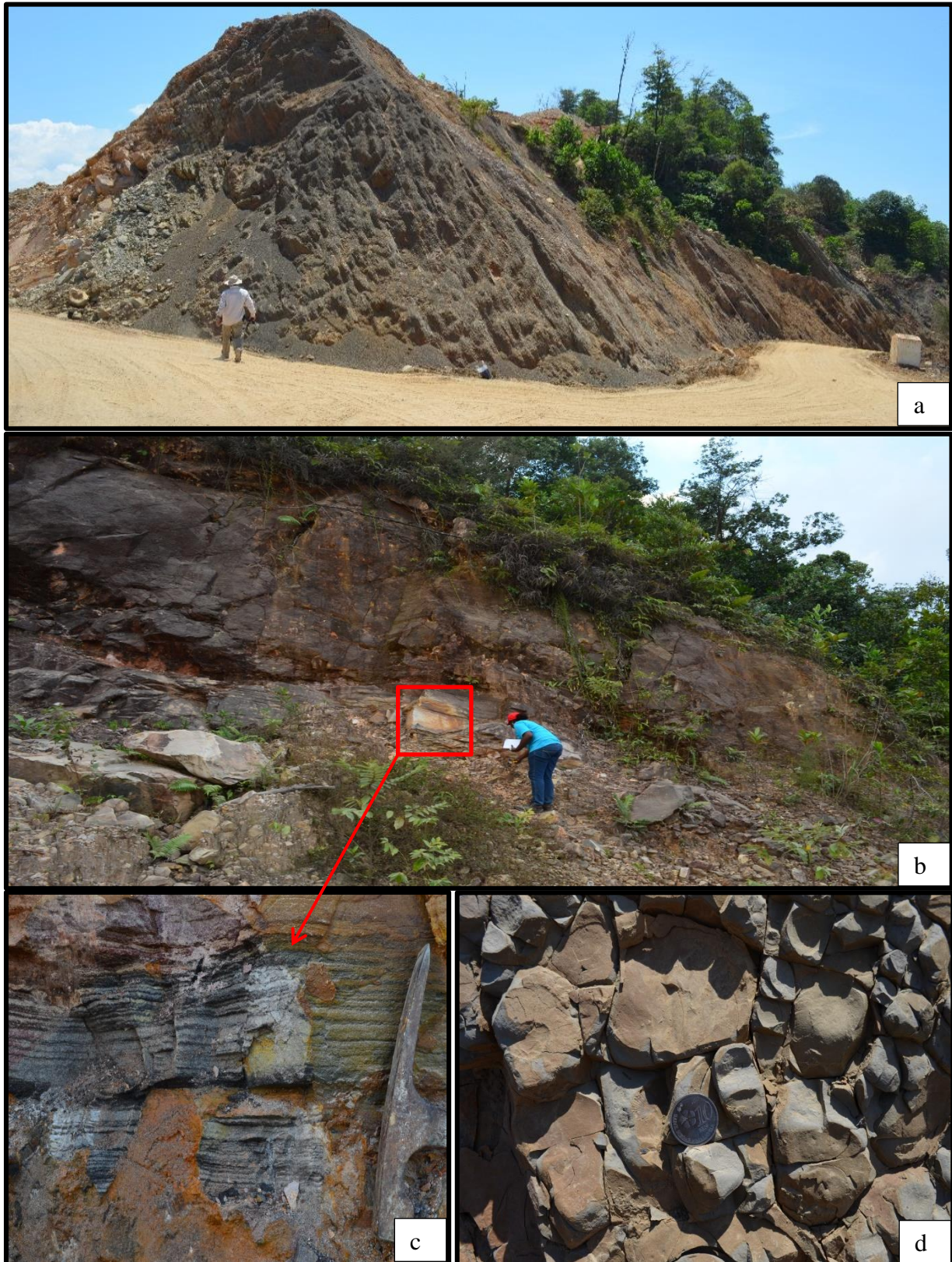


Plate 5.5. Field Observation of Meligan Formation in Sipitang area. a) Outcrop view of steeply dipping sandstone and mudstones beds; b) laminated sandstone with abundant carbonaceous materials (full view); c) laminated sandstone with abundant carbonaceous materials (close view); d) mudstone with abundant sideritic concretions.



Plates 5.6. Field observation in Locality (137) Sipitang-Tenom road representing the Temburong Formation; a) Outcrop view of steeply dipping thick shale and thin sandstone beds; b) laminated sandstone; c) *Paleodictyon* ichnofossils and burrows tracks bed; d) vertical and horizontal burrows in shale beds; e) brittle deformation in the shales.

5.2.7 West Crocker Formation

The sedimentary records of the West Crocker Formation were well recorded by e.g. William et al. (2003), Crevello et al.(2007), Lambiase et al. (2008), Jackson et al. (2009) Zakaria et al.(2013). The outcrops under current investigation are selected exposures in Kota Kinabalu and Sipitang.

The logged section in the Kota Kinabalu area popularly called the Kingfisher outcrop (Nizam et al., 2008; Jackson et.al. 2009) is over 100 m of steeply dipping medium to thick-bedded sandstone and mudstone that are exposed on the cut slopes of this outcrop. The sandstone facies is predominantly fine grained, though some are medium to coarse and even pebbly (granular) in places. Many have sharp tops and bases. Internally they appear to be structureless, though faint consolidation lamination. Rip-up clasts are also common, indicative of the high energy deposition flows. Bouma Sequence Ta, Tb, Td and Te are common. The most spectacular feature of this outcrop is the occurrence of slump intervals, consisting of several large sandstone blocks “floating” in a muddy matrix. The sandy nature of the succession and the slump features suggest that the succession represents part of mass-transport complex in a proximal submarine fan (mid-fan). The slump features was also observed in the Sipitang areas which supports the wide occurrence and extension of the mass transport complex in Western Sabah onshore and offshore areas as reported by Algar et al. (2011).

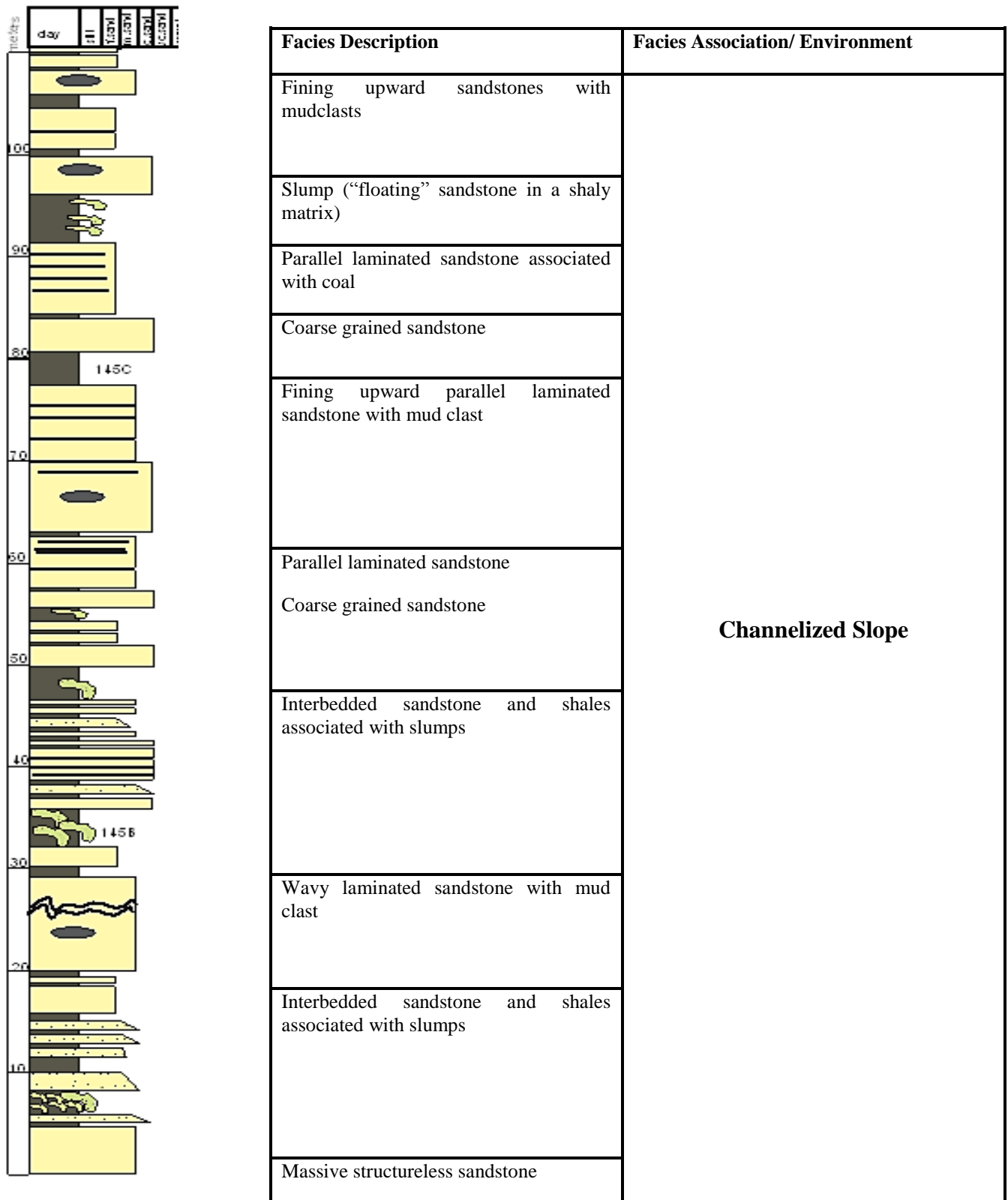


Figure 5.7. Sedimentary log of West Crocker Formation in Locality (145) KK, popularly known as the kingfisher outcrop.

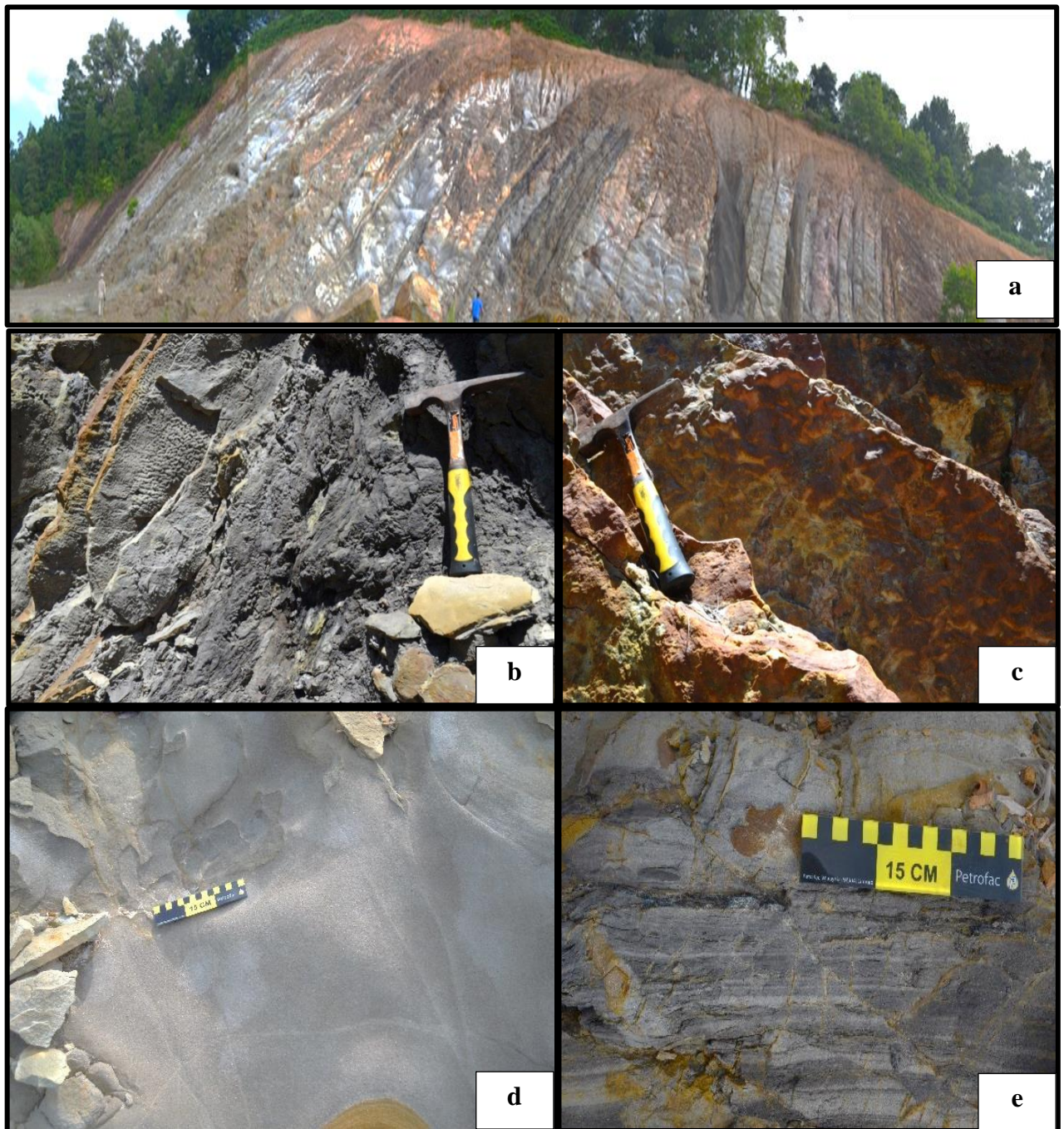


Plate 5.7. Field observation of West Crocker Formation, a) outcrop view of the sandy dominated turbiditic sequences in KK; b) slump deposits; c) flute marks at the base of sandstone in Sipitang ; d) massive structureless sandstone bed typical of high density turbidites; e) laminated sandstone facies associated with resinous coaly layers in KK.

5.2.8 Undifferentiated Formation

The Batu Linting section shows deep water sequences and was previously reported by Tan (2010) to be Meligan Formation. Thus, the field observation of the current study does not fit the well-known fluvio-deltaic to shallow marine Meligan Formation (e.g. Hutchison, 2005). The section is characterized by alternating thick, fine to medium sandstones which grade upward from medium grained sand to parallel laminated sand which contains abundant carbonaceous material and often capped with wavy beds (Plate 5.8b). Abundant deep water trace fossils including *Paleodictyon* and *Nereites* ichnofossils were found in the section. Allochthonous coal debris are present in the medium grained sandstones. Although, the lithofacies and ichnofossils assemblages suggests deep water environments which may likely relate to the Temburong or West Crocker formation, the geochemical signature is quite different from the above mentioned submarine fan sequences which generates lots of uncertainties in assigning this sequence to a specific formation. The characteristics are well discussed in the subsequent sections.



Plate 5.8. Field Observations of the undifferentiated Formation; a) steeply dipping sandstone beds ; b) close up view of sandstone beds with laminations; c) Ichnofossils indicative of deep water environment; d) coaly debris within the sandstones.

5.3 Organic Petrographic Data

The organic petrological studies performed include maceral analysis, vitrinite reflectance and visual kerogen typing (palynofacies analysis). This study was carried out to evaluate the quality and thermal maturity of organic matter using microscopic observation. The integration of petrographic with geochemical data are discussed in the next chapter.

5.3.1 Maceral Analysis

Maceral analysis was carried out on selected samples to investigate the occurrence and type of organic matter present in the deltaic and submarine fan sequences.

Reflected light microscopy indicates that the deltaic sequences contain phytoclasts (dispersed organic matter) and mineral matter (Plate 5.9). The phytoclasts is made up predominatly of vitrinitic material with low –common occurrence of liptinite and inertinite macerals (Table 5.1). The liptinite was identified by their different fluorescence intensity in ultra violet light and their morphological characteristics (Plate 5.9 c-f). The common liptinites in the studied deltaic sequences samples are cutinite, suberinite, sporinite and bituminite, which were characterised by bright yellow to yellow and orange fluorescence (Plate 5.9 c-f). Resinite, bituminite and amorphous organic matter is the common liptinite maceral in the submarine fan sequences (Plate 5.10 c-g). The Temburong formation samples shows weaker fluorescence compared to the intense fluorescing samples from the undifferentiated formation in Batu Liting which suggests high level of thermal maturity of the Temburong Formation.

Table 5.1. Organic petrology results including palynofacies (under transmitted light (%), kerogen composition (under reflected light (%)) and thermal maturity indicators (vitrinite reflectance measurements (%Ro

| Formation | Samples | %Ro | Palynofacies (%) | | | Kerogen composition (%) | | | |
|----------------------------|-------------|------|------------------|-----|------|-------------------------|-----|-------|-----------|
| | | | Phy | AOM | Paly | Vit | Lip | Ine | Min. Mat. |
| Deltaic Sequences | | | | | | | | | |
| Lambir | L-02-SS | 0.41 | 86 | 4 | 10 | 33 | 10 | 2 | 55 |
| | L-03-SH | 0.39 | 90 | 3 | 7 | 30 | 5 | 5 | 60 |
| | L-05-SS | 0.42 | 89 | 2 | 9 | 33 | 5 | 2 | 60 |
| | L-07-SH | 0.45 | 89 | 5 | 6 | 32 | 6 | 2 | 60 |
| | L-14-SH | 0.41 | 89 | 4 | 7 | 35 | 5 | 5 | 55 |
| Miri | M-01-SH | 0.48 | 88 | 4 | 8 | 25 | 3 | 10 | 62 |
| | M-03-SH | 0.42 | 86 | 4 | 10 | 25 | 5 | 5 | 65 |
| | M-05-SH | 0.43 | 87 | 4 | 9 | 30 | 3 | 7 | 60 |
| | M-08-SH | 0.41 | 92 | 2 | 6 | 35 | 5 | 5 | 55 |
| | M-11-SS | 0.45 | 88 | 3 | 9 | 35 | 5 | 7 | 53 |
| Tukau | T-01-SS | 0.41 | 88 | 2 | 10 | 30 | 5 | 2 | 63 |
| | T-03-SH | 0.45 | 88 | 2 | 10 | 35 | 5 | 3 | 62 |
| | T-04-SH | 0.42 | 90 | 2 | 8 | 35 | 5 | 5 | 60 |
| | T-08-SH | 0.43 | 86 | 4 | 10 | 35 | 3 | 5 | 57 |
| | T-10-SS | 0.42 | 83 | 6 | 9 | 40 | 5 | 5 | 50 |
| Belait | BL-A2-SH | 0.46 | 86 | 6 | 8 | 25 | 5 | 5 | 55 |
| | BL-A3-SH | 0.44 | 86 | 6 | 8 | 30 | 5 | 10 | 55 |
| | BL-A5-SS | 0.45 | 88 | 4 | 8 | 30 | 5 | 7 | 58 |
| | BL-A6-SS | 0.46 | 90 | 3 | 7 | 20 | 5 | 5 | 60 |
| | BL-A7-SH | 0.43 | 89 | 4 | 7 | 20 | 5 | 5 | 60 |
| | BL-B1-SH | 0.44 | 86 | 4 | 10 | 22 | 5 | 5 | 68 |
| | BL-C2-SH | 0.45 | 84 | 6 | 10 | 30 | 3 | 10 | 57 |
| Meligan | ME-130B-SH | 0.87 | 88 | 4 | 8 | 20 | 5 | 5 | 70 |
| | ME-130C-SS | 0.74 | 86 | 6 | 8 | 25 | 5 | 5 | 65 |
| | ME-130F-SH | 0.69 | 88 | 4 | 8 | 25 | 5 | 5 | 55 |
| | ME-133A-SS | 0.72 | 88 | 4 | 8 | 30 | 5 | 5 | 60 |
| | ME-134A-SH | 0.71 | 88 | 2 | 10 | 30 | 10 | 5 | 55 |
| Submarine Fan Sequences | | | | | | | | | |
| Temburong | TE-137A-SH | 1.08 | 60 | 35 | 5 | 15 | 4 | 1 | 80 |
| | TE-137B-SS | 1.14 | 62 | 33 | 5 | 5 | 3 | 2 | 83 |
| | TE-140-SH | 0.99 | 55 | 35 | 10 | 15 | 4 | 1 | 80 |
| West Crocker | WC-129B-SH | 0.79 | 58 | 35 | 7 | 25 | 7 | 1 | 67 |
| | WC-129E-MTD | 0.82 | 48 | 40 | 12 | 30 | 15 | 1 | 54 |
| | WC-135B-SS | 0.89 | 60 | 33 | 7 | 35 | 10 | 2 | 53 |
| | WC-144A-MTD | 0.92 | 47 | 43 | 10 | 30 | 15 | trace | 55 |
| | WC-145B-MTD | 1.14 | 46 | 42 | 12 | 35 | 15 | trace | 50 |
| Undifferentiated Formation | UD-01-SS | 0.46 | 65 | 30 | 5 | 30 | 10 | 5 | 55 |
| | UD-02-SS | 0.49 | 55 | 40 | 5 | 20 | 10 | 5 | 60 |

%Ro: vitrinite reflectance, Phy: phytoclast, AOM: amorphous organic matter, Paly: palynomorphs (spores+pollen), Vit: vitrinite, Lip: liptinite, Ine: inertinite, Min. Mat.: mineral matter

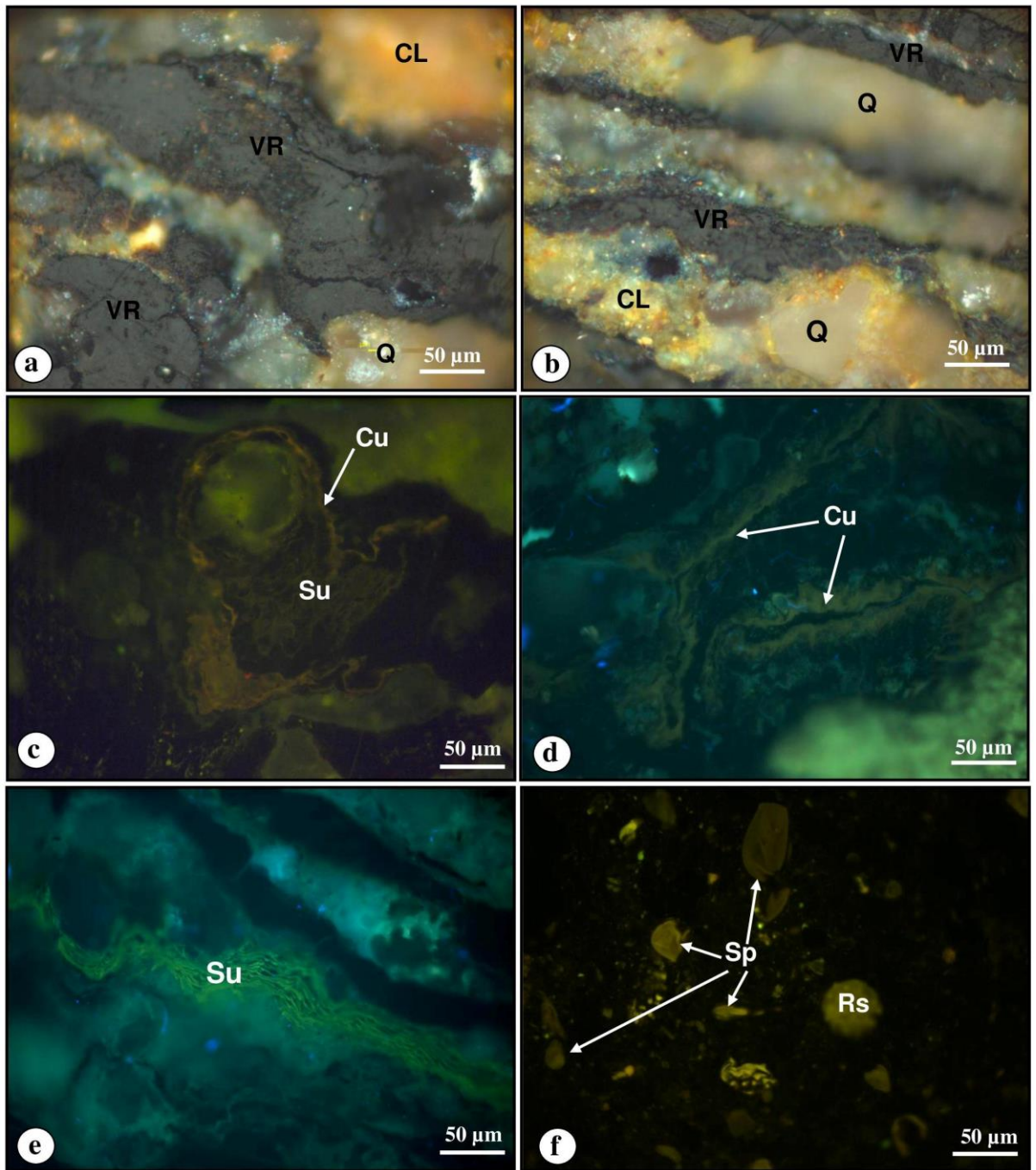


Plate 5.9. Photomicrograph of common maceral constituents of the studied northwest Sarawak formations. (a) and (b) vitrinite phytoclasts (VR) associated with Quartz (Q) and clay minerals (CL) under white light; (c) Yellow to greenish fluorescing cutinite (Cu) associated with greenish fluorescing suberinite (Su); (d) Greenish fluorescing cutinite (Cu); (e) Greenish fluorescing suberinite (Su); (f) Yellow fluorescing sporinite (Sp) associated with resinite (Rs).

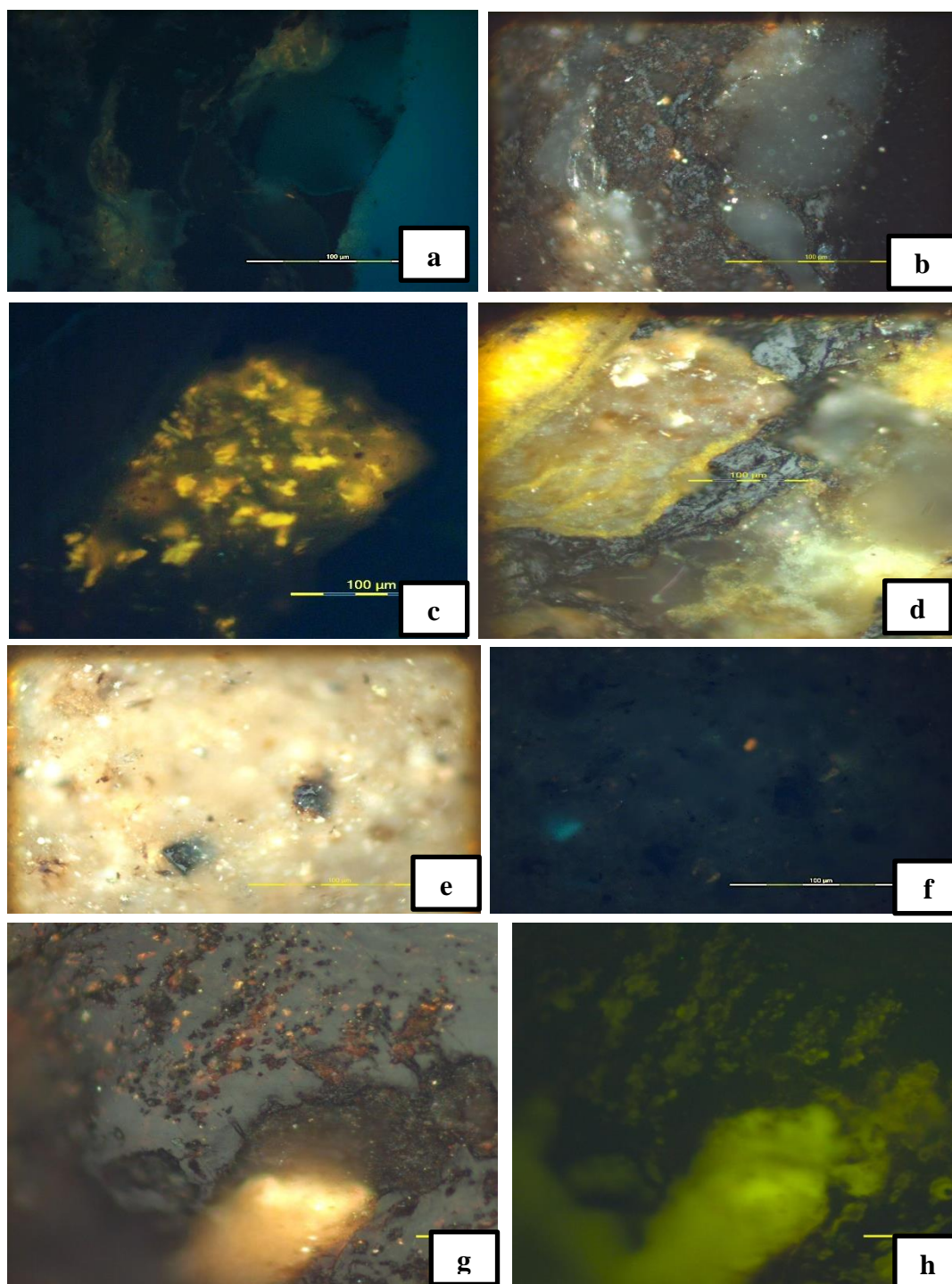


Plate 5.10. a) and b) weakly fluorescing bitumen stain around vitrinite rim in Meligan sample c) and d) amorphous organic matter in Slump sample from West Crocker Formation, e) and f) sparse vitrinite phytoclast and weakly fluorescing resinite in the Temburong Formation sample, g) and h) Intense fluorescing bituminite in the undifferentiated deep water sample from Klias Peninsula.

5.3.2 Palynofacies analysis

Combaz (1964) originally defined the term palynofacies to encompass the total complement of acid-resistant organic matter recovered from a sediment or sedimentary rock by palynological processing techniques, using hydrochloric acid and hydrofluoric acid, as seen under a microscope. Powell et al. (1990) redefined the term as “a distinctive assemblage of palynoclasts whose composition reflects a particular sedimentary environment”. Tyson (1995), however, added that apart from reflecting a specific set of environmental conditions it is also associated with a characteristic range of hydrocarbon-generating potential.

The palynofacies classification terms used here follows that of Tyson (1995): phytoclasts, opaques, (black debris), Amorphous organic matter (AOM) and palynomorphs. Phytoclasts include structured terrestrial plants fragments such as cuticles, wood tracheid and cortex tissues. The structure may be displayed, only faintly discernible or suggested, sometimes merely by the fact that it is a membrane or filament that has a clearly defined, non-amorphous outline (Batten, 1996). They are mainly derived from terrestrial sources and they show high concentrations in places close to the parent flora, near the mouth of rivers and in oxidizing conditions. Opaque (black debris) are made up of oxidized brownish black to black coloured woody tissues including charcoal. They are produced as a result of oxidation and natural pyrolysis on terrestrial plant tissues. AOM includes all particulate organic materials that appear structure less with no cellular structure preserved. They appear in different forms and are referred to as fluffy, granular, fibrous, or membranous. AOM normally dominates sediments deposited in oxygen deficient conditions and the increase of AOM indicates reducing conditions, distal dysoxic – anoxic shelf and high marine productivity (Tyson, 1995; Batten, 1981, 1996).

Quantitative analysis of palynofacies in the studied formations is shown in Table 5.1. From the varying characters and distribution of the organic matter in the studied

sequences, four palynofacies types have been identified. Variation in the palynofacies types and composition of the palynomorphs assemblage may provide information regarding the depositional environments which is discussed in Chapter 6.

Palynofacies type I is dominated by structured phytoclast with an average relative abundance of more than 80% structured and unstructured phytoclasts and an average content of 5% for AOM. Palynomorphs are with an average of 10%. This assemblage is related to proximal depositional conditions, with the main controlling factor being the short transport of the particles. The phytoclasts are well preserved, translucent and structured (mainly cuticles and tracheid). Palynomorphs though few, are mainly well preserved spores and some pollen. This palynofacies type is common in the deltaic sequence. Palynofacies type II is dominated by phytoclast more than 60% consisting of dominant opaque, lesser translucent phytoclast and AOM more than 30% Palynomorphs are less than 10%. This occurs in most samples from Temburong and West Crocker Formation.

Palynofacies type III is mostly made up of AOM and phytoclast in relative abundance. Opaque phytoclasts are more abundant than the translucent phytoclasts in this type. Palynomorphs are less than 15% with minor occurrence of dinoflagellate. The major type of AOM is possibly resins and this occurs in the slump facies within the West Crocker Formation.

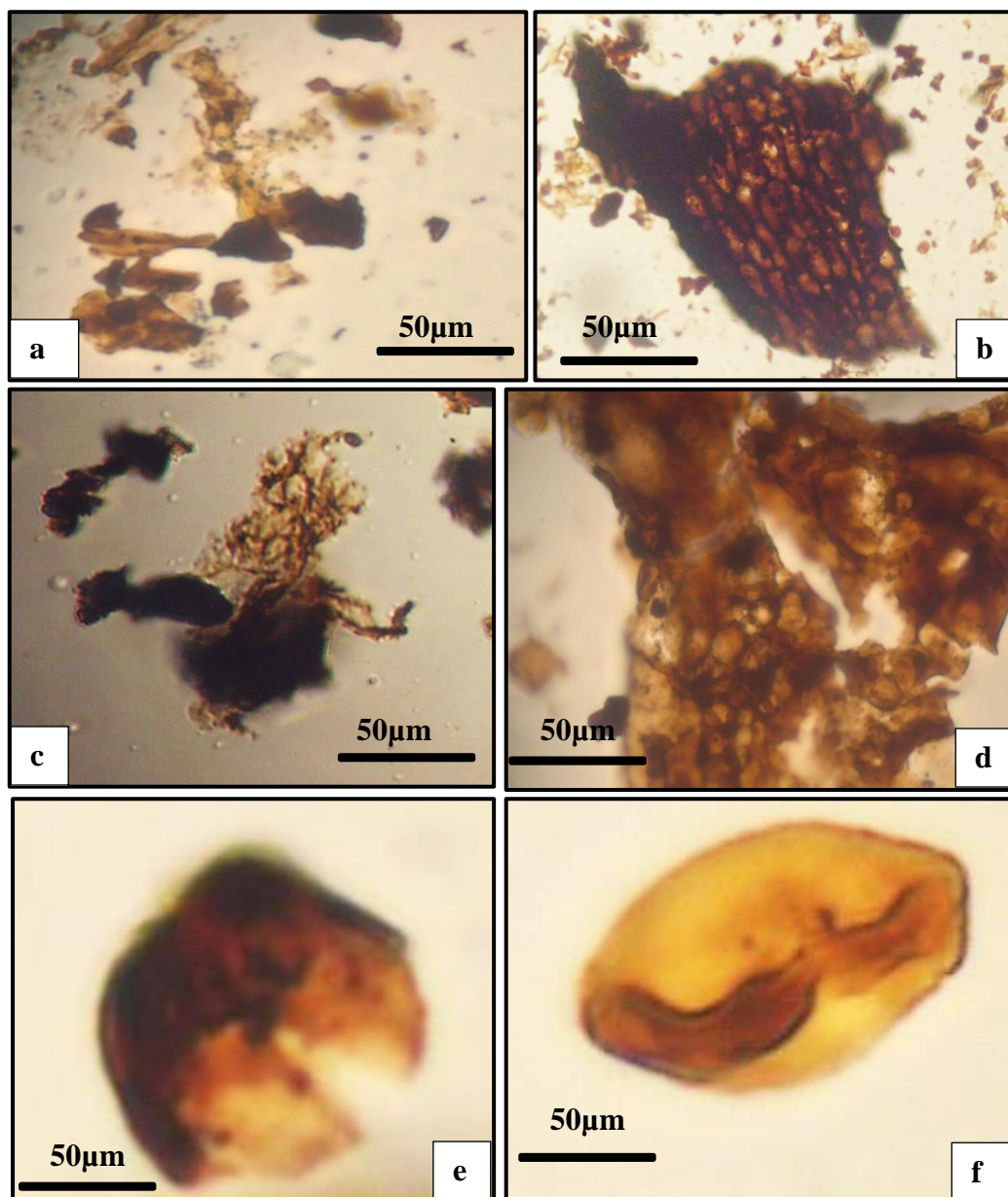


Plate 5.11. Photomicrograph of common palynofacies in the studied formations. a) opaque and translucent phytoclasts; b) structured woody phytoclasts; c) dinoflagellate macerated from submarine fan deposits; d) amorphous resinous organic matter; e) spores; f) pollen.

5.3.3 Vitrinite Reflectance

Vitrinite reflectance values for main phase of oil generation ranges from (0.6-1.3) %Ro and values greater than 2.0 %Ro indicate dry gas generation (Tissot and Welte, 1984; Teichmüller et al., 1998; Killops and Killops, 2005). The vitrinite reflectance values for the deltaic sequences range from 0.39-0.48 %Ro for Tukai, Miri, Lambir and Belait formation samples while the values of 0.69-0.79 %Ro was recorded in the Meligan Formation (Table 5.1). The submarine fan sequences shows vitrinite reflectance values in the range of 0.99-1.14%Ro and 0.79-1.14%Ro (Table 5.1) for Temburong and West Crocker formations respectively. The undifferentiated Formation has lower vitrinite reflectance values compared to Temburong and West Crocker formations in the range of 0.46 -0.49 %Ro. The spatial distribution of vitrinite reflectance within the studied formations is shown in Figure 5.8. See Appendix A for more information on the measured vitrinite reflectance.

5.4 Organic Geochemistry

In this study organic geochemical analyses were performed to evaluate the organic matter content, type and thermal maturity as well as to interpret depositional environment conditions based on total organic matter content, pyrolysis, elemental and molecular composition. Sixty-two samples were selected to represent the sandy, shaly and slump facies within the studied formations. Total organic carbon, source rock analysis, extractable organic matter (EOM) and hydrocarbon yield of selected samples were used to identify source richness in terms of hydrocarbon generation potential. These data are discussed in the next chapter.

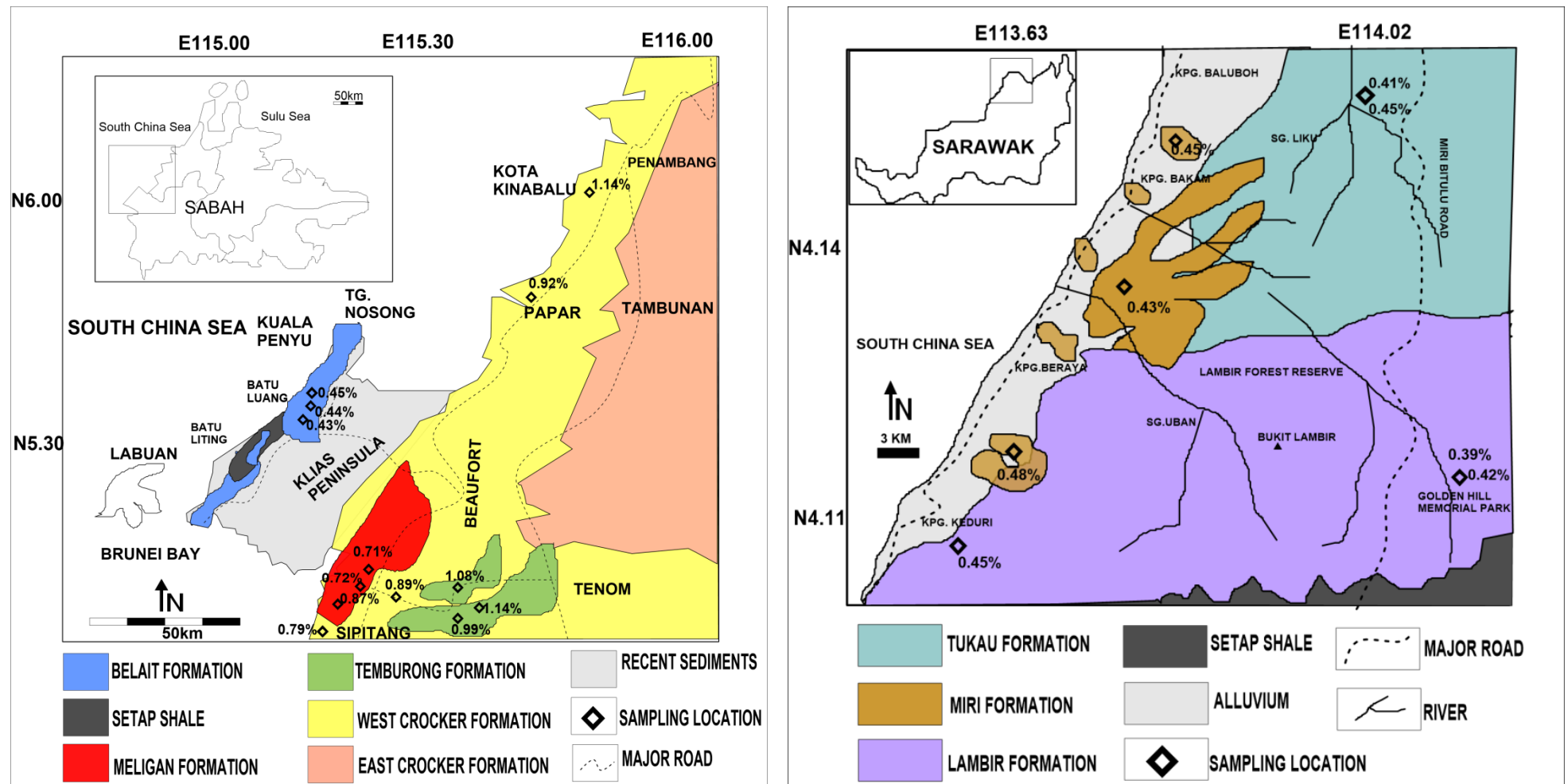


Figure 5.8. Map showing distribution of vitrinite reflectance in the western Sabah and northern Sarawak studied formations.

5.4.1 Extractable Organic Matter and Hydrocarbon Yield

A summary of the extractable organic matter (EOM) and petroleum yield is shown in in Table 5.2. The total amount of EOM is high in the sandy and shaly facies of all the deltaic sequences with average EOM concentration more than 1000ppm compared to most samples from submarine fan sequences with average EOM concentration of less than 700 ppm. Some samples from the slump facies in West Crocker Formation and the undifferentiated Formation have values over 1000 ppm. The concentrations of the aromatic, aliphatic and NSO fractions from the EOM are shown in Figure 5.9. Aromatic hydrocarbon fraction is higher than the aliphatic in all the analysed samples except for the slump facies in the West Crocker Formation where the values of aromatic and aliphatic yielded are close. There are relatively high values of NSO fractions compared to total hydrocarbons (aliphatic and aromatic) in the Tukai, Miri, Lambir, Belait samples which is in agreement with the immature or the every early mature stage (Tissot and Welte, 1984)

5.4.2 Total Organic Carbon

Total Organic carbon (TOC) analysis was carried out to determine the amount of organic matter. Most of the studied samples contain high organic matter content (TOC >1.0 wt.%, Table 5.3). In terms of source rocks quantity, most of the studied samples have relatively good TOC content (as defined by Peters and Cassa, 1994). There are variations in TOC content relative to facies. In general, the sandy facies are found to have higher TOC, when compared to the shaly facies, except in Temburong Formation where the TOC content value is higher in the shales. The sandy facies have higher TOC values because they are commonly associated with coals and carbonaceous debris. This is typical to terrestrial and marginal depositional environment.

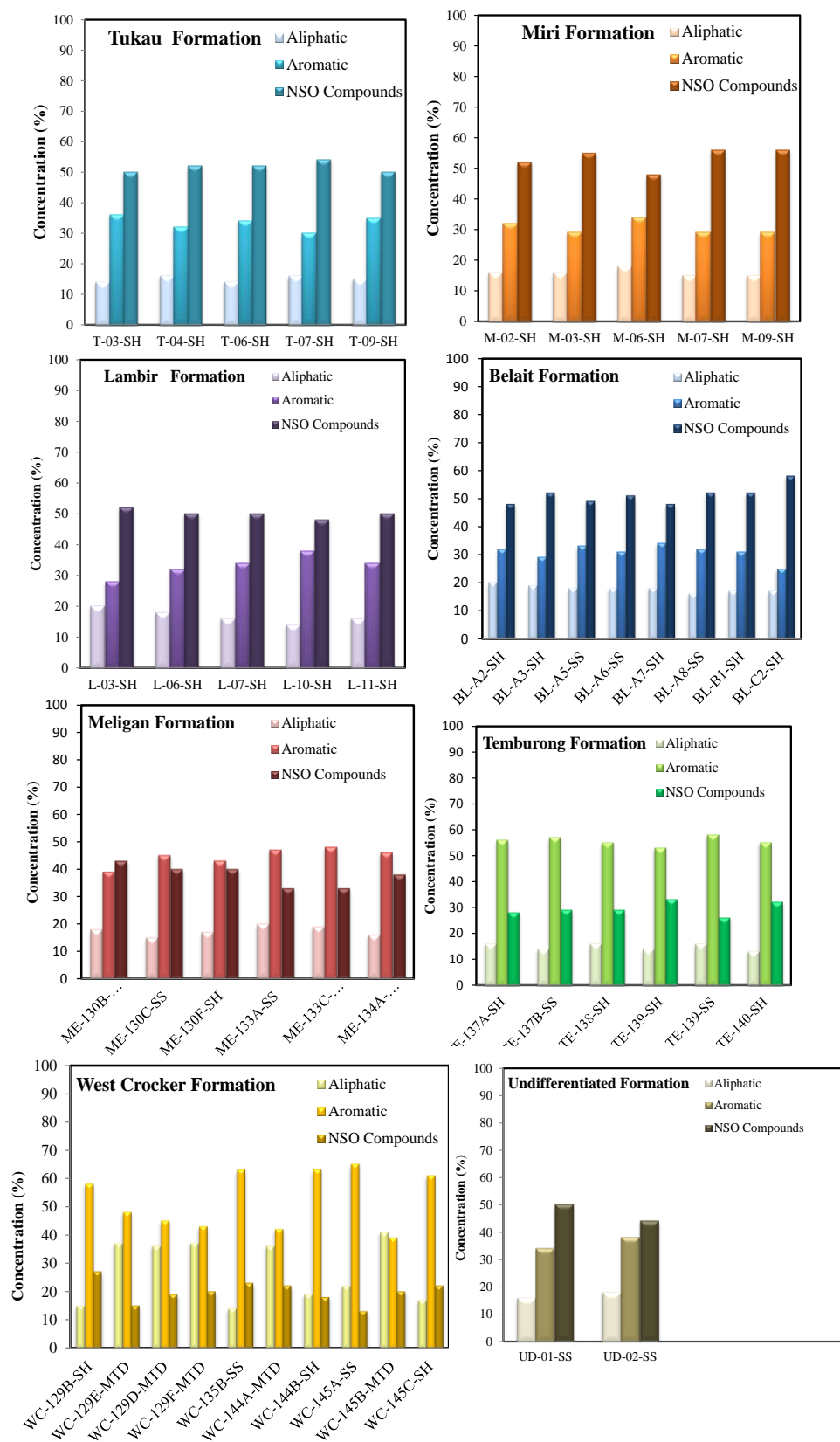


Figure 5.9. Concentrations of EOM fractions in the studied samples.

Table 5.2. Extractable organic matter and hydrocarbon yield from the studied samples

| | Sample ID | TOC (wt.%) | EOM (wt.%) | EOM (ppm) | ALI (%) | ARO (%) | NSO (%) | ALI (ppm) | ARO (ppm) | NSO (ppm) | HC yield (ppm) |
|------------------|--------------------------|---------------|---------------|--------------|------------|------------|------------|--------------|--------------|--------------|----------------------|
| Deltaic Sequence | <i>Tukau Formation</i> | | | | | | | | | | |
| | T-03-SH | 1.61 | 0.13 | 1320 | 15 | 35 | 50 | 198 | 462 | 660 | 660 |
| | T-04-SH | 1.52 | 0.12 | 1204 | 15 | 35 | 50 | 181 | 421 | 602 | 602 |
| | T-06-SH | 1.54 | 0.12 | 1220 | 14 | 34 | 52 | 171 | 415 | 634 | 586 |
| | T-07-SH | 1.21 | 0.12 | 1240 | 16 | 30 | 54 | 198 | 372 | 670 | 570 |
| | T-09-SH | 1.38 | 0.13 | 1308 | 15 | 35 | 50 | 196 | 458 | 654 | 654 |
| | T-01-SS | 2.91 | 0.16 | 1580 | 14 | 36 | 50 | 221 | 569 | 790 | 790 |
| | T-10-SS | 2.54 | 0.15 | 1450 | 16 | 32 | 52 | 232 | 464 | 754 | 696 |
| | <i>Miri Formation</i> | | | | | | | | | | |
| | M-02-SH | 1.14 | 0.13 | 1290 | 16 | 32 | 52 | 206 | 413 | 671 | 619 |
| | M-03-SH | 1.06 | 0.13 | 1240 | 16 | 29 | 55 | 198 | 360 | 682 | 558 |
| | M-06-SH | 1.14 | 0.13 | 1276 | 18 | 34 | 48 | 230 | 434 | 612 | 664 |
| | M-07-SH | 1.24 | 0.13 | 1287 | 15 | 29 | 56 | 193 | 373 | 721 | 566 |
| | M-09-SH | 1.59 | 0.13 | 1299 | 15 | 29 | 56 | 195 | 377 | 727 | 572 |
| | M-08-SS | 2.32 | 0.11 | 1298 | 15 | 30 | 55 | 195 | 390 | 714 | 585 |
| | M-11-SS | 2.54 | 0.12 | 1346 | 15 | 32 | 53 | 202 | 431 | 713 | 634 |
| | <i>Lambir Formation</i> | | | | | | | | | | |
| | L-03-SH | 1.28 | 0.12 | 1214 | 16 | 34 | 50 | 195 | 412 | 607 | 607 |
| | L-06-SH | 1.07 | 0.13 | 1284 | 18 | 32 | 50 | 231 | 411 | 642 | 642 |
| | L-07-SH | 2.76 | 0.14 | 1376 | 16 | 34 | 50 | 220 | 468 | 688 | 688 |
| | L-10-SH | 1.45 | 0.11 | 1089 | 14 | 38 | 48 | 152 | 414 | 523 | 566 |
| | L-11-SH | 1.62 | 0.11 | 1124 | 16 | 34 | 50 | 180 | 382 | 562 | 562 |
| | L-02-SS | 11.11 | 0.35 | 3484 | 20 | 28 | 52 | 697 | 976 | 1812 | 1672 |
| | L-05-SS | 3.45 | 0.18 | 1842 | 18 | 32 | 50 | 332 | 589 | 921 | 921 |
| | <i>Belait Formation</i> | | | | | | | | | | |
| | BL-A2-SH | 1.71 | 0.14 | 1420 | 20 | 32 | 48 | 284 | 454 | 682 | 738 |
| | BL-A3-SH | 5.03 | 0.22 | 2210 | 19 | 29 | 52 | 420 | 641 | 1149 | 1061 |
| | BL-A5-SS | 4.18 | 0.21 | 2082 | 18 | 33 | 49 | 375 | 687 | 1020 | 1062 |
| | BL-A6-SS | 1.08 | 0.10 | 1005 | 18 | 31 | 51 | 181 | 312 | 513 | 492 |
| | BL-A7-SH | 1.05 | 0.10 | 1030 | 18 | 34 | 48 | 185 | 350 | 494 | 536 |
| | BL-A8-SS | 7.87 | 0.17 | 1654 | 16 | 32 | 52 | 265 | 529 | 860 | 794 |
| | BL-B1-SH | 2.27 | 0.19 | 1850 | 17 | 31 | 52 | 315 | 574 | 962 | 888 |
| | BL-C2-SH | 1.19 | 0.11 | 1050 | 17 | 25 | 58 | 179 | 263 | 609 | 441 |
| | <i>Meligan Formation</i> | | | | | | | | | | |
| | ME-130B-SH | 0.98 | 0.14 | 1420 | 18 | 39 | 43 | 256 | 554 | 611 | 809 |
| | ME-130C-SS | 1.34 | 0.11 | 1053 | 15 | 45 | 40 | 158 | 474 | 421 | 632 |
| | ME-130F-SH | 2.85 | 0.11 | 1070 | 17 | 43 | 40 | 182 | 460 | 428 | 642 |
| | ME-133A-SS | 3.03 | 0.09 | 852 | 20 | 47 | 33 | 170 | 400 | 281 | 571 |
| | ME-133C-SH | 1.77 | 0.20 | 1582 | 19 | 48 | 33 | 253 | 727 | 600 | 980 |
| | ME-134A-SH | 2.42 | 0.16 | 1980 | 16 | 46 | 38 | 377 | 951 | 654 | 1328 |

Table 5.2. Extractable organic matter and hydrocarbon yield from the studied samples (continuation).

| | Sample ID | TOC (wt.%) | EOM (wt.%) | EOM (ppm) | ALI (%) | ARO (%) | NSO (%) | ALI (ppm) | ARO (ppm) | NSO (ppm) | HC yield (ppm) |
|---------------|-----------------------------------|---------------|---------------|--------------|------------|------------|------------|--------------|--------------|--------------|----------------------|
| Submarine Fan | <i>Temburong Formation</i> | | | | | | | | | | |
| | TEM-137A-SH | 1.10 | 0.03 | 420 | 16 | 56 | 28 | 99 | 147 | 174 | 246 |
| | TEM-137B-SS | 0.51 | 0.04 | 445 | 14 | 57 | 29 | 76 | 211 | 158 | 287 |
| | TEM-138-SH | 1.38 | 0.05 | 482 | 16 | 55 | 29 | 93 | 220 | 169 | 313 |
| | TEM-139-SH | 1.26 | 0.03 | 483 | 14 | 53 | 33 | 96 | 188 | 125 | 284 |
| | TEM-139-SS | 0.58 | 0.04 | 342 | 16 | 58 | 26 | 54 | 100 | 67 | 221 |
| | TEM-140-SH | 0.71 | 0.03 | 381 | 13 | 55 | 32 | 89 | 176 | 116 | 265 |
| | <i>West Crocker Formation</i> | | | | | | | | | | |
| | WC-129B-SH | 1.23 | 0.07 | 698 | 15 | 58 | 27 | 105 | 405 | 188 | 510 |
| | WC-129E-MTD | 2.26 | 0.18 | 1784 | 37 | 48 | 15 | 660 | 856 | 268 | 1516 |
| | WC-129D-MTD | 1.73 | 0.16 | 1560 | 36 | 45 | 19 | 562 | 702 | 296 | 1264 |
| | WC-129F-MTD | 2.40 | 0.19 | 1850 | 37 | 43 | 20 | 685 | 796 | 370 | 1480 |
| | WC-135B-SS | 3.94 | 0.18 | 1058 | 14 | 63 | 23 | 148 | 667 | 243 | 815 |
| | WC-144A-MTD | 10.63 | 0.42 | 4200 | 36 | 42 | 22 | 1512 | 1764 | 924 | 3276 |
| | WC-144B-SH | 1.72 | 0.07 | 726 | 19 | 63 | 18 | 138 | 457 | 131 | 595 |
| | WC-145A-SS | 0.65 | 0.08 | 456 | 22 | 65 | 13 | 166 | 491 | 98 | 358 |
| | WC-145B-MTD | 6.32 | 0.41 | 4098 | 41 | 39 | 20 | 1680 | 1598 | 820 | 3278 |
| | WC-145C-SH | 1.06 | 0.07 | 659 | 17 | 61 | 22 | 112 | 402 | 145 | 514 |
| | <i>Undifferentiated Formation</i> | | | | | | | | | | |
| | UD-01-SS | 2.27 | 0.15 | 1480 | 16 | 34 | 50 | 237 | 503 | 740 | 740 |
| | UD-02-SS | 1.82 | 0.14 | 1360 | 18 | 38 | 44 | 245 | 517 | 598 | 762 |

TOC, total organic carbon content

EOM, extractable organic matter

ALI, aliphatic fraction

ARO, aromatic fraction

NSO, nitrogen, oxygen and sulphur compounds

HC yield, total hydrocarbon yield (aliphatic + aromatic)

5.4.3 Pyrolysis

5.4.3.1 Source Rock Analysis

In the pyrolysis analyses, free hydrocarbons (S_1), the amount of hydrocarbon (S_2) and CO_2 (S_3) expelled from pyrolysis of kerogen are measured and the results are shown in Table 5.3. The amount of hydrocarbon yield (S_2) expelled during pyrolysis can be used to evaluate the generative potential of the source rocks (Bordenave, 1993). Most of the samples analysed have S_2 yield less than 5.0 mg HC/g rock and this indicates poor to fair hydrocarbon generative potential. However, some of the sandy and slump samples from Lambir, Belait and West Crocker formation have S_2 yield more than 5.0 mg HC/g rock indicating good to very good hydrocarbon generative potential. In addition, T_{max} values which represents the temperature at the point where S_2 peak is the maximum is also determined (Espitalie et al., 1977). The T_{max} values is higher in Meligan, Temburong and West Crocker formations samples compared to Tukai, Miri, Lambir and Belait formations samples (Table 5.3) and this is significant in determining the thermal maturity of the studied samples. The hydrogen index (HI) values are generally less than 150 mg HC/g TOC is most of the studied samples except for the samples from the slump facies in the West Crocker Formation which show significant high HI values (up to 300 mg HC/g TOC; Table 5.3). Hydrocarbon generative capacity depends on the quality (HI_o; as defined in Table 5.3) of organic matter in thermally immature source rocks (Peters et al., 2005). However, petroleum generation decreases the remaining generative potential as measured by present day HI. Thus, the need to reconstruct of original source rock generative potential for thermally matured organic matter with respect to its original generation potential in order to understand the true characteristics of the organic matter. Adopting empirical equations from Banerjee et.al (1998) in relation to the T_{max} ($>435^\circ C$), the corrected HI values are shown in Table 5.3. There are no much differences in the characteristics of the organic matter in terms of hydrocarbon generative potential and

source rock quality after correction except from few samples from West Crocker Formation. This parameter is combined with other parameters to give information of the source rock quality present in all the studied formations and is further discussed in the next chapter.

5.4.3.2 Py-GC

The pyrolysis products of the oil prone Type I and II kerogen extend out to the high molecular weight range of compounds. Type I and II kerogen produces abundant long-chained n-alkenes, as shown by the prominent peaks in the pyrograms in the C₁₅ range. In contrast, Type III kerogen shows the bulk of the pyrolysis products confined to the low molecular weight part of the pyrogram (Dembicki, 2009). The Py-GC pyrograms of most of the analysed kerogen samples from Tukai, Miri, Lambir, Belait and West Crocker formations are dominated by low molecular weight compounds relative to the homologous series of n-alkane /alkene doublets as shown in Figure 5.10, these are characteristics of Type III kerogen and typically gas prone. Temburong Formation shows Type IV kerogen (Figure 5.10) fingerprints which may be due to the effect of low grade metamorphism on the organic matter. It is interesting to note that the slump samples from the West Crocker Formation display Type II kerogen with dominance of n-alkene/alkane doublets over aromatic compound (Figure 5.10) which indicate oil proneness. See Appendix B for the quantitative data based on the peak height measurements of the Py-GC pyrograms.

Table 5.3 Bulk geochemical characteristics (TOC content , pyrolysis) of the studied formations

| Sample ID | TOC Wt.% | | Pyrolysis (SRA) data | | | | | | | | |
|-------------------|----------|--------------------------|--------------------------|--------------------------|--|--------------|-----|-------|----|------|-------|
| | | S ₁ (mg/g) | S ₂ (mg/g) | S ₃ (mg/g) | S ₂ /S ₃ (mg/g) | Tmax (°C) | HI | HI(o) | OI | PI | GP |
| Deltaic Sequences | | | | | | | | | | | |
| Lambir Formation | | | | | | | | | | | |
| L-02-SS | 11.11 | 0.14 | 10.21 | 3.78 | 2.70 | 426 | 92 | - | 34 | 0.01 | 10.35 |
| L-03-SH | 1.28 | 0.08 | 1.12 | 0.27 | 4.17 | 401 | 88 | - | 21 | 0.07 | 1.20 |
| L-04-SS | 6.57 | 0.09 | 6.51 | 1.97 | 3.30 | 413 | 99 | - | 30 | 0.01 | 6.60 |
| L-05-SS | 3.45 | 0.10 | 2.10 | 0.76 | 2.77 | 418 | 61 | - | 22 | 0.05 | 2.20 |
| L-06-SH | 1.07 | 0.04 | 1.03 | 0.25 | 4.19 | 421 | 96 | - | 23 | 0.04 | 1.07 |
| L-07-SH | 2.76 | 0.07 | 1.92 | 0.83 | 2.32 | 426 | 70 | - | 30 | 0.04 | 1.99 |
| L-09-SH | 1.38 | 0.04 | 1.06 | 0.43 | 2.48 | 410 | 77 | - | 31 | 0.04 | 1.10 |
| L-10-SH | 1.45 | 0.06 | 1.14 | 0.36 | 3.14 | 412 | 79 | - | 25 | 0.05 | 1.20 |
| L-11-SH | 1.62 | 0.13 | 1.18 | 0.45 | 2.60 | 418 | 73 | - | 28 | 0.10 | 1.31 |
| L-14-SH | 1.85 | 0.09 | 1.53 | 0.48 | 3.18 | 416 | 83 | - | 26 | 0.06 | 1.62 |
| Miri Formation | | | | | | | | | | | |
| M-01-SH | 1.36 | 0.44 | 1.03 | 0.33 | 3.16 | 434 | 76 | - | 24 | 0.30 | 1.47 |
| M-02-SH | 1.14 | 0.13 | 1.12 | 0.31 | 3.64 | 429 | 98 | - | 27 | 0.10 | 1.25 |
| M-03-SH | 1.06 | 0.05 | 1.08 | 0.34 | 3.18 | 421 | 102 | - | 32 | 0.04 | 1.13 |
| M-04-SH | 1.12 | 0.04 | 1.08 | 0.29 | 3.71 | 432 | 96 | - | 26 | 0.04 | 1.12 |
| M-05-SH | 1.87 | 0.09 | 1.18 | 0.71 | 1.66 | 434 | 63 | - | 38 | 0.07 | 1.27 |
| M-06-SH | 1.14 | 0.21 | 1.19 | 0.41 | 2.90 | 416 | 104 | - | 36 | 0.15 | 1.40 |
| M-07-SH | 1.24 | 0.09 | 1.17 | 0.47 | 2.48 | 416 | 94 | - | 38 | 0.07 | 1.26 |
| M-08-SS | 2.32 | 0.05 | 1.91 | 0.65 | 2.94 | 413 | 82 | - | 28 | 0.03 | 1.96 |
| M-09-SH | 1.59 | 0.11 | 1.41 | 0.43 | 3.28 | 424 | 89 | - | 27 | 0.07 | 1.52 |
| M-11-SS | 2.54 | 0.16 | 2.12 | 0.66 | 3.21 | 426 | 83 | - | 26 | 0.07 | 2.28 |
| Tukau Formation | | | | | | | | | | | |
| T-01-SS | 2.91 | 0.09 | 2.56 | 0.61 | 4.19 | 411 | 88 | - | 21 | 0.03 | 2.65 |
| T-02-SH | 1.24 | 0.05 | 1.23 | 0.31 | 3.97 | 423 | 99 | - | 25 | 0.04 | 1.28 |
| T-03-SH | 1.61 | 0.05 | 1.17 | 0.42 | 2.80 | 426 | 73 | - | 26 | 0.04 | 1.22 |
| T-04-SH | 1.52 | 0.09 | 1.18 | 0.41 | 2.88 | 429 | 78 | - | 27 | 0.07 | 1.27 |
| T-06-SH | 1.54 | 0.10 | 1.08 | 0.35 | 3.05 | 430 | 70 | - | 23 | 0.08 | 1.18 |
| T-07-SH | 1.21 | 0.18 | 1.20 | 0.34 | 3.54 | 430 | 99 | - | 28 | 0.13 | 1.38 |
| T-08-SH | 1.60 | 0.15 | 1.21 | 0.41 | 3.54 | 427 | 85 | - | 24 | 0.10 | 1.51 |
| T-09-SH | 1.38 | 0.08 | 1.06 | 0.41 | 2.56 | 428 | 77 | - | 30 | 0.07 | 1.14 |
| T-10-SS | 2.54 | 0.09 | 1.98 | 0.64 | 3.12 | 416 | 78 | - | 25 | 0.04 | 2.07 |
| T-12-SH | 1.26 | 0.06 | 1.20 | 0.33 | 3.66 | 420 | 95 | - | 26 | 0.05 | 1.26 |
| Belait Formation | | | | | | | | | | | |
| BL-A2-SH | 1.71 | 0.03 | 0.31 | 0.76 | 0.41 | 435 | 18 | 20 | 45 | 0.08 | 0.34 |
| BL-A3-SH | 5.03 | 0.16 | 5.19 | 2.26 | 2.30 | 428 | 103 | - | 45 | 0.03 | 5.35 |
| BL-A5-SST | 4.18 | 0.09 | 5.29 | 1.07 | 4.94 | 426 | 126 | - | 26 | 0.02 | 5.38 |
| BL-A6-SST | 1.08 | 0.06 | 0.39 | 0.47 | 0.83 | 437 | 36 | 41 | 44 | 0.13 | 0.45 |
| BL-A7-SH | 1.05 | 0.02 | 0.25 | 0.55 | 0.45 | 431 | 24 | - | 53 | 0.08 | 0.27 |
| BL-A8-SST | 7.87 | 0.58 | 12.8 | 2.58 | 4.96 | 418 | 163 | - | 33 | 0.04 | 13.38 |
| BL-B1-SH | 2.27 | 0.27 | 3.18 | 0.59 | 5.39 | 431 | 127 | - | 23 | 0.08 | 3.45 |
| BL-C2-SH | 1.19 | 0.08 | 0.39 | 0.50 | 0.78 | 432 | 33 | - | 42 | 0.17 | 0.47 |
| Meligan Formation | | | | | | | | | | | |
| ME-130B-SH | 0.98 | 0.04 | 0.2 | - | - | 458 | 20 | 42 | - | 0.17 | 0.24 |
| ME-130C-SS | 1.34 | 0.03 | 0.25 | 0.42 | 0.60 | 460 | 19 | 40 | 32 | 0.11 | 0.28 |
| ME-130F-SH | 2.85 | 0.22 | 0.64 | 0.48 | 1.33 | 444 | 22 | 43 | 17 | 0.26 | 0.86 |
| ME-133A-SS | 3.03 | 0.07 | 1.99 | 0.49 | 4.06 | 452 | 66 | 78 | 16 | 0.03 | 2.06 |
| ME-133C-SH | 1.77 | 0.15 | 0.99 | 0.56 | 1.76 | 471 | 56 | 77 | 32 | 0.13 | 1.14 |
| ME-134A-SH | 1.90 | 0.19 | 1.05 | - | - | 472 | 54 | 75 | - | 0.15 | 1.24 |

Table 5.3 Bulk geochemical characteristics (TOC content , pyrolysis) of the studied formations (Continuation)

| Sample ID | TOC Wt. % | Pyrolysis (SRA) data | | | | | | | | | |
|----------------------------|-----------|--------------------------|--------------------------|--------------------------|--|--------------|-----|-------|----|------|-------|
| | | S ₁ (mg/g) | S ₂ (mg/g) | S ₃ (mg/g) | S ₂ /S ₃ (mg/g) | Tmax (°C) | HI | HI(o) | OI | PI | GP |
| Submarine Fan Sequence | | | | | | | | | | | |
| Temburong Formation | | | | | | | | | | | |
| TE-137A-SH | 1.1 | 0.07 | 0.59 | 0.17 | 3.47 | 492 | 54 | 60 | 15 | 0.11 | 0.66 |
| TE-137B-SS | 0.51 | 0.17 | 0.19 | - | - | 497 | 37 | 40 | - | 0.47 | 0.36 |
| TE-138-SH | 1.38 | 0.03 | 0.32 | 0.35 | 0.91 | 487 | 23 | 29 | 25 | 0.09 | 0.35 |
| TE-139-SH | 1.26 | 0.02 | 0.22 | - | - | 490 | 17 | 25 | - | 0.08 | 0.24 |
| TE-139-SS | 0.58 | 0.01 | 0.25 | 0.13 | 1.92 | 492 | 43 | 59 | 22 | 0.04 | 0.26 |
| TE-140-SH | 0.71 | 0.05 | 0.32 | 0.17 | 1.88 | 474 | 45 | 52 | 24 | 0.14 | 0.37 |
| West Crocker Formation | | | | | | | | | | | |
| WC-129B-SH | 1.23 | 0.03 | 0.18 | 0.28 | 0.64 | 455 | 14 | 26 | 23 | 0.15 | 0.21 |
| WC-129D-MTD | 1.73 | 0.44 | 1.66 | 0.31 | 5.35 | 450 | 96 | 121 | 18 | 0.21 | 2.10 |
| WC-129E-MTD | 2.26 | 0.08 | 0.82 | 0.47 | 1.74 | 453 | 86 | 113 | 21 | 0.09 | 0.90 |
| WC-129F-MTD | 2.4 | 0.11 | 0.95 | 0.24 | 3.96 | 459 | 40 | 84 | 10 | 0.10 | 1.06 |
| WC-135B-SS | 3.94 | 0.07 | 4.69 | 0.44 | 10.66 | 465 | 119 | 211 | 11 | 0.01 | 4.76 |
| WC-144A-MTD | 10.63 | 0.09 | 35.83 | 0.52 | 68.90 | 463 | 337 | 387 | 5 | 0.00 | 35.92 |
| WC-144B-SH | 1.72 | 0.01 | 0.18 | 0.79 | 0.23 | 473 | 10 | 11 | 46 | 0.08 | 0.19 |
| WC-145A-SS | 0.65 | 0.01 | 0.03 | 0.29 | 0.10 | 515 | 5 | 6 | 44 | 0.14 | 0.04 |
| WC-145B-MTD | 6.32 | 0.06 | 3.25 | 0.46 | 7.07 | 503 | 151 | 282 | 7 | 0.02 | 3.31 |
| WC-145C-SH | 1.06 | 0.01 | 0.02 | 0.29 | 0.07 | 488 | 2 | 10 | 27 | 0.20 | 0.03 |
| Undifferentiated Formation | | | | | | | | | | | |
| UD-01-SS | 2.27 | 0.27 | 3.18 | 0.59 | 5.39 | 431 | 127 | - | 33 | 0.08 | 3.45 |
| UD-02-SS | 1.82 | 0.05 | 2.03 | 0.42 | 4.83 | 434 | 111 | - | 30 | 0.06 | 1.87 |

TOC: total organic carbon (wt. %)

S₁: volatile hydrocarbon (HC) content, mg HC/g rock

S₂: remaining HC generative potential, mg HC/g rock

S₃: carbon dioxide yield, mgCO₂/g rock

HI: hydrogen index = S₂ 100/TOC, mg HC/g TOC

OI: oxygen index = S₃ 100/TOC, mg CO₂/g TOC; PI: production index = S₁/ (S₁ + S₂)

GP: genetic potential=S₁+S₂

T_{max} = Temperature at maximum generation

Ro= vitrinite reflectance

HIo= Original Hydrogen Index= HI. $1/(a \cdot \exp.b \cdot (T_{max} - 435)) + HI_o$ (Banergee et al., 1998)

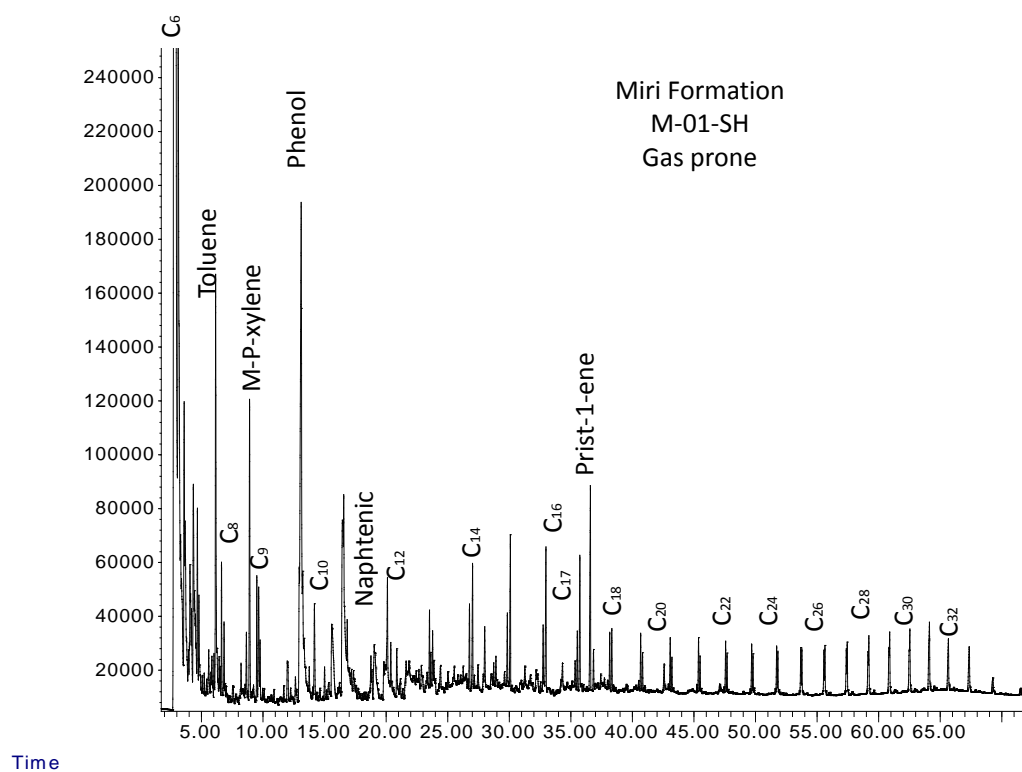
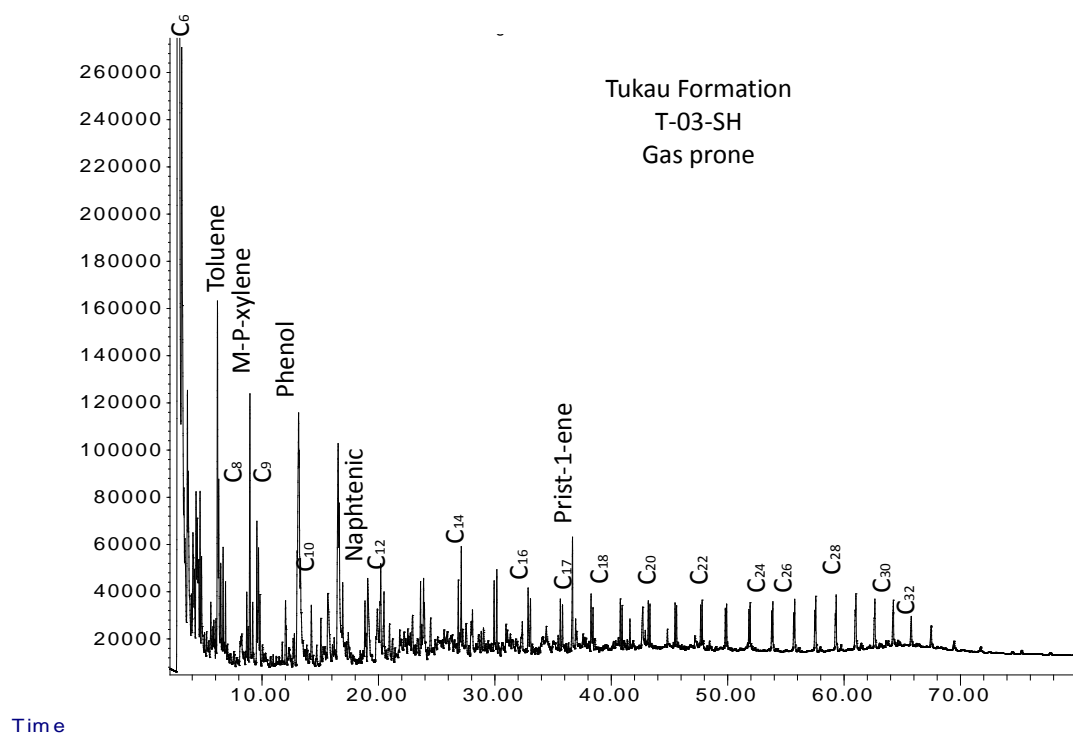


Figure 5.10. Pyrograms of the studied formations showing quality of kerogen.

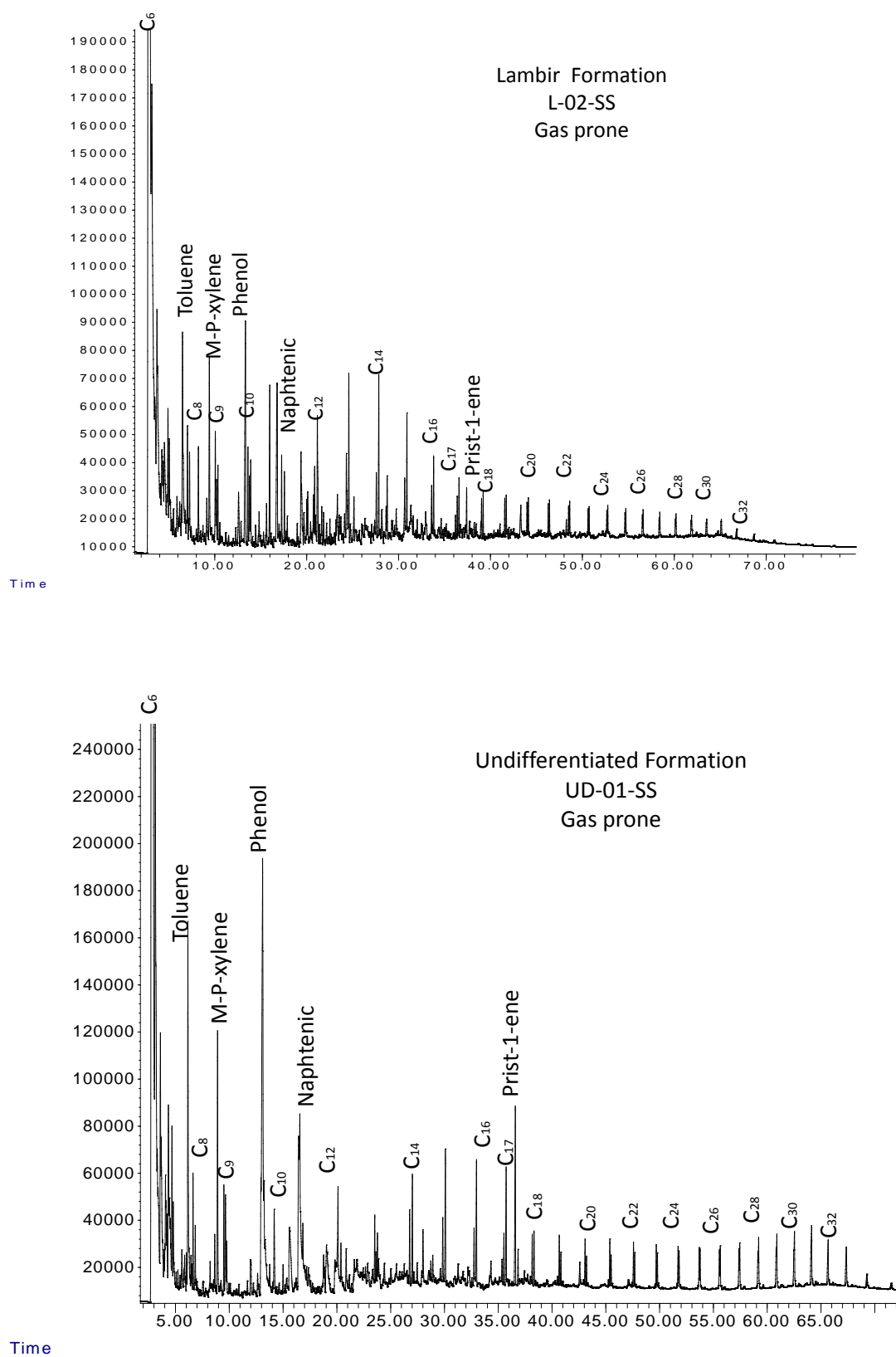


Figure 5.10. Pyrograms of the studied formations showing quality of kerogen (cont.)

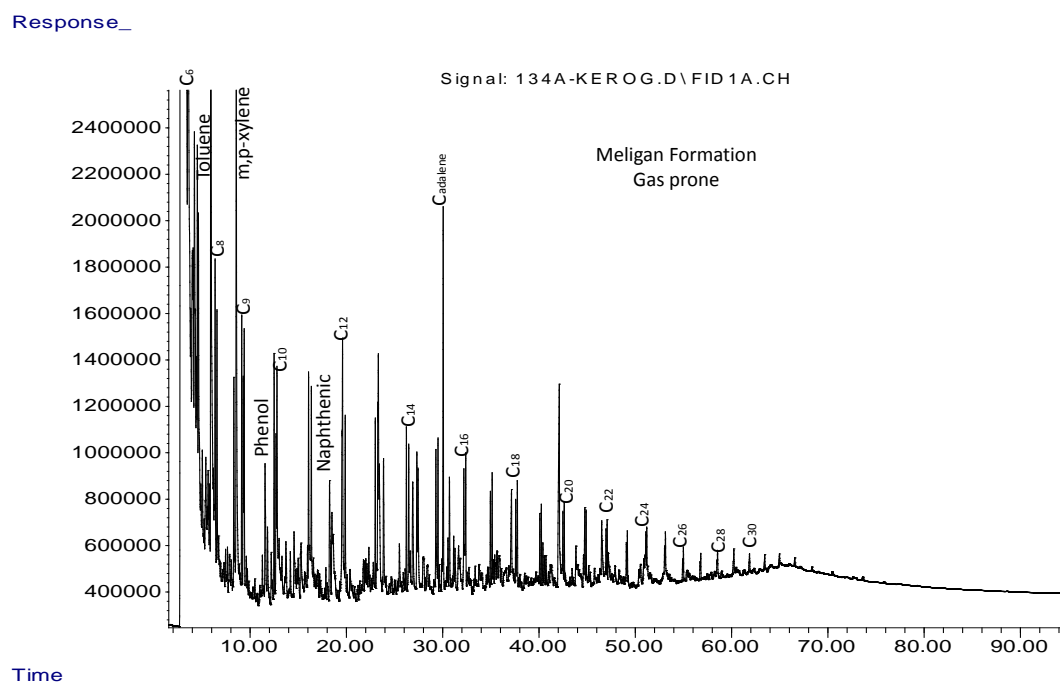
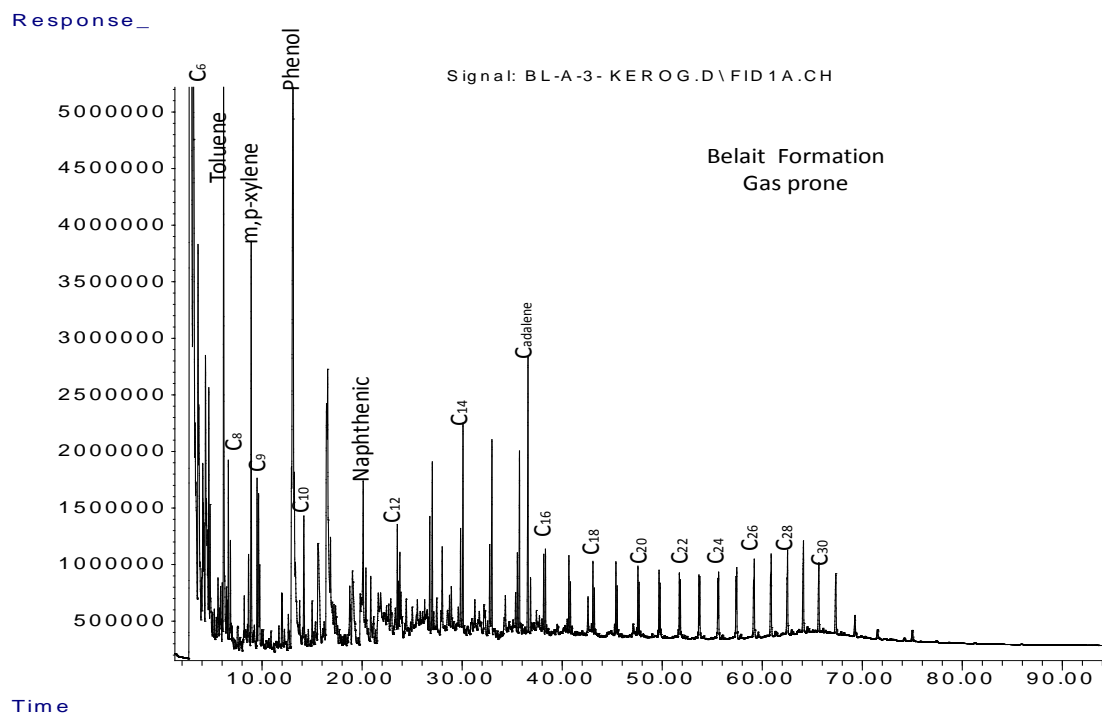


Figure 5.10. Pyrograms of the studied formations showing quality of kerogen (cont.).

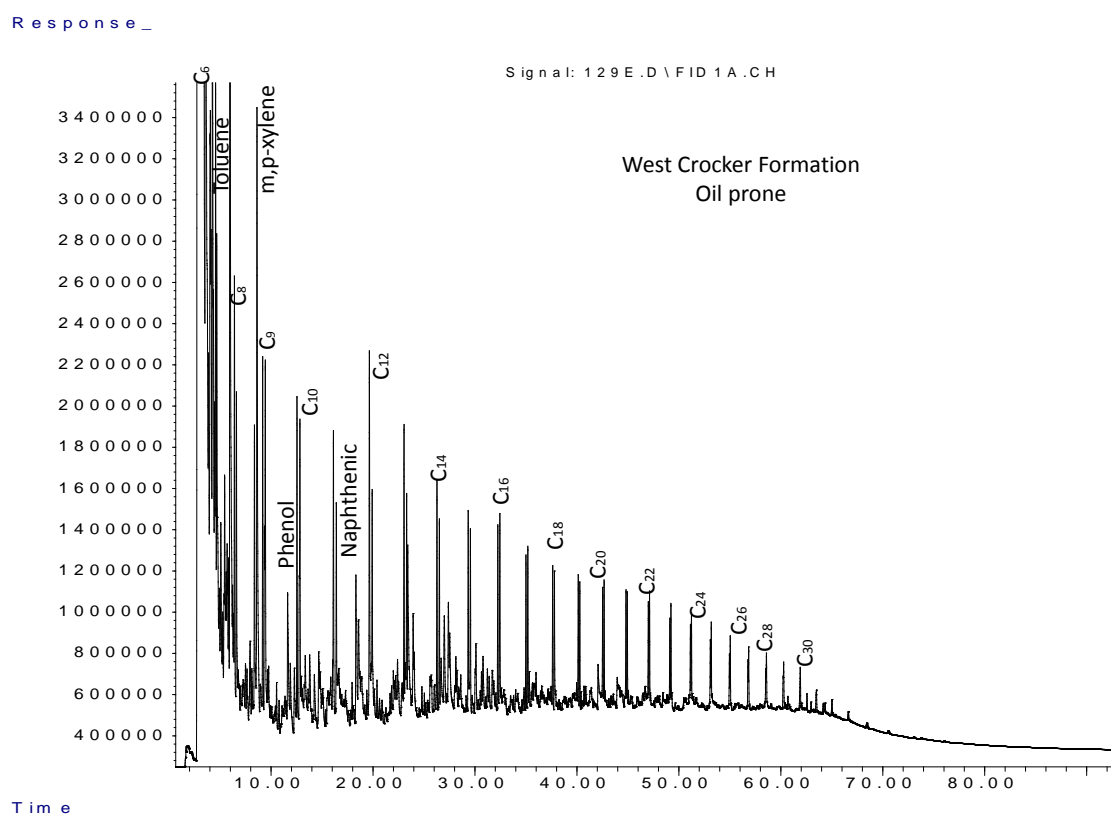
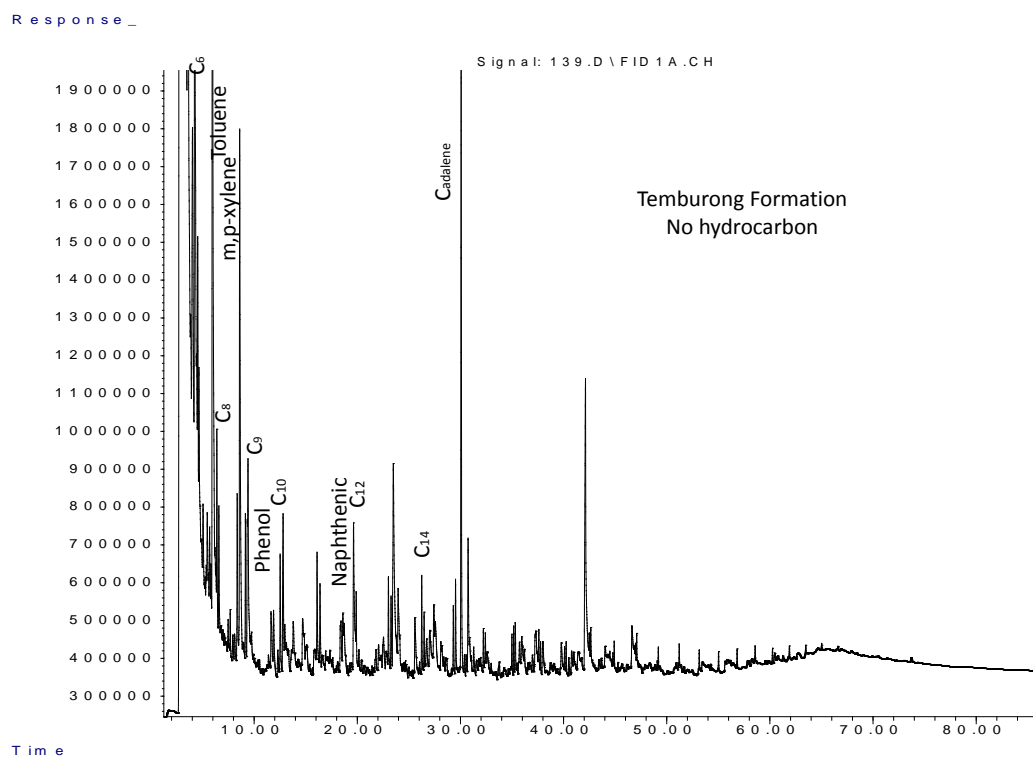


Figure 5.10. Pyrograms of the studied formations showing quality of kerogen (cont.).

5.4.4 Elemental Analytical Data

Representative whole rock and isolated kerogen samples from Belait, Meligan, Temburong and West Crocker formations were analysed for total sulphur (TS), carbon, hydrogen and nitrogen (CHN). The results in Table 5.4 were used to assess the type of organic matter, source input and depositional conditions. The atomic H/C ratios are less than 1 in most of the samples and significantly lower in the Temburong Formation samples (Table 5.4). This may be due to increased thermal decomposition of the Temburong Formation. Total sulphur contents are very low in most of the studied samples and this indicates presence of oxygen in the deposition of the organic matter present in the studied Formations. Total nitrogen is also low and this may suggest high terrestrial influence in the studied formations. These are further discussed in the next chapter.

5.4.5 Molecular Composition

The fragmentograms of n-alkanes and isoprenoids (m/z 85) and phenanthrenes (m/z 178+192) of the representative samples of the studied formations are presented in Figures 5.11 and 5.12. The calculated parameters are shown in Table 5.5 for aliphatic and aromatic hydrocarbon respectively.

5.4.5.1 n-alkanes and isoprenoids

The distribution of n-alkanes and isoprenoids are represented by mass fragmentogram (m/z 85). The n-alkanes ranging from n-C₁₆ to n-C₃₃, pristane, and phytane were identified in all the analysed samples (Figure 5.11). The distributions based on integrated peak areas of n-alkanes and isoprenoids identified in each sample are listed in Table 5.5. The implication for source input, depositional conditions and thermal maturity will be discussed in Chapter 6.

Table 5.4. TOC and elemental analysis data of the studied formations.

| | <i>Sample ID</i> | <i>TOC</i> | <i>TS</i> | <i>TN</i> | <i>C</i> | <i>H</i> | <i>H/C</i> | <i>TOC/TS</i> | <i>TOC/TN</i> |
|-------------------------|--------------------------|------------|-----------|-----------|----------|----------|------------|---------------|---------------|
| Deltaic Sequence | <i>Tukau Formation</i> | | | | | | | | |
| | T-01-SS | 2.91 | 0.45 | 0.11 | 62.05 | 4.24 | 0.82 | 6.54 | 25.98 |
| | T-03-SH | 1.61 | 0.30 | 0.06 | 59.45 | 4.36 | 0.88 | 5.37 | 28.25 |
| | T-04-SH | 1.52 | 0.34 | 0.06 | 71.70 | 4.84 | 0.81 | 4.54 | 27.64 |
| | T-08-SH | 1.60 | 0.33 | 0.09 | 56.18 | 4.12 | 0.88 | 4.86 | 18.82 |
| | T-10-SS | 2.54 | 0.55 | 0.05 | 65.22 | 4.62 | 0.85 | 4.64 | 47.92 |
| | <i>Miri Formation</i> | | | | | | | | |
| | M-01-SH | 1.36 | 0.32 | 0.06 | 64.27 | 4.82 | 0.90 | 4.29 | 22.67 |
| | M-03-SH | 1.06 | 0.28 | 0.04 | 60.55 | 4.44 | 0.88 | 3.79 | 24.09 |
| | M-05-SH | 1.87 | 0.45 | 0.07 | 56.09 | 4.02 | 0.86 | 4.13 | 26.71 |
| | M-08-SS | 2.32 | 0.58 | 0.09 | 57.27 | 4.20 | 0.88 | 4.00 | 25.78 |
| | M-11-SS | 2.54 | 0.68 | 0.11 | 59.86 | 4.39 | 0.88 | 3.72 | 23.09 |
| | <i>Lambir Formation</i> | | | | | | | | |
| | L-02-SS | 11.11 | 1.85 | 0.46 | 58.76 | 4.26 | 0.87 | 6.01 | 24.15 |
| | L-03-SH | 1.28 | 0.35 | 0.05 | 62.45 | 4.58 | 0.88 | 3.69 | 27.23 |
| | L-05-SS | 3.45 | 0.57 | 0.13 | 59.58 | 4.22 | 0.85 | 6.07 | 27.60 |
| | L-11-SH | 1.62 | 0.36 | 0.07 | 62.02 | 4.60 | 0.89 | 4.45 | 24.92 |
| | L-14-SH | 1.85 | 0.31 | 0.07 | 61.46 | 4.20 | 0.82 | 5.99 | 25.69 |
| | <i>Belait Formation</i> | | | | | | | | |
| | BL-A2-SH | 1.71 | 0.7 | 0.08 | 60.28 | 4.98 | 0.99 | 2.44 | 21.16 |
| | BL-A3-SH | 5.03 | 0.62 | 0.24 | 61.18 | 4.86 | 0.95 | 8.11 | 21.07 |
| | BL-A5-SST | 4.18 | 0.91 | 0.20 | 60.86 | 4.56 | 0.90 | 4.59 | 20.84 |
| | BL-A6-SST | 1.08 | 0.76 | 0.05 | 60.24 | 4.38 | 0.87 | 1.42 | 21.22 |
| | BL-A7-SH | 1.05 | 0.82 | 0.05 | 60.14 | 4.78 | 0.95 | 1.28 | 20.46 |
| | BL-B1-SH | 2.27 | 0.86 | 0.11 | 60.85 | 4.85 | 0.96 | 2.64 | 21.18 |
| | BL-C2-SH | 1.19 | 0.31 | 0.04 | 71.87 | 4.74 | 0.79 | 3.84 | 27.06 |
| | <i>Meligan Formation</i> | | | | | | | | |
| | ME-130B-SH | 0.98 | 0.35 | 0.04 | 64.25 | 4.14 | 0.77 | 2.80 | 24.5 |
| | ME-130C-SS | 1.34 | 0.39 | 0.06 | 62.38 | 4.48 | 0.86 | 3.44 | 23.45 |
| | ME-130F-SS | 2.85 | 0.57 | 0.13 | 64.62 | 4.58 | 0.85 | 5.00 | 22.24 |
| | ME-133A-SS | 3.03 | 0.62 | 0.12 | 65.27 | 4.21 | 0.77 | 4.89 | 24.54 |
| | ME-133C-SH | 1.77 | 0.33 | 0.07 | 60.7 | 4.24 | 0.84 | 5.36 | 24.48 |
| | ME-134A-SH | 2.42 | 0.44 | 0.09 | 80.41 | 4.62 | 0.69 | 5.50 | 27.89 |

Table 5.4. TOC and elemental analysis data of the studied formations (cont.).

| | <i>Sample ID</i> | <i>TOC</i> | <i>TS</i> | <i>TN</i> | <i>C</i> | <i>H</i> | <i>H/C</i> | <i>TOC/TS</i> | <i>TOC/TN</i> |
|----------------------|-----------------------------------|------------|-----------|-----------|----------|----------|------------|---------------|---------------|
| Submarine Fan | <i>Temburong Formation</i> | | | | | | | | |
| | TEM-137A-SH | 1.1 | 0.78 | 0.06 | 67.86 | 3.89 | 0.59 | 1.41 | 18.43 |
| | TEM-138-SH | 1.38 | 0.72 | 0.07 | 75.45 | 4.12 | 0.60 | 1.92 | 19.84 |
| | TEM-139-SH | 1.26 | 0.65 | 0.06 | 78.46 | 3.92 | 0.59 | 1.94 | 19.89 |
| | TEM-140-SH | 0.71 | 0.55 | 0.04 | 78.13 | 3.65 | 0.46 | 1.29 | 20.01 |
| | <i>West Crocker Formation</i> | | | | | | | | |
| | WC-129B-SH | 1.23 | 0.76 | 0.07 | 53.49 | 3.2 | 0.72 | 1.62 | 18.46 |
| | WC-129D-MTD | 1.73 | 0.75 | 0.10 | 57.25 | 4.39 | 0.92 | 2.31 | 17.89 |
| | WC-129E-MTD | 2.26 | 0.75 | 0.13 | 53.15 | 4.21 | 0.95 | 3.01 | 17.4 |
| | WC-129F-MTD | 2.4 | 0.74 | 0.13 | 53.97 | 4.34 | 0.96 | 3.24 | 18.2 |
| | WC-135B-SS | 3.94 | 0.99 | 0.19 | 58.95 | 4.02 | 0.82 | 3.98 | 20.76 |
| | WC-144A-MTD | 10.63 | 3.07 | 0.56 | 52.24 | 5.12 | 1.18 | 3.46 | 18.99 |
| | WC-145B-MTD | 6.32 | 1.92 | 0.33 | 54.2 | 4.17 | 0.92 | 3.29 | 19.02 |
| | WC-145C-SH | 1.06 | 0.82 | 0.05 | 57.26 | 4.28 | 0.90 | 1.29 | 20.04 |
| | <i>Undifferentiated Formation</i> | | | | | | | | |
| | UD-01-SS | 2.27 | 0.68 | 0.15 | 58.06 | 4.50 | 0.93 | 3.33 | 15.13 |
| | UD-02-SS | 1.82 | 0.72 | 0.12 | 60.20 | 4.84 | 0.96 | 2.53 | 15.17 |

TOC: total organic carbon content

TS: total sulphur

TN: total nitrogen

C: carbon

H:hydrogen

5.4.5.2 Phenanthrene and alkyl derivatives

The m/z 178 and 192 fragmentograms showing the distribution of phenanthrene and methyl phenanthrenes in the studied samples are shown in Figure 5.12. Phenanthrene and four methylphenanthrene (MP) were detected in the aromatic fraction of the studied samples. The calculated parameters based on peak heights are recorded in Table 5.5. The implication for source input and thermal maturity will be discussed in Chapter 6.

5.5 Trace elements distributions

Selected trace elements concentrations of Lambir, Miri and Tukai samples are listed in Table 5.6, along with the several widely used geochemical ratios. Trace elements such as V, Ni and Cr in sediments are sensitive indicators of paleo-redox conditions and may allow oxic, dysoxic and anoxic depositional settings to be identified (Galarraga et al., 2008). Vanadium (V) is usually enriched in comparison with Nickel (Ni) in suboxic to anoxic marine environments (Barwise, 1990; Peters and Moldowan, 1993). The concentration of vanadium (V) is higher than nickel (Ni) in all the analyzed samples (Table 5.6) indicating the prevalence of alternating oxic and anoxic conditions in the study area. Cobalt and Scandium are in much lower concentration in all the analysed samples except for high Cobalt concentrations recorded in some of Miri Formation samples and that indicate prevailing oxic conditions during deposition. These results are discussed in the context of paleoenvironment in the next chapter.

Table 5.5. Source and maturity parameters derived from n-alkanes, isoprenoids and phenanthrenes.

| | Sample ID | n-alkane and Isoprenoids | | | | | Phenanthrenes | | | |
|------------------|-------------------|--------------------------|----------------------|----------------------|------|------|---------------|------|--------------|-------|
| | | Pr/Ph | Pr/n-C ₁₇ | Ph/n-C ₁₈ | CPI | OEP | TAR | Paq | 9MP/9M P+1MP | MPI-1 |
| Deltaic Sequence | Tukau Formation | | | | | | | | | |
| | T-03-SH | 3.16 | 2.76 | 0.68 | 1.78 | 1.76 | 1.96 | 0.34 | 0.50 | 0.44 |
| | T-04-SH | 2.86 | 2.19 | 0.71 | 1.31 | 1.34 | 2.86 | 0.42 | 0.54 | 0.42 |
| | T-06-SH | 3.20 | 1.71 | 0.75 | 1.80 | 1.82 | 2.40 | 0.32 | 0.62 | 0.44 |
| | T-07-SH | 2.89 | 2.14 | 0.95 | 1.96 | 1.96 | 2.52 | 0.40 | 0.44 | 0.42 |
| | T-09-SH | 2.24 | 1.18 | 0.86 | 2.24 | 2.20 | 2.65 | 0.36 | 0.58 | 0.40 |
| | Miri Formation | | | | | | | | | |
| | M-02-SH | 1.43 | 1.52 | 0.65 | 1.23 | 1.30 | 2.54 | 0.40 | 0.52 | 0.48 |
| | M-03-SH | 3.25 | 2.4 | 0.63 | 1.50 | 1.48 | 1.98 | 0.40 | 0.50 | 0.42 |
| | M-06-SH | 2.25 | 1.42 | 0.64 | 1.67 | 1.68 | 1.84 | 0.38 | 0.48 | 0.46 |
| | M-07-SH | 2.74 | 2.60 | 0.72 | 1.28 | 1.28 | 1.75 | 0.36 | 0.63 | 0.46 |
| | M-09-SH | 1.84 | 2.27 | 0.86 | 2.54 | 2.48 | 2.02 | 0.40 | 0.52 | 0.42 |
| | Lambir Formation | | | | | | | | | |
| | L-03-SH | 2.54 | 1.21 | 0.58 | 1.75 | 1.70 | 2.81 | 0.38 | 0.56 | 0.41 |
| | L-06-SH | 2.43 | 2.8 | 0.76 | 1.50 | 1.50 | 2.32 | 0.34 | 0.64 | 0.43 |
| | L-07-SH | 3.21 | 2.54 | 0.83 | 2.20 | 2.22 | 2.46 | 0.40 | 0.72 | 0.45 |
| | L-10-SH | 3.20 | 2.31 | 0.8 | 1.74 | 1.70 | 2.08 | 0.38 | 0.58 | 0.44 |
| | L-11-SH | 2.95 | 1.64 | 0.82 | 1.66 | 1.68 | 2.24 | 0.38 | 0.50 | 0.42 |
| | Belait Formation | | | | | | | | | |
| | BL-A2-SH | 2.54 | 1.1 | 0.8 | 1.93 | 2.10 | 2.01 | 0.40 | 0.42 | 0.48 |
| | BL-A3-SH | 2.9 | 0.91 | 0.49 | 1.65 | 1.75 | 1.75 | 0.42 | 0.52 | 0.46 |
| | BL-A5-SS | 2.72 | 1.3 | 0.56 | 1.89 | 1.83 | 1.96 | 0.38 | 0.43 | 0.45 |
| | BL-A6-SS | 2.68 | 1.65 | 0.86 | 2.03 | 2.01 | 1.78 | 0.42 | 0.56 | 0.48 |
| | BL-A7-SH | 2.54 | 1.05 | 0.45 | 2.04 | 2.06 | 1.31 | 0.40 | 0.58 | 0.46 |
| | BL-A8-SS | 3.82 | 1.39 | 0.61 | 1.89 | 1.78 | 2.76 | - | - | - |
| | BL-B1-SH | 2.5 | 1.37 | 0.48 | 1.23 | 1.25 | 1.86 | 0.45 | 0.52 | 0.48 |
| | BL-C2-SH | 4.2 | 3.1 | 0.67 | 1.71 | 1.72 | 2.54 | - | - | - |
| | Meligan Formation | | | | | | | | | |
| | ME-130B-SH | 2.86 | 1.08 | 0.39 | 1.01 | 1.00 | 1.98 | 0.48 | 0.62 | 0.85 |
| | ME-130C-SS | 2.8 | 0.86 | 0.15 | 1.01 | 0.98 | 1.72 | - | - | - |
| | ME-130F-SH | 2.84 | 1.72 | 0.53 | 1.01 | 1.00 | 1.84 | 0.45 | 0.53 | 0.76 |
| | ME-133A-SS | 3.04 | 1.39 | 0.43 | 0.99 | 0.92 | 2.01 | 0.43 | 0.42 | 0.7 |
| | ME-133C-SH | 2.12 | 0.7 | 0.15 | 1.00 | 0.99 | 1.96 | 0.43 | 0.50 | 0.74 |
| | ME-134A-SH | 3.6 | 1.07 | 0.36 | 1.00 | 1.00 | 2.34 | 0.43 | 0.43 | 0.7 |

Table 5.5. Source and maturity parameters derived from n-alkanes, isoprenoids and phenanthrenes (Continuation).

| | Sample ID | n-alkane and Isoprenoids | | | | | | Phenanthrenes | | |
|------------------------|-----------------------------------|--------------------------|----------------------|----------------------|------|------|------|---------------|--------------|-------|
| | | Pr/Ph | Pr/n-C ₁₇ | Ph/n-C ₁₈ | CPI | OEP | TAR | Paq | 9MP/9M P+1MP | MPI-1 |
| Submarine Fan Sequence | <i>Temburong Formation</i> | | | | | | | | | |
| | TEM-137A-SH | 1.21 | 0.98 | 0.58 | 0.98 | 0.99 | 1.84 | 0.45 | 0.38 | 1.1 |
| | TEM-137B-SS | 1.42 | 0.40 | 0.12 | 1.00 | 0.9 | 1.52 | 0.48 | 0.38 | 1.1 |
| | TEM-138-SH | 1.6 | 0.55 | 0.22 | 0.98 | 1.00 | 1.48 | 0.46 | 0.36 | 1.08 |
| | TEM-139-SH | 1.28 | 0.65 | 0.24 | 1.01 | 1.00 | 1.5 | 0.35 | 0.34 | 1.14 |
| | TEM-139-SS | 1.34 | 0.73 | 0.47 | 0.99 | 1.00 | 1.62 | - | - | - |
| | TEM-140-SH | 1.42 | 0.82 | 0.5 | 1.01 | 1.2 | 1.48 | - | - | - |
| | <i>West Crocker Formation</i> | | | | | | | | | |
| | WC-129B-SH | 1.74 | 1.9 | 0.85 | 0.9 | 0.9 | 1.65 | 0.36 | 0.38 | 0.8 |
| | WC-129E-MTD | 1.62 | 1.75 | 0.76 | 0.98 | 0.99 | 1.62 | 0.37 | 0.39 | 0.99 |
| | WC-129D-MTD | 1.48 | 0.86 | 0.33 | 0.99 | 0.98 | 1.82 | 0.37 | 0.35 | 0.92 |
| | WC-129F-MTD | 1.34 | 1.15 | 0.68 | 0.99 | 0.99 | 1.46 | 0.35 | 0.34 | 0.9 |
| | WC-135B-SS | 2.7 | 1.33 | 0.41 | 1.01 | 0.99 | 1.54 | 0.36 | 0.36 | 0.99 |
| | WC-144A-MTD | 1.7 | 0.56 | 0.18 | 1.01 | 1.01 | 1.68 | 0.45 | 0.36 | 0.89 |
| | WC-144B-SH | 1.42 | 0.72 | 0.28 | 1.01 | 1.01 | 1.78 | - | - | - |
| | WC-145A-SS | 1.38 | 1.21 | 0.62 | 0.99 | 0.99 | 1.24 | - | - | - |
| | WC-145B-MTD | 1.62 | 1.1 | 0.52 | 1.00 | 1.00 | 1.62 | - | - | - |
| | WC-145C-SH | 1.72 | 0.98 | 0.62 | 1.01 | 0.99 | 1.48 | - | - | - |
| | <i>Undifferentiated Formation</i> | | | | | | | | | |
| | UD-01-SS | 1.84 | 1.54 | 0.86 | 1.54 | 1.52 | 1.60 | 0.40 | 0.42 | 0.45 |
| | UD-02-SS | 1.58 | 1.23 | 0.62 | 1.48 | 1.46 | 1.78 | 0.42 | 0.46 | 0.48 |

Pr:pristane

Ph: phythane

CPI: carbon preference index

OEP: odd-even predominance

TAR: terrigenous-aquatic ratio

Paq= nC₂₃ + nC₂₅/ nC₂₃ + nC₂₅ + nC₂₉ + nC₃₁ – Alkanes

MPI-1 = 1.5 (2-MP + 3-MP)/ 0.69P + 1-MP + 9-MP

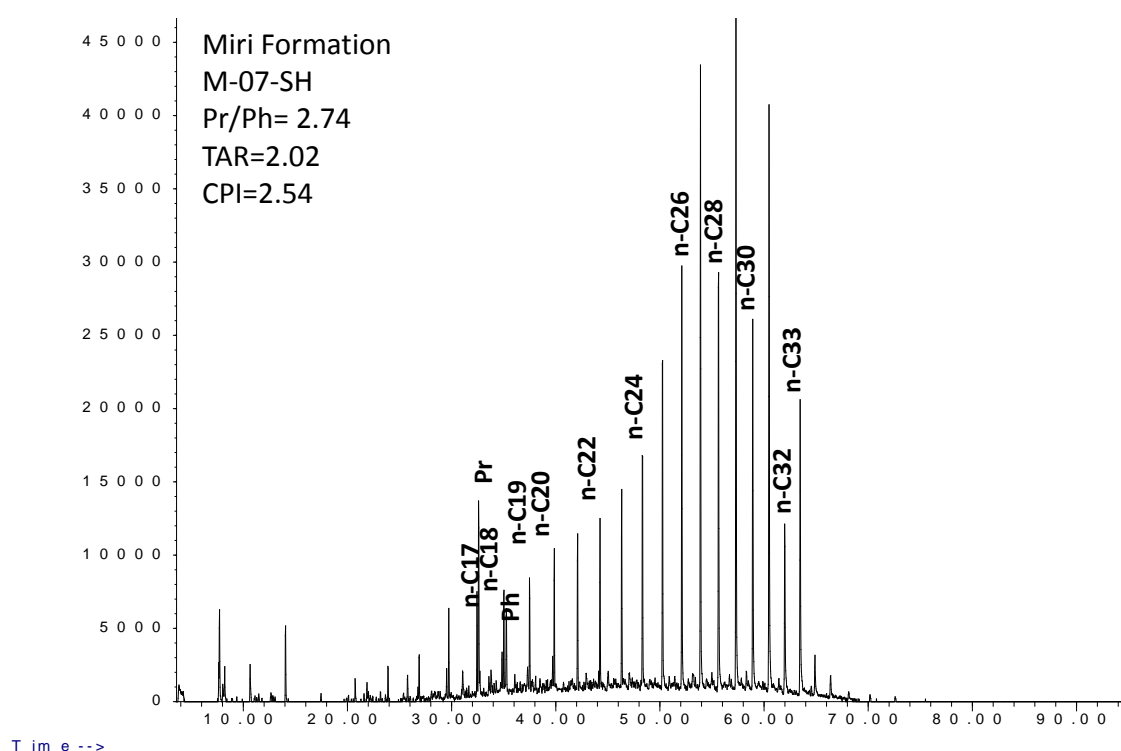
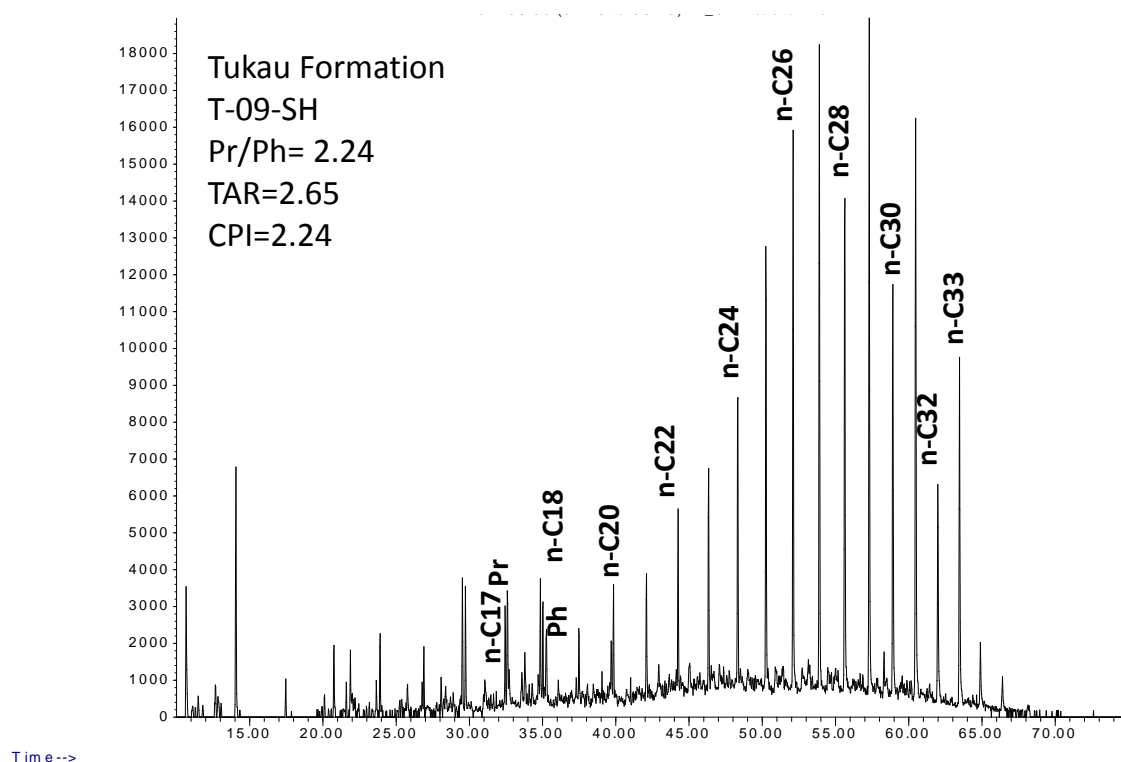


Figure 5.11. Representative m/z 85 fragmentogram showing the distribution of n-alkanes and isoprenoids.

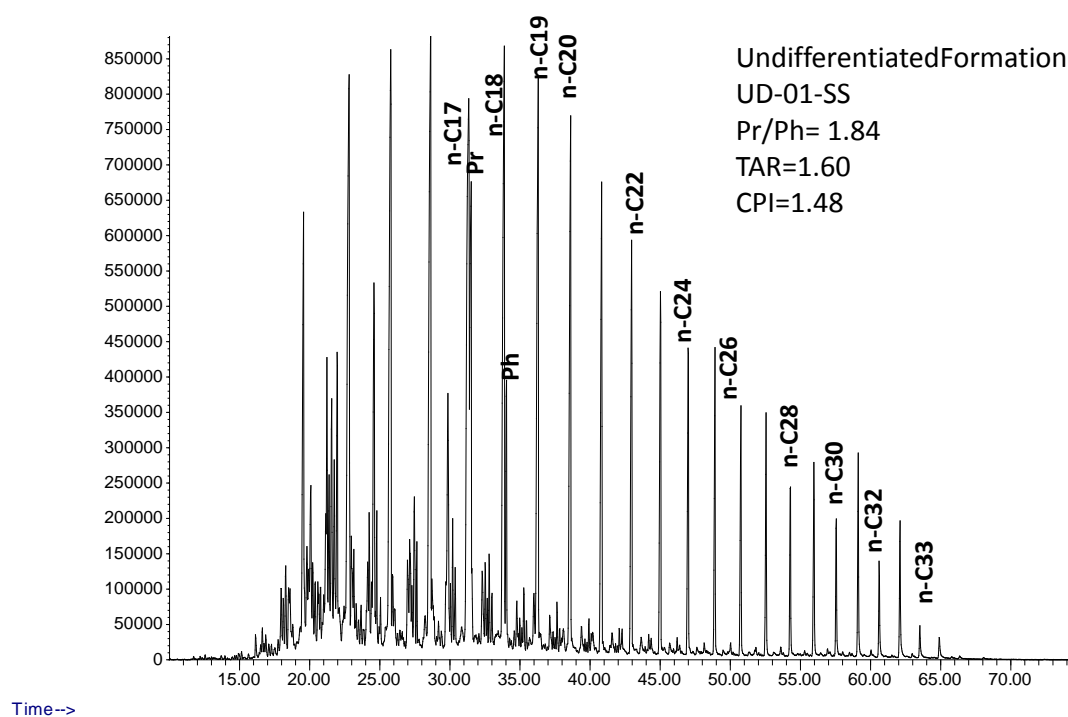
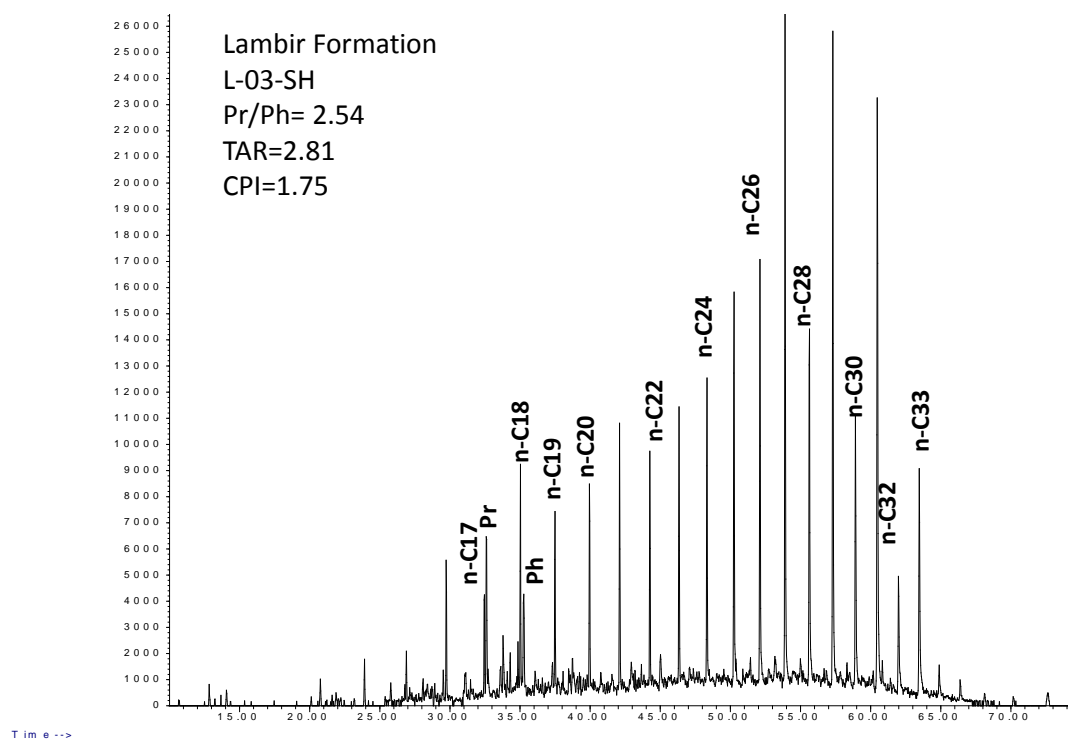


Figure 5.11. Representative m/z 85 fragmentogram showing the distribution of n-alkanes and isoprenoids (cont.).

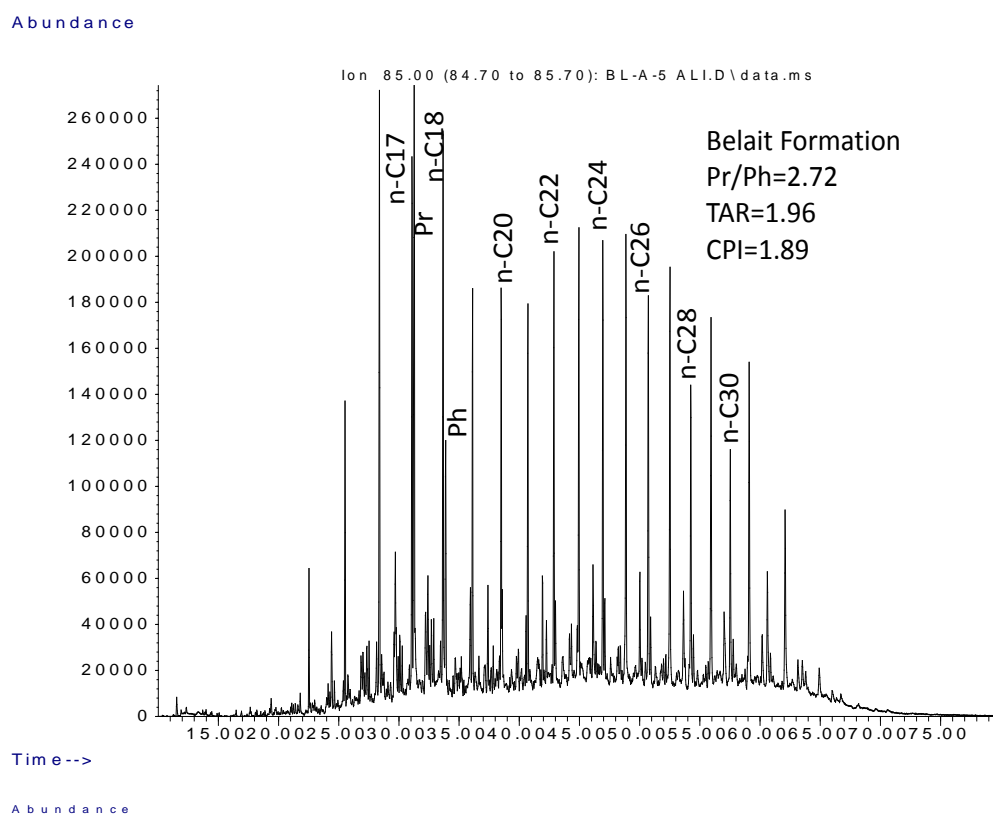
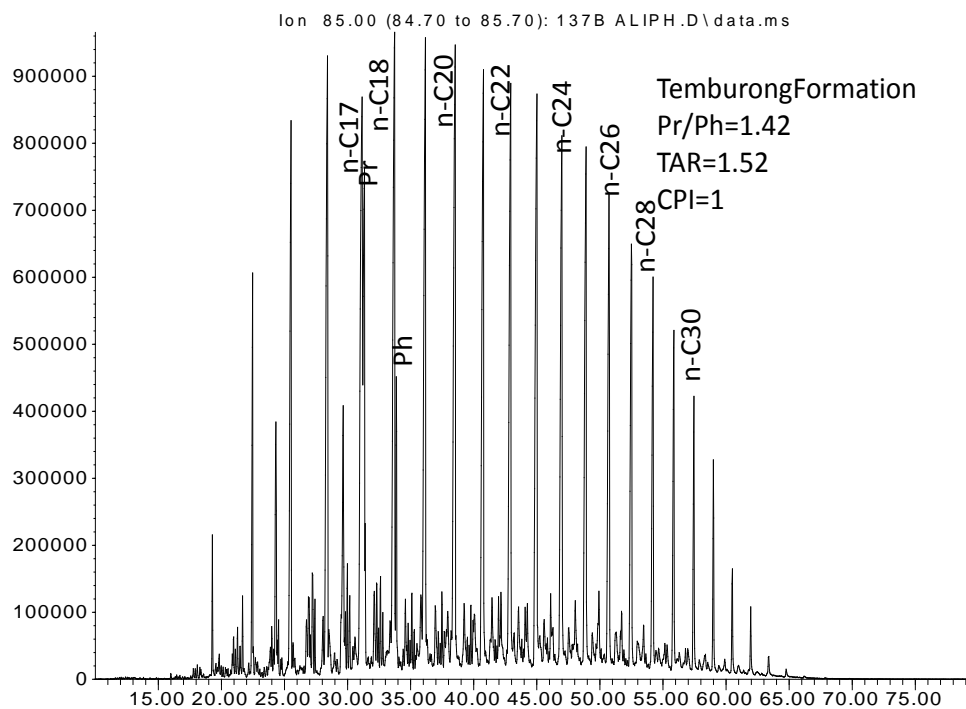


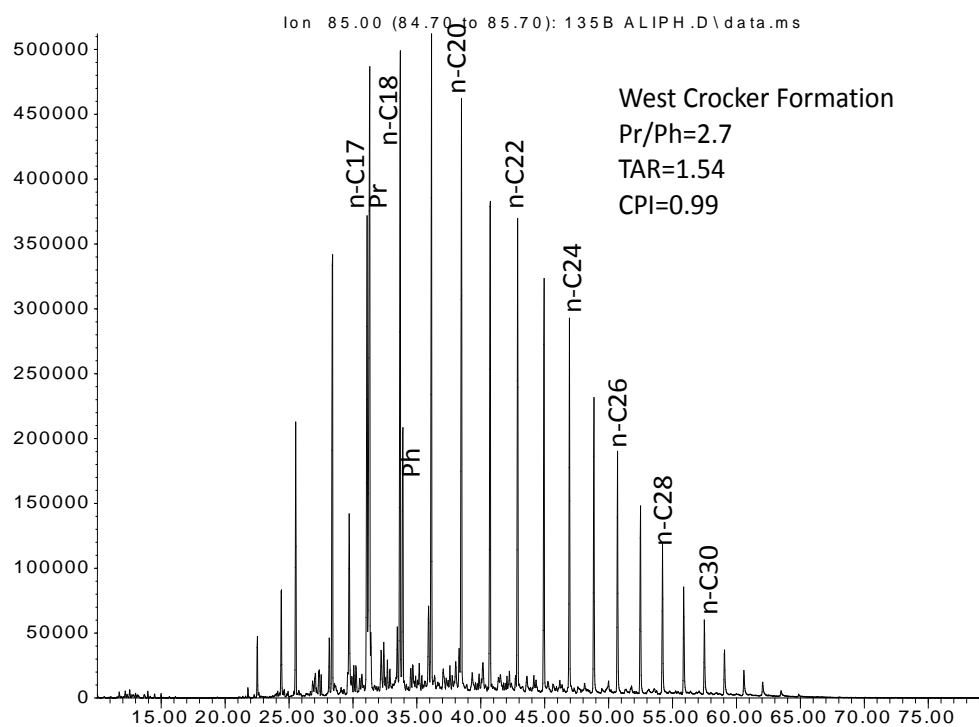
Figure 5.11. Representative m/z 85 fragmentogram showing the distribution of n-alkanes and isoprenoids (cont.).

Abundance



Time-->

Abundance



Time-->

Figure 5.11. Representative m/z 85 fragmentogram showing the distribution of n-alkanes and isoprenoids (cont.).

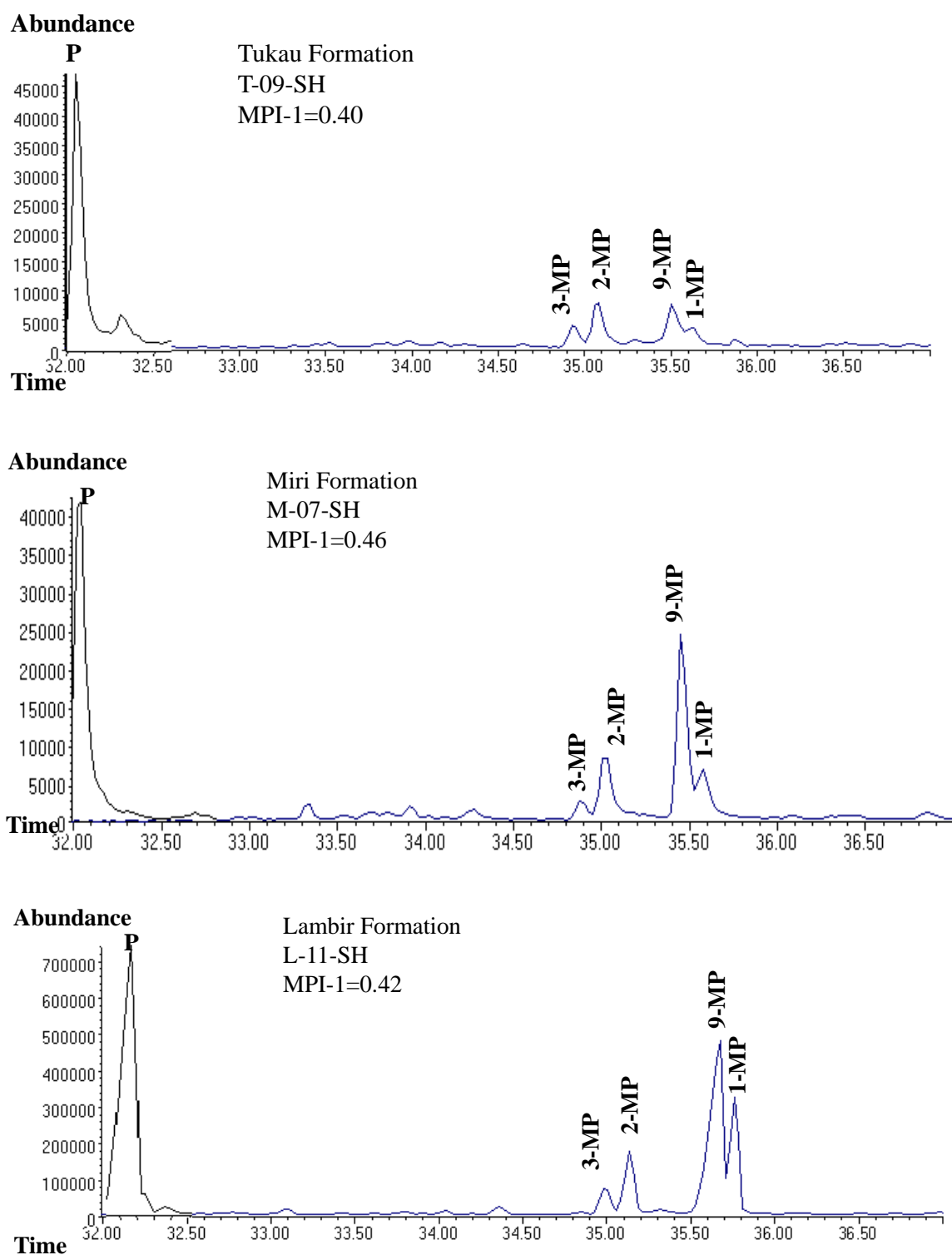


Figure 5.12. m/z 178 +192 fragmentograms showing the distribution of phenanthrenes (P) and methyl-phenanthrenes (MP) in the studied formations.

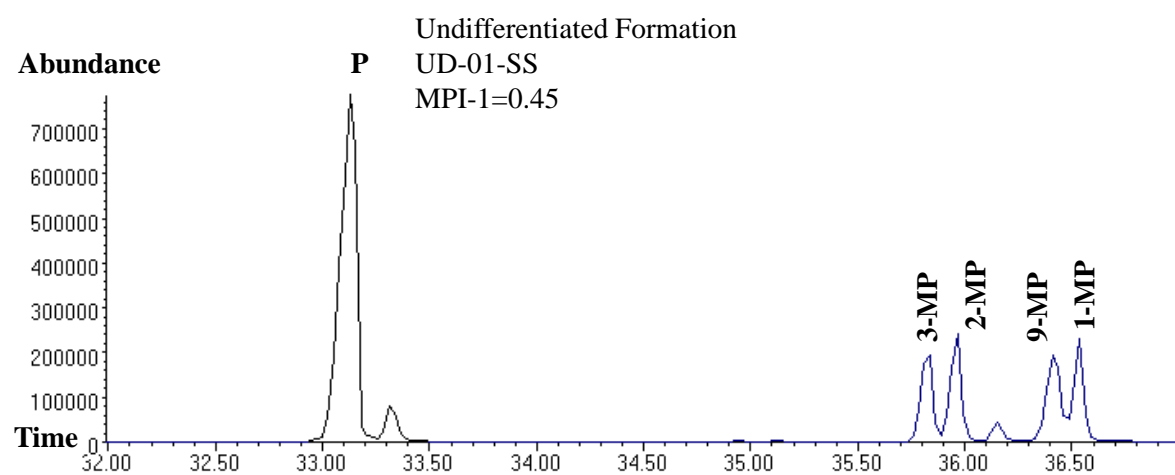
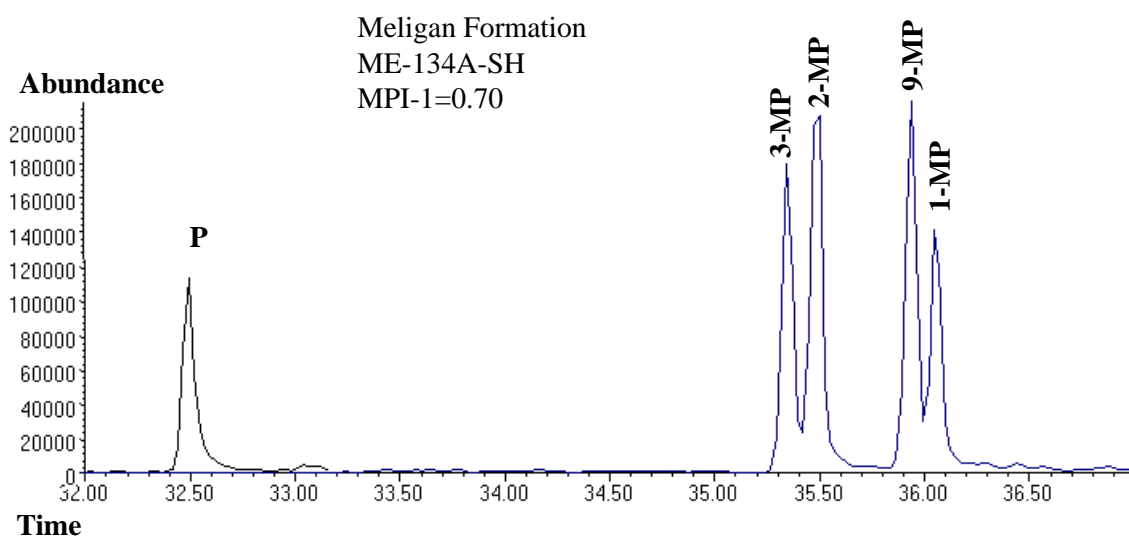
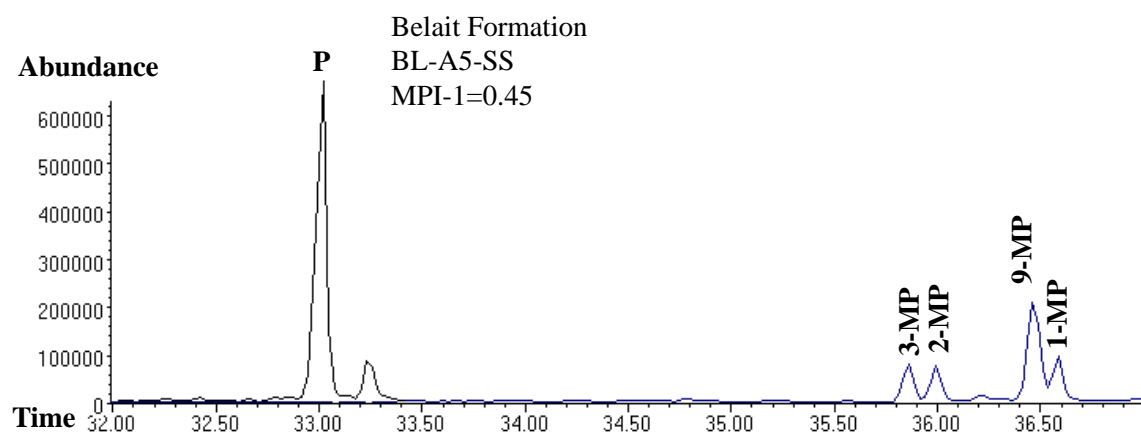


Figure 5.12. m/z 178 + 192 fragmentograms showing the distribution of phenanthrenes (P) and methyl-phenanthrenes (MP) in the studied formations (cont.).

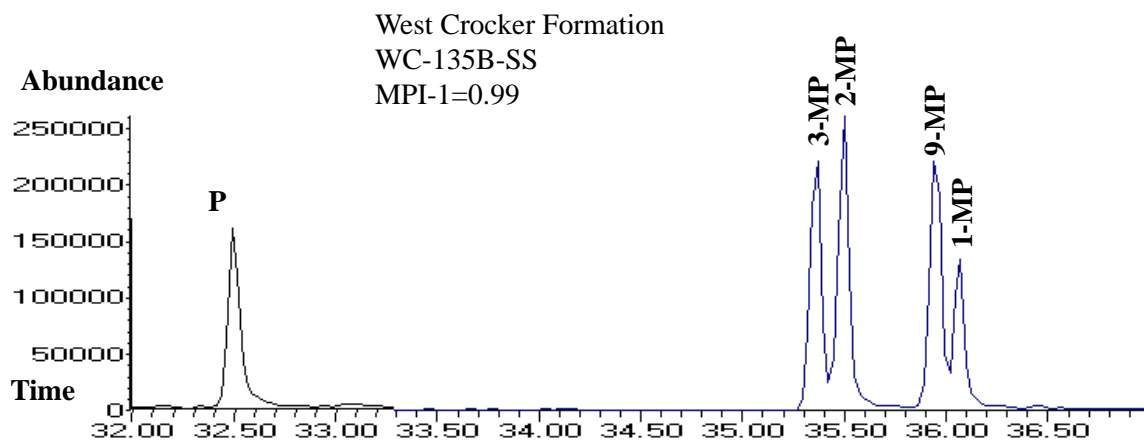
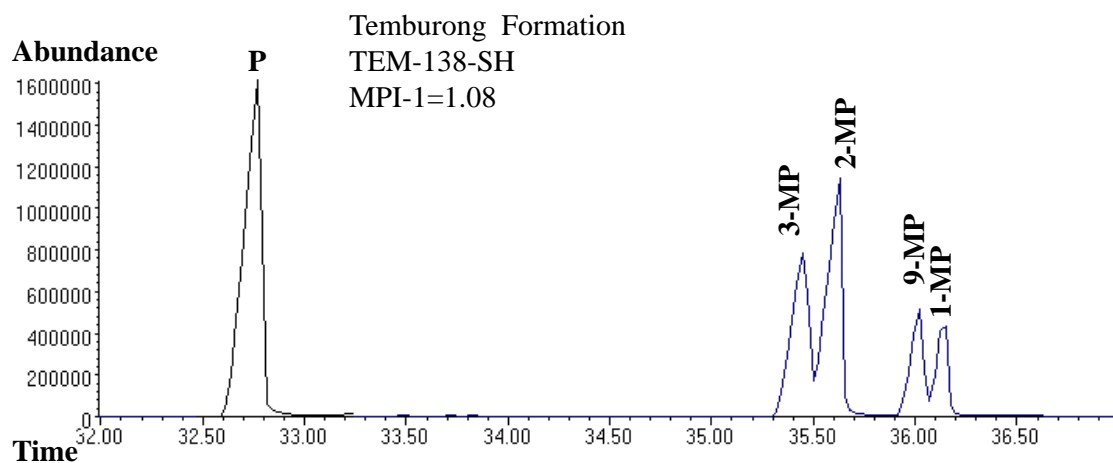


Figure 5.12. m/z 178 +192 fragmentograms showing the distribution of phenanthenes (P) and methyl-phenanthenes (MP) in the studied formations (cont.).

Table 5.6. Trace elements concentrations and ratios in the studied samples.

| | Sample ID | V | Ni | Cr | Co | Sc | V/Ni | V/Cr | V/Sc | Ni/Co |
|------------------|--------------------------|-------|-------|-------|-------|------|------|------|-------|-------|
| Deltaic Sequence | <i>Tukau Formation</i> | | | | | | | | | |
| | T-03-SH | 60.21 | 25.02 | 24.69 | 4.98 | 4.2 | 2.40 | 2.43 | 14.29 | 5.02 |
| | T-04-SH | 48.19 | 31.89 | 31.58 | 11.64 | 4.24 | 1.50 | 1.52 | 11.32 | 2.75 |
| | T-06-SH | 46.09 | 26.05 | 20.54 | 5.16 | 4.56 | 1.77 | 2.24 | 10.09 | 5.04 |
| | T-07-SH | 50.34 | 39.87 | 30.86 | 13.38 | 3.26 | 1.25 | 1.62 | 15.34 | 2.99 |
| | T-09-SH | 36.48 | 18.02 | 16.82 | 3.49 | 4.24 | 2.00 | 2.14 | 8.49 | 5.16 |
| | <i>Miri Formation</i> | | | | | | | | | |
| | M-02-SH | 38.21 | 28.05 | 17.59 | 13.59 | 3.42 | 1.36 | 2.16 | 11.11 | 2.06 |
| | M-03-SH | 54.25 | 32.03 | 20.69 | 15.69 | 3.9 | 1.69 | 2.61 | 13.85 | 2.04 |
| | M-06-SH | 48.34 | 31.98 | 40.00 | 14.29 | 4.2 | 1.50 | 1.20 | 11.43 | 2.24 |
| | M-07-SH | 45.12 | 26.79 | 21.95 | 4.99 | 4.82 | 1.73 | 2.05 | 9.34 | 5.21 |
| | M-09-SH | 50.04 | 30.28 | 33.78 | 12.50 | 4.65 | 1.67 | 1.48 | 10.75 | 2.40 |
| | <i>Lambir Formation</i> | | | | | | | | | |
| | L-03-SH | 48.06 | 17.96 | 18.46 | 3.46 | 3.86 | 2.67 | 2.60 | 12.44 | 5.20 |
| | L-06-SH | 42.03 | 23.83 | 17.50 | 4.63 | 3.80 | 1.75 | 2.40 | 11.05 | 5.18 |
| | L-07-SH | 26.05 | 17.78 | 17.57 | 6.29 | 4.52 | 1.44 | 1.48 | 5.75 | 2.86 |
| | L-10-SH | 48.04 | 24.86 | 21.72 | 11.06 | 3.72 | 1.92 | 2.21 | 12.90 | 2.26 |
| | L-11-SH | 30.15 | 16.02 | 26.32 | 5.37 | 3.24 | 1.88 | 1.14 | 9.26 | 2.98 |
| | <i>Belait Formation</i> | | | | | | | | | |
| | BL-A2-SH | 48.46 | 24.70 | 23.76 | 4.75 | 3.72 | 1.96 | 2.04 | 13.02 | 5.20 |
| | BL-A3-SH | 46.83 | 24.40 | 18.70 | 4.80 | 3.52 | 1.92 | 2.50 | 13.30 | 5.08 |
| | BL-A5-SST | 44.34 | 20.24 | 13.02 | 7.41 | 4.57 | 2.19 | 3.41 | 9.71 | 2.73 |
| | BL-A6-SST | 52.06 | 20.97 | 16.25 | 3.99 | 2.77 | 2.48 | 3.20 | 18.82 | 5.26 |
| | BL-A7-SH | 25.16 | 15.00 | 17.24 | 3.41 | 3.18 | 1.68 | 1.46 | 7.91 | 4.40 |
| | BL-A8-SST | 30.80 | 20.00 | 16.92 | 4.35 | 3.72 | 1.54 | 1.82 | 8.28 | 4.60 |
| | BL-B1-SH | 48.26 | 20.34 | 22.64 | 4.18 | 4.03 | 2.37 | 2.13 | 11.96 | 4.86 |
| | BL-C2-SH | 32.84 | 24.30 | 26.00 | 4.99 | 4.57 | 1.35 | 1.26 | 7.19 | 4.87 |
| | <i>Meligan Formation</i> | | | | | | | | | |
| | ME-130B-SH | 35.34 | 22.00 | 20.83 | 4.94 | 4.27 | 1.61 | 1.70 | 8.28 | 4.45 |
| | ME-130C-SS | 36.43 | 19.00 | 18.18 | 3.89 | 3.96 | 1.92 | 2.00 | 9.21 | 4.89 |
| | ME-130F-SS | 27.34 | 15.00 | 15.70 | 3.74 | 3.13 | 1.82 | 1.74 | 8.75 | 4.01 |
| | ME-133A-SS | 35.45 | 22.00 | 18.82 | 4.44 | 3.91 | 1.61 | 1.88 | 9.05 | 4.96 |
| | ME-133C-SH | 45.26 | 24.00 | 23.44 | 4.74 | 4.99 | 1.89 | 1.93 | 9.07 | 5.06 |
| | ME-134A-SH | 38.50 | 21.70 | 19.15 | 5.45 | 4.32 | 1.77 | 2.01 | 8.92 | 3.98 |

Table 5.6. Trace concentrations and ratios in the studied samples (Continuation).

| | Sample ID | V | Ni | Cr | Co | Sc | V/Ni | V/Cr | V/Sc | Ni/Co |
|---------------|-----------------------------------|-------|-------|-------|------|------|------|------|-------|-------|
| Submarine Fan | <i>Temburong Formation</i> | | | | | | | | | |
| | TE-137A-SH | 43.45 | 18.20 | 10.63 | 4.08 | 2.34 | 2.39 | 4.09 | 18.53 | 4.46 |
| | TE-137B-SS | 50.28 | 26.00 | 17.30 | 4.19 | 3.02 | 1.93 | 2.91 | 16.67 | 6.20 |
| | TE-138-SH | 40.14 | 18.20 | 13.99 | 2.87 | 2.82 | 2.21 | 2.87 | 14.25 | 6.34 |
| | TE-139-SH | 58.74 | 26.77 | 27.87 | 3.89 | 3.62 | 2.19 | 2.11 | 16.22 | 6.88 |
| | TE-139-SS | 54.28 | 24.11 | 19.15 | 4.10 | 3.06 | 2.25 | 2.83 | 17.73 | 5.88 |
| | TE-140-SH | 49.26 | 21.46 | 17.79 | 3.41 | 2.97 | 2.30 | 2.77 | 16.58 | 6.29 |
| | <i>West Crocker Formation</i> | | | | | | | | | |
| | WC-129B-SH | 84.45 | 33.87 | 29.37 | 5.21 | 4.23 | 2.49 | 2.88 | 19.95 | 6.50 |
| | WC-129E-MTD | 75.04 | 30.12 | 27.17 | 4.64 | 3.99 | 2.49 | 2.76 | 18.81 | 6.49 |
| | WC-129D-MTD | 45.21 | 22.90 | 17.44 | 3.35 | 2.61 | 1.97 | 2.59 | 17.30 | 6.84 |
| | WC-129F-MTD | 68.74 | 33.01 | 25.00 | 5.19 | 3.51 | 2.08 | 2.75 | 19.59 | 6.36 |
| | WC-135B-SST | 66.32 | 30.84 | 23.91 | 5.28 | 3.40 | 2.15 | 2.77 | 19.51 | 5.84 |
| | WC-144A-MTD | 70.24 | 28.00 | 22.29 | 4.51 | 3.90 | 2.51 | 3.15 | 18.02 | 6.21 |
| | WC-144B-SH | 52.28 | 23.70 | 14.69 | 3.49 | 2.61 | 2.21 | 3.56 | 20.03 | 6.80 |
| | WC-145A-SST | 68.80 | 30.63 | 20.66 | 4.91 | 3.89 | 2.25 | 3.33 | 17.69 | 6.24 |
| | WC-145B-MTD | 84.60 | 43.30 | 34.53 | 6.83 | 4.99 | 1.95 | 2.45 | 16.94 | 6.34 |
| | WC-145C-SH | 69.12 | 33.17 | 17.93 | 5.18 | 3.49 | 2.08 | 3.86 | 19.80 | 6.40 |
| | <i>Undifferentiated Formation</i> | | | | | | | | | |
| | UD-01-SS | 67.82 | 20.19 | 28.26 | 5.78 | 3.46 | 3.36 | 2.40 | 19.60 | 3.49 |
| | UD-02-SS | 64.76 | 22.34 | 24.30 | 5.30 | 3.86 | 2.90 | 2.67 | 16.78 | 4.21 |

V: Vanadium

Ni: Nickel

Cr: Chromium

Co: Cobalt

Sc: Scandium

CHAPTER 6

DISCUSSION

6.1 Introduction

This chapter discusses the integration of petrographical and geochemical data to interpret the source rock characteristics, as well as the source and preservation of the organic matter in the studied sequences. Greater emphasis been given in comparing sandy and shaly facies.

6.2 Source Rock Evaluation

Source rocks are capable of generating petroleum (Tissot and Welte, 1984). Source rock evaluation consists of assessing the hydrocarbon generating potential of sediments by evaluating their capacity for hydrocarbon generation, the type of organic matter, what hydrocarbons might be generated, thermal maturity and how it influences generation and expulsion (Dembicki, 2009). The source rock characteristics of the studied deltaic and submarine fan sequences is discussed based on organic richness (quantity), type of kerogen and potential hydrocarbon (oil and/or gas) and thermal maturity.

6.2.1 Organic matter richness and hydrocarbon generative potential

The organic richness of a rock is usually expressed as the total organic carbon (TOC) content in wt%. The minimum acceptable TOC value for clastic type rocks indicating good source potential is 1.0% (Peters and Cassa, 1994., Hunt, 1996).

Deltaic Sequence

The TOC values in most of the samples in the Tukai, Miri, Lambir, Belait and Meligan formations exceed the minimal 1.0 wt.% and thus, in terms of source rock organic richness, the deltaic sequences have good to excellent TOC contents (as defined by Peters and Cassa, 1994; Hunt, 1996). There is variation in TOC content in the shaly and sandy

facies of the deltaic sequences. Most of the sandy facies have higher TOC than the shaly facies with exceptionally high values of 7.87 wt. % and 11.1 wt. % recorded in Belait and Lambir sandy facies respectively. Moreover, the amount of hydrocarbon yield (S_2) generated during pyrolysis is a useful parameter to evaluate the hydrocarbon generation potential of source rocks (Peters, 1986; Bordenave, 1993). Generally, the hydrocarbon (S_2) yields in the deltaic sequence can be regarded as fair to good hydrocarbon generation potential as shown in Figure 6.1. Some sandy facies from the Lambir and Belait Formation have significant higher values of S_2 yield, which implies higher hydrocarbon generative potential (Figure 6.1). The hydrocarbon generative potential in the studied deltaic sequences was also been supported based on extractable organic matter (EOM, ppm) and hydrocarbon yields (Table 5.2). The source rock richness rating is shown in TOC (wt. %) versus hydrocarbon yields crossplot (Figure 6.2), which indicate that most of the samples from Tukai, Miri, Lambir, Belait and Meligan formations have fair to good hydrocarbon generative potential.

Submarine Fan Sequences

There is variation in TOC in the shaly and sandy facies of the submarine fan deposits. Most of the sandy facies in the studied formations have higher TOC than the shaly facies except in the Temburong Formation where the shaly facies have higher TOC content. Most of slump facies samples within the West Crocker Formation show significantly high amount of organic matter and this means they contain more than sufficient organic matter required to be a source rock. The hydrocarbon (S_2) yields in the submarine fan deposits can generally be referred to as poor to fair hydrocarbon generating potential with exceptions to the slump samples and the sandy facies from the undifferentiated formation which shows quite good to excellent hydrocarbon generating characteristics. This is further supported by TOC and hydrocarbon yield (Figure 6.2).

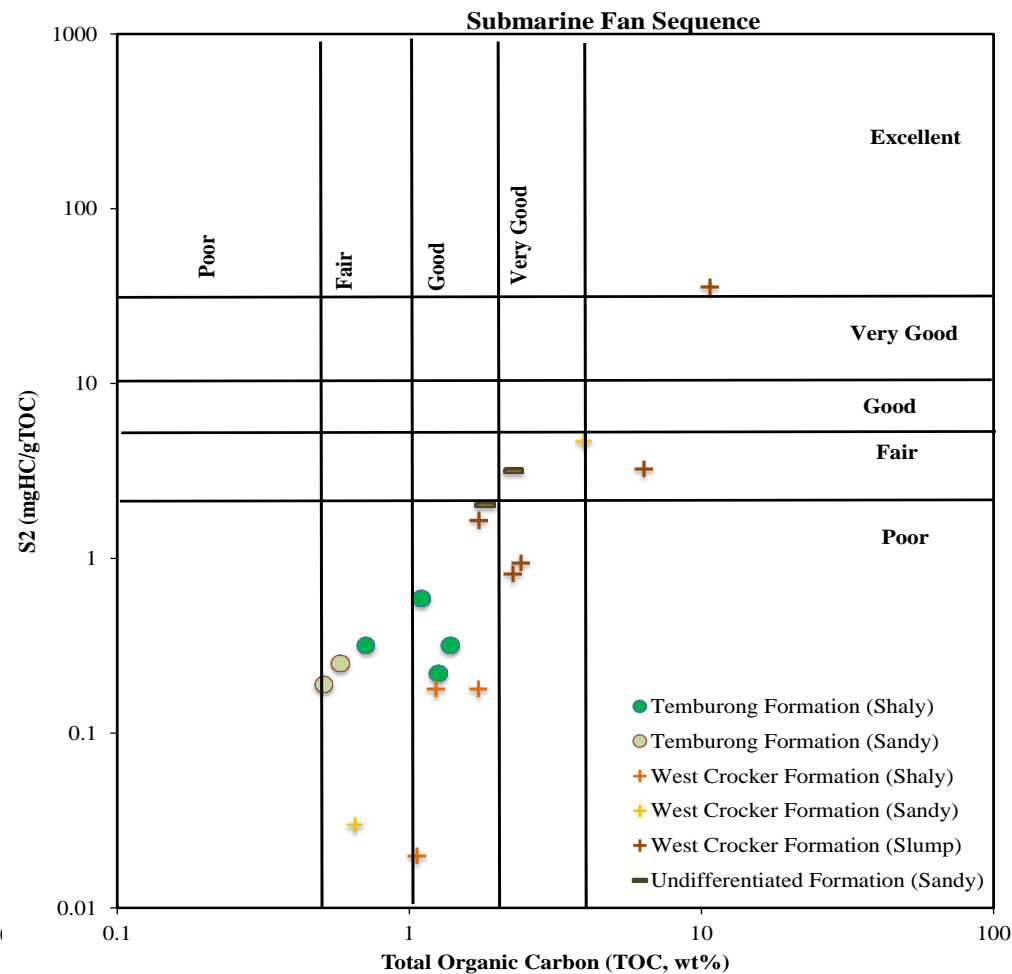
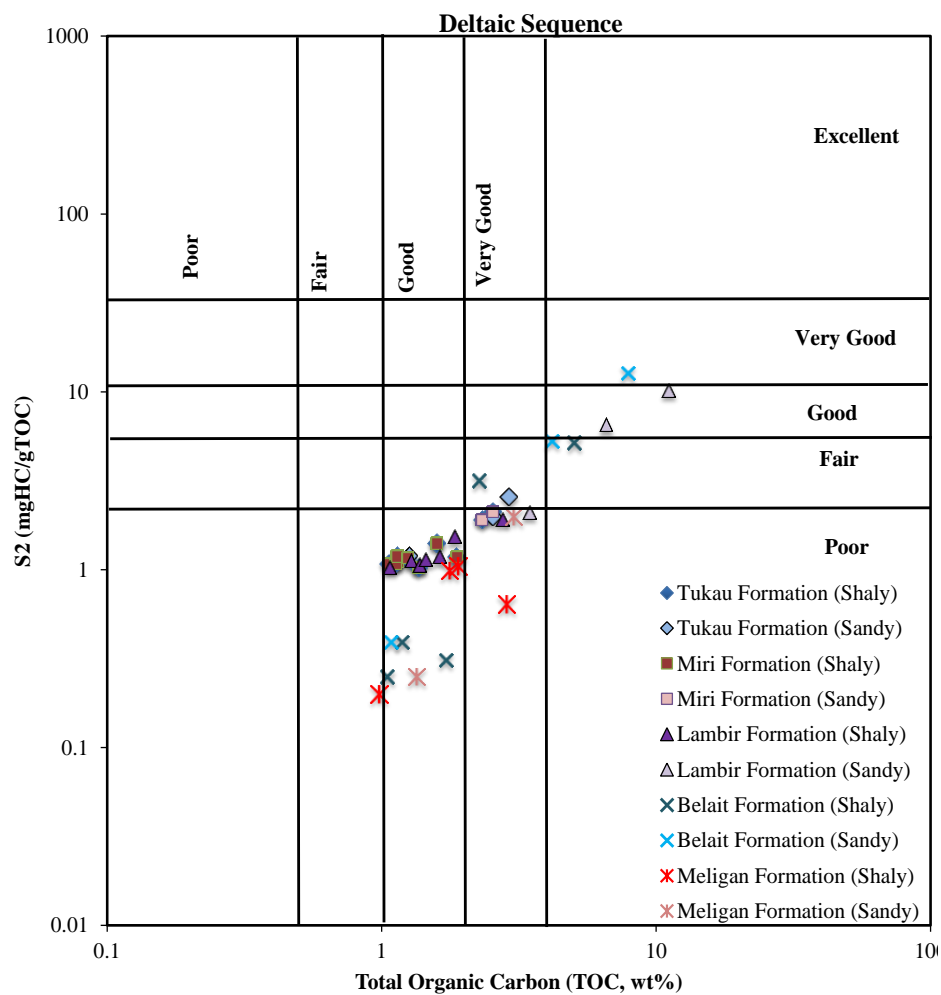


Figure 6.1. Plot of total organic carbon (TOC) versus hydrocarbon yield (S₂) showing the hydrocarbon generative potential of the studied deltaic and submarine fan samples.

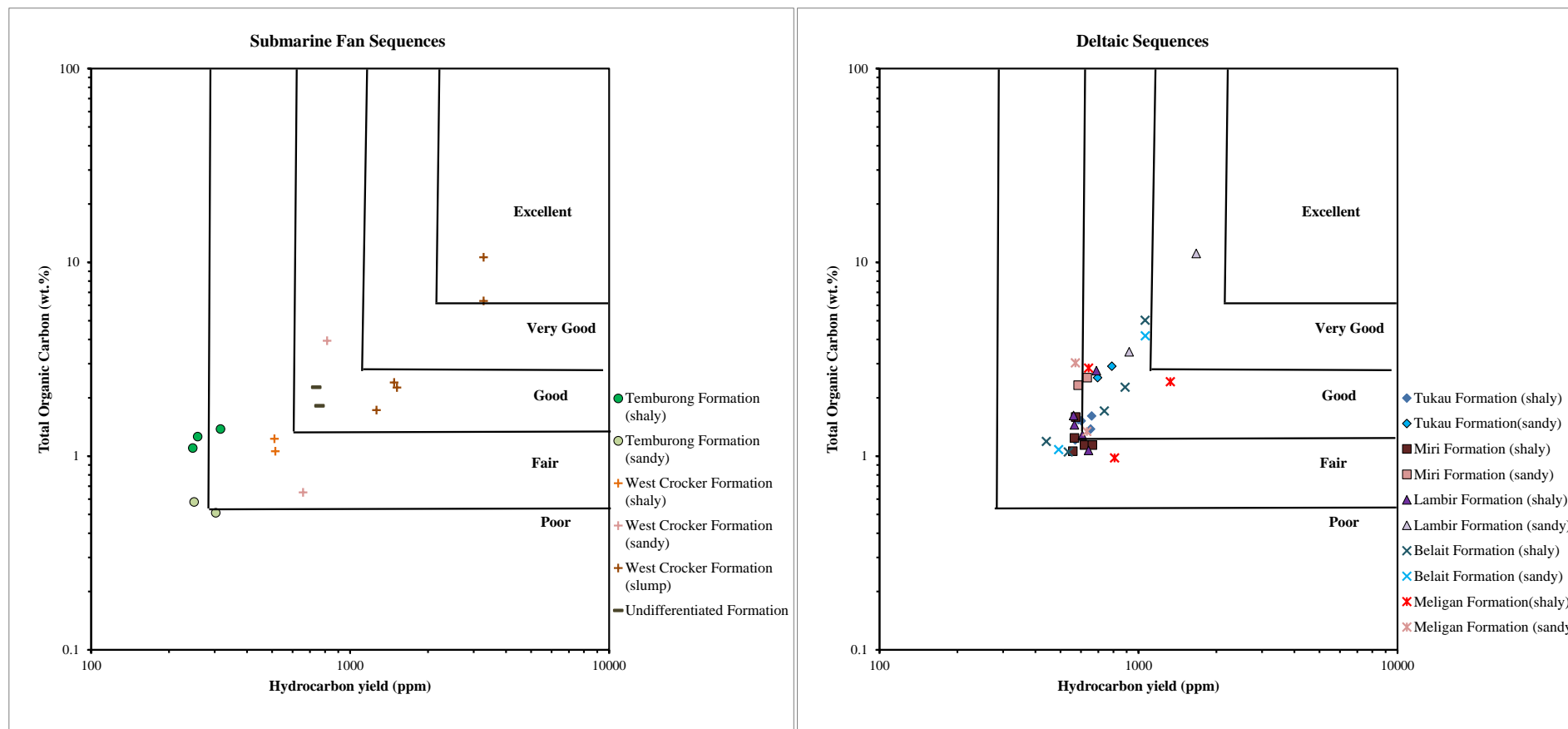


Figure 6.2. Plot of TOC versus hydrocarbon yield plot showing source rock richness and hydrocarbon potential.

6.2.2 Bulk kerogen Characteristics

Bulk kerogen and type were characterized based on pyrolysis (SRA and Py-GC), elemental data and petrographic characteristics.

Deltaic Sequences

A van Krevelen plot of whole rock hydrogen and oxygen indices can be used to classify the dominant type of organic matter in potential source rocks (Bordenave, 1993; Figure 6.3). Most of the samples from Tukai, Miri, Lambir, Belait and Meligan formations plot in the field of Type III kerogen. This suggests that the organic matter in these formations contain predominantly gas prone Type III kerogen. In addition, TOC versus pyrolysis S2 can be used to indicate the type of organic matter (Figure 6.4). Based on this relationship, most of the samples have Type III kerogen. This is further supported by low atomic H/C ratios. The atomic H/C (hydrogen to carbon) ratio of kerogen has been used to assess the quality of organic matter in source rocks. For oil prone source rocks, Type I kerogens have H/C ratios of 1.35-1.50, whereas Type II kerogens have H/C ratios of 1.20-1.35. Gas prone Type III kerogen have H/C ratios <1 while Type IV kerogen has H/C ratios of 0.5 (Baskin, 1997; Killips and Killips, 2005). Most of the analysed samples have low H/C (<1) which is typical of gas prone Type III kerogen.

Pyrolysis (SRA) hydrogen and oxygen indices (HI and OI) does not always accurately represent the types of kerogen present and types of hydrocarbon that may be generated by the source rocks (Dembicki, 2009). The application of SRA technique can provide more accurate assessments of kerogen type when integrated with pyrolysis-gas chromatography (Py-GC) method (Dembicki, 1993 and Dembicki, 2009). The Py-GC analysis provides information regarding the quantitative chemistry of the thermal decomposition products of the kerogen. This gives a direct indicator of the kerogen types

and types of hydrocarbons that can be generated by the kerogen during maturation process (Giraud, 1970; Larter and Douglas, 1980; Horsfield, 1989; Eglinton et. al., 1990; Dembicki, 2009). Bahar and Pelet, (1985) and Dembicki (2009) show clearly how the three main types of kerogen can be distinguished by the carbon number distribution of n-alkanes. These authors stated that Type I kerogen pyrogram contain large amounts of n-alkanes/n-alkenes in C₂₀-C₃₀ range, whereas a Type III pyrogram shows most products in the <C₁₀ fraction. The fingerprint observed in the analysed kerogen samples from the studied formations indicates the dominance of gas prone Type III kerogen characterized by dominance of aromatic compounds over n-alkane/alkene doublets.

The relative percentages of three pyrolysate components (*m,p*-xylene, phenol and *n*-octene) were used to define kerogen type using the diagram of Figure 6.5 as defined by Larter (1984). These three pyrolysate components represent the aliphatic and aromatic structures within the macromolecular organic matter. Based on the relative abundance of the three pyrolysate components (*m,p*-xylene, phenol and *n*-octene), the majority of the analysed samples fall within the field of the Type III kerogen (Figure 6.5), consistent with their HI indices. Thus provide further support that the Type III is the main organofacies within the deltaic samples.

The kerogen composition of the Tukai, Miri, Lambir, Belait and Meligan formations samples has also been evaluated by petrographic examination. The phytoclasts consist predominantly of vitrinitic material with low-common occurrence of liptinite and inertinite macerals. Based on the type of organic matter under reflected light microscopy, a high proportion of Type III kerogen was observed as illustrated in Figure 6.6.

Submarine Fan

Type III and IV kerogens are the dominant kerogen types within the studied formations except for a slump sample in the West Crocker Formation with HI value of 337 mg HC/g TOC indicative of Type II kerogen. The type of kerogen has also been classified using the modified van Krevelen diagram (Figure 6.3) and S_2 versus TOC plot as shown in Fig.6.4. This is further supported by the dominance of terrestrially derived woody phytoclasts in the studied formations as discussed

The Py-GC fingerprints observed in the analysed kerogen samples from the studied formations indicates the dominance of gas prone Type III kerogen characterized by dominance of aromatic compounds over n-alkane/alkene doublets with exception to Temburong Formation which shows Type IV kerogen fingerprints which may be due to the effect of low grade metamorphism on the organic matter. It is interesting to note that the slumps from the West Crocker Formation display Type II kerogen with dominance of n-alkene/alkane doublets over aromatic compounds. This is further supported by the ternary diagram as defined by Larter(1984) that has been applied to assess the kerogen characteristics by using the relative percentage of three pyrolysates compounds (m-p-xylene, phenol, and n-octene)(Figure 6. 5 and 6.6). The dominance of kerogen Type III is further supported by a ternary plot of the three main macerals as shown in Figure 6.6.

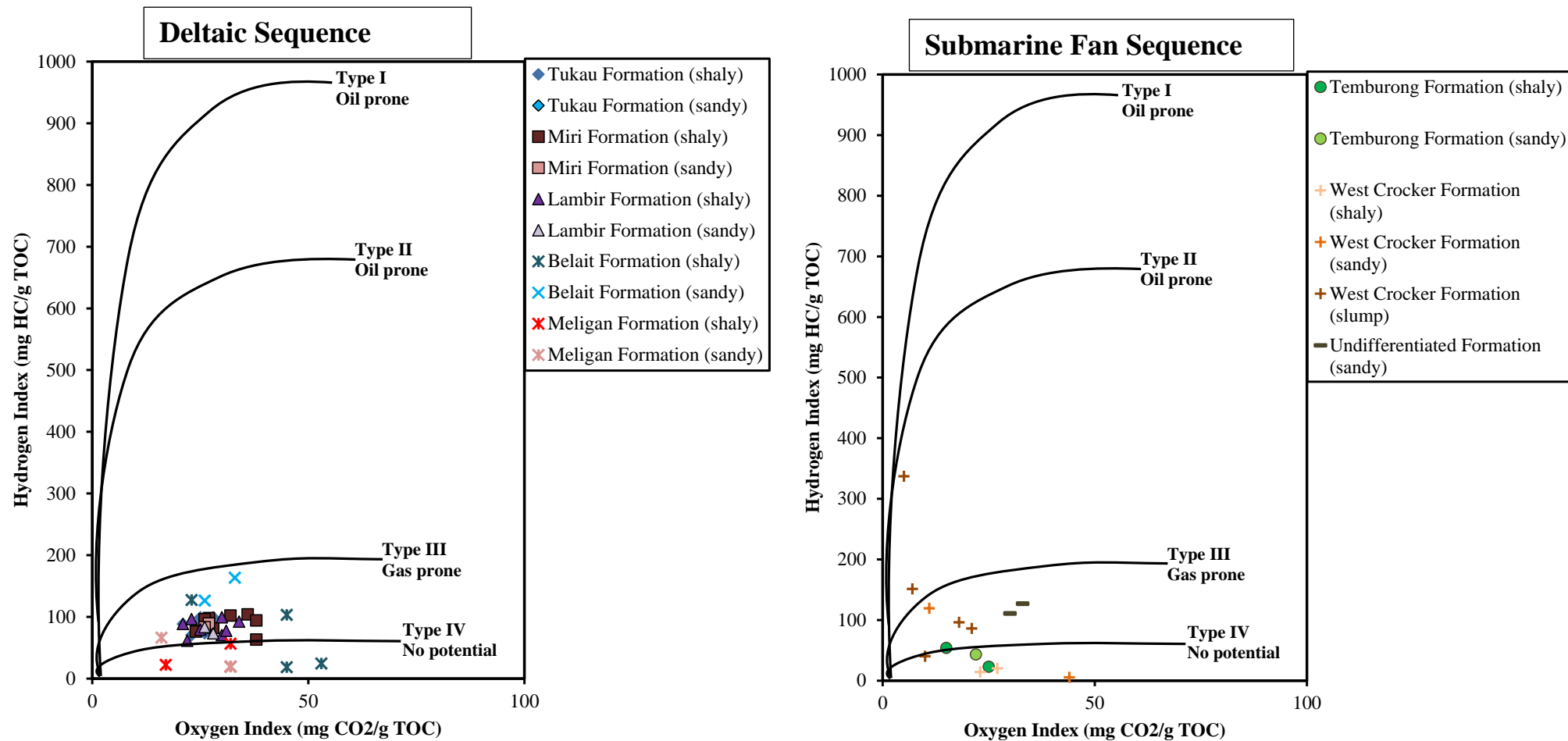


Figure 6.3 Modified van Krevelen diagram of Hydrogen index (HI) versus Oxygen index (OI) showing kerogen quality of the studied formations.

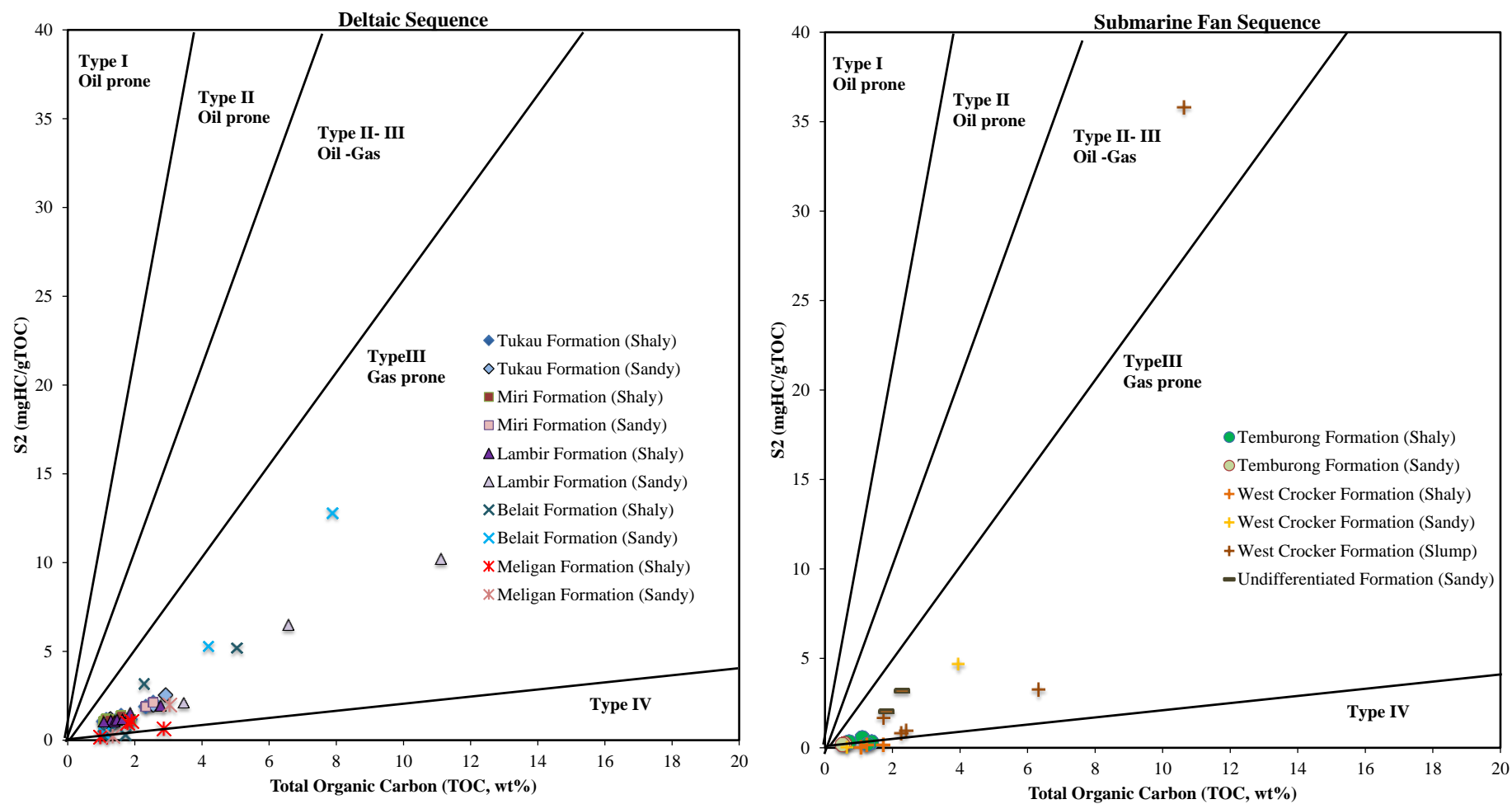


Figure 6.4. Crossplot of total organic carbon (TOC in wt. %) and remaining hydrocarbon potential (S2 in mg HC/g rock) showing the quality of kerogen in the studied formations

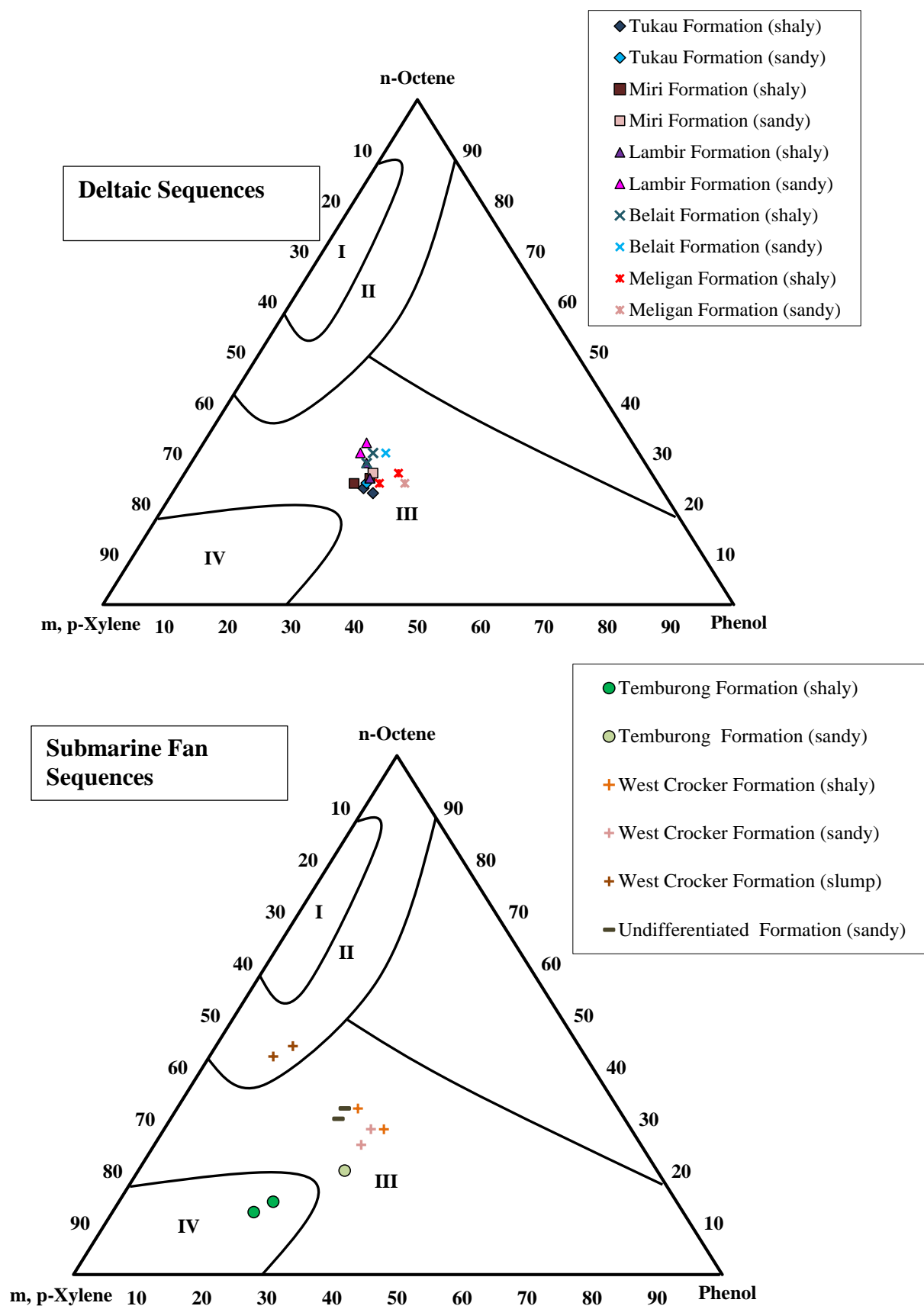


Figure 6.5. The ternary diagram to assess the kerogen characteristics based on the relative percentages m-p-xylene, phenol, and n-octene (Larter, 1984).

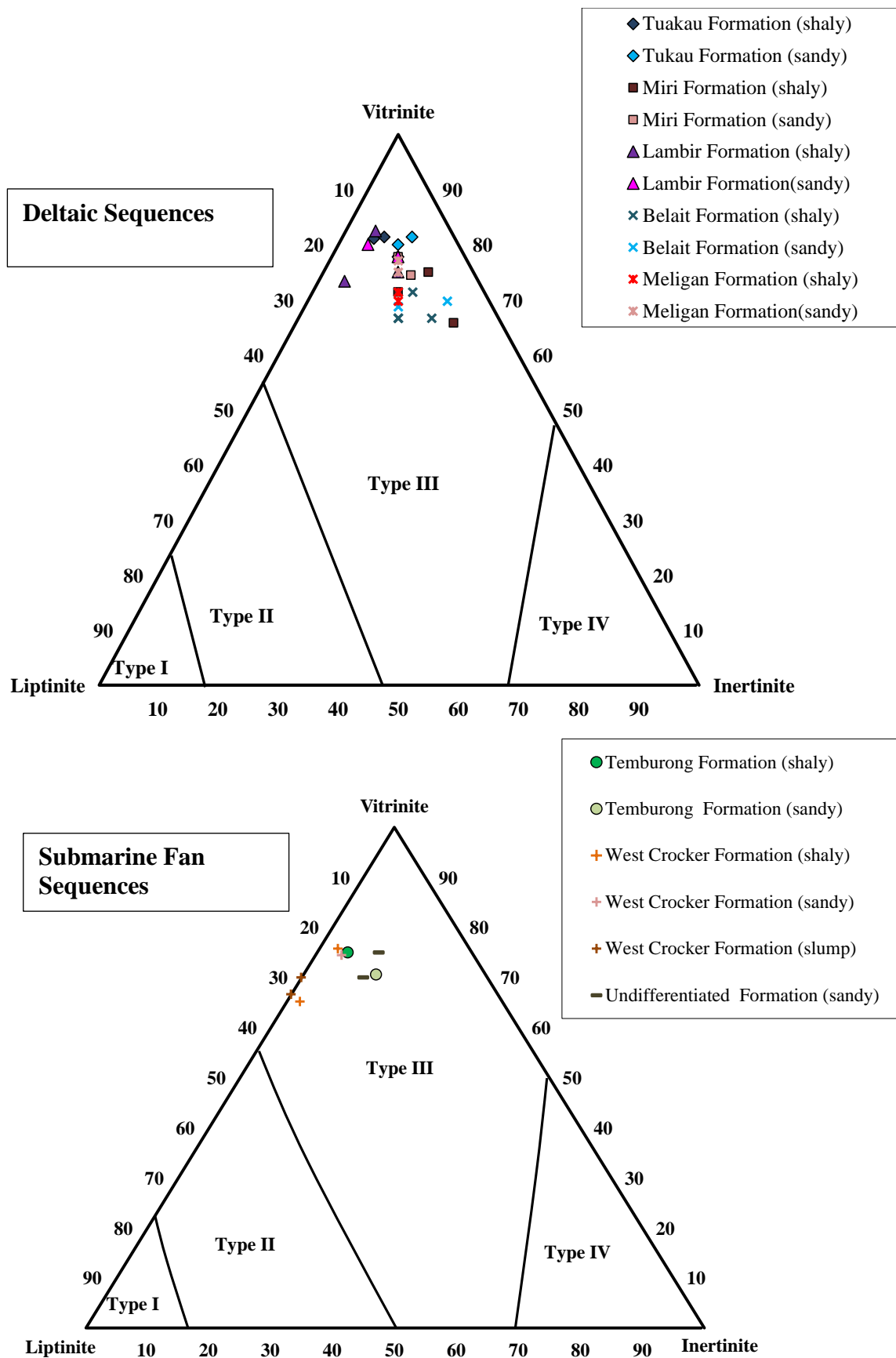


Figure 6.6. Ternary plot of classification of kerogen type based on major organic constituents observed under reflected light microscopy (modified after Cornford et al., 1998).

6.2.3 Thermal Maturity of Organic Matter

For an organic rich source rock to become effective source rock, it must reach a maturity level sufficient to generate hydrocarbons (Tissot and Wellte, 1984). Thermal maturity describes the impact of heat during burial of sediments. This thermal exposure converts kerogen into petroleum. Several data types and parametrs have been used to evaluate the level of organic maturity; these include vitrinite reflectance data (%Ro), pyrolysis Tmax and molecular parameters.

Deltaic Sequences

Vitrinite reflectance (VR) is more satisfactory and widely accepted by many authors and exploration geologists as a technique for measuring the thermal maturity of source rocks (Teichmüller, 1958; Tissot and Welte, 1984; Bordenave, 1993). Vitrinite reflectance values for main phase of oil generation ranges from (0.6-1.3) %Ro and values greater than 2.0 %Ro indicate dry gas generation (Tissot and Welte, 1984). The vitrinite reflectance values for the deltaic sequences range from 0.39-0.48 %Ro for Tukai, Miri, Lambir and Belait formation samples which indicates that they are thermally immature for hydrocarbon generation while the values of 0.69-0.79 %Ro recorded in the Meligan Formation samples indicates peak of oil generation to late oil window level of thermal maturity for hydrocarbon generation.

The pyrolysis Tmax indicates the temperature of the maximum generation of S2 peak. Generally, the threshold of the oil zone is at Tmax of 430°C - 435°C for Type II and III kerogen while gas zone ranges from 450°C - 455°C and 465°C - 470°C for Type II and type III respectively (Killops and Killops, 2005, Peters et al., 2005, Sykes and Raine, 2008). The pyrolysis Tmax values for most of the Tukai, Miri, Lambir and Belait formations samples is less than 435°C, indicating immature to very early mature stage. The pyrolysis Tmax values in the Meligan Formation samples range from 458-472 °C

indicating peak of oil generation to late oil window level of thermal maturity. This is in good agreement with the measured vitrinite reflectance data as illustrated in the HI versus Tmax plot of Figure 6.7.

The fractions of the EOM can be used to determine the level of thermal maturity. Nitrogen, Sulphur and Oxygen compounds (NSO), tends to be abundant in immature organic matter as recorded in Tukai, Miri, Lambir and Belait formations samples and decreases with increasing maturity. Also, there is increase in the aromaticity as maturity increases. This is displayed by the mature samples of Meligan Formation as described in Section 5.4.1.

The proportion of odd versus even carbon numbered n-alkanes may be used to obtain a rough estimate of organic maturation level of sediments (Bray and Evans 1961; Peters and Moldowan 1993; Peters et al. 2005). These measurements include the carbon preference index (CPI) proposed by Peters and Moldowan (1993), which is an improved odd-even preference (OEP) by Scalan and Smith (1970). CPI or OEP values significantly above 1.0 (odd preference) or below 1.0 (even preference) indicate thermal immaturity while values of 1.0 suggest that the organic matter is thermally mature (Peters and Moldowan 1993). Tukai, Miri, Lambir and Belait samples have CPI more than 1.0 with prevalence of odd carbon number over even carbon number. This indicates that all the analysed samples are thermally immature in terms of hydrocarbon generation (Bray and Evans 1961). The CPI and OEP values in the Meligan Formation samples are close to 1 and suggest these samples are thermally mature for hydrocarbon generation maturity. Also, the MPI-1 values correlate well with the measured vitrinite reflectance data.

Submarine Fan Sequence

The Submarine fan sequences shows vitrinite reflectance values in the range of 0.99-1.14%Ro and 0.79-1.14%Ro for Temburong and West Crocker formations samples respectively and this also indicates they are thermally mature for hydrocarbon generation. However, the undifferentiated Formation samples shows low thermal maturity with vitrinite reflectance values in the range 0.45-0.46%Ro.

The Temburong and West Crocker formations samples have Tmax values in the range of 474-492°C and 450-515°C respectively indicative of over-maturity for the Temburong Formation and peak of oil window to over-maturity for West Crocker Formation samples as described by Peters and Cassa (1994). This is supported by the plot of present day Hydrogen Index versus pyrolysis Tmax as shown in Figure 6.7. There is also a good agreement with the measured vitrinite reflectance data. This is further supported by the increase in aromaticity as recorded from EOM fractionation (see Section 5.4.1). The CPI and OEP values are close to 1 thereby suggest the analysed samples are thermally mature. The measured MPI-1 from phenanthrenes and alkyl derivatives is in good agreement with the measured vitrinite reflectance of the studied samples.

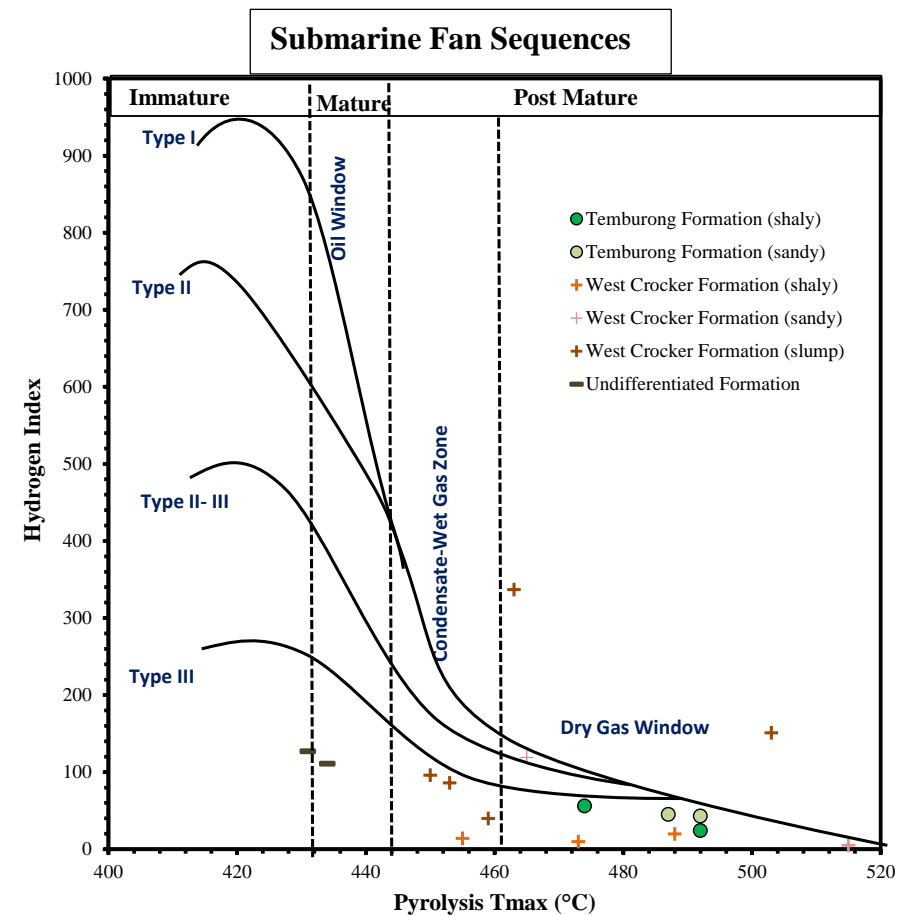
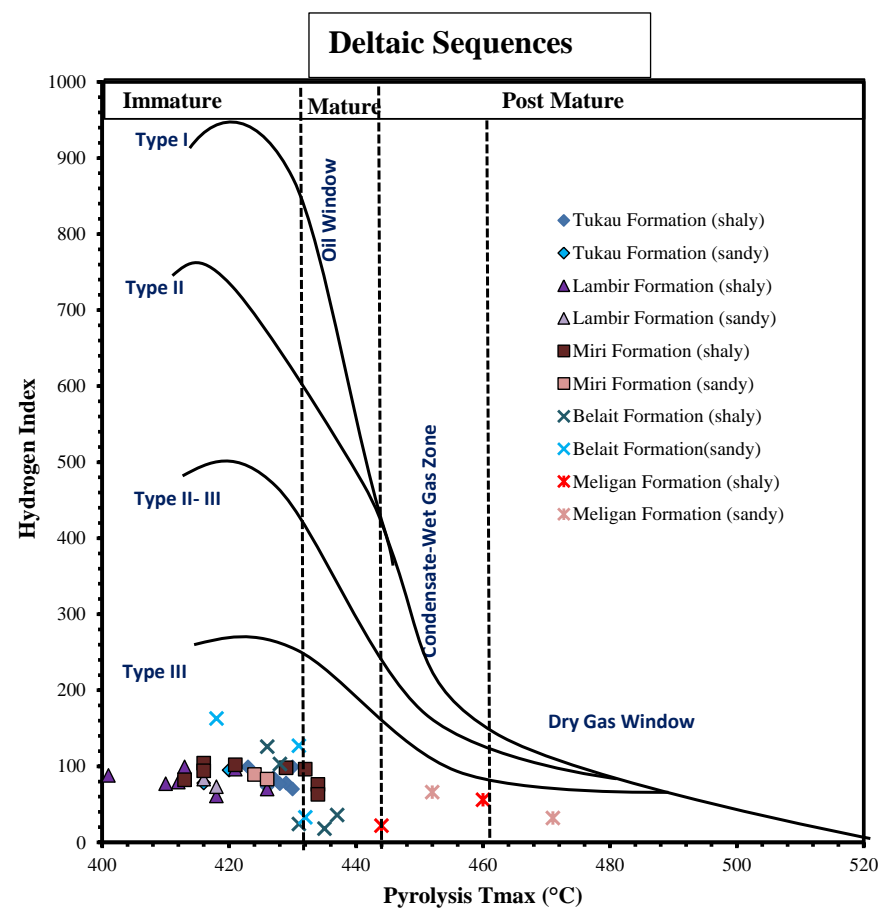


Figure 6.7 Plot of Hydrogen Index versus Tmax showing the type of kerogen and thermal maturity of the studied samples.

6.2.4 Prospect for Liquid Hydrocarbon Generation

The prospect of the studied samples for hydrocarbon generation and expulsion was evaluated based on bulk and quantitative pyrolysis techniques and organic petrological study. Capability for liquid hydrocarbon generation potential will be discussed in this section although the majority of the analysed samples have been shown to be gas prone.

Deltaic Sequences

The deltaic sequences (Tukau, Miri, Lambir, Belait, and Meligan) generally have pyrolysis HI values less than 150 mg HC/g TOC, indicating that Type III kerogen is the dominant kerogen in these sediments. This interpretation is supported by kerogen composition using pyrolysis products of pyrolysis–gas chromatography (Py-GC). The Type III kerogen has also been confirmed by high contribution of terrigenous organic matter input as indicated by the presence of vitrinitic-rich phytoclasts with minor occurrence of spores and pollen. These types of organic matters can generate mainly gaseous hydrocarbons if they are subjected to sufficient burial and heating as shown in the ternary diagram shown in Figure 6.8. However, some of the deltaic sequences show potential to generate liquid hydrocarbon (mainly wet gas/condensate) as supported by the display of mixed kerogen fingerprints of predominantly n-alkane/alkene doublets and aromatic compounds. In the Miri, Lambir and Belait formations samples, the pyrolysis – GC is dominated by the n-alkane/alkene doublets that extend beyond C₃₀, indicative of the aliphatic–richness with significant aromatic compounds, suggesting capability to generate waxy hydrocarbon and/or wet gas. In contrast, the samples from Meligan and Tukau formations show relatively low n-alkane/alkene doublets, indicative of the aliphatic–poor, and with significant aromatic compounds, suggesting the main generation products are gas. While the Meligan Formation samples are thermally mature for hydrocarbon generation, the Tukau, Miri, Lambir and Belait formations samples are immature to very early-mature,

thus indicate they have not been buried to a sufficient depth for hydrocarbon generation, but the stratigraphic offshore equivalents are known to have been buried to deeper depth and could therefore act as predominantly gas source rocks with limited oil generating potential.

Submarine Fan Sequences

The submarine fan sequences (West Crocker and Temburong formations) are generally lower in organic richness compared to the deltaic sequences, although within the West Crocker Formation abundant resinous coaly fragments do occur within the slump or debris flow mass transport deposits. Gas prone Type III and IV kerogen are the most common organic constituents in these sequences although occurrence of oil prone Type II kerogen was commonly observed in the slump deposits. The oil generative features were observed to be associated with perhydrous vitrinite and abundant resinous constituents, was also observed as well as appreciably presence of amorphous organic matter (Figure 6.8) and this is supported by pyrolysis HI up to 300 mg HC/g TOC. This is further supported by dominance of n-alkane/alkene doublets over aromatic compounds suggesting the main generation products of the slumps deposit are liquid hydrocarbon. The Temburong Formation samples are in late maturity stages of hydrocarbon generation while the West Crocker Formation samples shows variable thermal maturity ranging from early oil to gas generation stage. It is possible that the oil prone slump deposits within the West Crocker acts as effective liquid hydrocarbon source rock in NW Sabah due to large scale occurrence in the offshore part as reported by Algar et al. (2011).

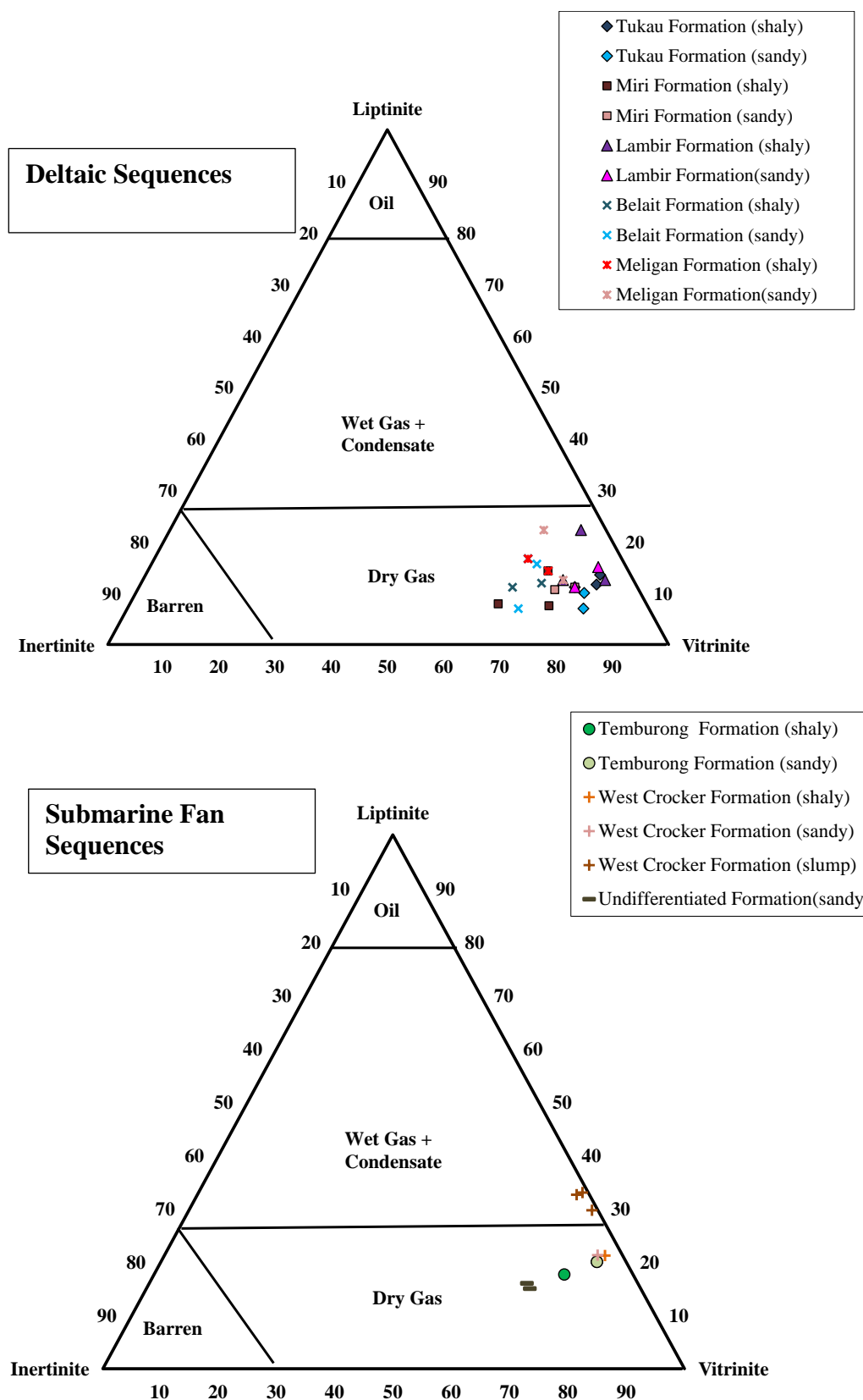


Figure 6.8. Predicted hydrocarbon in the studied sequences

6.3 Source of Organic Matter and Depositional Conditions

The organic matter source input and depositional conditions of the studied sequences were examined based on petrographic characteristics (palynofacies), molecular composition (n-alkanes and phenanthrenes) and elemental data.

6.3.1. Palynofacies Indicators

The AOM-phytoclast-palynomorph (APP) plot of Tyson (1993) is applied to give paleoenvironmental interpretation of the studied sequences.

The palynofacies assemblages in Lambir, Miri, Tunku and Belait formations shows dominance of phytoclasts group with high content of translucent phytoclasts related to proximal depositional conditions, with the main controlling factor being the short transport of the particles. This interval can be interpreted as high energy environment due to the presence of high percentage of cuticle thus being dominated by terrestrial input (Boulter and Riddick, 1986; Zavattieri et al., 2008). The phytoclast contents of this facies suggest the proximity to a fluvio-deltaic source and moderately suboxic depositional conditions (Kholeif and Ibrahim, 2010). This is supported by Tyson (1993) ternary diagram where the studied samples from these formations plot in palynofacies field I (Figure 6.9).

Palynofacies assemblages in the Meligan Formation show predominance of phytoclast group with high content of opaque phytoclast. According to Kholeif and Ibrahim (2010), opaque are derived from the oxidation of translucent woody material either during prolonged transport or post-depositional alteration. Tyson (1993) has stated that, the high frequency of opaque phytoclasts indicates oxidizing conditions and either proximity to terrestrial sources or redeposition of terrestrial organic matter from fluvio-deltaic environment.

The Submarine Fan sequences are characterized by almost equal content of phytoclasts group and AOM with low abundance of palynomorphs. The amorphous

organic matter comprises mostly resin. The palynomorphs are mostly spores and pollen grains of terrestrial origin with a few dinoflagellates. The presence of dinoflagellates may indicate minor input of marine organic matter in the submarine fan sequences. The high percentage of AOM in the Submarine Fan sequences indicates enhanced preservation in reducing conditions and increased stability of water column, resulting in suboxic or anoxic bottom conditions (Tyson, 1993, 1995; Ibrahim et al. 2002). In oxygen deficient basins, with high AOM preservation, allochthonous terrestrial material is dominant in the immediate vicinity of fluvio-deltaic sources or within turbidites (Tyson, 1987, 1993). Zavatierra et al. (2008) described similar palynofacies association in Neuquen basin, Argentina, and interpreted it as a relatively high-energy reducing environment with a terrestrial organic input. Kholeif and Ibrahim (2010) suggest that the very low presence of palynomorphs suggest a proximal suboxic –anoxic basin environment. Unlike the deltaic sequences, these assemblages indicate that sediments must have been transported farther away from land and into nearshore/marine environment as supported by the plot related to palynofacies field II and IV on Tyson (1993) ternary plot (Figure 6.9).

6.3.2 Molecular Indicators for Source Input and Depositional Conditions

The use of n-alkanes to evaluate organic matter source input is based on short chain alkanes (n-C₁₅ to n-C₁₉) being predominantly derived from marine algae and long chain alkanes (n-C₂₅ to n-C₃₁) being derived from land plant waxes (Peters et al.2005). The Terrigenous/Aquatic ratio (TAR) is defined as: $(n-C_{27} + n-C_{29} + n-C_{31}) / (n-C_{15} + n-C_{17} + n-C_{19})$. Values >1 for this parameter indicate more land plant sources than marine algae sources and low values (<1) indicate more marine algae sources than land plant sources. TAR values for the deltaic samples range from 2.08 -2.86 for Lambir samples, 1.26-1.98 for Miri samples , 1.98-2.81 for Tukai samples, 2.4-3.2 for Belait samples and 2.06-3.14 in

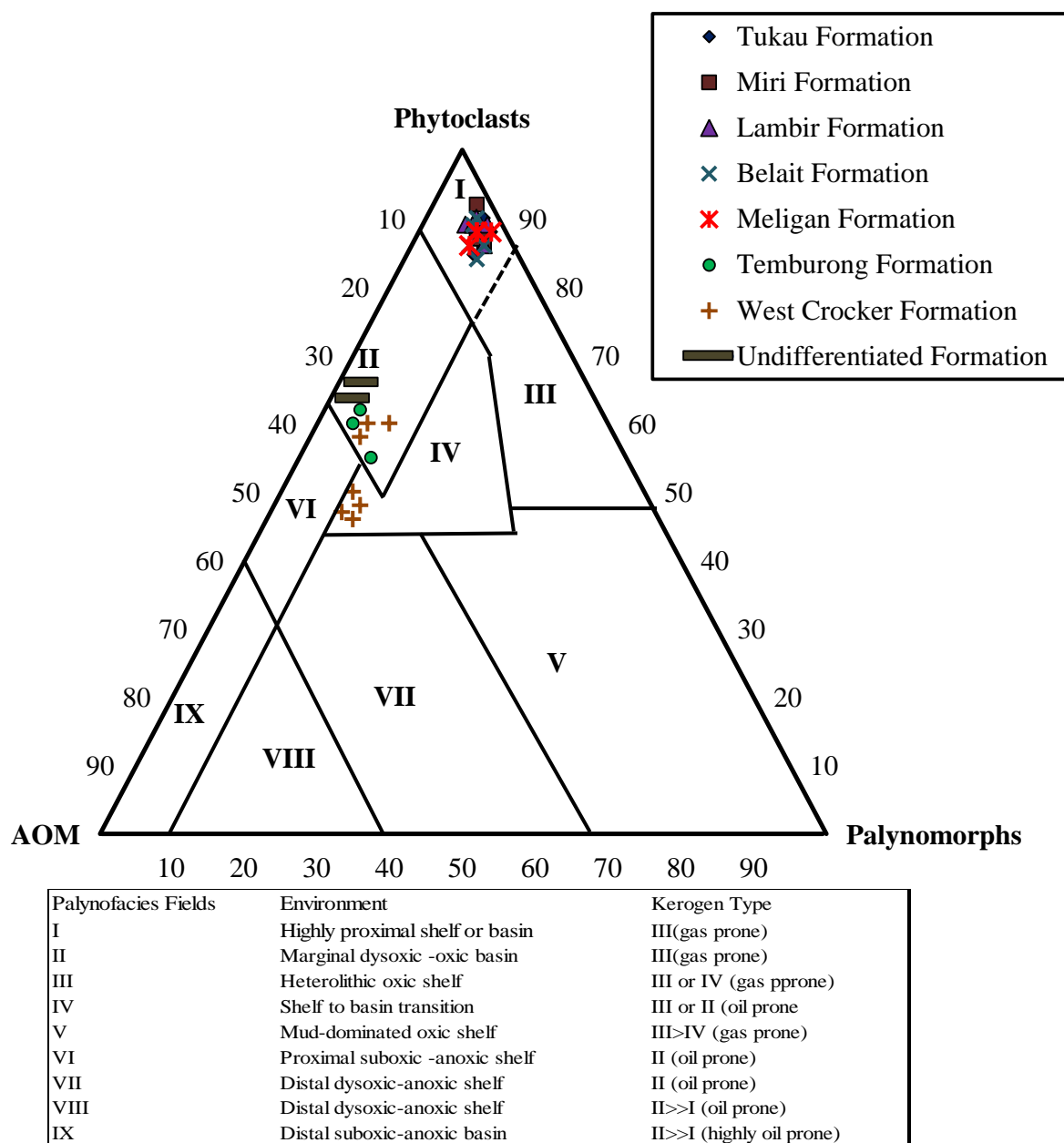


Figure 6.9. Ternary amorphous organic matter–phytoclast–palynomorph (APP) kerogen plot based to characterize the kerogen assemblage and environments under transmitted light microscopy (modified after Tyson, 1995).

Meligan samples suggesting the dominance of land-derived organic matter in these formations. The TAR values in the submarine fan samples range from 1.89-2.01 for Temburong samples and 1.56-2.12 in the West Crocker samples. The undifferentiated formation has TAR values range from 1.58-1.60. This also suggests terrigenous source input.

Pristane (Pr) and phytane (Ph) are usually the most important acyclic isoprenoid hydrocarbons in terms of concentration (Powell and McKirdy, 1973), and reflect the palaeoenvironmental conditions of source rocks and are considered as potential indicators of the redox conditions during sedimentation and diagenesis (Didyk et al., 1978; Chandra et al., 1994). Pr/Ph ratio values greater than 3.0 indicate oxic conditions, values below 1.0 indicate anoxic conditions, and values between 1.0 and 3.0 indicate suboxic conditions (Didyk et al.1978; Peters et al.2005). The Pr/Ph ratio values range from 1-3 in both the deltaic and submarine sequences and this suggests alternation of oxic and anoxic conditions during deposition. Some researchers (e.g. ten Haven *et al.*1987; Peters et al. 2005;) have raised objections to interpreting redox conditions from the Pr/Ph ratio, suggesting possible sources other than chlorophyll for pristane and phytane and possible influence of thermal maturity on the ratio. However, in this study redox interpretations using the Pr/Ph ratio are consistent with interpretations using other biomarker redox indicators (e.g. Pr/n-C₁₇ versus Ph/n-C₁₈). The Pr/n-C₁₇ versus Ph/n-C₁₈ plots (Figure 6.10) shows dominance of oxic conditions in the deltaic sequences compared to submarine fan sequences. The plot also discriminates the source input in the deltaic sequences and submarine fan. There is indicator of minor contributions of marine organic matter in the submarine fan sequences, although few samples from the Belait formation also plot in mixed organic matter field (Figure 6.10) suggesting minor input of marine derived organic matter in some of the analysed Belait Formation samples.

Source input indicator based on phenanthrenes also indicates that the source of the organic matter in the deltaic and submarine fan sequences is predominantly terrigenous. Ficken et al. (2000) established that aquatic macrophyte n-alkane proxy (Paq) <0.1 indicates pure terrestrial organic matter, 0.1-0.4 and 0.4-1 indicates dominating contribution of emergent plants and submerged plants respectively. This is clearly depicted in the plot of 9MP/PMP+1MP ratio against Paq (Figure 6.11) to distinguish between various sources of organic input for the samples analysed in this study.

6.3.3. Elemental Indicators

Organic carbon and total sulphur contents in sediments may provide insight into the depositional environment and microbial sulphate reduction (Berner and Raiswell 1983, Raiswell et al. 1987; Berner 1989; Hedges and Keil 1995; Adegoke et al. 2014). According to Hedges and Keil (1996), TOC/TS values of >5 indicates oxic conditions, while values between 1.5 and 5 indicates suboxic conditions. Anoxic conditions have TOC/TS values less than 1.5. The TOC/TS values in the deltaic samples range from 2.44-8.05 wt. % which suggests oxic to suboxic deposition conditions. The submarine fan samples show lower TOC/TS in the range of 1.29-3.98 wt. % and this indicates deposition under suboxic conditions. This is well depicted in the plot of organic carbon and sulphur contents as shown in Figure 6.12.

The relationship between total organic carbon and nitrogen from bulk organic matter have been used in many studies to distinguish between phytoplankton and terrestrial plant sources (e.g. Meyers 1997; Bechtel et al. 2001; Lamb et al. 2006; Gao et al. 2012). The former typically yields low values (4-10), and terrestrial plant sources tend to have ratios greater than 20 (Meyers 1997), while lacustrine and marine systems close to land generally show intermediate TOC/TN values (Silliman et al. 1996; Muller and Methesius 1999).

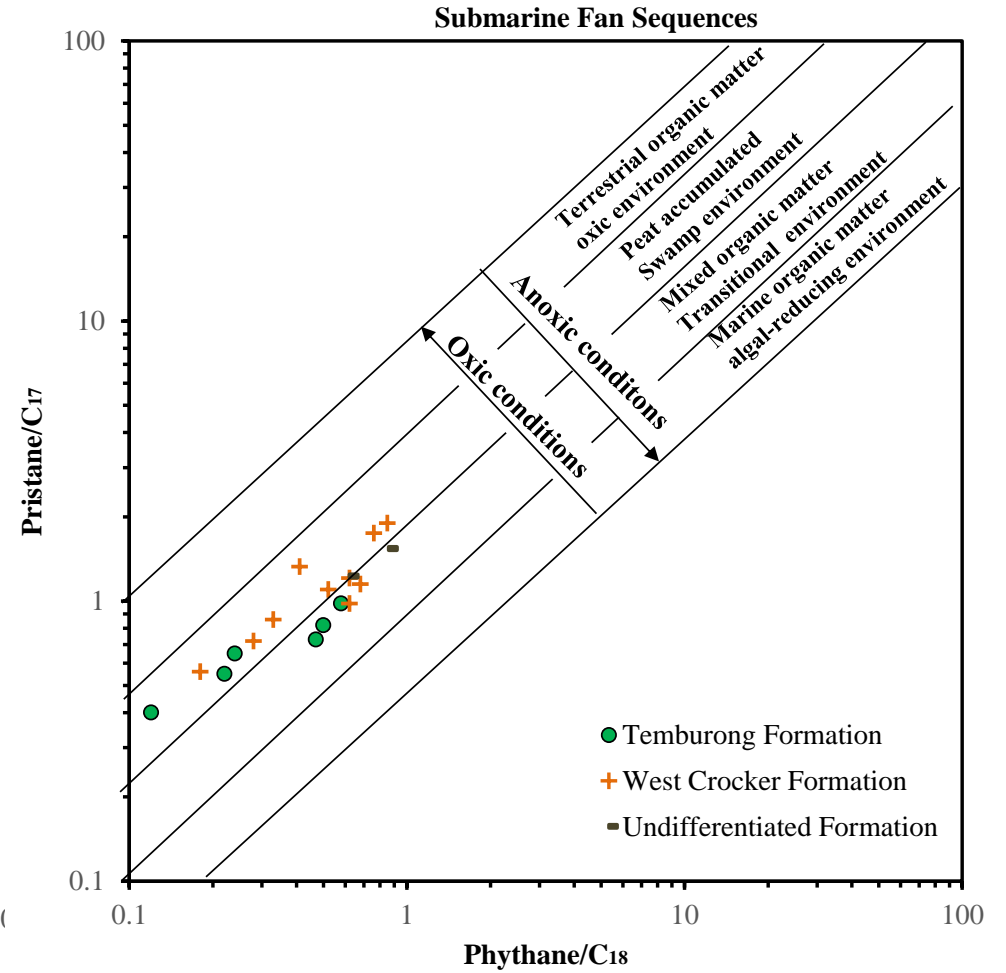
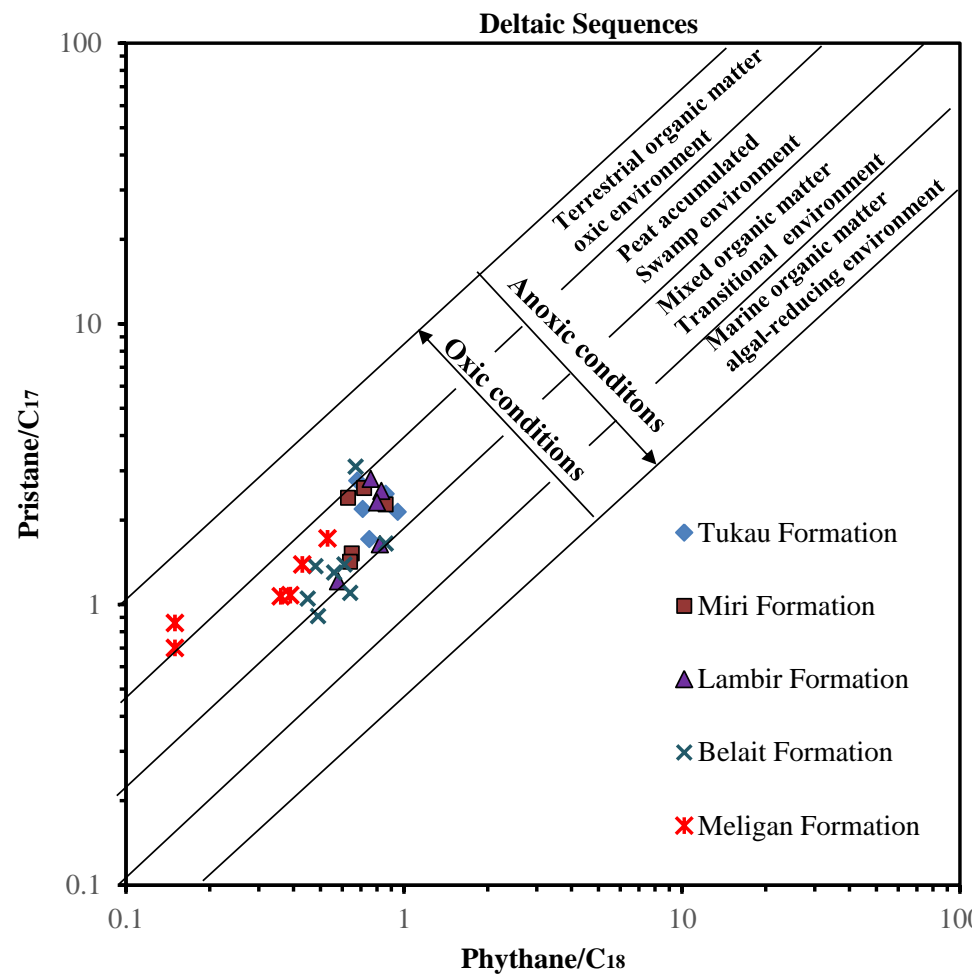


Figure 6.10. Plot of Pr/n-C₁₇ vs Ph/n-C₁₈ showing the deposition conditions of the preserved organic matter in the studied formations

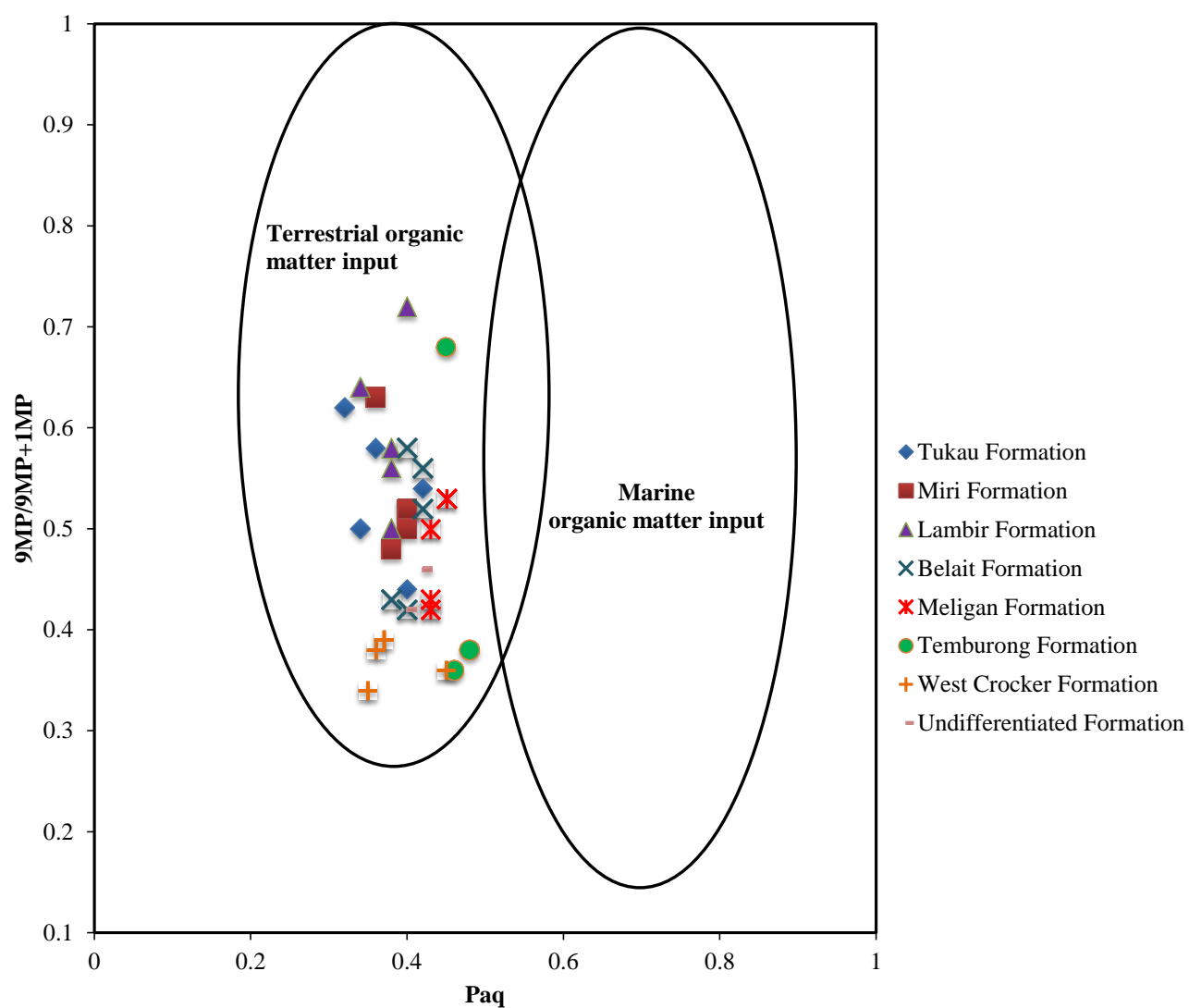


Figure 6.11 . Plot of 9MP/9MP+1MP ratio against aquatic macrophyte n-alkane proxy (Paq) of the analysed samples (after Ficken et al., 2000).

The TOC/TN ratios in all the deltaic samples are greater than 20 and this reflect major contributions of terrigenous organic matter. However, the TOC/TN ratios in most submarine fan samples are slightly lower than 20 which may suggest presence of mixed organic matter (i.e minor contributions of marine organisms). The mixed organic source input is supported by minor occurrence of dinoflagellates as described in section 6.3.1 and as indicated based on the plot of Pr/n-C₁₇ vs Ph/n-C₁₈ (Figure 6.10)

6.3.4 Trace Elements

The trace elements concentrations and ratios reveal the paleo-redox conditions during sedimentation of siliciclastic rocks (e.g. Harris et al.2004; MacDonald et al.2010; Fu et al.2011; Adegoke et al.2014).

Vanadium–nickel relationship: Vanadium (V) and Nickel (Ni) are important indicators for the redox conditions during deposition (Bechtel et al.2001; Galarraga et al.2008). The relative proportions of V and Ni are controlled by the depositional environment (Lewan 1984). A V/Ni ratio greater than 3 indicates deposition in a reducing environment; V/Ni ratios ranging from 1.9 to 3 or less than 1.9 indicate deposition under suboxic conditions and oxic conditions respectively (Galarraga et al.2008). The cross plot of V and Ni (Figure 6.13) indicates the deposition of terrigenous organic matter in oxygen influenced environment.

The *Vanadium-Chromium* (V/Cr) ratio has been suggested and employed as an index of paleo-oxygenation in a number of studies (e.g Jones and Manning, 1994; Algeo and Maynard 2004; Tribovillard et al., 2006). Chromium is usually incorporated within the detrital clastic fraction of a sediment, where it may substitute for Al within clays, be adsorbed, or occur as chromite (Patterson et al., 1986; Jones and Manning, 1994). In contrast, vanadium may be bound to organic matters by the incorporation of V⁴⁺ into porphyrins, and is concentrated in sediments deposited under reducing conditions (Jones

and Manning, 1994; Tribovillard et al., 2006). So, higher V/Cr ratios are thought to represent more anoxic (reducing) depositional conditions. The V/Cr ratio above 4 may be indicative of anoxic depositional conditions and the V/Cr ratio below 2 may indicate oxic depositional conditions (Jones and Manning, 1994). The V/Cr ratio in the deltaic sequences range between 1.0-3.5 which suggests oxic and suboxic depositional conditions while the ratio in the submarine fan sequences range from 2-4 and suggests mainly suboxic depositional conditions

The *Nickel-Cobalt* (Ni/Co) ratio suggested from the studies of Lewan (1984) and Tribovillard et al. (2006) can also be used to interpret the depositional conditions. The thermodynamics predict that the Ni/Co ratio will decrease as the environment becomes more oxidising due to the enrichment of cobalt (Telnaes et al., 1991). The Ni/Co ratio of less than 5 suggests oxic conditions while more than 7 suggests anoxic conditions. Most the deltaic samples have Ni/Co ratios less than 5 which suggest high level of oxygen during deposition. The submarine fan sequences have Ni/Co ratios between 5 and 7 and this suggests suboxic depositional conditions. This is further supported by the cross plot of Ni/Co versus V/Cr (Figure 6.13 a).

Powell et al. (2003) also revealed that Ni/Co and V/Sc ratios preserved the most detailed record of paleo-redox conditions. Values of $V/Sc < 9.1$ correspond to oxic environment, whereas $V/Sc \geq 10.0$ corresponds to low-oxygen depositional environments. Based on the cross plot of Ni/Co against V/Sc ratios (Powell et al., 2003), the submarine fan samples were deposited in suboxic marine conditions while the deltaic samples were deposited in much oxygen influence environment, thus also in agreement with previously discussed organic geochemical parameters such as total sulphur content and Pr/n-C₁₇ vs Ph/n-C₁₈ plot.

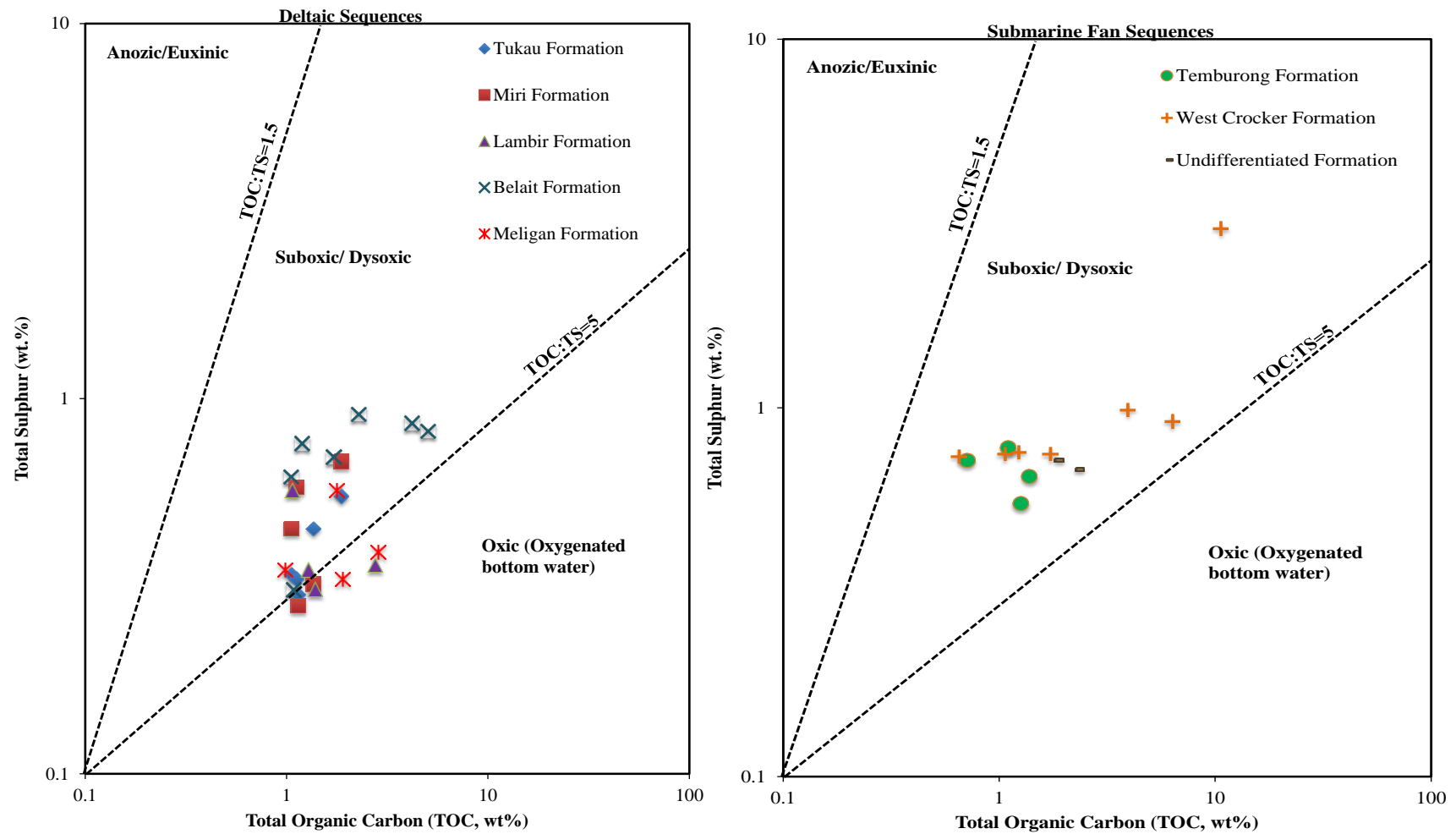


Figure 6.12. Relationship between total organic carbon (TOC) and total sulphur (TS) showing the depositional conditions of the analysed samples (Trendline after Hedges and Keil, 1996).

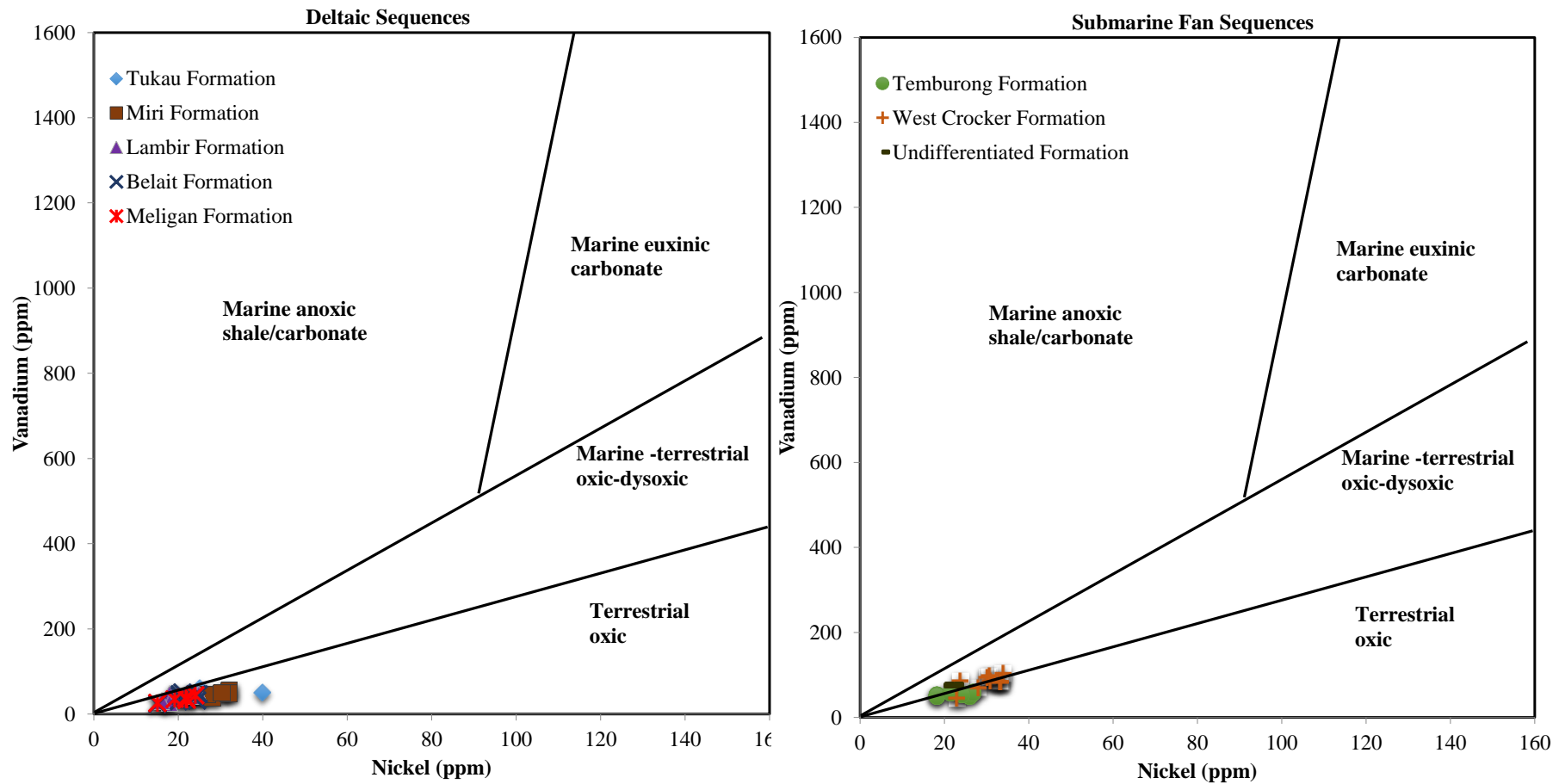


Figure 6.12. Plots of nickel against vanadium (modified after Akinlua et al. 2013).

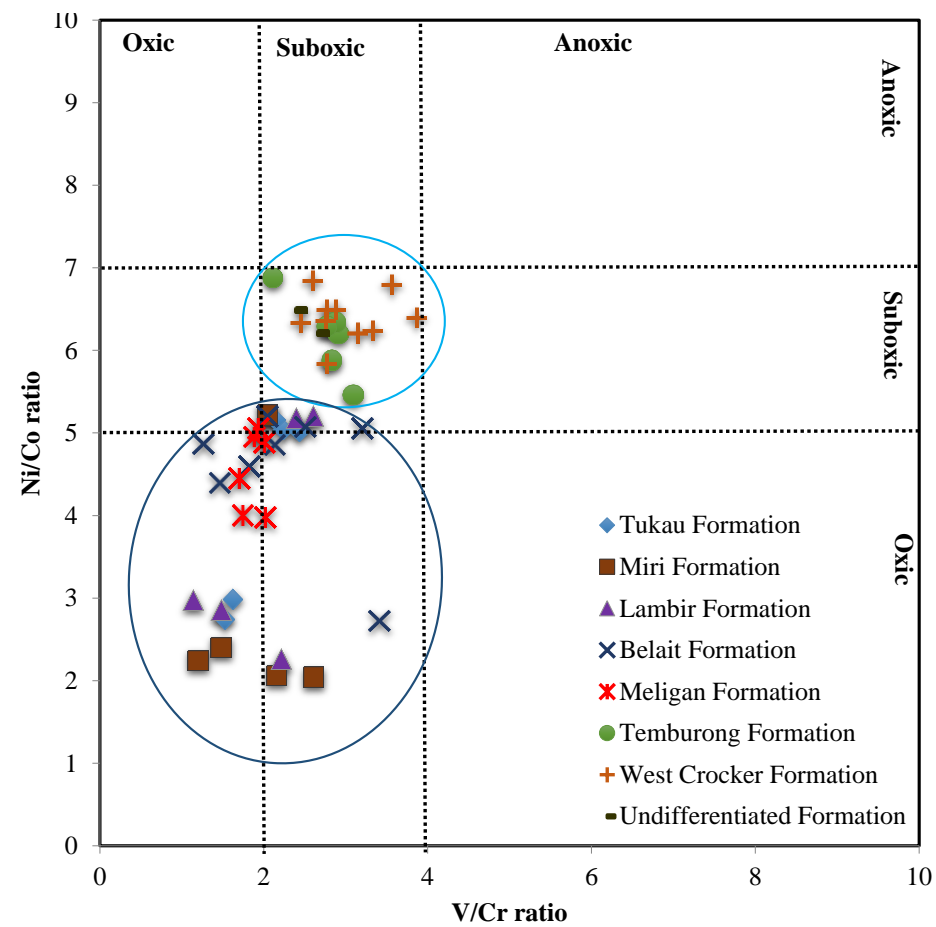
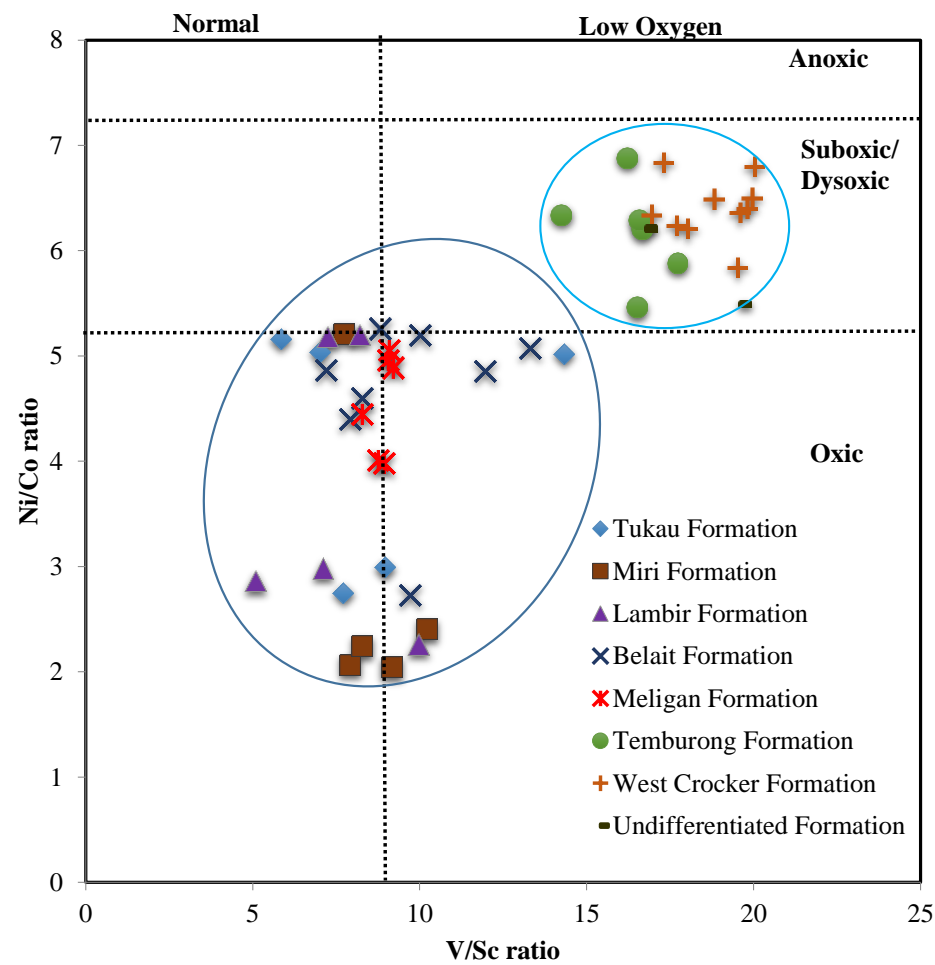


Figure 6.13 a) Plot of Ni/Co against V/Sc ratios (modified after Powell et al. 2003), b) Plot of Ni/Co and V/Cr (modified after Jones and Manning, 1994)

CHAPTER 7

CONCLUSIONS

This thesis integrates petrology and geochemistry in order to evaluate for potential source rocks in the deltaic (Tukau, Miri, Lambir, Belait, Meligan formations) and submarine fan (West Crocker and Temburong) deposits. Also, to provide more information on the source of organic matter and the conditions under which the organic matter was preserved.

There is variation in TOC in the shaly and sandy facies of the studied Formations. Most of the sandy facies in the studied formations have higher TOC than the shaly facies except in the Temburong Formation where the shaly facies have higher TOC content and this is supported by high EOM yield. This indicates most of the samples within the studied formations have sufficient total organic carbon content to act as petroleum source rocks. However, the pyrolysis S_2 yields show that most of the deltaic samples have fair to good hydrocarbon generating potential while the submarine fan deposits shows poor to fair hydrocarbon generating potential. The slump facies within the West Crocker formation shows good to excellent hydrocarbon generating potential. This is supported by the hydrocarbon yield fraction of the EOM.

The organic matter in most of the deltaic and submarine fan sediments is predominantly Type III kerogen and is gas prone, as indicated by low pyrolysis HI values of mostly less than 150 mg HC/ g TOC. However, there is evidence of oil prone Type II kerogen in the West Crocker Formation slump deposits. The dominance of Type III kerogen is confirmed by low initial H/C atomic ratios in the range of 0.82-0.90 and abundance of terrestrial-derived organic matter (i.e., vitrinite phytoclasts) as generally observed in all of the studied samples.

Thermal maturity assessed from pyrolysis Tmax and the vitrinite reflectance indicate that the organic matter in the submarine fan deposits is thermally mature to overmature for hydrocarbon generation with exception from the sandy facies from the undifferentiated Formation. The studied deltaic deposits are mostly immature to very early mature for hydrocarbon generation except for the Meligan Formation samples which display relatively higher thermal maturity. The maturity inference is supported by CPI, OEP and MPI-1 obtained from aliphatic and aromatic molecular parameters.

The organic material in the submarine fans and deltaic sediments are derived mainly from terrestrial environments that were eroded and carried towards the deeper parts of the basin, via a delta system and submarine canyons. An n-alkane distribution with high to medium molecular weight typical of terrestrial derived organic matter is most common especially in the deltaic deposits while some of the submarine fan deposits show evidence of low molecular weight compounds that suggest minor contribution of marine organic matter. This is further supported by the occurrence of marine plankton (dinoflagellate) in the submarine fan deposits. The organic matter present in all the studied samples is mostly preserved under oxic to suboxic conditions as revealed by n-alkane /isoprenoids ratios and trace elements distributions. This paleoenvironment conditions is further supported by the palynofacies assemblages in the analysed organic matter.

Integration of all geochemical-petrographic analyses indicate that the immature deltaic deposits and the slump deposits of the submarine fan has a possible hydrocarbon potential of mainly gas with minor oil and should attract further research. This could include detailed sedimentology logging for adequate information on the lateral extent and volumes of these strata . Also, biomarker study based on hopane and sterane distributions that could be directly correlated with the known occurrences of oil accumulation within the petroleum prolific basins of offshore Sarawak and Sabah.

REFERENCES

- Abdullah, W.H., (1999). Oil generating potential of Tertiary coals and other organic –rich sediments of the Nyalau Formation, onshore Sarawak. *Jour. Asian Earth Sci.*, 17, 255-267.
- Abdul Jalil, M., Mohd Jamaal, H., (1992). Possible source for the Tembungo Oils: Evidences from Biomarker Fingerprints . *GSM*, 32, 213-232.
- Abdullah, W.H., (2003). Coaly source rocks of NW Borneo: role of suberinite and bituminite in oil generation and expulsion. *Geological Society of Malaysia Bulletin* 47, 153–163.
- Abeida, H.S., Abdul Hadi, A., Zuhair Zahir, T.H., (2005). Facies, Depositional Framework and Sequence Stratigraphy of the Miri Formation (Middle Miocene), Miri, Sarawak. *PGCE*, 6 December, Kuala Lumpur.
- Adedosu , T.A, Sonibare, O.O., Tuo, J., Ekundayo, O., (2012). Biomarkers, carbon isotopic composition and source rock potentials of Awgu coals, middle Benue trough, Nigeria. *Journal of African Earth Sciences*, 66, 13-21.
- Adegoke, A.K, Abdullah, W.H, Hakimi, M.H, Sarki Yandoka, B.M, Mustapha, K.A, Aturamu, A.O., (2014). Trace elements geochemistry of kerogen in Upper Cretaceous sediments, Chad (Bornu) Basin, northeastern Nigeria: Origin and paleo-redox conditions. *Journal of African Earth Sciences* 100:675-683.
- Akinlua, A., Adekola, S.A., Swakamisa, O., Fadipe, O.A., Akinyemi, S.A., (2010). Trace element characterisation of Cretaceous Orange Basin hydrocarbon source rocks. *Applied Geochemistry* 25:1587-1595.
- Alberdi-Genolet, M., Tocco, R., (1999). Trace metals and organic geochemistry of the Machiques Member (Aptian-Albian) and La Luna Formation (Cenomanian-Campanian), Venezuela. *Chemical Geology* 160:19-38.
- Agostinelli, E., M. R. A. Tajuddin, E. Antollielli, and M. M. Aris (1990), Miocene-Pliocene palaeogeographic evolution of a tract of Sarawak offshore between Bintulu and Miri, *Bull. Geol. Soc. Malays.*, 27, 117–135.

- Alexander, R., Kagi, R. I. , Woodhouse, G. W. (1981). Geochemical correlation of Windalia oil and extract of winning group (Cretaceous) Potential source rock, Barrow Sub-basin, Western Australia, AAPG Bulletin, 65, 235-50.
- Algar, S., C. Milton, H. Upshall, J. Roestenburg, Crevello, P., (2011). Mass-transport deposits of the deep-water north western Borneo margin (Malaysia); characterization from seismic reflection, borehole, and core data with implications for hydrocarbon exploration and exploitation, in R.C. Shipp, P. Weimer, and H.W. Posamentier, (eds.), Mass transport deposits in deep-water settings: Society for Sedimentary Geology, Special Publication 96, p. 351-366.
- Algar, S.C., (2012). Big Oil from “Gas Prone” Source Rocks and Leaking Traps: Northwest Borneo. AAPG ICE, Singapore.
- Algeo, T.J., Maynard, J.B., (2004). Trace-element behavior and redox facies in core shales of Upper Pennsylvanian Kansas-type cyclothems: Chemical Geology, v. 206, p. 289- 318.
- Anuar, A., Hoesni, M.J., (2008). The Hydrocarbon Property Variation in the West Baram Delta Petroleum System: Unravelling the Respective Effects of Biodegradation and Source Facies. AAPG International Conference and Exhibition, Cape Town, South Africa. October 22.
- Anuar A., Kinghorn, R.F., (1994). Sterane and triterpane biomarker characteristics from oil and sediments extracts of the Middle-Upper Miocene sequences, Northern Sabah Basin. GSM Bulletin, 37.
- Anuar, A., Abdul Jalil, M., (1997). A comparison of source rock facies and hydrocarbon types of the Middle Miocene sequence, offshore NW Sabah Basin Malaysia. In: Howes, J.V.C. and Noble , R.A eds, Proceedings of the IPA Petroleum Systems of SE Asia and Australia, 21-23 May 1997, Indonesian Petroleum Association, Jakarta, 773-786.
- Arfaoui, A., Montacer, M., Kamoun, F. and Rigane, A., (2007) Comparative study between Rock-Eval pyrolysis and biomarkers parameters: A case study of Ypresian source rocks in central-northern Tunisia. Marine and Petroleum Geology, 24, 566-578.
- Armstroff A. et.al., (2006). Aromatic hydrocarbon biomarkers in terrestrial organic matter of Devonian to Permian age. Paleogeography, Palaeoclimatology, Palaeoecology (240) 253-274

- Back, S., Morley, C.K., Simmons, M.D., Lambiase, J.J., (2001). Depositional environment and sequence stratigraphy of Miocene deltaic cycles exposed along the Jerudong anticline, Brunei Darussalam. *Journal of Sedimentary Research*, 71, 913-921.
- Back, S., Strozyk, F., Kukla, P., Lambiase, J.J., (2008). Three-dimensional restoration of original sedimentary geometries in deformed basin fill, onshore Brunei Darussalam, NW Borneo. *Basin Research*, 20, 99-117.
- Back, S., Tioe Hak Jing, Tran Xuan Thang, Morley, C.K., (2005). Stratigraphic development of synkinematic deposits in a large growth-fault system, onshore Brunei Darussalam. *Journal of the Geological Society, London*, 162, 243-258.
- Balaguru, A., Nichols, G.J., Hall, R., (2003). The origin of the circular basins of Sabah, Malaysia. *Geological Society of Malaysia Bulletin* 46, 335–351.
- Balaguru, A., Nichols, G.J., (2004). Tertiary stratigraphy and basin evolution, southern Sabah (Malaysian Borneo). *Journal of Asian Earth Sciences* 23, 537–554.
- Baskin, D.K. (1997). Atomic H/C ratio of kerogen as an estimate of thermal maturity and organic matter conversion. *AAPG Bulletin* 8, 1437-1450.
- Bastow, T.P., Alexander, R., Sosrowidjojo, I.B. and Kagi, R.I., (1998). Pentamethylnaphthalenes and related compounds in sedimentary organic matter. *Organic Geochemistry* 28.9-10:585-595.
- Bastow, T.P., Alexander, R., Fisher, S.J., Singh, R.K., van Aarssen, B.G.K. and Kagi, R.I., (2000). Geosynthesis of organic compounds. Part V-methylation of alkyl naphthalenes. *Organic Geochemistry* 31:523-534.
- Batten, D. J., (1981). Palynofacies, organic maturation and source potential for petroleum. In: Brooks J. (Ed), *Organic maturation studies and fossil fuel exploration*. Academic Press, London, pp. 201 – 223.
- Batten, D.J., (1996). Palynofacies and paleoenvironmental interpretation. In Jansonius J, McGregor DC (Eds.), *Palynology: Principles and applications*; Amer. Assoc. Strat. Palynol. Found., 3: 1011-1064.
- Batten, D.J., (1999). Small palynomorphs. In: Jones TP, Rowe NP (eds) *Fossil plants and spores: modern techniques*. Geological Society, London, pp 15–19

- Barwise, A.J.G., (1990). Role of nickel and vanadium in petroleum classification. *Energy Fuels* 4:647-652.
- Bechtel, A., Gratzer, R., Sachsenhofer, R.F., (2001) Chemical characteristics of Upper Cretaceous (Turonian) jet of the Gosau Group of Gams/Hieflau (Styria, Austria). *International Journal of Coal Geology* 46:27-49.
- Berner, R.A., (1989). Biogeochemical cycles of carbon and sulfur and their effect on atmospheric oxygen over phanerozoic time. *Palaeogeography, Palaeoclimatology, Palaeoecology* 75:97-122.
- Berner, R.A., Raiswell, R., (1983). Burial of organic carbon and pyrite sulfur in sediments over phanerozoic time: a new theory. *Geochimica et Cosmochimica Acta* 47:855-862.
- Banerjee, A., Sinha, A. K., Jain, A. K., Thomas, N. J., Misra, K. N., & Chandra, K. (1998). A mathematical representation of Rock-Eval Hydrogen index vs Tmax profiles. *Organic Geochemistry*, 28, 43–55.
- Barckhausen, U., Roeser, H.A., (2004). Seafloor spreading anomalies in the South China Sea revisited. In: Clift, P., Wang, P., Kuhnt, W., Hayes, D.E. (Eds.), *Continent–Ocean Interactions within the East Asian Marginal Seas*, vol. 149. American Geophysical Union Geophysical Monograph, pp. 121–125.
- Bol, A.J., van Hoorn, B., (1980). Structural style in western Sabah offshore. *Bulletin of the Geological Society of Malaysia* 12, 1–16.
- Boulter, M., C., Riddick, A., (1986). Classification and analysis of palynodebris from the Paleocene sediments of the Forties Field: *Sedimentology*, 33, 871–886.
- Bourbonniere, R. A. and Meyers, P. A., (1996). Sedimentary geolipid records of historical changes in the watersheds and productivities of the Lakes Ontario and Erie, *Limnology and Oceanography*, 41, 352-59.
- Bordenave, M. L., Espitalie, J., Leplat, P., Oudin, J. L. and Vendenbroucke, M., (1993). Screening techniques for source rock evaluation. In: Bordenave, M. L. (Ed.), *Applied Petroleum Geochemistry Editions Technip, Paris*, pp. 237-255.

- Bostick, N.H., (1979), Microscopic measurement of the level of catagenesis of solid organic matter in sedimentary rocks to aid exploration for petroleum and to determine former burial temperatures -- a review, in P.A. Scholle, and P.R. Schluger, eds., *Aspects of Diagenesis: S.E.P.M. Special Publication 26*, p. 17-43.
- Bray, E. E. and Evans, E. D., (1961). Distribution of n-paraffin's as a clue to recognition of source beds. *Geochimica et Cosmochimica Acta*, 22, 2-15.
- Brooks, J. D., Gould, K. and Smith, J. W., (1969). Isoprenoids hydrocarbons in coal and petroleum. *Nature*, 222, 257-9.
- Budzinski, H. et. al., (1995). Alkylated phenanthrene distributions as maturity and origin indicators in crude oils and rock extracts. *Geochimica et Cosmochimica Acta*. 59, 2043– 2056.
- Briaies, A., Patriat, P., Trapponier, P., (1993). Updated interpretation of magnetic anomalies and seafloor spreading stages in the South China Sea: implications for the Tertiary tectonics of Southeast Asia. *Journal of Geophysical Research*, 98, 6299-6328.
- Carvalho, M.A., Filho, J.G.M., Menezes, T.R., (2006). Paleoenvironmental reconstruction based on palynofacies analysis of the Aptian-Albian succession of the Sergipe Basin, North eastern Brazil, *Marine Micropaleontol.* 59: 56-81
- Crevello, P.D et al. (2006). "Mixed braided and leveed-channel turbidites, West Crocker fan system, northwest Borneo," in *Atlas of Deep-Water Outcrops, AAPG Studies in Geology 56*.
- Curiale, J., Morelos, J., Lambiase, J., Mueller, W., (2000). Brunei Darussalam—characteristics of selected petroleum and source rocks. *Organic Geochemistry* 31, 1475–1493.
- Combaz, A., (1964). Les palynofaciès. *Revue de Micropaléontologie*, v. 7, p. 205-218.
- Darlymple, R.W., Zaitlin, B.A., Boyd, R., (1992). Estuarine facies models: Conceptual basis and stratigraphic implications. *Journal of Sedimentary Petrology*, 62: 1130-1146.
- Dembicki, H.J., 2009. Three common source rock evaluation errors made by geologists during prospect or play appraisals *Am. Assoc. Pet. Geol. Bull.*, 93 (3) pp. 341–35.

- Dembicki, H.J., Horsfield, B., & Thomas, T.Y.H., (1983). Source rock evaluation by pyrolysis-gas chromatography. American Association of Petroleum Geologists Bulletin 67(7), pp. 1094-1103.
- Dembicki Jr., H., (2009). Three common source rock evaluation errors made by geologists during prospects or play appraisals. American Association of Petroleum Geologists Bulletin 93(3), 341-356
- Demaison, G. J. and Moore, G. T., (1980). Anoxic environments and oil source bed genesis. AAPG Bulletin, 64, 1179-1209.
- Derenne, S., Largeau, C., Casadevall, E. and Connan, J., (1988). Comparison of torbanites of various origins and evolutionary stages. Bacterial contribution to their formation. Cause of lack of botryococcane in bitumens. Organic Geochemistry, 12, 43-59.
- Dyman, T. S., Palacas, J. G., Tysdal, R. G., Perry, W. G., Pawlewicz, M. J., (1996). Source rocks potentials of middle Cretaceous rocks in south western Montana. AAPG Bulletin 80, 1177-84.
- Didyk, B. M., Simoneit, B. R. T., Brassell, S. C., Eglinton, G., (1978). Organic geochemical indicators of paleoenvironmental conditions of sedimentation. Nature, 272, 216-22.
- Durand, B., Monin, J.C., (1980). Elemental analysis of kerogens (C, H, O, N, S, Fe), In: B. Durand (Ed.), Kerogen, Editions Technip, Paris (1980), pp. 113–142.
- Eglinton, T.I, Sinninghe Damsté, J.S, Kohnen, M.E.L., de Leeuw, J.W., (1990). Rapid estimation of the organic sulphur content of kerogens, coals and asphaltenes by pyrolysis-gas chromatography. Fuel, 69, pp. 1394–1404
- Eglinton, G. and Hamilton, R. G., (1967). Leaf epicuticular waxes. Science 156, 1322–1344.
- Ehinola, O. A., Sonibare, O. O., Jave, D. M. and Oluwole, E. A., (2008). Geochemical appraisal of organic matter in the Mid-Cretaceous sediments of the Calabar Flank, Southeastern, Nigeria. European Journal of Scientific Research, 23 (4), 567-77.
- Emerson, S., (1985). Organic carbon preservation in marine sediments, American Geophysical Union, Washington DC, 78-86

- Espitalie, J., Marques, F. and Barsony, I., (1984). Geochemical logging. In: Voorhees, K.J. (Ed.), *Analytical Pyrolysis-Techniques and Applications*: Boston, Butterworth, p. 276-304.
- Ficken, K.J., Li, B., Swain, D.L. and Eglinton, G., (2000). An n-alkane proxy for the sedimentary input of submerged/floating fresh water aquatic macrophytes. *Organic Geochemistry* 31.7-8:745-749.
- Gao, X., Yang, Y., Wang, C., (2012). Geochemistry of organic carbon and nitrogen in surface sediments of coastal Bohai Bay inferred from their ratios and stable isotopic signatures. *Marine Pollution Bulletin* 64:1148-1155.
- Galarraga, F., Reategui, K., Martínez, A., Martínez, M., Llamas, J., Márquez, G., (2008). V/Ni ratio as a parameter in palaeoenvironmental characterisation of nonmature medium-crude oils from several Latin American basins. *Journal of Petroleum Science and Engineering* 61:9-14.
- Gartrell, A., Torres, J., Hoggmascall, N., (2011). A regional approach to understanding basin evolution and play systematic in Brunei – unearthing new opportunities in a mature basin. In: *International Petroleum Technology Conference*, Bangkok, Thailand, IPTC 1571, 1–5.
- Giraud, A., (1970). Application of pyrolysis and gas chromatography to the geochemical characterization of kerogen in sedimentary rocks. *Bull. Am. Assoc. Pet. Geol.*, 54, pp. 439–455
- Gogou, A., Bouloubassi, I. and Stephanou, E. G., (2000). Marine organic geochemistry of the Eastern Mediterranean: 1. Aliphatic and polyaromatic hydrocarbons in Cretan Sea surficial sediments. *Marine Chemistry*, 68, 265-82.
- Hakimi, M.H., Wan Hasiah, A., & Shalaby, M.R., (2011). organic geochemical characteristics and depositional environments of Jurassic shales in the Masila basin of Eastern Yemen, *Geo Arabia* 16(1), pp. 47-64.
- Hakimi, M.H., Abdullah, W.H., Sia, G.S., Makeen, Y.M., (2013). Organic geochemical and petrographic characteristics of Tertiary coals in the northwest Sarawak, Malaysia: Implications for palaeoenvironmental conditions and hydrocarbon generation potential. *Marine and Petroleum Geology* 48, 31-46.
- Haile, N., Ho, C., (2014). Geological field guide, Sibu-Miri Traverse, Sarawak. 37p

- Hall, R., (1996). Reconstructing Cenozoic SE Asia. In: Hall, R. & Blundell, D. J., (eds.) Tectonic Evolution of SE Asia. Geological Society, London, Special Publications 106, 153- 184.
- Hall, R., and Nichols, G., (2002). Cenozoic sedimentation and tectonics in Borneo: climatic influences on orogenesis. In: Jones S J, Frostick, L. (eds.), Sediment Flux to Basins: Causes, Controls and Consequences, Geological Society London Special Publication, 191:5–22.
- Hall, R., and C. K. Morley (2004), Sundaland basins, in Continent-Ocean Interactions within East Asian Marginal Seas, Geophys. Monogr. Ser, vol. 149, edited by P. Clift et al., pp. 55–85, AGU, Washington, D. C.
- Hall, R., van Hattum, M.W.A., Spakman, W., (2008). Impact of India–Asia collision on SE Asia: the record in Borneo. *Tectonophysics* 451, 366–389.
- Hall, R., (2013). Contraction and extension in northern Borneo driven by subduction rollback. *J. Asian Earth Sci.* 76, 399-411
- Harris, N. B., Freeman, K. H., Pancost, R. D., White, T. S. and Mitchell, G. D. (2004). The character and origin of lacustrine source rocks in the Lower Cretaceous synrift section, Congo Basin, west Africa. *AAPG Bulletin* 88, 1163– 1184.
- Hazebroek, H. P., and Tan, D. N. K., (1993). Tertiary tectonic evolution of the NW Sabah continental margin, in *Proceedings of the Symposium on Tectonic Framework and Energy Resources of the Western Margin of Pacific Basin*, edited by G. H. Teh, *Bull. Geol. Soc. Malays.*, 33, 195–210.
- Hesse, S., S. Back, and Franke, D., (2009). The deep-water fold-and-thrust belt offshore NW Borneo: Gravity-driven versus basement-driven shortening, *Geol. Soc. Am. Bull.*, 121, 939–953, doi:10.1130/B26411.1.
- Hinz, K., and Schlüter, H.U., (1985). Geology of the Dangerous Grounds, South China Sea and the continental margin off southwest Palawan: Results of SONNE cruises SO-23 and SO-27, *Energy*, 10, 297–315.
- Hinz, K., J. Fritsch, E. H. K. Kempter, A. Manaf Mohammad, J. Meyer, D. Mohammad, H. Vosberg, J. Weber, and J. Benavidez., (1989). Thrust tectonics along the north-western continental margin of Sabah/Borneo, *Geol. Rundsch.*, 78, 705–730,

- Hunt, J.M., (1996). *Petroleum Geochemistry and Geology*. W.H. Freeman and Company. New York. pp. 743
- Hutchison, C.S., (1996a). The 'Rajang accretionary prism' and 'Lupar Line' problem of Borneo. In: R. Hall and D.J. Blundell, (eds.) *Tectonic evolution of Southeast Asia*, Geological Society, London, Special Publication, 106, 247-261.
- Hutchison, C.S., (1996b). *South-East Asian Oil, Gas, Coal and Mineral Deposits*, Oxford Monographs on Geology and Geophysics, 36, Clarendon Press, Oxford, 265 p
- Hutchison, C.S., Bergman, S.C., Swauger, D.A., Graves, J.E., (2000). A Miocene collisional belt in north Borneo: uplift mechanism and isostatic adjustment quantified by thermochronology. *Journal of the Geological Society*, London, 157, 783–793.
- Hutchison, C.S., (2005). *Geology of North-West Borneo*. Elsevier. pp.42.
- Horsfield, B., (1989). Practical criteria for classifying kerogens: some observations from pyrolysis–gas chromatography. *Geochim. Cosmochim. Acta*, 53.
- Horsfield, B., (1997). The bulk composition of first-formed petroleum in source rocks. In: D.H. Welte, B. Horsfield, D.R. Backer (Eds.), *Petroleum and Basin Evolution; Insights from Petroleum Geochemistry, Geology and Basin Modeling*, Springer, Berlin.
- Horsfield, B., Dueppenbecker, S., (1991). The decomposition of Posidonia Shale and Green River Shale kerogens using microscale sealed vessel (MSSV) pyrolysis. *J. Anal. Appl. Pyrolysis* 20, 107-123.
- Hedges J, Keil R (1995) Sedimentary organic matter preservation: an assessment and speculative synthesis. *Marine Chemistry* 49:81-115.
- Ibrahim, M. I. A., Al-Saad, H, Kholeif, S.E.,(2002).Chronostratigraphy, palynofacies, source rock potential, and organic thermal maturity of Jurassic rocks of Qatar. *GeoArabia*, 7: 675 – 696.
- Ingram, G. M., T. J. Chisholm, C. J. Grant, C. A. Hedlund, P. Stuart-Smith, and J. Teasdale (2004). Deepwater North West Borneo: Hydrocarbon accumulation in an active fold thrust belt, *Mar. Pet. Geol.*, 21, 879– 887,

- Jones, B., Manning, D. A.C., (1994). Comparison of geochemical indices used for the interpretation of paleoredox conditions in ancient mudstones: *Chemical Geology*, v. 111, p. 111-129.
- Jackson, C.A.L, Zakaria, A.A., Johnson, H.D., Tongkul, F., Crevello, P.D., (2009). Sedimentology, stratigraphic occurrence and origin of linked debrites in the West Crocker Formation (Oligo-Miocene), Sabah, NW Borneo. *Marine and Petroleum Geology* 26, p.1957-1973.
- James, D.M.D., (1984). Regional geological setting, In: D.M.D. James, (ed.) *The Geology and Hydrocarbon Resources of Negara Brunei Darussalam*. Brunei Museum and Brunei Shell Petroleum Company, 34-42.
- Killops, S.D., Killops, V.J., (2005). *Introduction to organic geochemistry*. Blackwell Pub., Malden, MA.
- Kholeif, S.H.E, Ibrahim, M.I, (2010). Palynofacies Analysis of Inner Continental Shelf and Middle Slope Sediments offshore Egypt, South-eastern Mediterranean, *Geobios* 43: 333-340.
- Kessler, F.L., (2010). Observations on sediments and deformation characteristics of the Sarawak Foreland, Borneo Island. *Warta Geologi* 35,1-10
- Kessler, F.L., (2005). Comments on the evolution of Bukit Lambir area; PGCE, 6 December, Kuala Lumpur.
- King, R. C., M. R. P. Tingay, R. R. Hillis, C. K. Morley, and J. Clark (2010). Present-day stress orientations and tectonic provinces of the NW Borneo collisional margin, *J. Geophys. Res.*, 115, B10415, doi:10.1029/2009JB006997.
- Lamb, A.L., Wilson, G.P., Leng, M.J., (2006). A review of coastal palaeoclimate and relative sea-level reconstructions using $\delta^{13}\text{C}$ and C/N ratios in organic material. *Earth-Science Reviews* 75:29-57.
- Larter, S.R., (1984). Application of analytical pyrolysis technique to kerogen characterization and fossil fuel exploitation. In: K. Voorhees (Ed.), *Analytical Pyrolysis*, Butterworth's, London, pp. 212–275

- Larter, S.R., Douglas, A.G., (1980). A Pyrolysis –gas chromatographic method for kerogen typing. In: A.G. Douglas, J.R. Maxwell (Eds.), *Advances in Organic Geochemistry*. Pergamon Press, New York, pp. 579–584.
- Larter, S.R., Senftle, J.T., (1985). Improved kerogen typing for petroleum source rock analysis. *Nature* 318, 277-280.
- Lambiase, J.J. and Suraya Tulot, (2013). Low energy, low latitude wave-dominated shallow marine depositional systems: examples from northern Borneo. *Journal of Marine Geophysics*.
- Lambiase, J.J. and A. B. Cullen, (2013). Sediment supply systems of the Champion "Delta" of NW Borneo: implications for deepwater reservoir sandstones. *Journal of Southeast Asian Earth Sciences*, 76, 356-371.
- Lambiase, J.J., Tzong, T.Y., William, A.G., Cullen, A.B., (2008). The WestCrocker formation of NW Borneo: an Eocene accretionary prism. In: Draut, A.E., Clift, R.D., Scholl, D.W. (Eds), *Formation and Applications of the Sedimentary record in Arc Collision Zones*. Geological Society of America, Special Paper, 436, pp. 171–184.
- Lambiase, J.J., Ovinda, (2006). Reservoir geometry, lateral facies continuity and permeability heterogeneities in outcropping shoreface sandstones, Brunei Darussalam. In: *American Association of Petroleum Geologists International Conference*, Perth.
- Leong, K.M., (1999). Geological Setting of Sabah. *The Petroleum Geology and Resources of Malaysia*. Petroliaam Nasional Berhard (PETRONAS). Kuala Lumpur. 293-341.
- Lesslar, P. and Wannier , M., (2001). Destination Mri: A geological tour of Northern Sarawak's National Parks and Giant Caves. Multimedia in Ecomedia Software, Miri Sarawak.
- Leichti P, Roe FN, Haile NS, Kirk HJC (1960) The geology of Sarawak, Brunei and western part of north Borneo. *Sarawak Geological Survey* 3:
- Lewan, M.D. Maynard, J.B., (1982). Factors controlling enrichment of vanadium and nickel in the bitumen of organic sedimentary rocks: *Geochimica et Cosmochimica Acta*, v. 46, p.2547-2560.

- Lewan, M.D., (1984). Factors controlling the proportionality of vanadium to nickel in crude oils: *Geochimica et Cosmochimica Acta*, v. 48, p. 2231-2238.
- Levell, B.K., (1987). The nature and significance of regional unconformities in the hydrocarbon-bearing Neogene sequence offshore West Sabah. *Geological Society of Malaysia Bulletin*, 21, 55-90.
- Leong, K.M., Azlina Anuar (1999). Sabah Basin. *The Petroleum Geology and Resources of Malaysia*. Petroliaam Nasional Berhard (PETRONAS). Kuala Lumpur. 499-515.
- Mazlan b. Haji Madon (1997) Sedimentological aspects of the Temburong and Belait Formations, Labuan (Offshore west Sabah, Malaysia). *Geol. Soc. Malay. Bull.*, 41, 61-84
- Mackenzie, A. S. (1984). Application of biological markers in petroleum geochemistry. In: *Advances in Petroleum Geochemistry Vol.1* (J. Brooks and D. H. Welte, eds.), Academic Press, London, p. 115-214.
- Madon, M.B.H., Abolins, P.. (1999). Balingian Province. In *The Petroleum Geology and Resources of Malaysia* pp-343-346, PETRONAS , Kuala Lumpur, Malaysia
- Madon, M. B. H., (1999a). Geological Setting of Sarawak, in *The Petroleum Geology and Resources of Malaysia*, pp. 273–290, PETRONAS, Kuala Lumpur, Malaysia.
- Madon, M. B. H., (1999b). Basin types, tectono-stratigraphic provinces, structural styles, in *The Petroleum Geology and Resources of Malaysia*, pp. 77–112, PETRONAS, Kuala Lumpur, Malaysia.
- Mango, F. D. (1991). The stability of hydrocarbons under time-temperature condition of petroleum genesis. *Nature* 352, 146-148.
- Moldowan, J. M., Seifert, W. K. and Gallegos, E. J., (1985). Relationship between petroleum composition and depositional environment of petroleum source rocks. *AAPG Bulletin*, 69:12, 55-68.
- Meyers, P. A., (1997). Organic geochemical proxies of Paleooceanographic, Paleolimnologic, and Paleoclimatic processes. *Organic Geochemistry*, 27, 213-50.

- Milsom, J., Holt, R., Bin Ayub, D., Smail, R., (1997). Gravity anomalies and deep structural controls at the Sabah-Palawan margin, South China Sea. In: Frazer, A.J., Matthews, S.J., Murphy, R.W., (eds.). *Petroleum Geology of Southeast Asia*. Geological Society, London, Special Publication, 126, 417-427.
- Morley, C. K., (2003). Mobile shale related deformation in large deltas developed on passive and active margins, in *Subsurface Sediment Mobilization*, edited by P. van Rensbergen et al., *Geol. Soc. Spec. Publ.*, 216, 335–357.
- Morley, C.K., Back, S., (2008). Estimating hinterland exhumation from late orogenic basin volume, NW Borneo. *Journal of Geological Society*, London, 165, 353-364.
- Morrison, K., Lee, W. C., (2003). Sequence stratigraphic framework for Northwest Borneo. *Bulletin of the Geological Society of Malaysia*, 47, 127-138
- MacDonald, R., Hardman, D., Sprague, R., Meridji, Y., Mudjiono, W., Galford, J., Rourke, M., Dix, M., Kelto, M., (2010). Using elemental geochemistry to improve sandstone reservoir characterization: a case study from the Unayzah A interval of Saudi Arabia. In: *SPWLA 51st Annual Logging Symposium*. pp 1-16
- Muller, A., Voss, M., (1999). The palaeoenvironments of coastal lagoons in the southern Baltic Sea, II. $\delta^{13}C$ and $\delta^{15}N$ ratios of organic matter – sources and sediments. *Palaeogeography, Palaeoclimatology, Palaeoecology* 145:17-32.
- Nissenbaum, A., Swaine, D., (1976). Organic matter-metal interactions in Recent sediments: the role of humic substances. *Geochimica et Cosmochimica Acta* 40:809-816
- Nagarajan R., (2013). Geochemistry of Neogene sedimentary rocks of Borneo Basin, East Malaysia: Paleo-weathering, provenance and tectonic setting. *Chemie Erde-Geochemistry*.
- Nøhr-Hansen, H., (1989). Visual and chemical kerogen analyses of the Lower Kimmeridge Clay, Westbury, England. In: Batten DJ, Keen MC (eds) *Northwest European micropalaeontology and palynology*. Ellis Horwood Limited, Chichester, pp 118–132
- Nizam , A.B., Abudul Hadi, A., Mazlan, M., (2008). The West Crocker Formation (Early Oligocene to Middle Miocene) in the Kota Kinabalu Area, Sabah: Facies, Sedimentary Processes and Depositional Setting. *PGCE*, 14 January, Kuala Lumpur

- Nor Azidin, N.F., Balaguru, A., Ahmad, N., (2011). Structural Styles of the North West Sabah and West Sulawesi Fold Thrust Belt Regions and its Implication to the Petroleum System – A Comparison. PGCE , 03 July, Kuala Lumpur
- Patterson, J.H., A.R. Ramsden, L.S. Dale, and J.J. Fardy, (1986), Geochemistry and mineralogical residences of trace elements in oil.
- Paramanathan, S., (1998). Malaysian Soil Taxonomy (Second Approximation). Mal. Soc. Soil Sci. and Param Agric .Soil Surveys, March
- PETRONAS., (2013), Petronas announces oil and gas discovery onshore Sarawak. Petronas Media Release. Retrieved from <http://www.petronas.com.my/media-relations/media-releases/Pages/article/PETRONAS-ANNOUNCES-OIL-AND-GAS-DISCOVERY-ONSHORE-SARAWAK.aspx>. January 18
- PETRONAS, (1999). The Petroleum Geology and Resources of Malaysia: Kuala Lumpur, Malaysia, Petrolia Nasional Berhad, 665p
- Peters, K. E. (1986) Guidelines for evaluating petroleum source rock using programmed pyrolysis. AAPG bulletin, 70, 318-329.
- Peters, K.E., Cassa, M.R., (1994). Applied source rock geochemistry. In: Magoon , L.B., Dow, W.G. (Eds), The Petroleum System-From Source to Trap. American Association of Petroleum Geologists Memoir, vol 60, pp.93-120.
- Peters, K.E., Walters, C.C., Moldowan, J.M., (2005). The biomarker guide. Cambridge University Press, Cambridge, UK
- Peters, K.E., Moldowan, J.M., (1993) The biomarker guide. Prentice Hall, Englewood Cliffs, N.J.
- Pepper, A. S., Corvi, P., (1995) Simple kinetic models of petroleum formation. Part 1: Oil and gas generation from kerogen. Marine and Petroleum Geology, 12, 291-319.

- Pereira, W.E., Hostettler, F.D., Luoma, S.N., van Geen, A., Fuller, C.C., Anima, R.J., (1999). Sedimentary record of anthropogenic and biogenic polycyclic aromatic hydrocarbons in San Francisco Bay, California. *Mar. Chem.* 64, 99–113.
- Philp, R. P. (1985). *Fossil Fuel Biomarkers. Methods in Geochemistry and Geophysics*, Elsevier, New York, 23, p. 294.
- Powell, T. G., (1988). Pristane/Phytane ratio as environmental indicator. *Nature*, 333, 604.
- Powell, A.J., Dodge, J.D., Lewis, J., (1990). Late Neogene to Pleistocene palynological facies of the Peruvian continental margin upwelling, Leg 112. *Proceedings of the Ocean Drilling Project, Scientific Results*, 112, pp. 297–321
- Powell, W.G., Johnston, P.J., Collom, C.J., (2003). Geochemical evidence for oxygenated bottom waters during deposition of fossiliferous strata of the Burgess Shale Formation. *Palaeogeography, Palaeoclimatology, Palaeoecology* 201, 24–268.
- Pi, D.H., Cong-Qiang, L., Shields-Zhond, A.G., Shao-Yong J., (2013). Trace and rare earth element geochemistry of black shale and kerogen in the early Cambrian Niutitang Formation in Guizhou province, South China: constraints for redox environments and origin of metal enrichments. *Precamb. Res.*, 225, 218–229.
- Piper, D.Z., (1994). Seawater as the source of minor elements in black shales, phosphorites and other sedimentary rocks. *Chemical Geology* 114:95-114.
- Raiswell, R., Buckley, F., Bern, R.A., (1988). Degree of Pyritization of Iron as a Paleoenvironmental Indicator of Bottom-Water Oxygenation. *SEPM Journal of Sedimentary Research*.
- Rangin, C., Bellon, H., Bernard, F., Letouzey, J., Muller, C. & Sanudin, T., (1990). Neogene arc-continent collision in Sabah, northern Borneo (Malaysia). *Tectonophysics* 183, 305-319.
- Radke, M. and Welte, D.H., (1983). The methylphenanthrene index (MPI): a maturity parameter based on aromatic hydrocarbons. In: Bjoroy M, editor. *Advances in Organic Geochemistry* 10:51-63.

- Radke, M., Welte, D. and Willsch, H., (1986). Maturity parameters based on aromatic hydrocarbons: influence of the organic matter type. *Organic Geochemistry* 10:51-63.
- Radke, M., (1987). Organic geochemistry of aromatic hydrocarbons. In: Brooks, J., Welte, D.H. (Eds.). *Advances in Petroleum Geochemistry, Vol.2*. London: Academic Press. 141-207.
- Radke, M., Welte, D.H. and Willsch, H. (1990). Methylated dicyclic and tricyclic aromatic hydrocarbons in crude oils from Handil Field (Indonesia). *Organic Geochemistry* 15:17-34.
- Radke, M., Hilkert, A. and Rullkoter, J., (1998). Molecular stable carbon isotope compositions of alkylphenanthrenes in coals and marine shales related to source and maturity. *Organic Geochemistry* 28.12: 785-795.
- Rijks, E.J.H., (1981). Baram delta geology and hydrocarbon occurrence. Geo. Survey Malaysia Bulletin, 14, 1-18
- Sandal, S.T., (1996). The geology and hydrocarbon resources of Negara Brunei Darussalam: Brunei Darussalam, Brunei Shell Petroleum Company Sendirian Berhad and Brunei Museum, 243 p
- Scalan, K. S. and Smith, J. E. (1970). An improved measure of odd even predominance in the n-alkanes of sediment extract and petroleum, *Geochimica et Cosmochimica Acta*, 34, 611-620.
- Scherer, F.C., (1980). Exploration in East Malaysia over the past decade. In: Halbouty, M.T., ED., *Giant Oil and Gas Fields of the Decade 1968-1978*. AAPG Memoir, 30, 423-440
- Schwark, L., Ferretti, A., Papazzoni, C. A. and Trevisani, E. (2009) Organic geochemistry and paleoenvironment of the Early Eocene "Pesciara di Bolca" Konservat-Lagerstätte, Italy. *Palaeogeography, Palaeoclimatology, Palaeoecology*, 273, 272-85.
- Simoneit, B. R. T. (2004) Biomarkers (Molecular fossils) as geochemical indicators of life. *Advances in Space Research*, 33, 1255-61.

- Seah, E., Zulkifli S. and Awang Sapawi, A.J. (1987). Rock Eval Analyses and Total Organic Carbon analyses of Core and Surface Samples from Sarawak. PETRONAS Report No. MGK/08/87.
- Simons, W. J. F., et al. (2007), A decade of GPS in Southeast Asia: Resolving Sundaland motion and boundaries, *J. Geophys. Res.*, 112, B06420,
- Silliman JE, Meyers PA, Bourbonniere RA (1996) Record of postglacial organic matter delivery and burial in sediments of Lake Ontario. *Organic Geochemistry* 24:463-472.
- Tan, D.N.K., Abdul Hadi, A., Azlina Anuar, Boniface, B., Chow K.T.,(1999). West Baram Delta. The Petroleum Geology and Resources of Malaysia. *Petroleum Nasional Bernhard (PETRONAS)*. Kuala Lumpur. 293-341.
- Tan, C.H., (2010), Facies Distribution and Stratigraphic Development on a Shale-Cored Ridge, Klias Peninsula, Malaysia, *Bulletin of Earth Sciences of Thailand*, 3 (2), p.9- 11241–260.
- Taylor, G.H., M. Teichmüller, A. Davis, C.F.K. Diessel, R. Littke, and P. Robert, (1998), *Organic petrology*: Berlin & Stuttgart, Gebrüder Borntraeger, 704 p
- Taylor, B., Hayes, D.E., (1983). Origin and history of the South China Sea Basin. In: D.E. Hayes (ed.), *The Tectonic and Geologic Evolution of Southeast Asian Seas and Islands Part 2, Geophysical Monograph, 27, American Geophysical Union, Washington, D.C.*, 23-56.
- Teichmüller M, Littke R, Robert P, (1998). Coalification and maturation. In: Taylor GH, Teichmüller M, Davis A, Diessel CF, Littke R, Robert P (ed) *Organic Petrology*, Berlin: Gebrüder Borntraeger, 86–174.
- ten Haven HL, de Leeuw JW, Rullkötter J, Sinninghe Damsté JS (1987) Restricted utility of the pristane/phytane ratio as a palaeoenvironmental indicator. *Nature* 330:641-643.

- Tissot, B. P., Califet-Debyser, Y., Deroo, G. and Oudin, J. L. (1971) Origin and evolution of hydrocarbons in early Toarcian shales, Paris Basin, France. AAPG Bulletin, 55, 2177-93.
- Tissot, B.T. and Welte, D.H., (1984). Petroleum Formation and Occurrences. Second Edition. Berlin: Springer-Verlag.
- Tjia, H.D., (2012). The Paleo-Orientations of Northwestern Borneo and Adjacent to South China Sea Bains. Indonesian Journal of Geology, 7(2), 67-76
- Tongkul, F., (1989). "The sedimentology and structure of the Crocker Formation in the Kota Kinabalu area," GEOSEA VI Proceedings, Jakarta 1987, Indonesian Association of Geologists, pp. 135-156.
- Tulloch, A. P., (1976). Chemistry of waxes of higher plants. In: Kolattukudy, P. E(Ed.), Chemistry and Biochemistry of Natural Waxes. Elsevier, Amsterdam, p. 236.
- Tyson, R.V., (1995). Sedimentary organic matters: organic facies and palynofacies. Chapman & Hall, London, p 615.
- Telnaes, N., B.S. Cooper, and B. Jones, (1991). Kerogen facies, biomarker, trace metal contents, and spectral logs as indicators of oxicity and salinity, Upper Jurassic, North Sea, in
- Tribovillard, N., T.J. Algeo, T. Lyons, and A. Riboulleau, (2006). Trace metals as paleoredox and paleoproductivity proxies: An update: Chemical Geology, v. 232, p. 12-32.
- Tyson, R.V., (1987). The genesis and palynofacies characteristics of marine petroleum source rocks. In: Brooks J, Fleet A J. (Eds), Marine petroleum source rocks. Geol. Soc. Special Publ., 26: 47 – 67.

- Tyson, R.V., (1998). Late Jurassic palynofacies trends, Piper and Kimmeridge Clay formation, UK onshore and offshore. In: Batten D J, Keen M C (Eds), Northwest European Micropalaeontology and Palynology. Brit. Micropalaeontol. Soc. Series, Ellis Horwood, Chichester, pp. 135 – 172.
- Tyson, R.V. (1993). Palynofacies analysis. In: Jenkins DJ (Ed), Applied Micropaleontology, Kluwer Academic publishers, Dordrecht, pp. 153-191
- Tyson, R.V., (1995). Sedimentary Organic matter - Organic facies and palynofacies. Chapman and Hall, London. pp 615
- Van Hattum, M.W.A., Hall, R., Pickard, A.L., Nicols, G., (2013). Provenance and Geochronology of Cenozoic Sandstones of Northern Borneo. Journal of Asian Earth Sciences, 76, 266-282
- Van Hattum, M.W.A., Hall, R., Pickard, A.L., Nicols, G., (2006). Southeast Asian sediments not from Asia: Provenance and geochronology of north Borneo sandstones. Geology, 34 (7), 589-592.
- Wan Hasiah Abdullah, 1999. Oil-generating potential of Tertiary coals and other organic-rich sediments of the Nyalau Formation, onshore Sarawak. Journal of Asian Earth Sciences 17, 255-267
- Wannier M, Lesslar PH, Lee CH, Raven H, Sorkhabi R, and Ibrahim A. (2011) Geological Excursions Around Miri, Sarawak. EcoMedia, Miri, Malaysia, 308 p.
- William A.G., Lambiase, J.J., Back, S., Mohd Khalid, J., (2003). Sedimentology of the Jalan Salaiman and Bukit Melinsung outcrops, western Sabah: is the West Crocker Formation an analogue for Neogene turbidites offshore?. Geol. Soc. Malaysia, Bulletin 47, 63-75.
- Wilson, R.A.M., (1964). The Geology and Mineral Resources of Labuan and Padas Area, Sabah, Malaysia. Mem. 17, Geol. Sur. Borneo Region, Malaysia.
- Wignall, P.B., and J.R. Maynard, (1993). The sequence stratigraphy of transgressive black shales, in: Katz, B.J., Pratt, L.M., Eds., Source Rocks in a Sequence Stratigraphic Framework: AAPG Studies in Geology, vol. 37, p. 35-47.

- Wilford, G.E. (1961). The Geology and Mineral Resources of Brunei and adjacent part of Sarawak. British Borneo Geological Survey Memoir 10, 617-740.
- Yensepbayev, T., Izart, A., Joltaev, G., Hautevelle, Y., Elie, M. and Suarez-Ruiz, I., (2010). Geochemical characterization of source rocks and oils from the eastern part of the Precaspian and Pre-Uralian Basins (Kazakhstan): Palaeoenvironmental and palaeothermal interpretation. *Organic Geochemistry*, 41, 242-62.
- Zavattieri, A.N., Rosenfield, U., Volkheimer, W., (2008). Palynofacies analysis and sedimentary environment of Early Jurassic coastal sediments at the southern border of the Neuquen Basin, Argentina. *J. South Am. Earth Sci.* 25: 245-277

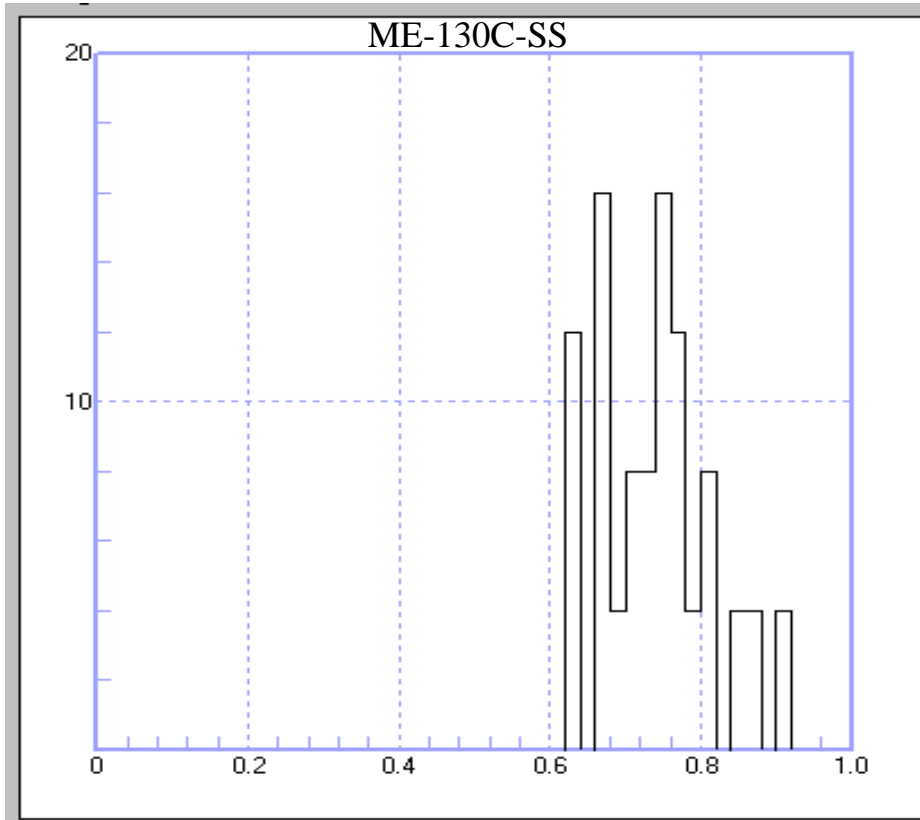
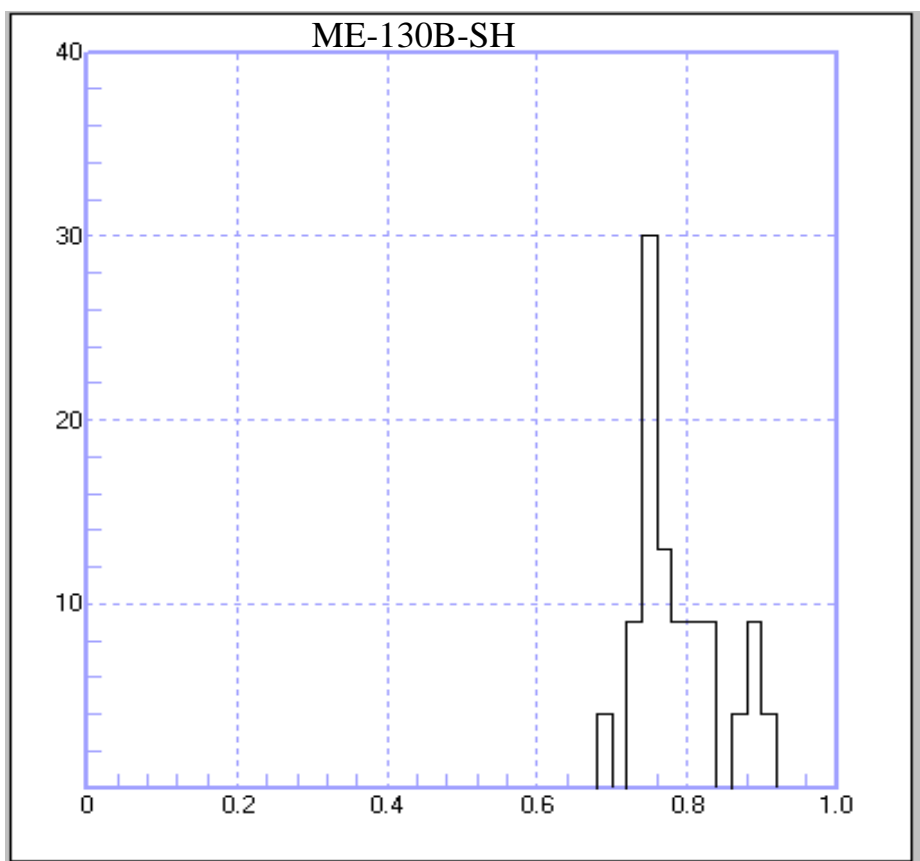
LIST OF PUBLICATIONS AND CONFERENCES

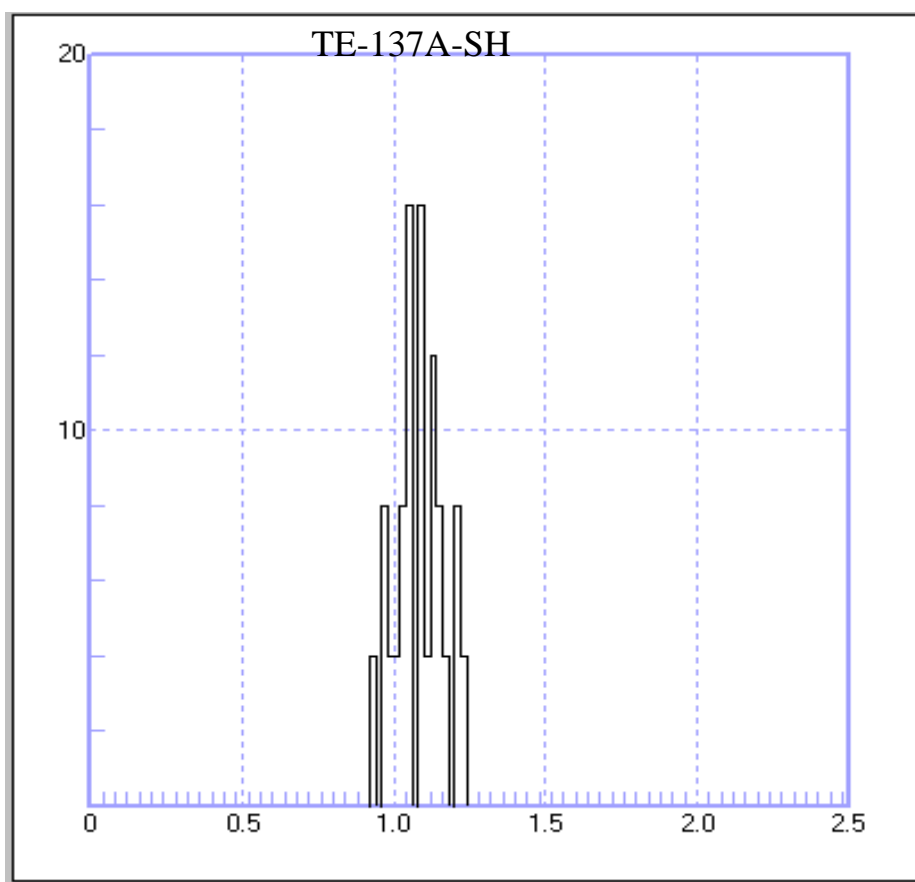
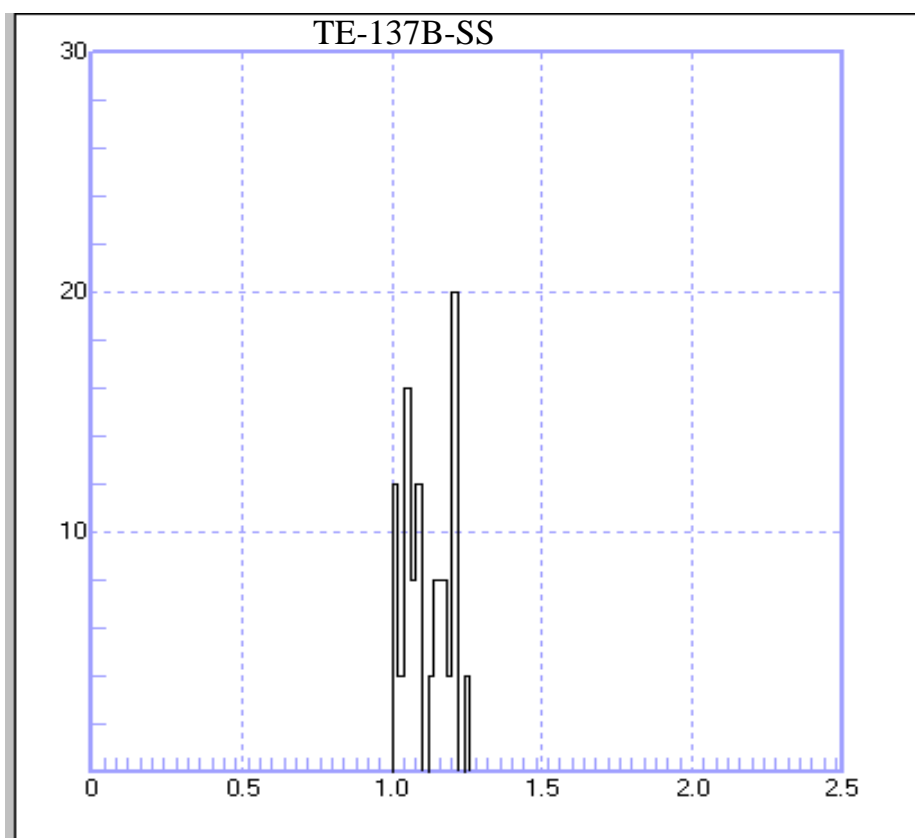
1. **Olayinka Serifat Togunwa**, Wan Hasiah Abdullah, Mohammed Hail Hakimi, Pedro Jose Barbeito, 2015. Organic geochemical and petrographic characteristics of Neogene organic-rich sediments from the onshore West Baram Delta Province, Sarawak Basin: Implications for source rocks and hydrocarbon generation potential. *Marine and Petroleum Geology* 63,115-126 (ISI-Cited Publication)
2. **Olayinka S. Togunwa** and Wan H. Abdullah 2015. Geochemical characterization of Neogene sediments from onshore West Baram Delta Province, Sarawak: Implications for paleoenvironment, source input and thermal maturity. *Central European Journal of Geosciences* (*under review*)
3. **Olayinka S. Togunwa** and Wan H. Abdullah. 2014. Biomarkers in the Lambir mudstones as indicators of source, paleoenvironment and thermal maturity, 9th Mathematics and Physical Graduate Congress, Malaysia. (*Poster presentation*)
4. Wan H. Abdullah, Felix Tongkul, Meor A. Hassan, **Olayinka S. Togunwa**, Khairul A. Mustapha. 2014. Petroleum Source Rock Potential of Cenozoic Sandy Facies of NW Borneo: Deepwater Submarine Fan of Crocker Formation versus Shallow Marine Deposits of Meligan Formation, Onshore Sabah, Malaysia. *AAPG ICE*, Istanbul. (*Poster presentation*)

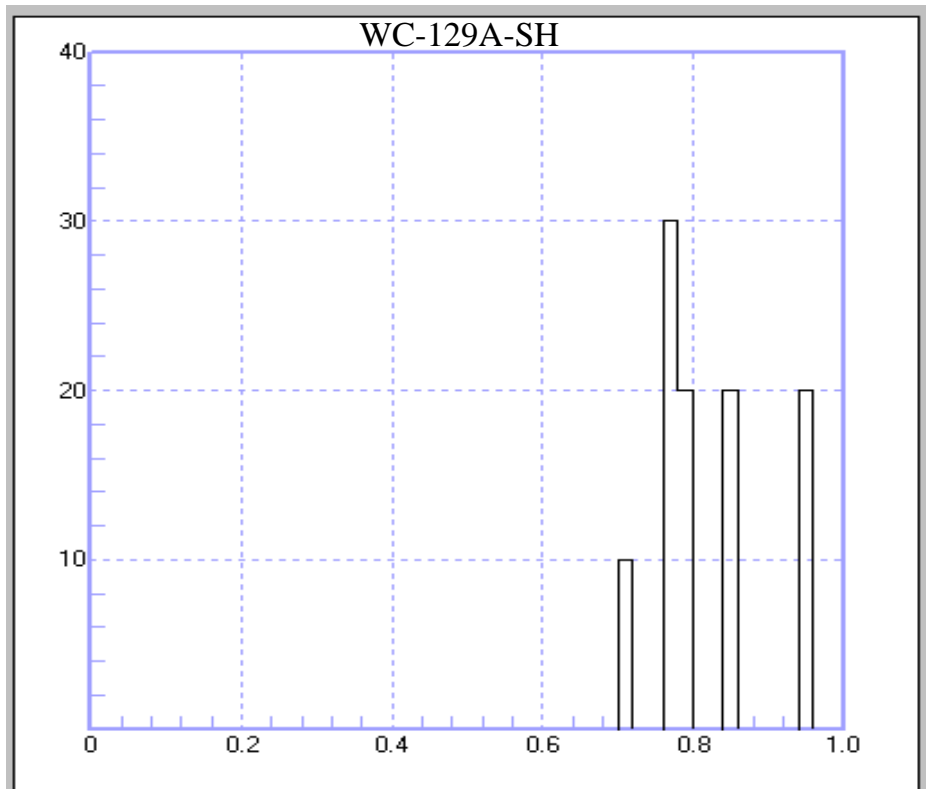
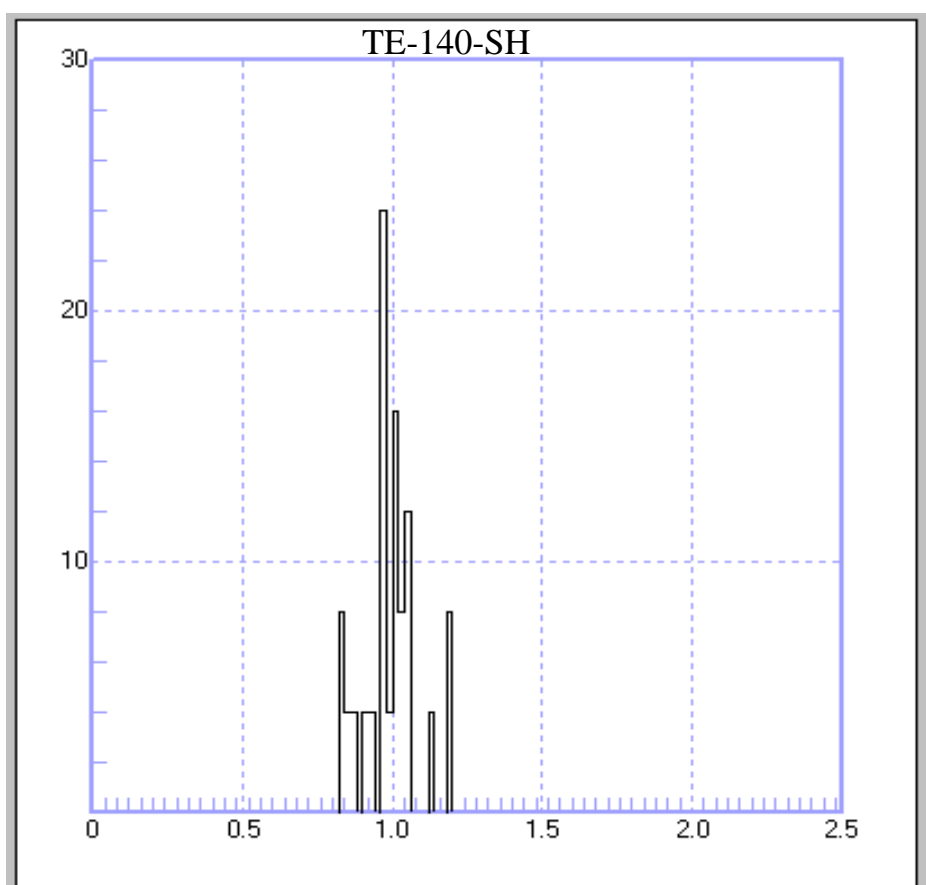
APPENDIX A

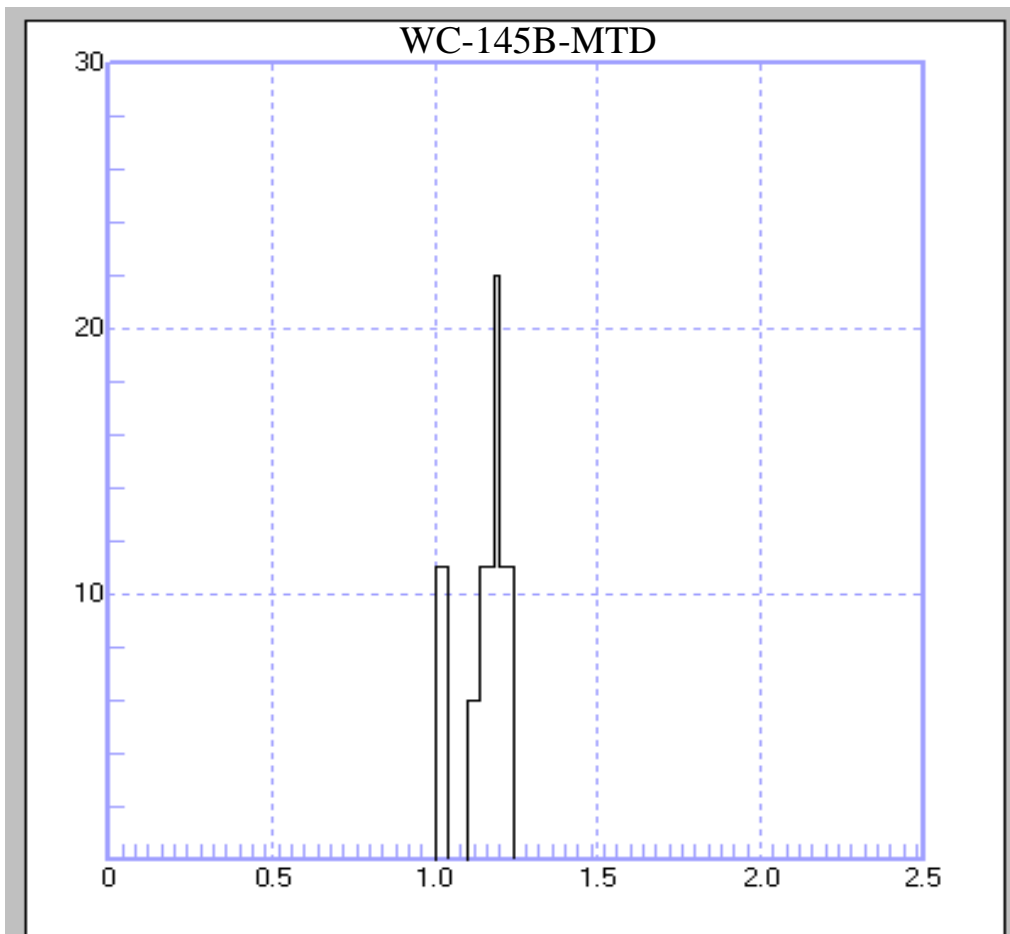
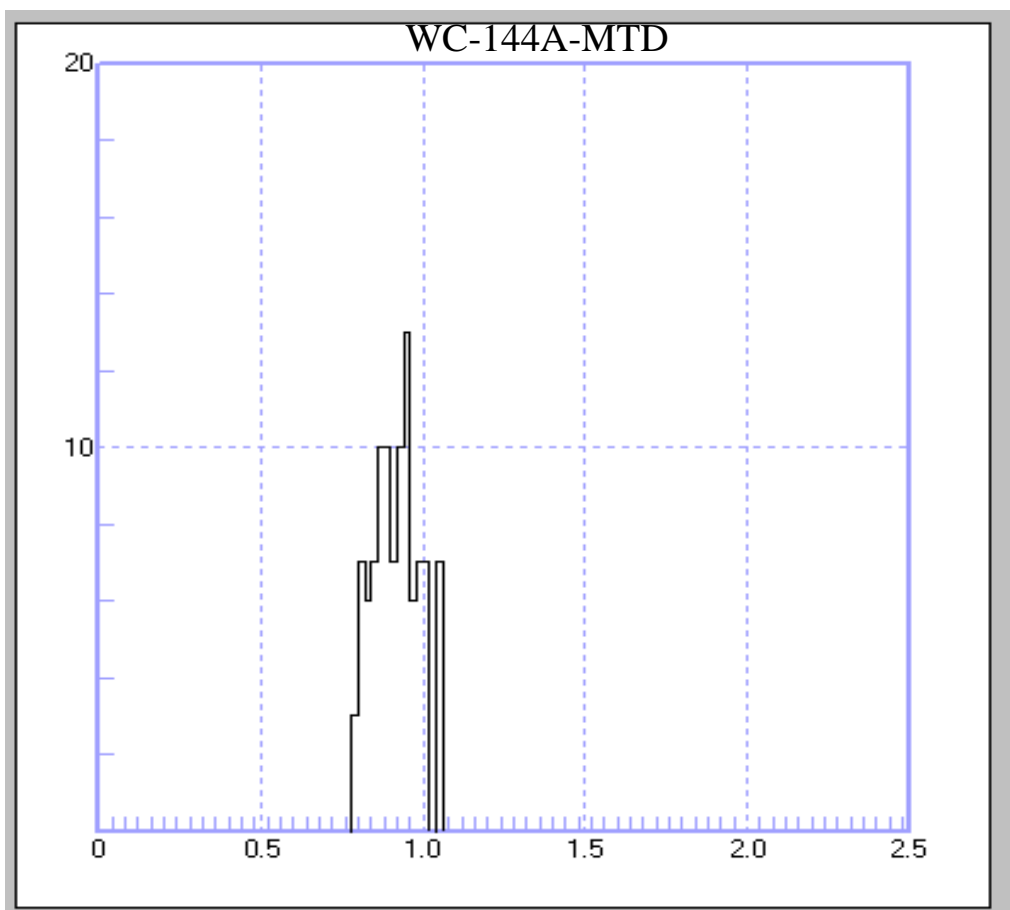
Vitrinite Reflectance Data and Histograms

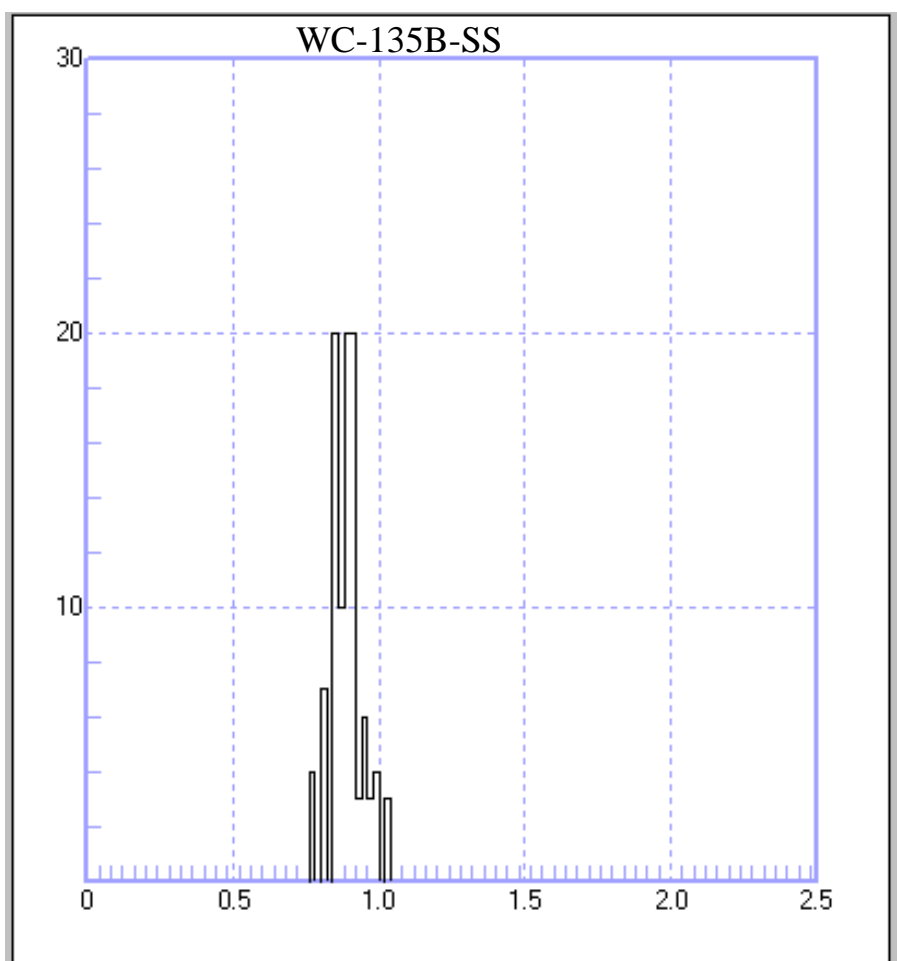
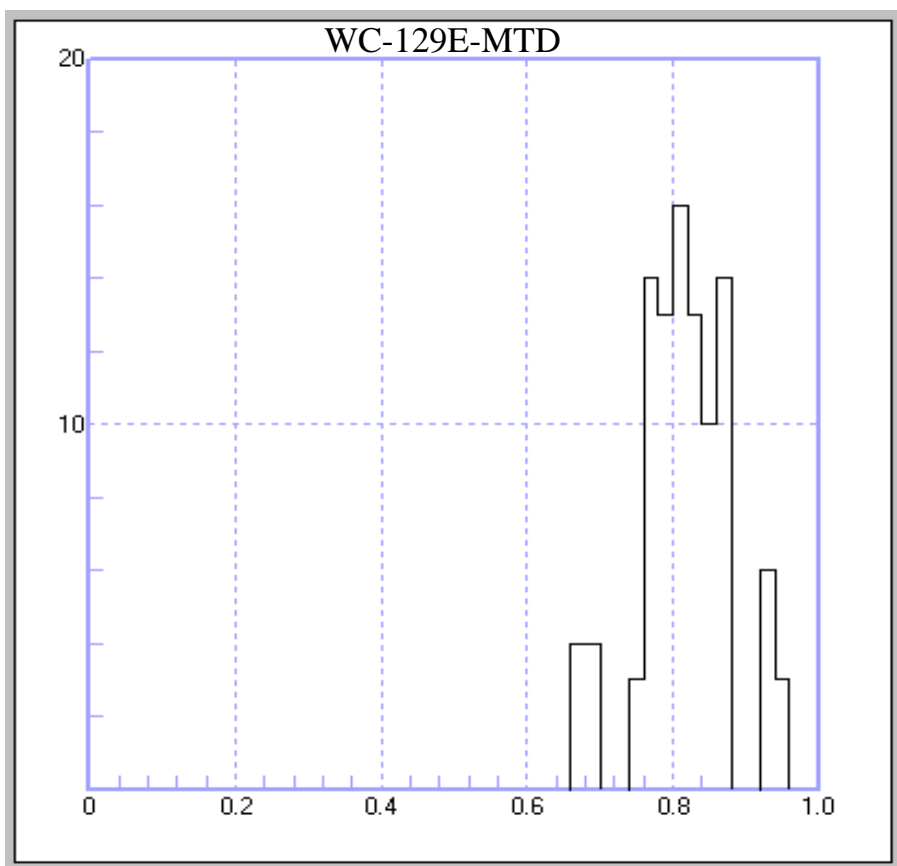
| Sample ID | Formation | Minimum | Maximum | Mean Ro % | N | Standard Deviation |
|-------------|------------------|---------|---------|-----------|----|--------------------|
| BL-A-5-SS | Belait | 0.40 | 0.52 | 0.45 | 45 | 0.03 |
| BL-C-2-SH | Belait | 0.40 | 0.51 | 0.46 | 20 | 0.03 |
| BL-A-7-SH | Belait | 0.41 | 0.50 | 0.45 | 20 | 0.02 |
| BL-A-3-SH | Belait | 0.41 | 0.49 | 0.44 | 60 | 0.02 |
| BL-A-2-SH | Belait | 0.41 | 0.52 | 0.45 | 43 | 0.03 |
| BL-A-6-SS | Belait | 0.40 | 0.47 | 0.43 | 30 | 0.02 |
| BL-B-1-SH | Belait | 0.41 | 0.47 | 0.44 | 21 | 0.02 |
| ME-130B-SH | Meligan | 0.79 | 0.91 | 0.79 | 23 | 0.06 |
| ME-133A-SS | Meligan | 0.65 | 0.78 | 0.72 | 50 | 0.03 |
| ME-134A-SS | Meligan | 0.58 | 0.83 | 0.71 | 30 | 0.07 |
| ME-130C-SS | Meligan | 0.62 | 0.91 | 0.74 | 25 | 0.07 |
| TE-137A-SH | Temburong | 0.93 | 1.22 | 1.08 | 25 | 0.08 |
| TE-137B-SS | Temburong | 1.01 | 1.24 | 1.11 | 25 | 0.08 |
| TE-140-SH | Temburong | 0.83 | 1.19 | 0.99 | 25 | 0.09 |
| WC-135B-SS | West Crocker | 0.77 | 1.03 | 0.89 | 30 | 0.05 |
| WC-129A-SH | West Crocker | 0.70 | 0.96 | 0.82 | 10 | 0.08 |
| WC-129E-MTD | West Crocker | 0.67 | 0.94 | 0.82 | 30 | 0.06 |
| WC-144A-MTD | West Crocker | 0.78 | 1.05 | 0.92 | 30 | 0.07 |
| WC-145B-MTD | West Crocker | 1.01 | 1.62 | 1.14 | 18 | 0.07 |
| UD-01-SS | Undifferentiated | 0.42 | 0.50 | 0.46 | 55 | 0.02 |
| UD-02-SS | Undifferentiated | 0.45 | 0.55 | 0.49 | 30 | 0.03 |
| L-02-SS | Lambir | | | 0.41 | | |
| L-03-SH | Lambir | | | 0.39 | | |
| L-05-SS | Lambir | 0.38 | 0.48 | 0.42 | 50 | 0.03 |
| L-07-SH | Lambir | | | 0.45 | | |
| L-14-SH | Lambir | | | 0.41 | | |
| M-01-SH | Miri | 0.46 | 0.50 | 0.48 | 50 | 0.09 |
| M-03-SH | Miri | | | 0.42 | | |
| M-05-SH | Miri | | | 0.43 | | |
| M-08-SH | Miri | | | 0.41 | | |
| M-11-SS | Miri | 0.40 | 0.47 | 0.45 | 50 | 0.03 |
| T-01-SS | Tukau | | | 0.41 | | |
| T-03-SH | Tukau | | | 0.45 | | |
| T-04-SH | Tukau | | | 0.42 | | |
| T-08-SH | Tukau | | | 0.43 | | |
| T-10-SS | Tukau | | | 0.42 | | |

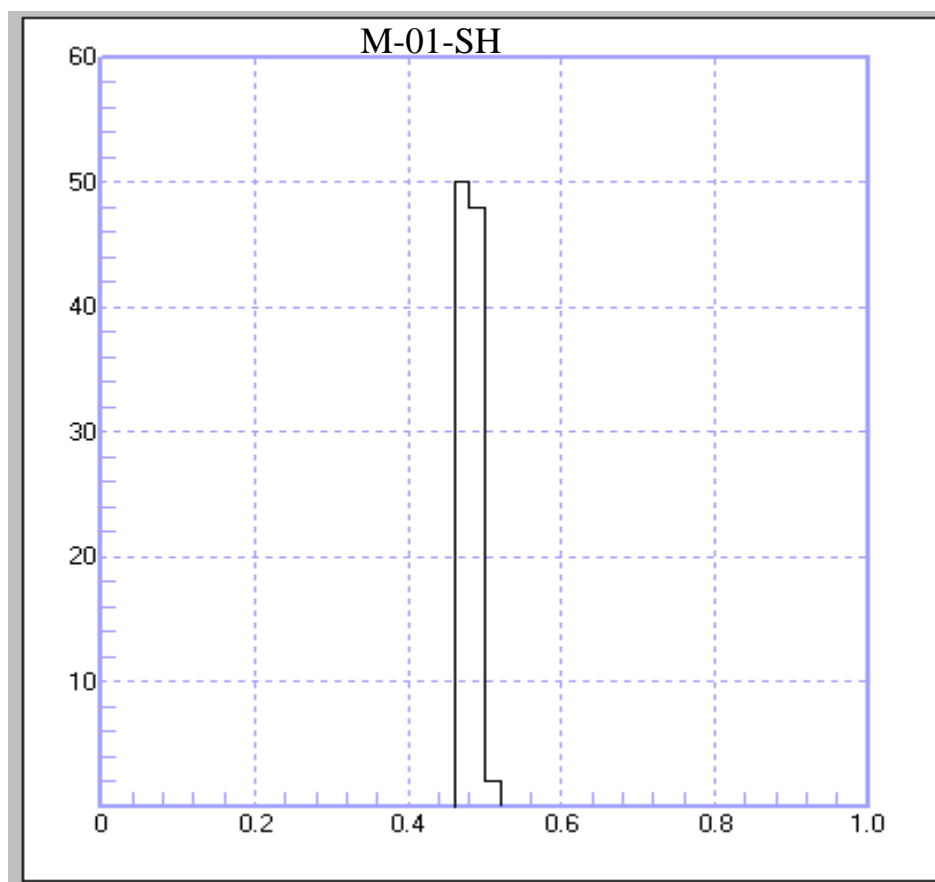
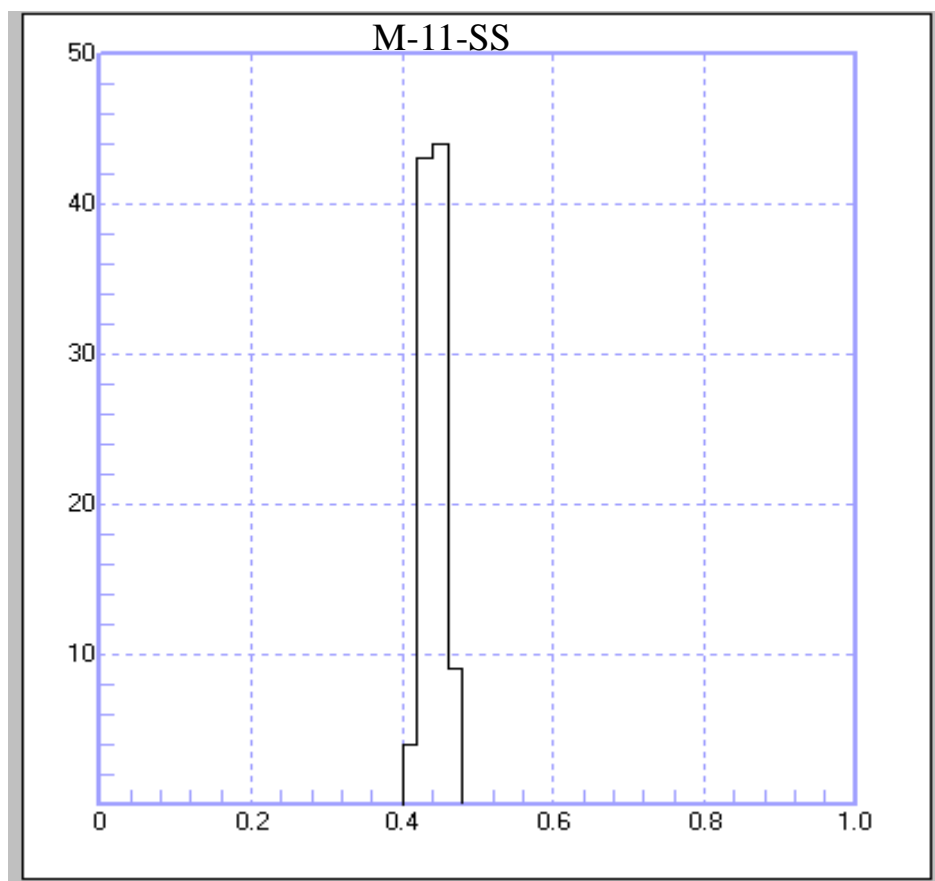


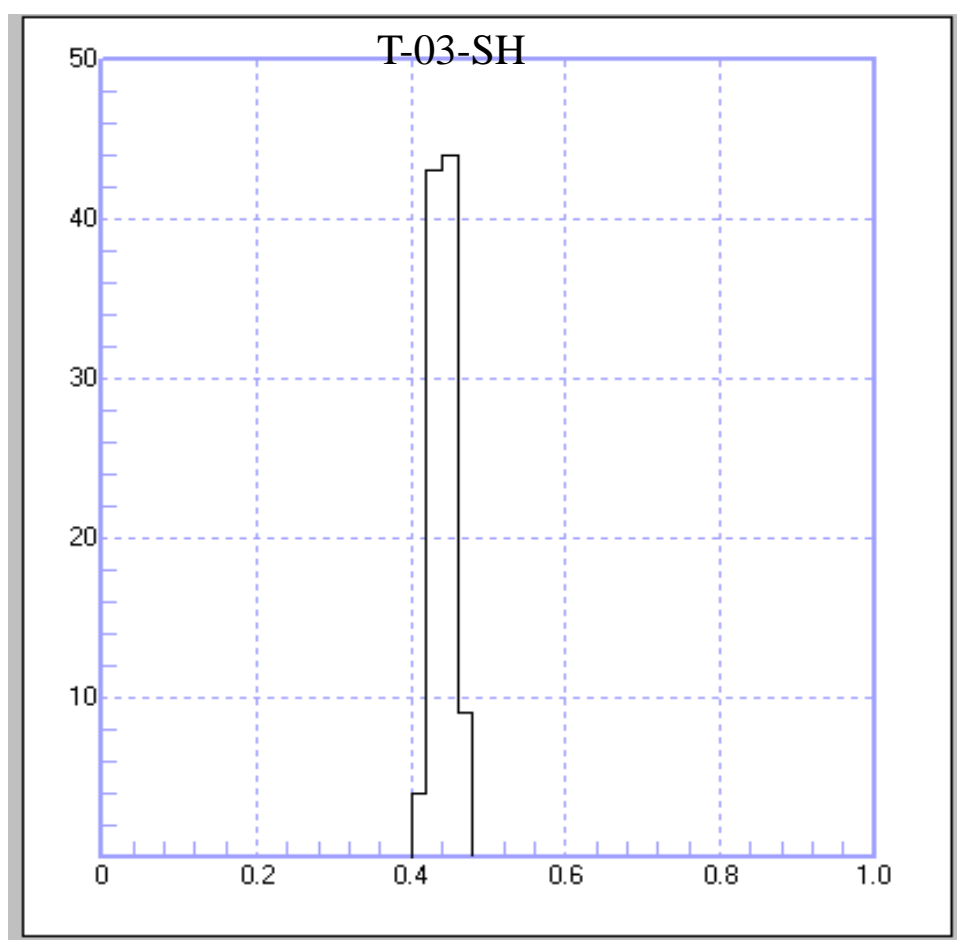
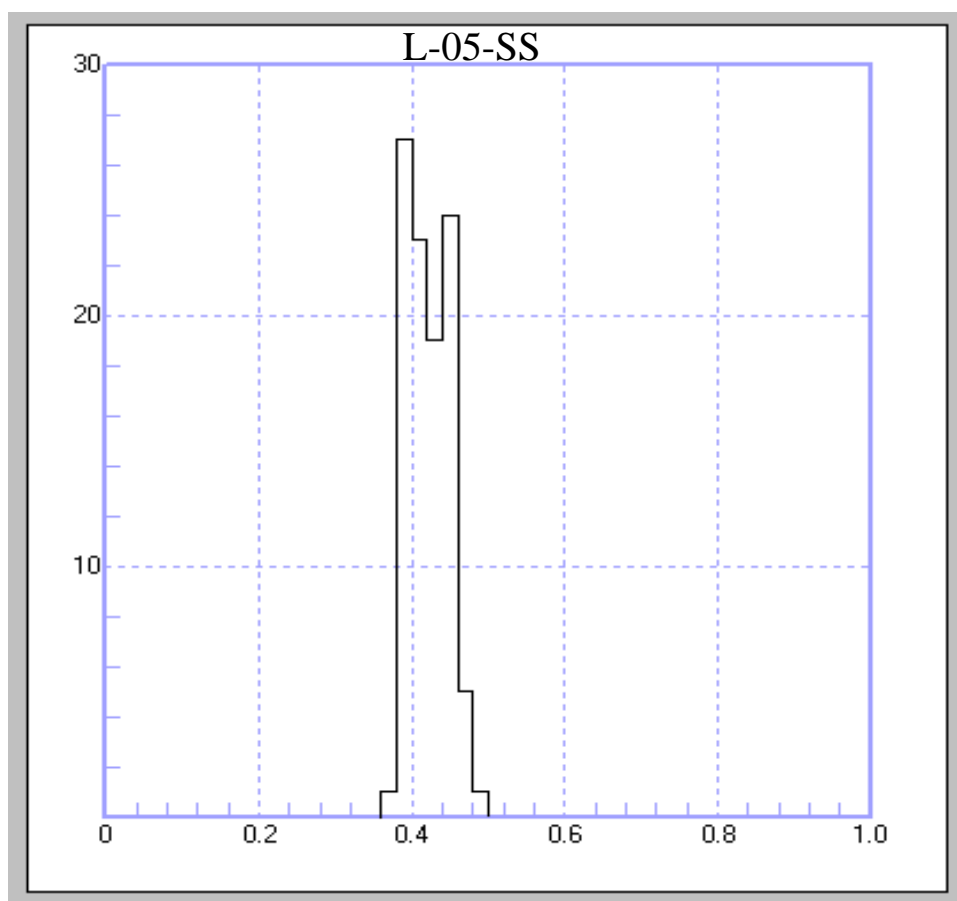


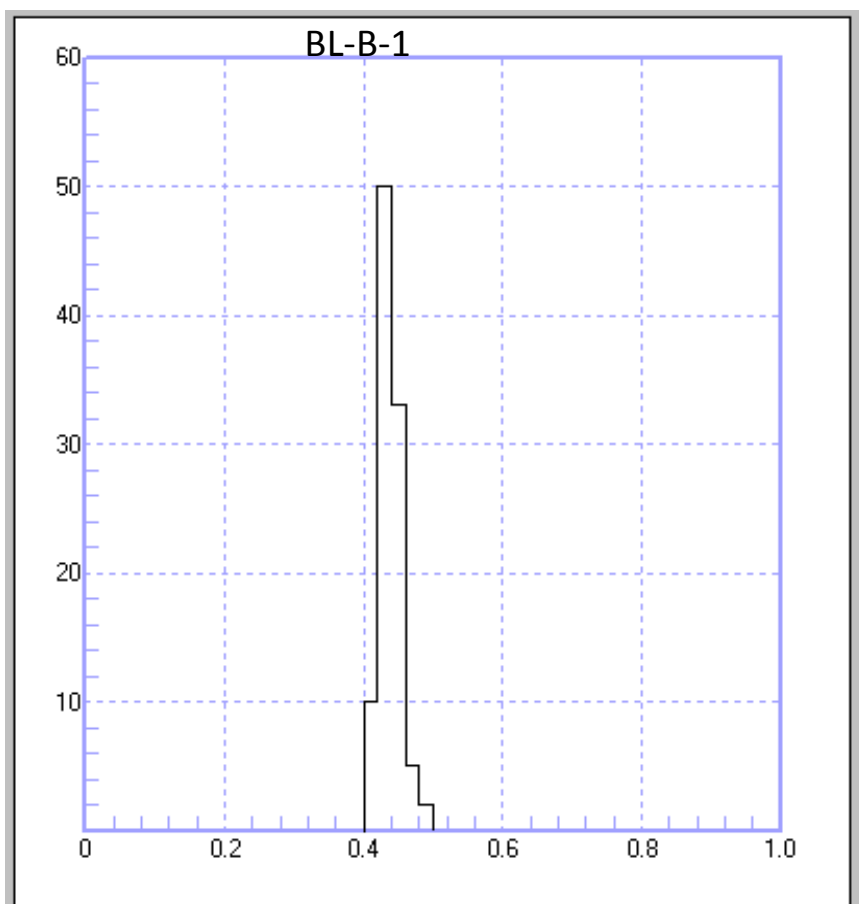
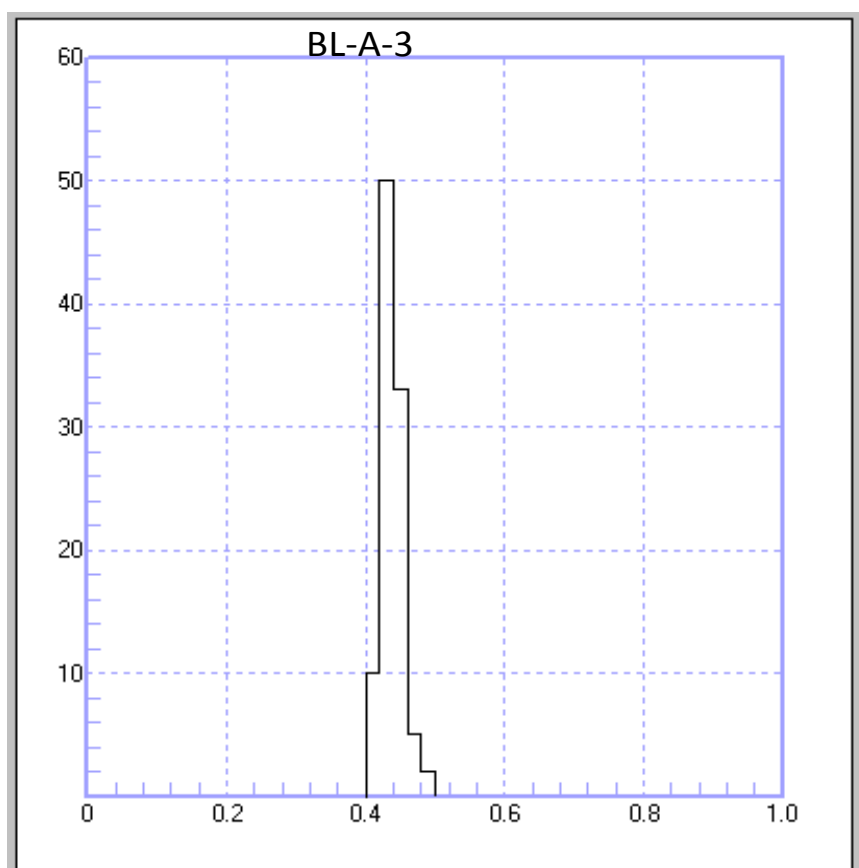


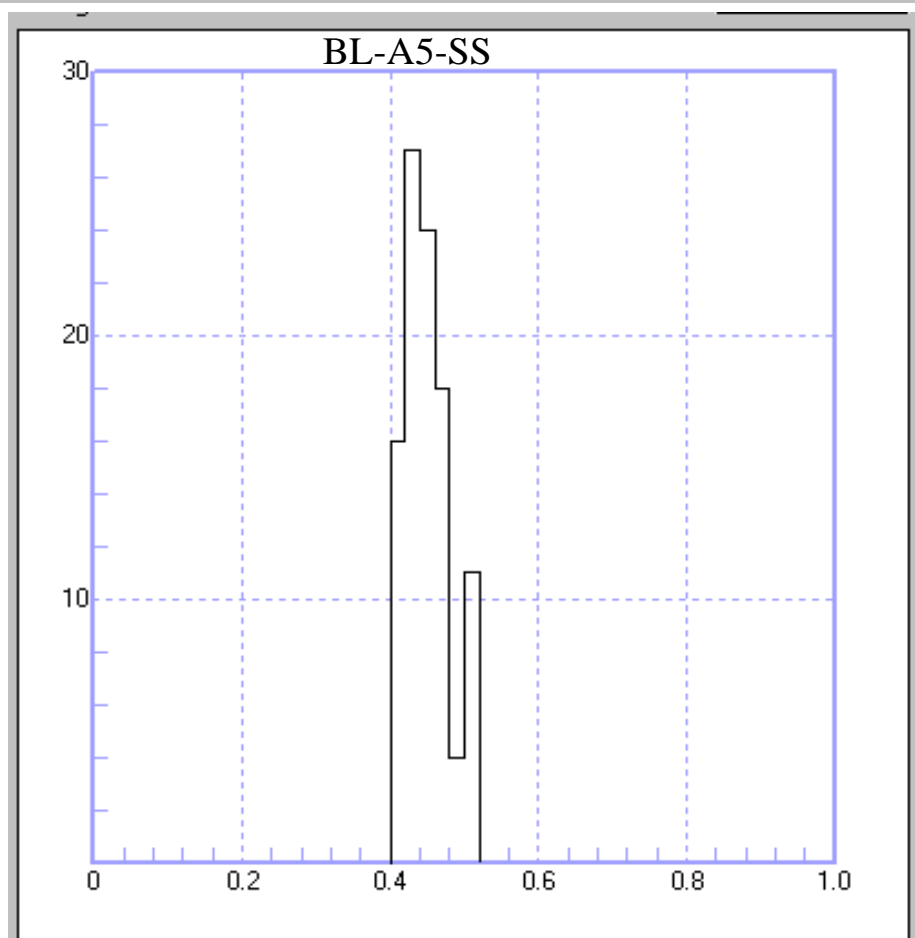
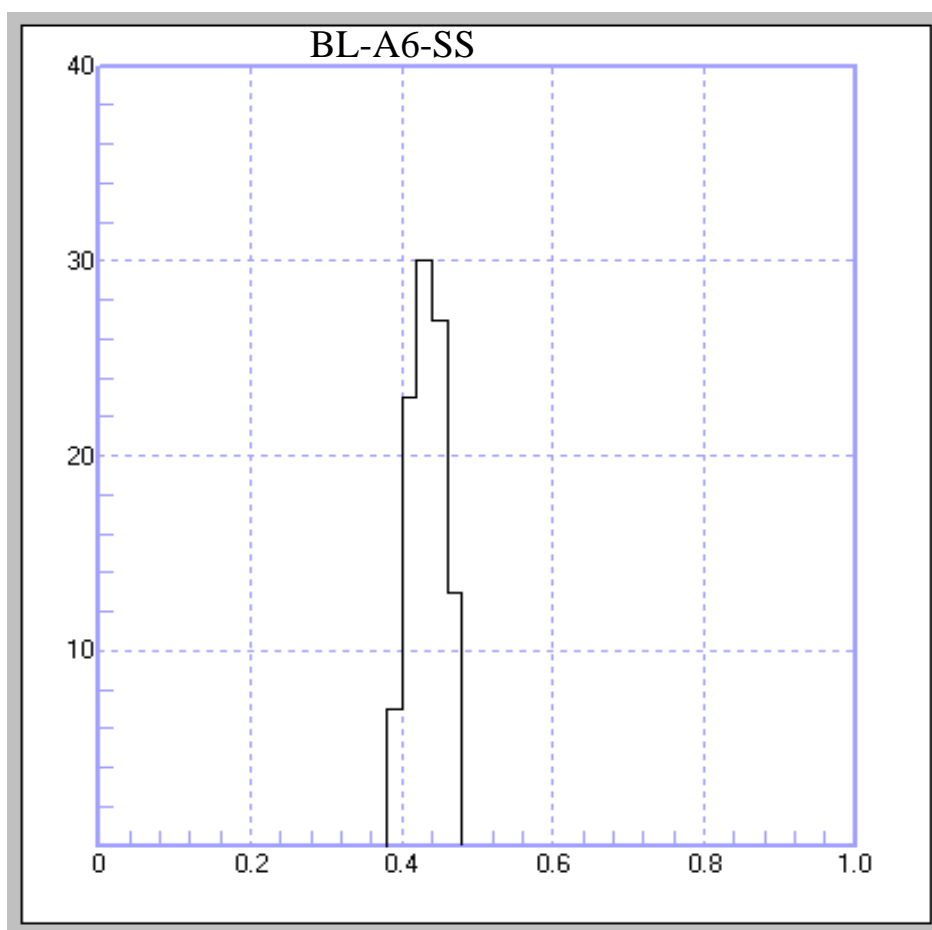


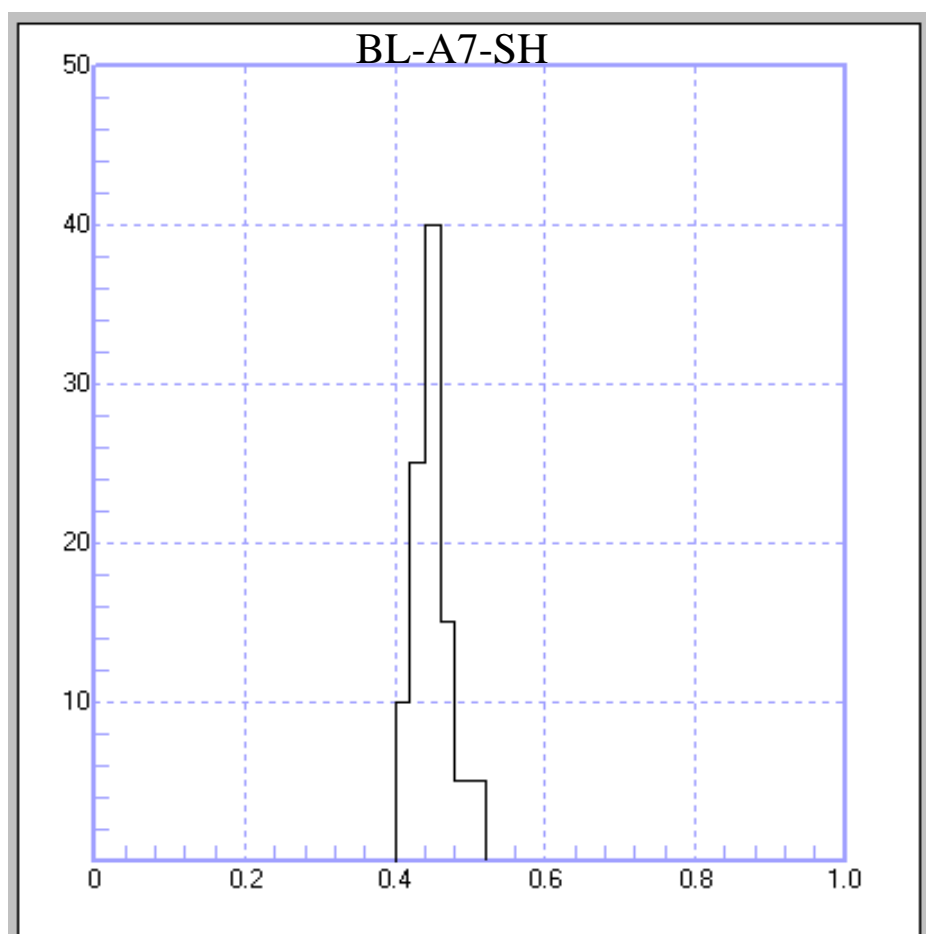
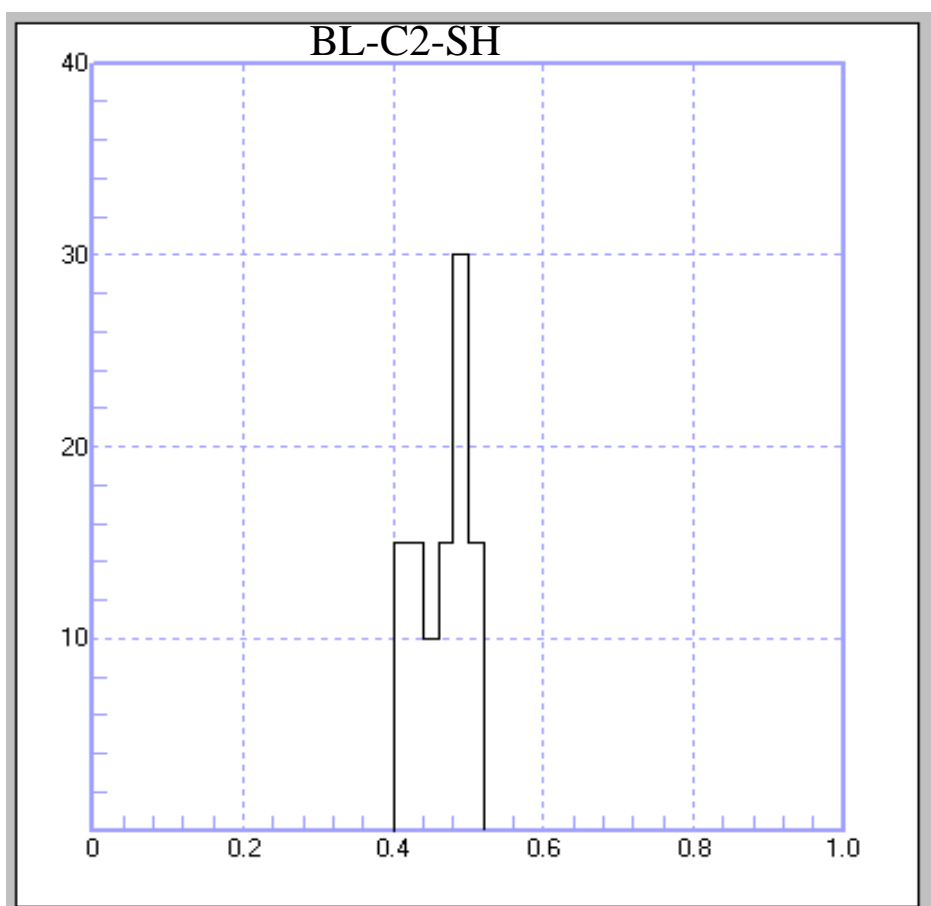












APPENDIX B

Py-GC Pyrogram Quantitative Data

| Sample | Formation | C ₈ | Xy | Phe | C ₈ % | Xy % | Phe % |
|-------------|------------------|----------------|-----|-----|------------------|------|-------|
| T-03-SH | Tukau | 1.2 | 3.2 | 3.5 | 15 | 41 | 44 |
| T-04-SH | Tukau | 1.6 | 3.4 | 3.4 | 19 | 40 | 40 |
| T-10-SS | Tukau | 1.2 | 3.6 | 3.5 | 14 | 43 | 42 |
| M-01-SH | Miri | 1.6 | 3.8 | 6.4 | 14 | 32 | 54 |
| M-03-SH | Miri | 1.4 | 3.2 | 5.8 | 13 | 31 | 56 |
| M-05-SH | Miri | 1.4 | 3.6 | 5.8 | 13 | 33 | 54 |
| M-08-SH | Miri | 1.3 | 3.3 | 6.2 | 12 | 31 | 57 |
| M-11-SS | Miri | 1.2 | 3.5 | 5.5 | 12 | 34 | 54 |
| L-02-SS | Lambir | 1.7 | 2.8 | 3.3 | 22 | 36 | 42 |
| L-03-SH | Lambir | 1.5 | 2.8 | 3.2 | 20 | 37 | 43 |
| L-05-SS | Lambir | 1.8 | 3.2 | 3.5 | 21 | 38 | 41 |
| L-07-SH | Lambir | 1.5 | 2.5 | 3.2 | 21 | 35 | 44 |
| L-14-SH | Lambir | 1.5 | 3.1 | 3.2 | 19 | 40 | 41 |
| BL-A3-SH | Belait | 2.2 | 5.2 | 7.1 | 15 | 36 | 49 |
| BL-A5-SS | Belait | 2.4 | 5.5 | 6.8 | 16 | 37 | 46 |
| BL-A6-SS | Belait | 2.2 | 4.8 | 8.2 | 14 | 32 | 54 |
| BL-B1-SH | Belait | 2.6 | 5.6 | 7.8 | 16 | 35 | 49 |
| BL-C2-SH | Meligan | 2.8 | 8.4 | 4.2 | 18 | 55 | 27 |
| ME-134A-SH | Meligan | 3.5 | 6.2 | 1.6 | 31 | 55 | 14 |
| ME-130F-SH | Meligan | 3 | 7.2 | 5 | 20 | 47 | 33 |
| ME-133A-SS | Meligan | 2.6 | 7.6 | 3.8 | 19 | 54 | 27 |
| TE-139-SH | Temburong | 2.2 | 6.7 | 0.7 | 23 | 70 | 7 |
| TE-137A-SH | Temburong | 1.2 | 7.2 | 0.5 | 13 | 81 | 6 |
| TE-140-SH | Temburong | 1.4 | 7.4 | 0.3 | 15 | 81 | 3 |
| WC-129E-MTD | West Crocker | 5.8 | 7.6 | 1.2 | 52 | 43 | 8 |
| WC-144A-MTD | West Crocker | 6 | 8.4 | 1.6 | 53 | 38 | 10 |
| WC-145B-MTD | West Crocker | 4 | 8.2 | 1.2 | 30 | 61 | 9 |
| WC-129B-SH | West Crocker | 2.8 | 6.2 | 0.8 | 29 | 63 | 8 |
| WC-135B-SS | West Crocker | 3.2 | 5.6 | 1.2 | 32 | 56 | 12 |
| UD-01-SS | Undifferentiated | 1.7 | 4 | 6.3 | 14 | 33 | 53 |
| UD-02-SS | Undifferentiated | 1.5 | 3.8 | 5.8 | 14 | 34 | 52 |

C₈: n-Octene Xy: Xylene Phe: Phenol